BLACK-HOLE ELECTRODYNAMICS

Thesis by

Douglas Alan Macdonald

In Partial Fulfillment of the Requirements

for the Degree of

Doctor of Philosophy

California Institute of Technology

Pasadena, California

1984

(Submitted November 7, 1983)

ACKNOWLEDGEMENTS

I would like to thank my advisor, Kip Thorne, for his support and guidance during my years at Caltech. The encouragement and friendship of my office-mates, Yekta Gürsel and Ian Redmount, have also been invaluable in helping me through sometimes difficult times. There are many people without whom this thesis would not have been possible: my sister Fiona and my father, and especially Bert and Bessie Bailey. And Elizabeth Wood, who came into my life at just the right time.

This dissertation was supported in part by the National Science Foundation under Grant Numbers (AST79-22012) and (AST82-14126) and (PHY77-27084).

ABSTRACT

This dissertation considers several aspects of the structure and dynamics of electromagnetic fields around black holes. The four-dimensional, covariant laws of electrodynamics are reformulated in a 3 + 1 (space+time) language in which the key quantities are three-dimensional vectors lying in hypersurfaces of a constant global time t. This formulation is applied to the Blandford-Znajek model of power generation in quasars, which consists of a supermassive black hole surrounded by an accretion disk that holds a magnetic field on the hole, with the rotational energy and angular momentum of the hole and disk being extracted by electromagnetic torques. The 3 + 1 formalism allows the theory of stationary, axisymmetric black holes and their magnetospheres to be couched in an "absolute-space/universal-time" language very similar to the flat-spacetime theory of pulsar electrodynamics; and this similarity allows flat-space pulsar concepts to be extended to curved-space black holes. The Blandford-Znajek quasar model is reformulated in terms of a DC circuit-theory analysis, and action principles describing the overall structure of the magnetosphere and the field distribution on the horizon are developed. A general prescription for constructing global models of force-free magnetospheres is developed and this prescription is used to generate numerical models of black-hole magnetospheres for a variety of field configurations and black-hole angular velocities. The electromagnetic boundary conditions at the horizon of a black hole are described in terms of a recently developed "membrane viewpoint". The necessity and efficacy of using a "stretched horizon" in the membrane viewpoint is discussed, and is illustrated by two simple dynamical problems involving electromagnetic fields near black-hole horizons.

TABLE OF CONTENTS

CHAPTER I

INTRODUCTION AND SUMMARY

3 + 1 Formulation of Electrodynamics

One of the most important results to emerge from the theory of relativity in the past two decades is the striking simplicity of the black-hole solutions of Einstein's equations. If a black hole is isolated, that is, if there is no matter surrounding it, then the spacetime will be completely characterized by just three quantities: the mass of the black hole, its angular momentum and its charge. This is true regardless of the physical complexities of the situation which led to the formation of the black hole. Even if the hole is formed by a highly asymmetric collapse, the higher-order multipoles of both the gravitational and electromagnetic fields will be radiated off on a timescale of the order of the light-travel time across the hole, until they attain the values characterizing the Kerr-Newman geometry and the spacetime is described by just the three above-mentioned quantities. This simplicity of form has been aptly characterized by John A. Wheeler in his statement "A black hole has no hair."

A black hole in isolation, therefore, is not a very good candidate for detection by earth-based observations. Its external gravitational field is the same as that of a star of similar mass, but it emits no radiation by which it might be observed. The deflection of starlight by its gravitational field (the lens effect) might be observable, but a distant observer could not distinguish the effect from that due to a dim star of the same mass. Nor is a charged black hole likely to be observable by the effects of its electromagnetic field. The electromagnetic field is stationary and is not likely to be strong enough either to affect the geometry or to be astrophysically important, since the charge on a black hole is known to be limited by selective accretion and quantum effects (Damour & Ruffini 1975,

Blandford & Znajek 1977).

Thus, if one is interested in the possibility of detecting a real astrophysical black hole, one must consider situations of non-isolated black holes. If a black hole is surrounded by matter, it can have as much hair as the matter wishes to hold on it. There are several scenarios which might lead to non-isolated black holes. If a black hole of stellar mass is part of a binary system, it may drag mass off its companion to form an accretion disk which is slowly dragged into the hole, radiating its gravitational energy as it falls in. Similarly, the supermassive black holes which are invoked to explain the enormous power output of quasars and active galactic nuclei would be expected to be continuously accreting interstellar gas as well as gas from stars which have come too close and been disrupted.

Matter in the vicinity of a black hole can serve to anchor electromagnetic fields near the hole which may be far stronger than any fields due to a charge on the hole. This raises interesting possibilities. Models have been proposed (Ruffini & Wilson 1975, Blandford & Znajek 1977, Phinney 1983) for the extraction of the rotational energy of a black hole by electromagnetic fields. Similar models also exist for energy extraction by infalling particles, but such models involve somewhat strained assumptions and are unlikely to be realistic as astrophysical power sources. On the other hand, the electromagnetic processes, particularly the Blandford-Znajek process, are considered by many investigators to be realistic candidates for the power source of quasars. The study of electromagnetic fields in the neighborhood of black holes is therefore of crucial importance in answering the question of their detectability.

Much work has been done in this area. Only a few completely self-consistent, analytic solutions of the Einstein-Maxwell equations are known (Wheeler 1955, Melvin 1964), and fewer still of these represent black holes in

electromagnetic fields (Ernst 1976, Ernst & Wild 1976); but there is a plethora of analytic solutions in which the electromagnetic field is treated as a test field too weak to perturb the spacetime geometry. These range from simple idealized physical models involving specified configurations of charge and current (Petterson 1975, Hanni & Ruffini 1973, Znajek 1978a, Linet 1976, 1979) or asymptotic fields (Hanni & Ruffini 1976, Wald 1974) to detailed studies of realistic magnetohydrodynamic configurations around black holes (Lovelace 1976, Blandford & Znajek 1977, Phinney 1983; see Coroniti 1983 for a recent brief review).

The study of electromagnetic fields around black holes is made more difficult by the inescapably relativistic nature of the problem. Even for as condensed an object as a neutron star, relativity does not play a critical role in determining the structure of the magnetosphere; the theory of pulsar electrodynamics can be couched entirely in the language of flat-space electrodynamics (Goldreich & Julian 1969, Mestel, Phillips & Wang 1979, Michel 1982), making only minor errors. Any attempt to ignore relativity when dealing with the magnetospheres of black holes, however, is doomed to failure.

But the necessity of a fully relativistic treatment does not mean that the equations of black-hole electrodynamics have to be explicitly four-dimensional; they can perfectly well be made three-dimensional to facilitate contact with laboratory and neutron-star intuition. Even the equations of flat-space electrodynamics, after all, are four-dimensional when expressed in their most elegant form: they are couched in terms of such quantities as the electromagnetic field tensor $F_{\mu\nu}$ and the 4-current density J_{μ}. It is only when one chooses a time coordinate and an associated family of fiducial three-dimensional spacelike hypersurfaces of constant time ("3 + 1 split") and projects the four-dimensional field quantities into them that one obtains the familiar equations of flat-space electrodynamics, couched in terms of such quantities as the electric field $\mathbf{E}$, the

magnetic field **B**, the 3-current density **j** and the charge density ρ_e.

One can do the same thing in a general curved spacetime. In fact, one effectively has a great deal more freedom in the choice of the splitting in a curved spacetime than one has in flat spacetime. There is a "natural" set of choices of the family of spatial 3-hypersurfaces in flat spacetime, i.e. any set associated with a congruence of inertial observers all moving with the same velocity throughout spacetime. There will generally be no such natural choice in a curved spacetime. The fiducial 3-hypersurfaces may be chosen with as many hills and valleys as desired, so long as they are everywhere spacelike; in fact, in a generic spacetime, the curvature makes it impossible to choose the spatial sections without such hills and valleys.

In any problem with a degree of symmetry, however, there will often be natural choices of splitting singled out. For a stationary problem, for instance, it would be foolish not to choose all of the 3-hypersurfaces to have the same geometry, independent of the "ignorable" time coordinate. Similarly, if the problem is axisymmetric, the 3-hypersurfaces should obviously be chosen to share this axisymmetry. All of the problems considered in this thesis will have such natural choices of splitting.

The 3 + 1 formulation of curved-space electrodynamics can be simply integrated with a recently developed paradigmatic view of black-hole horizons which will be described below.

Paradigmatic View of Black-Hole Physics

General relativity is unique among the branches of physics in the wide latitude of possible viewpoints it allows of its subject matter. This is due to the fact that it was originally created with the intent of writing the laws of physics in a form invariant with respect to all coordinate transformations, and it thus

expresses these laws in an extremely general form which is valid in the reference frame of any arbitrarily chosen family of fiducial observers.

Although the invariance of physical law as described by general relativity has always been recognized intellectually, it has often been a source of confusion, usually due to the fact that the large freedom in choice of reference frames allows one all too easily to choose sets of fiducial observers whose coordinate systems become degenerate in particular regions of spacetime. These degeneracies can cause certain quantities measured by the fiducial observers (e.g. components of vectors and tensors) to be infinite even though all physical quantities (e.g. scalars and physical components of vectors and tensors) are finite.

This confusion over coordinate systems has nowhere been more marked than in the study of black holes. Schwarzschild discovered the spherically symmetric black-hole solution bearing his name in 1916, only a few weeks after the general theory of relativity was published. This solution had an apparent singularity at radial coordinate $r = 2M$, where M is the mass of the black hole. Eddington, in 1924, constructed a coordinate system based on infalling observers which was explicitly nonsingular at $r = 2M$, but it was not until 1933 that the singularity was recognized by Lemaître to be wholly fictitious, a manifestation of a pathology in the coordinate system rather than in the structure of spacetime. The nature of the apparent singularities at the horizons of black-hole spacetimes is now well understood, but a good choice of fiducial reference frame is still important in investigating any problem as an aid to physical intuition and to avoid obscuring the physics with coordinate problems.

Several distinct viewpoints for the study of black holes will be described below. Although the differences between these viewpoints will actually amount to nothing more than differing choices of fiducial reference frames and different

interpretations of physical quantities measured in these frames, the relationships between these viewpoints and the resolution of apparent contradictions between them are subtle enough that we will, with an appropriate recognition of the inherent hubris, refer to these viewpoints as *paradigms* (Kuhn 1962, Thorne *et al.* 1984).

A particularly instructive way of illustrating the relationship between the various paradigms for black holes is to consider a particle falling into a black hole. If one looks at events from the viewpoint of an observer stationary outside the black hole, then since the event horizon is a surface of infinite redshift, the infalling particle and any fields it may carry will never be seen to cross the horizon, but rather will hover just outside it and asymptotically approach it. For a black hole formed by stellar collapse, in fact, the stationary observer could in principle see the original material of the collapsed star if he or she could look close enough to the horizon. This viewpoint is the basis for the Russian name "застывший звезда" for a black hole, which means "frozen star", and it will therefore be called the *frozen-star paradigm.*

The star is anything but frozen from the viewpoint of an observer riding on an infalling particle. This observer passes through the horizon and hits the singularity at $r = 0$ (which is a true spacetime singularity) in a finite amount of his own proper time. This viewpoint is the basis of what will be called the *black-hole paradigm.* The resolution of the apparent contradiction between the two viewpoints lies in the fact the coordinate system of the external stationary observer becomes degenerate at the horizon, while that of the infalling observer is well-behaved there.

In the spherically symmetric Schwarzschild black-hole spacetime, the natural choice of the stationary observers for the frozen-star paradigm is that set of observers moving along trajectories of constant Schwarzschild time t,

while two (of many) possible choices of the infalling observers for the black-hole paradigm are the infalling observers of Novikov coordinates and the infalling observers of ingoing Eddington-Finkelstein coordinates.

If an infalling particle has a charge and generates electromagnetic fields, one may ask which of these paradigms is most useful in studying the behavior of the fields during and after the infall. The answer is that neither is ideal for the purpose. The black-hole paradigm is a poor choice because its fiducial observers do not stay outside the horizon, and also because they are non-stationary, which will introduce unnecessary complications if the background spacetime is stationary. The frozen-star paradigm does not suffer from either of these problems, but it has the disadvantage that it emphasizes a part of the field geometry which quickly becomes irrelevant as the particle falls into the hole. As mentioned above, and as discussed qualitatively in chapter II, not only does the infalling particle appear to hover, "frozen", just above the horizon, but so also do its fields. The fields form a layered structure, lying just above the horizon and asymptotically approaching it, which contains relic fields reflecting the entire past evolution of the field, including the infall of the particle. These layered fields not only make it difficult to define boundary conditions on fields at the horizon, but at times large compared to the infall timescale of the particle, they turn out to be completely irrelevant to the overall structure of the field farther out. Thus, although one can use the frozen-star paradigm in treating problems of electromagnetic fields outside horizons, it does not give much intuitive insight into the behavior of the fields associated with the particle long after the particle has fallen into the hole.

A viewpoint which has been developed over the last few years by Znajek (1978b), Damour (1978, 1982) and Carter (1979) is much more conducive to understanding the behavior of electromagnetic fields outside the horizon than is

the frozen-star paradigm. This point of view regards the horizon as a bubble or membrane endowed with familiar physical properties such as shear and bulk viscosity, surface pressure and electrical conductivity; this new viewpoint is therefore known as the *membrane paradigm.*

The membrane paradigm is particularly useful as an aid to physical intuition when combined with a 3 + 1 split of spacetime as described in chapter II and in Thorne *et al.* (1984). In this formulation, the boundary conditions on electromagnetic fields at the horizon are applied not on the actual horizon, but rather on a *stretched horizon* displaced outward slightly from the true horizon. This obviates the necessity of considering the irrelevant relic horizon fields described above, since they are hidden beneath the stretched horizon. The surface electrical resistivity of the true horizon in the membrane paradigm is $R^H = 4\pi/c = 377$ ohms, which is equal to the impedance of the vacuum at the end of an open waveguide, so the boundary conditions at the horizon amount to a prohibition of outgoing waves there. This prohibition can equally well be applied at a stretched horizon as long it is near enough to the true horizon that reflection of waves from the part of the wave-equation effective potential between the stretched and true horizons is negligible. Another condition affecting the choice of the stretched horizon is the requirement that its proper distance from the true horizon be smaller than the distance light travels in the timescale of evolution of the field, so that important features of the field are not neglected beneath the stretched horizon. As long as these criteria are met, the amount by which the horizon is stretched does not greatly affect the solution for the external field structure.

As an example of how the predictions of the various paradigms may be reconciled, consider the solutions and field line diagrams given by Hanni & Ruffini (1973) for a charged particle at rest outside a Schwarzschild black hole

(See Fig. 1). If these solutions are regarded as successive stages in the quasistatic descent of the particle into the black hole, they show that as the particle approaches the horizon, the field ceases to depend on the position of the particle, and the electric field lines begin to look to an external observer as if they were emerging uniformly and radially from the hole's horizon. Since the electric field lines must be continuous, however, there is a layer near the horizon where the field lines bend away from the radial direction and run approximately parallel to the horizon in order to attach themselves to the charge. As the charge approaches the horizon, this layer plasters itself closer and closer to the horizon. If the horizon is stretched to just above this layer, the field lines emerging from it have just the pattern which would be expected of a uniformly charged conducting sphere, and the charged particle can be regarded as having descended into the hole's interior. In chapter V, two truly dynamical problems which show this same type of behavior will be solved.

The membrane paradigm and the associated 3 + 1 formalism have been under development in the Caltech relativity group for the past several years, most recently under the aegis of an informal group known as the Paradigm Society, including Kip Thorne, Richard Price, Ronald Crowley, Wojciech Zurek, Ian Redmount, Wai-mo Suen, L. Sam Finn, Xiao-He Zhang, and the present author. This group has worked to develop a self-consistent framework for the study of the electromagnetic and gravitational interactions of black holes from the viewpoint of the membrane paradigm, and to devise model problems clarifying its applications. This thesis comprises a substantial part of the work done by the Society on electromagnetic interactions.

This thesis is presented in five chapters. In chapter II, the general curved-spacetime 3 + 1 formulation of the laws of electrodynamics is developed. The four-dimensional equations of curved-spacetime electrodynamics are reexpressed in a language in which the key quantities are three-dimensional vectors such as the electric field $\mathbf{E}$ and the magnetic field $\mathbf{B}$ lying in hypersurfaces of a constant universal time t. In this language, Maxwell's equations, the Lorentz force law and the laws of energy and momentum conservation have forms closely resembling the analogous relations in flat spacetime. The general 3 + 1 equations are then specialized to the spacetime outside a stationary, axisymmetric black hole and the horizon boundary conditions ("membrane viewpoint") developed by Znajek (1978b) and Damour (1978, 1982) are reexpressed in 3 + 1 language. Chapter II also discusses in a qualitative way the necessity of stretching the horizon in order to define unequivocally the concept of a boundary condition on the horizon.

Chapter III applies the formalism derived in chapter II to the analytic study of a stationary, axisymmetric magnetosphere surrounding a black hole and held on it by the electrical conductivity of an accretion disk. The theory of electromagnetic extraction of the hole's rotational energy, developed by Blandford & Znajek (1977), is reformulated in 3 + 1 language and extended. The equations governing the field outside the black hole are written down under three successively more restricted assumptions: (i) Stationary, axisymmetric fields; (ii) Stationary, axisymmetric and degenerate ($\mathbf{E}\cdot\mathbf{B} = 0$) fields; and (iii) Stationary, axisymmetric and force-free ($\rho_e\mathbf{E} + (\mathbf{j}/c)\times\mathbf{B} = 0$) fields. The energy extraction process is analyzed from a torque-balance point of view and from a DC circuit-theory point of view, with the conclusion that the magnetic field lines threading the black hole should attain roughly half the angular velocity of the hole, resulting in optimum energy extraction. In the last section of chapter III, a general

method for constructing global models of force-free magnetospheres is outlined. The electromagnetic field structure is determined by a single scalar *stream function* $\psi(r,\theta)$ satisfying a second-order partial differential equation (originally derived by Blandford & Znajek). The boundary conditions to be imposed on ψ at the horizon and at the other boundaries of the force-free region are discussed, and it is proved that the field distributes itself over the horizon in such a way as to minimize the horizon's ohmic dissipation.

Chapter IV applies the equations and prescription derived in chapter III to the construction of numerical models of stationary black-hole magnetospheres. These models are constructed by spinning up static, vacuum magnetic field solutions in Schwarzschild spacetime, and they illustrate, for several different field configurations, the dependence of the magnetospheric fields on the angular velocity of the black hole.

Because chapters III and IV deal with stationary magnetospheres, there is no complex field structure near the true horizon and consequently no necessity to hide such structure by stretching the horizon. Chapter V turns attention to dynamical situations where stretching is needed. The concept of a stretched horizon is briefly explained and two simple time-dependent problems illustrating the concept are solved in detail. These problems are meant to elucidate the behavior of electromagnetic fields near the horizon and clarify the connections between the frozen-star and membrane paradigms. Both problems involve the relaxation of a specified initial field toward a stationary final state, and both show explicitly the near-horizon field behavior described qualitatively in chapter II.

REFERENCES

Blandford R. D. & Znajek, R. L., 1977. *Mon. Not. R. astr. Soc.*, **179**, 433.

Carter, B., 1979. In *General Relativity, An Einstein Centenary Survey*, p. 294, eds. Hawking, S. W. & Israel, W., Cambridge University Press.

Coroniti, F. V., 1983. UCLA Center for Plasma Physics and Fusion Engineering preprint.

Damour, T., 1978. *Phys. Rev. D*, **18**, 3598.

Damour, T., 1982. In *Proceedings of the Second Marcel Grossman Meeting on General Relativity*, p. 587, ed. Ruffini, R., North Holland, Amsterdam.

Damour, T. & Ruffini, R., 1975. *Phys. Rev. Lett.*, **35**, 463.

Ernst, F. J., 1976. *J. Math. Phys.*, **17**, 54.

Ernst, F. J. & Wild, W. J., 1976. *J. Math. Phys.*, **17**, 182.

Goldreich, P. & Julian, W. H., 1969. *Astrophys. J.*, **157**, 869.

Hanni, R. S. & Ruffini, R., 1973. *Phys. Rev. D*, **8**, 3259.

Hanni, R. S. & Ruffini, R., 1976. *Lettere al Nuovo Cimento*, **15**, 189.

Kuhn, Thomas S., 1962. *The Structure of Scientific Revolutions*, University of Chicago Press, Chicago.

Linet, B., 1976. *J. Phys. A*, **9**, 1081.

Linet, B., 1979. *J. Phys. A*, **12**, 839.

Lovelace, R. V. E., 1976. *Nature*, **262**, 649.

Melvin, M. A., 1964. *Phys. Lett.*, **8**, 65.

Mestel, L., Phillips, P., & Wang, Y. M., 1979. *Mon. Not. R. astr. Soc.*, **188**, 385.

Michel, F. C., 1982. *Rev. Mod. Phys.*, **54**, 1.

Petterson, J. A., 1975. *Phys. Rev. D*, **12**, 2218.

Phinney, E. S., 1983. In *Proceedings of the Torino Workshop on Astrophysical Jets*, p. 201, eds. Ferrari, A. & Pacholczyk, A. G., D. Reidel, Dordrecht, Holland.

Ruffini, R. & Wilson, J. R., 1975. *Phys. Rev. D*, **12**, 2959.

Thorne, Kip S., Price, Richard H., Crowley, Ronald J., Zurek, Wojciech, Suen, Wai-Mo, Redmount, Ian H., Macdonald, Douglas A., Finn, L. Sam, & Zhang, Xiao-He, 1984. In preparation, to be submitted to *Rev. Mod. Phys.*

Wald, R. M., 1974. *Phys. Rev. D*, **10**, 1680.

Wheeler, J. A., 1955. *Phys. Rev.*, **97**, 511.

Znajek, R. L., 1978a. *Mon. Not. R. astr. Soc.*, **182**, 639.

Znajek, R. L., 1978b. *Mon. Not. R. astr. Soc.*, **185**, 833.

FIGURE CAPTION

Figure 1. Electric field lines of a charge stationary outside a Schwarzschild black hole (cf. Hanni & Ruffini 1973) at various radii. These plots were obtained by using the analytic field expressions given by Linet (1976) rather than the multipole expansion given by Hanni & Ruffini. If these solutions are regarded as successive stages in the quasistatic descent of the charge into the black hole, they illustrate the layered near-horizon field structure described in chapter II and the lack of dependence of the rest of the field structure on this layered field. This behavior forms a heuristic justification for the introduction of the concept of a stretched horizon. In chapter V, two truly dynamical problems further illustrating this type of behavior will be discussed.

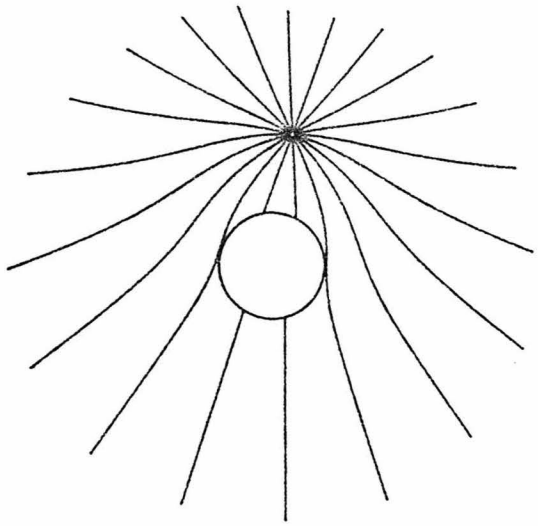

R = 5M

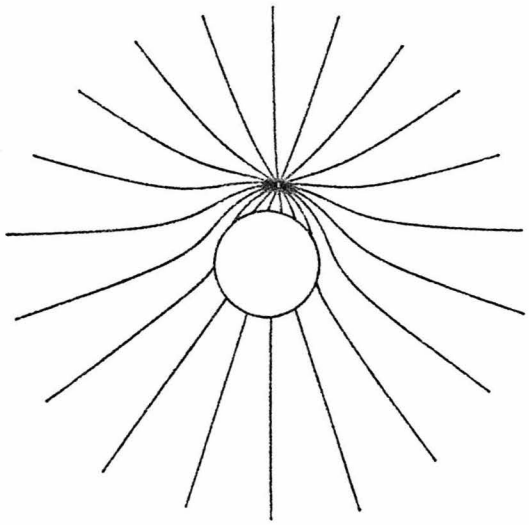

R = 3M

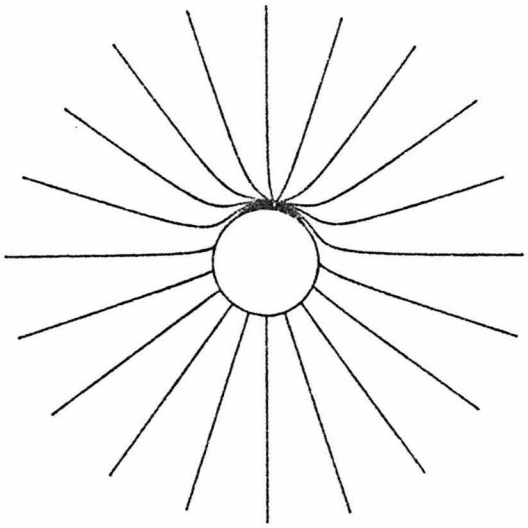

R = 2.2M

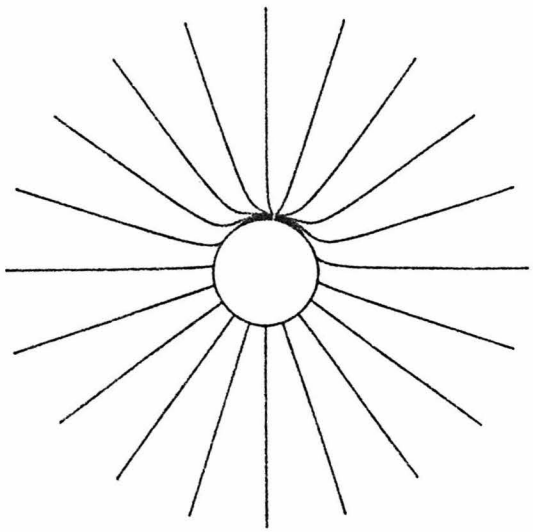

R = 2.1M

Fig. 1

CHAPTER II

OAP-615

ELECTRODYNAMICS IN CURVED SPACETIME: 3 + 1 FORMULATION*

KIP S. THORNE and DOUGLAS MACDONALD

W. K. Kellogg Radiation Laboratory
California Institute of Technology, Pasadena, California 91125

ABSTRACT

This paper develops the mathematical foundations for a companion paper on "Black-Hole Electrodynamics." More specifically, it reexpresses the equations of curved-spacetime electrodynamics in terms of a 3 + 1 (space + time) split, in which the key quantities are 3-dimensional vectors (electric field $\underset{\sim}{E}$, magnetic field $\underset{\sim}{B}$, etc.) that lie in hypersurfaces of constant time t. Three-dimensional vector analysis is used to express Maxwell's equations, the Gauss, Faraday, and Ampere laws, the Lorentz force law, and the laws of energy and momentum conservation in forms closely resembling their flat-spacetime counterparts.

After developing the 3 + 1 formalism for general spacetimes, this paper specializes to the spacetime outside a stationary but rotating black hole. The Znajek-Damour boundary conditions at the hole's horizon are reexpressed in 3 + 1 language. Because the black hole's hypersurfaces of constant time all have identical 3-dimensional geometries, one can abandon entirely Einstein's view of spacetime and return to Galileo's: The electric and magnetic fields $\underset{\sim}{E}$ and $\underset{\sim}{B}$ can be regarded as living in an absolute (but curved) 3-dimensional space, and as evolving in this space with the passage of universal time t. This viewpoint and associated mathematics are the foundation for a companion paper.

---

*Supported in part by the National Science Foundation [AST79-22012].

ONE OF THE ORANGE AID PREPRINT SERIES
IN NUCLEAR, ATOMIC & THEORETICAL ASTROPHYSICS

March 1981

1 Introduction

There is a close relationship between the theory of axisymmetric pulsar magnetospheres (e.g., Goldreich and Julian 1969; Mestel, Phillips, and Wang 1979), and the theory of black-hole and accretion-disk magnetospheres (Blandford and Znajek 1977). For this reason it is curious that astrophysicists have spent enormous effort on the axisymmetric pulsar problem, an idealized problem somewhat far from the structure of real (nonaxisymmetric) pulsars, but have put little effort into the theory of black-hole magnetospheres, for which the assumption of axisymmetry is probably justified in Nature.

We think that this may be due to the fact that general relativity plays crucial roles in the black-hole problem, but not in the pulsar problem, and that the language and mathematical formalism of black-hole electrodynamic theory (Blandford and Znajek 1977) are therefore somewhat different from those of pulsar electrodynamics, and somewhat alien to pulsar theorists. For example, the black-hole theory of Blandford and Znajek uses as its fundamental electrodynamic variables the components A_0, A_φ, $F_{r\theta}$, J^0, J^r, J^θ, J^φ of the 4-vector potential $\mathcal{A}$, the electromagnetic field tensor $\mathbf{F}$, and the charge-current 4-vector $\mathbf{J}$ — and those components are taken in the Boyer-Lindquist coordinate basis of Kerr spacetime. It is not easy for an astrophysicist to get an intuitive, physical feeling for these variables or for their relationship to the electric vector $\underset{\sim}{E}$, magnetic vector $\underset{\sim}{B}$, current vector $\underset{\sim}{j}$, and charge density ρ_e of his flat-space pulsar theory.

Fortunately, it is possible — indeed straightforward — to rewrite curved-spacetime black-hole electrodynamic theory in terms of the physically measured $\underset{\sim}{E}$, $\underset{\sim}{B}$, $\underset{\sim}{j}$, and ρ_e and thereby to obtain a formalism that is very similar to the theory of pulsar electrodynamics and that therefore might be a powerful

tool in future black-hole research. The prescription for this rewrite of the curved-spacetime theory is as follows: (i) Choose at each event in spacetime a fiducial reference frame; i.e., split spacetime up into three space directions and one uniquely chosen time direction ("3+1 split"). (ii) In this fiducial reference frame, split the electromagnetic field tensor $\mathbf{F}$ into electric and magnetic fields $\underset{\sim}{E}$ and $\underset{\sim}{B}$ in the usual manner of flat spacetime ($\underset{\sim}{E}$ is the time-space part of $\mathbf{F}$; $\underset{\sim}{B}$ is the space-space part). (iii) Similarly, in the fiducial frame, split the 4-current vector $\mathbf{J}$ into a time part $J^0 \equiv \rho_e$ = (charge density) and a 3-space part $\underset{\sim}{j}$ = (current density). (iv) Rewrite in terms of $\underset{\sim}{E}$, $\underset{\sim}{B}$, ρ_e, and $\underset{\sim}{j}$ the curved-spacetime Maxwell equations, the Lorentz force law, and the law of charge conservation.

Many relativity theorists dislike such a 3+1 split because of the arbitrariness of the choice of fiducial reference frame. However, in the case of stationary black-hole electrodynamics there is one set of fiducial frames preferred over all others: the frames of observers who are at rest in the hole's stationary gravitational field, and who see neighboring fiducial observers inertially fixed with respect to the gyroscopes of their inertial guidance systems ("ZAMO" or "zero angular momentum observers"). When one uses these ZAMO frames one finds that the "3+1" equations of black-hole electrodynamics are nearly identical to the flat-space equations of pulsar electrodynamics. Moreover, when using these frames one can mentally adopt a new viewpoint on the 3+1 formalism: one can regard electrodynamics and all other physics as occurring in a fixed, unchanging, absolute 3-dimensional space and one can regard time as merely a parameter which demarks the evolution of the matter and fields. In other words, one can return to the absolute-space and universal-time viewpoint of Galileo, which underlies most modern-day astrophysical intuition.

Previous research on black-hole electrodynamics has not used either the 3+1 viewpoint, or the absolute-space/universal-time viewpoint. The purpose of this paper and its companion is to introduce those viewpoints and thereby, we hope, to make it easier for astrophysicists to carry their pulsar-based intuition over to the black-hole problem.

We have split our presentation into two papers, so as to make the 3+1 formalism more accessible to astrophysicists. Paper I (this paper) derives 3+1 electrodynamics from the relativist's more usual 4-dimensional formalism—and in doing so it makes free use of the mathematical tools of general relativity theory. Paper II (Macdonald and Thorne 1981) reformulates the Blandford-Znajek theory of black-hole magnetospheres in 3+1 language, using the absolute-space/universal-time viewpoint—and in doing so it avoids the mathematics of general relativity.

Paper II can be read separately from Paper I if one is willing to accept the equations of 3+1 electrodynamics on faith.

This paper is organized as follows. Section 2 introduces the mathematics of the 3+1 split, including: a brief historical survey of the subject (§2.1); the fiducial observers and their hypersurfaces of simultaneity $\mathcal{S}_t$ with respect to which the 3+1 split is made (§2.2); the dot product, cross product, gradient, divergence, and curl of spatial vectors (3-vectors) lying in the fiducial hypersurfaces (§2.3); three different types of time derivative (§2.4); and identities for transforming volume, surface, and line integrals and their time derivatives into each other (§2.5).

Section 3 presents the 3+1 formulation of electrodynamics in terms of differential equations, including: the relationship between 3+1 electrodynamic quantities and 4-dimensional quantities (§3.1); the Maxwell equations (§3.2); expressions for $\underset{\sim}{E}$ and $\underset{\sim}{B}$ in terms of the scalar potential ϕ and vector

potential $\underset{\sim}{A}$ (§3.3); the law of charge conservation (§3.4); the Lorentz force law and equation of motion of a charged test particle (§3.5); and the differential laws of energy and momentum conservation for the electromagnetic field and a continuous medium (§3.6).

Section 4 presents the integral formulation of 3+1 electrodynamics: Gauss's law, Ampere's law, Faraday's law, and the law of charge conservation.

Section 5 specializes the 3+1 formalism to the spacetime of a stationary, axisymmetric black hole, including: the selection of the ZAMO observers as our fiducial observers and the resulting simplifications of various 3+1 kinematic equations (§5.1); the 3+1 electrodynamic equations specialized to our black-hole spacetime (§5.2); the pathological behavior of the hypersurfaces S_t near the hole's horizon, and the resulting delicate definition of "the limit of a physical quantity as one approaches the horizon" (§5.3); and the Znajek-Damour theory of electromagnetic boundary conditions at the horizon, rewritten in 3+1 language (§5.4).

Section 6 illustrates the 3+1 formalism by rewriting in 3+1 language two known solutions to the vacuum Maxwell equations: the electric field of a point charge outside a Schwarzschild hole (§6.1), and a uniform magnetic field surrounding and deformed by a Kerr hole (§6.2).

Throughout this paper we use the mathematical notation and conventions of Misner, Thorne, and Wheeler (1973; cited henceforth as MTW), including units in which the speed of light c is unity. (Nowhere, except in the examples of §5.3 and §6, do we need to set Newton's gravitation constant G to unity.) Electromagnetic quantities are expressed in Gaussian units (electric fields in statvolts per centimeter, magnetic fields in Gauss). We denote 4-vectors and 4-tensors by bold-face letters, e.g., $\mathbf{U}$ and $\mathbf{F}$, and their components by Greek indices, e.g., U^{α} and $F_{\alpha\beta}$. We denote spatial vectors (3-vectors) and

spatial tensors (3-tensors) by underscored letters, e.g., $\underset{\sim}{E}$ and $\underset{\sim}{\gamma}$, and their components by Latin indices, e.g., E^j and γ_{jk}.

2 3+1 Mathematical Formalism

2.1 HISTORICAL REMARKS

There are two rather different ways to make a 3+1 split of the laws of physics in curved spacetime. The first way selects a fiducial congruence of timelike world lines, and at each event identifies "time" as the direction along the fiducial world line and "space" as the three directions orthogonal to it. In this congruence approach the space directions at neighboring events will not mesh to form global spacelike hypersurfaces (3-spaces of constant time), unless the congruence is constrained to be "rotation-free".

The second approach selects a foliation of fiducial 3-dimensional hypersurfaces (3-spaces of constant time), and at each event identifies "space" as the directions lying in the hypersurface. In this hypersurface approach one can identify as "time" the direction orthogonal to the hypersurface — in which case the formalism is identical to the rotation-free limit of the congruence approach. Alternatively, one can identify as "time" a nonorthogonal direction (nonzero "shift vector").

The congruence approach to 3+1 splits was developed in brief form by Landau and Lifshitz (1941) and in greater detail by Zel'manov (1956, 1959), who refers to spatial vectors and tensors as "chronometric invariants". Today this congruence approach is much used by Russian relativistic astrophysicists, in no small measure because of the influence of Igor Novikov, who was a student of Zel'manov (see, e.g., §1.6 of Zel'dovich and Novikov, 1971). In the West the congruence approach was developed in brief form by Cattaneo (1959) and in great detail by Estabrook and Wahlquist (1964), who called it the "dyadic formalism". None of

these workers, Russian or Western, wrote down Maxwell's equations in 3+1 congruence language; that was done later, by Ellis (1973). And as far as we know, nobody has ever used the Ellis equations in astrophysics or relativity research, except for our present study of black-hole electrodynamics.

The hypersurface approach to 3+1 splits was developed by Lichnerowicz (1944) in his pioneering studies of the dynamical evolution of spacetime geometry; and it was further developed in the 1950's by Bergmann, Dirac, Wheeler, Arnowitt, Deser, Misner, and others as part of their efforts to create a Hamiltonian formulation of general relativity and thereby to lay the foundations for canonical quantization of the gravitational field; see Arnowitt, Deser, and Misner (1962) ("ADM"). As part of this program, Misner and Wheeler (1957) wrote down the curved-space, vacuum Maxwell equations in 3+1 hypersurface form, but using the language of exterior calculus rather than vector analysis; Arnowitt, Deser, and Misner (1960a,b) wrote down the 3+1 Maxwell equations with point charges, but using the language of vector densities rather than vectors; and Stachel (1969) wrote down those portions of the 3+1 Maxwell equations which are metric-independent, using the language of vectors and tensors. These "3+1 Maxwell equations" have been much used since 1960 as a guide to formal mathematical studies of the dynamics of geometry (see, e.g., chapter 21 of MTW). However, they seem never to have been used in astrophysics research. In recent years the full ADM 3+1 hypersurface formalism has been adopted as the canonical foundation for numerical solutions of the Einstein field equations and of hydrodynamical equations in curved spacetime ("numerical relativity"); see Smarr and York (1978), York (1979), Smarr, Taubes, and Wilson (1980). In the Soviet Union the hypersurface approach to 3+1 splits has been formulated by Zel'manov (1973); he refers to spatial vectors and tensors in this formalism as "kinematic invariants".

In the present work we shall use the ADM hypersurface approach to 3+1 splits. Initially we shall choose our time direction orthogonal to the hypersurfaces, thereby making our formalism identical to the rotation-free limit of

the congruence approach. This will permit us to use Ellis's beautiful 3+1 formulation of Maxwell's equations. Later, when specializing to black-hole spacetimes, we shall introduce a "shift" into our time direction, so that instead of being orthogonal to the fiducial hypersurfaces, it is along the Killing direction $\mathbf{k} = \partial/\partial t$ of the stationary spacetime geometry.

2.2 FIDUCIAL HYPERSURFACES AND CONGRUENCE

Our mathematical formalism for the fiducial hypersurfaces and congruence and for the 3+1 split is essentially the same as that used in current research on numerical relativity (e.g., York 1979), with these exceptions: (i) Our notation is slightly different; for example, we use index-free expressions $\underset{\sim}{A}\cdot\underset{\sim}{B}$, $\underset{\sim}{\nabla}\times\underset{\sim}{E}$, etc. and we "think" in coordinate-free language, whereas numerical relativists always have a coordinate mesh and use index notation $A^j B^k \gamma_{jk}$ with components taken on that mesh. (ii) In the early part of this paper we use different kinds of time derivatives than they — our D_τ and $\mathfrak{D}_\tau$. (iii) We develop and make extensive use of 3+1 integral identities, which are not part of present-day numerical relativity.

Consider a region $\mathcal{E}$ of 4-dimensional spacetime in which electrodynamic phenomena are to be studied. Introduce into $\mathcal{E}$ a family of spacetime-filling, 3-dimensional spacelike hypersurfaces; and introduce a parameter t which (i) labels the hypersurfaces, and (ii) increases smoothly as one moves forward in time from hypersurface to hypersurface, but (iii) is otherwise arbitrary. Denote by $\mathcal{S}_t$ the hypersurface which has label t. Give t the name "global time parameter" or simply "global time". See Figure 1.

There will exist a congruence of timelike curves which are orthogonal to the hypersurfaces. These curves can be regarded as the world lines of a family of "fiducial observers" [numerical relativists call them "Eulerian observers"]

who think of the hypersurfaces $\mathcal{S}_t$ as "slices of simultaneity". Parametrize each fiducial world line by the proper time τ of its observer. Then the observer's 4-velocity (unit tangent to the fiducial world line) is $\mathbf{U} = d/d\tau$. [In numerical relativity (e.g., York 1979) the notation $\mathbf{n}$ is used rather than $\mathbf{U}$. In this paper $\mathbf{n}$ is reserved for the normal to the horizon of a black hole (Eq. 5.23 below).] Proper time τ and global time t typically will not march forward at the same rate along a fiducial world line; the ratio of their rates is called the "lapse function" α

$$\alpha = (d\tau/dt)_{\text{along fiducial world line}} \quad . \tag{2.1a}$$

Since the fiducial 4-velocity $\mathbf{U}$ is orthogonal to hypersurfaces of constant t, it must be parallel to the 4-gradient of t with a proportionality constant determined by $\mathbf{U}^2 = -1$ and by $\mathbf{U} \cdot {}^{(4)}\boldsymbol{\nabla} t = dt/d\tau = \alpha^{-1}$:

$$\mathbf{U} = -\alpha\, {}^{(4)}\boldsymbol{\nabla} t \quad , \qquad \alpha = [-({}^{(4)}\boldsymbol{\nabla} t)^2]^{-1/2} \quad . \tag{2.1b}$$

Here and below we use a prefix (4) on the spacetime gradient ${}^{(4)}\boldsymbol{\nabla}$ to distinguish it clearly from the spatial gradient $\underset{\sim}{\nabla}$.

2.3 THREE-DIMENSIONAL VECTOR ANALYSIS

Any 4-vector $\mathbf{M}$ or 4-tensor $\mathbf{T}$ which is orthogonal to the fiducial 4-velocity, $M^\alpha U_\alpha = 0$ or $U_\alpha T^{\alpha\beta} = 0 = T^{\alpha\beta} U_\beta$, can be regarded as a purely spatial vector $\underset{\sim}{M}$ or tensor $\underset{\sim}{T}$ — i.e., it can be regarded as living in a fiducial hypersurface $\mathcal{S}_t$. When adopting the 3+1 viewpoint we shall denote it $\underset{\sim}{M}$ or $\underset{\sim}{T}$ and its components M_j or T_{jk}. When adopting the 4-dimensional spacetime viewpoint we shall use the notation $\mathbf{M}$, $\mathbf{T}$, M_α, $T_{\alpha\beta}$.

The most important spatial tensor we shall deal with is the metric $\underset{\sim}{\gamma}$ of the fiducial hypersurfaces $\mathcal{S}_t$. In 4-dimensional notation, $\gamma^{\alpha\beta}$ is the tensor

$$\gamma^{\alpha\beta} = g^{\alpha\beta} + U^{\alpha}U^{\beta} \tag{2.2}$$

which projects 4-vectors into the fiducial hypersurfaces. Here $g^{\alpha\beta}$ is the metric of 4-dimensional spacetime.

The 3+1 equations of physics will involve the kinematic properties of the fiducial world lines — their expansion θ, 4-acceleration $\underset{\sim}{a}$, and shear $\underset{\sim}{\sigma}$. (Their rotation $\underset{\sim}{\omega}$ vanishes because the fiducial world lines are hypersurface orthogonal.) Viewed as 4-dimensional quantities, θ, a^{α}, and $\sigma_{\alpha\beta}$ are defined by

$$\begin{aligned} \theta &= U^{\alpha}{}_{;\alpha} \quad , \qquad a^{\alpha} = U^{\alpha}{}_{;\beta}U^{\beta} \quad , \\ \sigma_{\alpha\beta} &= \tfrac{1}{2}\gamma_{\alpha}{}^{\mu}\,\gamma_{\beta}{}^{\nu}(U_{\mu;\nu} + U_{\nu;\mu}) - \tfrac{1}{3}\theta\,\gamma_{\alpha\beta} \quad , \end{aligned} \tag{2.3a}$$

which can be inverted to give

$$U_{\alpha;\beta} = -a_{\alpha}U_{\beta} + \sigma_{\alpha\beta} + \tfrac{1}{3}\theta\,\gamma_{\alpha\beta} \tag{2.3b}$$

(cf. Exercise 22.6 of MTW). Here the semicolon denotes the covariant derivative ${}^{(4)}\nabla$ with respect to the spacetime geometry. One can easily verify that a^{α} and $\sigma_{\alpha\beta}$ are orthogonal to U^{α} and are therefore a spatial vector and spatial tensor, respectively. A fiducial observer interprets θ as the fractional time rate of change $V^{-1}dV/d\tau$ of the volume V of a "fluid element" whose walls are attached to the world lines of nearby fiducial observers — i.e., $\theta = 3\times$ (Hubble expansion rate of fiducial observers averaged over all directions in space). If a fiducial observer carries an accelerometer, he interprets $\underset{\sim}{a}$ as the vector acceleration which it reads. If a fiducial observer studies the motions of other nearby fiducial observers, he interprets $\underset{\sim}{\sigma}$ as the rate of shear of those motions, as defined in nonrelativistic fluid mechanics. For further detail

see, e.g., Ellis (1971,1973). One can show, using equation (2.1b) and the definition of the spatial gradient given below, that the acceleration and the lapse function are related by

$$\underset{\sim}{a} = \underset{\sim}{\nabla} \ln \alpha \quad ; \tag{2.4}$$

and one can show using equations (2.3a) and (2.2), that the shear $\underset{\sim}{\sigma}$ is symmetric and trace-free

$$\sigma_{jk} = \sigma_{kj} \quad , \quad \sigma_{jk}\gamma^{jk} = \sigma_{\alpha\beta}\gamma^{\alpha\beta} = 0 \quad . \tag{2.5}$$

The "extrinsic curvature" $\underset{\sim}{K}$ of the hypersurface $\mathcal{S}_t$ is related to the shear and expansion of the fiducial congruence by

$$\underset{\sim}{K} = -(\underset{\sim}{\sigma} + \frac{1}{3}\theta\,\underset{\sim}{\gamma}) \quad . \tag{2.6}$$

Spatial vectors and tensors living in $\mathcal{S}_t$ can be manipulated in much the same manner as in flat space: If $\underset{\sim}{L}$ and $\underset{\sim}{M}$ are spatial vectors, their inner product and cross product are

$$\underset{\sim}{L}\cdot\underset{\sim}{M} = L_j M_k \gamma^{jk} \quad , \quad (\underset{\sim}{L}\times\underset{\sim}{M})^j = \varepsilon^{jk\ell} L_k M_\ell \tag{2.7}$$

where $\varepsilon^{jk\ell}$ is the spatial Levi-Civita tensor [equal to $(\det ||\gamma_{ij}||)^{-1/2}$ (anti-symmetric symbol)]. The spatial gradient operator (denoted $\underset{\sim}{\nabla}$ in abstract and $|_j$ in component notation) can be defined in either of two equivalent ways: as the 4-dimensional covariant derivative projected into $\mathcal{S}_t$, or as the spatial covariant derivative associated with the spatial metric γ_{jk}. From the former viewpoint, if $\underset{\sim}{M}$ is a spatial vector then $\underset{\sim}{\nabla}\underset{\sim}{M}$ is a spatial tensor with spacetime components

$$M^{\alpha}{}_{|\beta} = \gamma^{\alpha}{}_{\mu}\, \gamma_{\beta}{}^{\nu}\, M^{\mu}{}_{;\nu} \quad . \tag{2.8a}$$

From the latter viewpoint, $\underset{\sim}{\nabla}\underset{\sim}{M}$ has spatial components

$$M^{j}{}_{|k} = M^{j}{}_{,k} + \Gamma^{j}{}_{\ell k}\, M^{\ell} \tag{2.8b}$$

where $\Gamma^{j}{}_{\ell k}$ are connection coefficients computed in the usual way from the spatial metric γ_{jk}. The divergence and curl are defined in terms of $\underset{\sim}{\nabla}$ by

$$\underset{\sim}{\nabla} \cdot \underset{\sim}{M} = M^{j}{}_{|j} \quad , \qquad (\underset{\sim}{\nabla} \times \underset{\sim}{M})^{j} = \varepsilon^{jk\ell}\, M_{\ell|k} \quad . \tag{2.9}$$

Note that because the geometry of $\mathcal{S}_t$ is not flat, spatial gradients of vectors do not commute:

$$M^{j}{}_{|k\ell} - M^{j}{}_{|\ell k} = R^{j}{}_{i\ell k}\, M^{i} \tag{2.10}$$

where $R^{j}{}_{i\ell k}$ is the Riemann tensor of $\mathcal{S}_t$; cf. Exercise 16.3 of MTW. Despite this noncommutation, the following identities are valid for any vector field $\underset{\sim}{M}$ and scalar field ψ

$$\underset{\sim}{\nabla} \cdot \underset{\sim}{\nabla} \times \underset{\sim}{M} = 0 \quad , \qquad \underset{\sim}{\nabla} \times \underset{\sim}{\nabla}\psi = 0 \quad . \tag{2.11}$$

2.4 TIME DERIVATIVES OF SPATIAL VECTORS

Three different time derivatives are useful in studying the evolution of spatial vectors and tensors.

When focussing attention on physical measurements made by a fiducial observer, one may prefer a time derivative defined by Fermi transport ("gyroscope transport") along the fiducial world lines:

$$D_\tau M^\beta \equiv \gamma^{\beta\mu} M_{\mu;\nu} U^\nu$$

$$= M^\beta{}_{;\mu} U^\mu - U^\beta a_\mu M^\mu \quad . \tag{2.12}$$

Here M^α and $D_\tau M^\alpha$ are the spacetime components of a spatial vector $\underset{\sim}{M}$ and its time derivative $D_\tau \underset{\sim}{M}$. This is the type of time derivative used in the congruence version of the 3+1 formalism (e.g., Estabrook and Wahlquist 1964).

In deriving integral identities (§2.5 below) we shall find it easiest to make geometric constructions involving the Lie derivative of $\underset{\sim}{M}$ along fiducial world lines

$$\mathfrak{L}_\tau M^\beta \equiv \alpha^{-1} \mathfrak{L}_{\alpha \boldsymbol{U}} M^\beta$$

$$= \alpha^{-1}[M^\beta{}_{;\mu} \alpha U^\mu - (\alpha U^\beta)_{;\mu} M^\mu] \quad . \tag{2.13}$$

Note that all of the 4-vectors $\alpha \boldsymbol{U}$ whose tails sit on the same hypersurface $\mathcal{S}_t$ have their tips on the same hypersurface $\mathcal{S}_{t+1\,\text{second}}$. This together with the pictorial interpretation of the Lie derivative (Box 9.2 of MTW) guarantees that, just as $\underset{\sim}{M}$ is a 4-vector lying in $\mathcal{S}_t$, so $\mathfrak{L}_\tau \underset{\sim}{M}$ is a 4-vector lying in $\mathcal{S}_t$ — i.e., it is a spatial vector. This type of time derivative is occasionally used in the numerical relativity 3+1 formalism (e.g., York 1979, where $\alpha \mathfrak{L}_\tau$ is denoted $\mathfrak{L}_N$).

One can also define a third kind of time derivative: the Lie derivative along a "shifting congruence" with tangent vector $\alpha U^\mu + \beta^\mu$. Here $\underset{\sim}{\beta}$, the "shift vector", is a spatial vector field lying in $\mathcal{S}_t$. As measured by fiducial observers [called "Eulerian observers" by numerical relativists], the shifting congruence [called "Lagrangian congruence" by numerical relativists] has ordinary velocity

$$\underset{\sim}{\beta}/\alpha = d(\underset{\sim\sim\sim\sim\sim\sim\sim\sim\sim\sim\sim\sim\sim\sim}{\text{proper distance}})/d\tau \quad . \tag{2.14}$$

The shift vector field $\underset{\sim}{\beta}$ could be specified arbitrarily, but when we consider the case of stationary, axially symmetric spacetimes, a natural choice of $\underset{\sim}{\beta}$ presents itself, namely the one for which $\alpha\mathbf{U}+\boldsymbol{\beta}$ is equal to the Killing vector $\mathbf{k}$ associated with the time isometry of the spacetime. The time derivative along the shifting congruence will be defined by

$$\begin{aligned} \mathcal{L}_t M^\mu &\equiv \mathcal{L}_{\alpha\mathbf{U}+\boldsymbol{\beta}} M^\mu \\ &= M^\mu{}_{;\nu}(\alpha U^\nu + \beta^\nu) - (\alpha U^\mu + \beta^\mu)_{;\nu} M^\nu \quad . \end{aligned} \tag{2.15}$$

Just as $\underset{\sim}{M}$ is a spatial vector, so $\mathcal{L}_t\underset{\sim}{M}$ is a spatial vector. The mixed Eulerian-Lagrangian equations of numerical relativity are formulated in terms of this shifting time derivative $\mathcal{L}_t$ (York 1979; Smarr and York 1978; Smarr, Taubes, and Wilson 1980).

Physically the Fermi time derivative $D_\tau\underset{\sim}{M}$ describes the rate of change of $\underset{\sim}{M}$ with respect to proper time τ along a fiducial world line—the change being measured relative to an inertial guidance system of physical rods and gyroscopes carried by the fiducial observer; see §13.6 of MTW and Figure 2 of this paper. The Lie time derivative $\mathcal{D}_\tau\underset{\sim}{M}$ also describes the rate of change of $\underset{\sim}{M}$ with respect to proper time τ along a fiducial world line—but now the change is measured relative to the (changing) spatial locations of other fiducial observers; see Schild (1967) and Figure 2 of this paper. The Lie time derivative $\mathcal{L}_t\underset{\sim}{M}$ describes the rate of change of $\underset{\sim}{M}$ with respect to global time t along a trajectory of the shifting congruence—the change being measured relative to the spatial locations of other trajectories in the shifting congruence; see Figure 2.

The derivatives D_τ, $\mathcal{D}_\tau$, and $\mathcal{L}_t$ can act on scalar fields and 3-tensor fields as well as on vector fields. The action of D_τ is always defined by parallel

transport $U^{\alpha}\,{}^{(4)}\nabla_{\alpha}$, followed by projection with $\gamma^{\mu}{}_{\nu}$ on all indices; $\mathfrak{D}_{\tau}$ and $\mathfrak{L}_{t}$ are always defined by $\mathfrak{D}_{\tau} \equiv \alpha^{-1}\mathfrak{L}_{\alpha \boldsymbol{v}}$ and $\mathfrak{L}_{t} \equiv \mathfrak{L}_{\alpha \boldsymbol{v}+\boldsymbol{\beta}}$ where $\mathfrak{L}$ is the Lie derivative which acts on scalars and tensors in the usual fashion (Schild 1967). When acting on a scalar field these three derivatives are related by

$$D_{\tau}\psi = \mathfrak{D}_{\tau}\psi = \alpha^{-1}(\mathfrak{L}_{t}\psi - \underset{\sim}{\beta} \cdot \underset{\sim}{\nabla}\psi) \quad . \tag{2.16a}$$

When acting on a vector field they are related by

$$\mathfrak{D}_{\tau}\underset{\sim}{M} = D_{\tau}\underset{\sim}{M} - \underset{\sim}{\sigma} \cdot \underset{\sim}{M} - \frac{1}{3}\,\theta\,\underset{\sim}{M} \quad , \tag{2.16b}$$

$$\mathfrak{L}_{t}\underset{\sim}{M} = \alpha\,\mathfrak{D}_{\tau}\underset{\sim}{M} + \mathfrak{L}_{\underset{\sim}{\beta}}\underset{\sim}{M} \tag{2.16c}$$

where $\mathfrak{L}_{\underset{\sim}{\beta}}\underset{\sim}{M}$ is the Lie derivative of the spatial vector $\underset{\sim}{M}$ along the spatial vector $\underset{\sim}{\beta}$

$$\mathfrak{L}_{\underset{\sim}{\beta}}\underset{\sim}{M} = (\underset{\sim}{\beta} \cdot \underset{\sim}{\nabla})\underset{\sim}{M} - (\underset{\sim}{M} \cdot \underset{\sim}{\nabla})\underset{\sim}{\beta} \quad . \tag{2.17}$$

The 3-metric $\underset{\sim}{\gamma}$ is unchanging as measured by the Fermi time derivative D_{τ}, but it changes as measured by the Lie derivatives

$$D_{\tau}\underset{\sim}{\gamma} = 0 \tag{2.18a}$$

$$\mathfrak{D}_{\tau}\gamma_{jk} = 2(\sigma_{jk} + \frac{1}{3}\,\theta\,\gamma_{jk}) \tag{2.18b}$$

$$\mathfrak{L}_{t}\gamma_{jk} = 2\alpha(\sigma_{jk} + \frac{1}{3}\,\theta\,\gamma_{jk}) + \beta_{j|k} + \beta_{k|j} \quad . \tag{2.18c}$$

Because of this, one must be careful about scalar products when using $\mathfrak{D}_{\tau}$ and $\mathfrak{L}_{t}$; for example,

$$\mathfrak{L}_{t}(\underset{\sim}{E} \cdot \underset{\sim}{B}) = \underset{\sim}{E} \cdot \mathfrak{L}_{t}\underset{\sim}{B} + \underset{\sim}{B} \cdot \mathfrak{L}_{t}\underset{\sim}{E} + \underset{\sim}{E} \cdot (\mathfrak{L}_{t}\underset{\sim}{\gamma}) \cdot \underset{\sim}{B} \quad . \tag{2.19}$$

[Relations (2.16) and (2.18) are derived from the 4-dimensional definitions (2.12), (2.13), (2.15) of D_{τ}, $\mathfrak{D}_{\tau}$, and $\mathfrak{L}_{t}$. In (2.18b,c) note that $\sigma_{jk} + \frac{1}{3}\,\theta\,\gamma_{jk} =$

$-K_{jk}$ (extrinsic curvature; equation 2.6).]

Time derivatives do not commute with spatial gradients. From definitions (2.12) and (2.8a) one can show that for any scalar field ψ and spatial vector field $\underset{\sim}{M}$

$$D_\tau \underset{\sim}{\nabla}\psi = \frac{1}{\alpha}\,\underset{\sim}{\nabla}(\alpha D_\tau \psi) - \frac{1}{3}\,\theta\,\underset{\sim}{\nabla}\psi - \underset{\sim}{\sigma}\cdot\underset{\sim}{\nabla}\psi \quad , \tag{2.20a}$$

$$D_\tau(M_{j|k}) = \frac{1}{\alpha}\,(\alpha D_\tau M_j)_{|k} - \frac{1}{3}\,\theta\,M_{j|k} - \sigma_k{}^i\,M_{j|i} + \mathcal{R}^i{}_{jk}\,M_i$$
$$+ (\underset{\sim}{a}\cdot\underset{\sim}{M})(\sigma_{jk} + \frac{1}{3}\,\theta\,\gamma_{jk}) - M_i a_j(\sigma_k{}^i + \frac{1}{3}\,\theta\,\gamma_k{}^i) \quad . \tag{2.20b}$$

Here $\mathcal{R}^i{}_{jk}$ is a spatial tensor related to the Riemann curvature of 4-dimensional spacetime by

$$\mathcal{R}^\alpha{}_{\beta\gamma} = \gamma^\alpha{}_\mu\,\gamma_\beta{}^\nu\,\gamma_\gamma{}^\sigma\,{}^{(4)}R^\mu{}_{\nu\sigma\rho}\,U^\rho \quad . \tag{2.21a}$$

Using the Gauss-Codazzi equations along with (2.6), one can rewrite $\mathcal{R}^i{}_{jk}$ in terms of the kinematic quantities of the fiducial congruence:

$$\mathcal{R}_{ijk} = \sigma_{jk|i} - \sigma_{ik|j} + \frac{1}{3}\,(\gamma_{jk}\,\theta_{,i} - \gamma_{ik}\,\theta_{,j}) \quad . \tag{2.21b}$$

2.5 THREE-DIMENSIONAL INTEGRAL THEOREMS

In passing from the differential formulation of Maxwell's equations to the integral formulation, we shall use various integral identities. If $\mathcal{V}$ is a region of 3-dimensional space lying in $\mathcal{S}_t$ and $\partial\mathcal{V}$ is its closed 2-dimensional boundary, then Gauss's theorem says that for any vector field $\underset{\sim}{M}$

$$\int_{\mathcal{V}} \underset{\sim}{\nabla}\cdot\underset{\sim}{M}\,dV = \int_{\partial\mathcal{V}} \underset{\sim}{M}\cdot d\underset{\sim}{\Sigma} \quad . \tag{2.22}$$

Here dV is an element of spatial proper volume in $\mathcal{V}$, and $d\underset{\sim}{\Sigma}$ is an element of area in $\partial\mathcal{V}$ ($d\underset{\sim}{\Sigma}$ points orthogonally out of $\mathcal{V}$, and $|d\underset{\sim}{\Sigma}| = (\gamma^{jk}\,d\Sigma_j\,d\Sigma_k)^{1/2}$ is proper

area). If $\mathcal{A}$ is a 2-dimensional region lying in the 3-space $\mathcal{S}_t$ and $\partial\mathcal{A}$ is its closed 1-dimensional boundary, then Stokes's theorem says that for any vector field $\underset{\sim}{M}$

$$\int_{\mathcal{A}} (\underset{\sim}{\nabla} \times \underset{\sim}{M}) \cdot d\underset{\sim}{\Sigma} = \int_{\partial\mathcal{A}} \underset{\sim}{M} \cdot d\underset{\sim}{\ell} \quad . \tag{2.23}$$

Here $d\underset{\sim}{\Sigma}$ is an element of proper area in $\mathcal{A}$, $d\underset{\sim}{\ell}$ is an element of proper length along $\partial\mathcal{A}$, and the directions of $d\underset{\sim}{\ell}$ and $d\underset{\sim}{\Sigma}$ must be chosen in accord with the standard right-hand rule.

Gauss's theorem and Stokes's theorem involve spatial vector analysis in a single hypersurface $\mathcal{S}_t$, chosen once-and-for-all. We shall also need identities which relate integrals on one hypersurface $\mathcal{S}_t$ to integrals on an adjacent hypersurface $\mathcal{S}_{t+\Delta t}$. In these identities we must pay attention to the motion, relative to fiducial observers, of the regions of integration. For this purpose we give each point on a region of integration a label, and we define by

$$\underset{\sim}{v} = d(\underset{\sim\sim\sim\sim\sim\sim\sim\sim\sim\sim\sim\sim\sim\sim\sim\sim\sim\sim\sim}{\text{proper spatial distance}})/d\tau \tag{2.24}$$

the velocity of that labeled point as measured by a fiducial observer who sits beside it; see Figure 3.

Let ϕ be a smoothly varying scalar field in spacetime; let $\mathcal{V}(t)$ be a spatial volume in $\mathcal{S}_t$ which changes in some arbitrary but smooth manner as time passes; and let $\partial\mathcal{V}(t)$ be the 2-dimensional closed boundary of $\mathcal{V}(t)$ in $\mathcal{S}_t$. Then between global time t and time t+Δt the integral of ϕ over $\mathcal{V}$ changes by

$$\Delta \int_{\mathcal{V}} \phi \, dV = \int_{\mathcal{V}} (D_\tau \phi)\alpha\Delta t \, dV + \int_{\mathcal{V}} \phi(\theta\alpha\Delta t) \, dV + \int_{\partial\mathcal{V}} \phi(\underset{\sim}{v}\alpha\Delta t) \cdot d\underset{\sim}{\Sigma} \quad .$$

The first term accounts for the change $(D_\tau\phi)\Delta\tau = (D_\tau\phi)\alpha\Delta t$ in ϕ. The second

term accounts for the change $\Delta dV = (\theta dV)\Delta\tau$ in a physical volume element dV which is attached to fiducial observers. The third term accounts for the opening up of new volume (or closing off of old volume) at the moving boundary of $\mathcal{V}$, $\Delta dV = (\underset{\sim}{v}\Delta\tau) \cdot d\underset{\sim}{\Sigma}$. Dividing this equation by Δt and taking the limit $\Delta t \to 0$ we obtain the integral identity

$$\frac{d}{dt} \int_{\mathcal{V}(t)} \phi \, dV = \int_{\mathcal{V}(t)} \alpha(D_\tau \phi + \theta\phi) dV + \int_{\partial\mathcal{V}(t)} \alpha\phi \underset{\sim}{v} \cdot d\underset{\sim}{\Sigma} \quad . \tag{2.25}$$

Let $\underset{\sim}{M}$ be a smoothly varying vector field in spacetime; let $\mathcal{A}(t)$ be a 2-dimensional surface in $\mathcal{S}_t$ which changes in some arbitrary but smooth manner as time passes; and let $\partial\mathcal{A}(t)$ be the 1-dimensional closed boundary of $\mathcal{A}(t)$ with line element $d\underset{\sim}{\ell}$ related to the area element $d\underset{\sim}{\Sigma}$ of $\mathcal{A}$ by the right-hand rule. Then between global time t and t+Δt the integral of $\underset{\sim}{M}$ over $\mathcal{A}(t)$ changes by

$$\Delta \int_{\mathcal{A}(t)} \underset{\sim}{M} \cdot d\underset{\sim}{\Sigma} = \int_{\mathcal{A}(t)} (\alpha\Delta t)(\pounds_\tau \underset{\sim}{M}) \cdot d\underset{\sim}{\Sigma} + \int_{\mathcal{A}(t)} (\theta\alpha\Delta t)\underset{\sim}{M} \cdot d\underset{\sim}{\Sigma}$$

$$+ \int_{\mathcal{A}(t)} (\underset{\sim}{\nabla} \cdot \underset{\sim}{M})(\underset{\sim}{v}\alpha\Delta t) \cdot d\underset{\sim}{\Sigma} + \int_{\partial\mathcal{A}(t)} \underset{\sim}{M} \cdot (\underset{\sim}{v}\alpha\Delta t) \times d\underset{\sim}{\ell} \quad .$$

The first term accounts for changes $\Delta\underset{\sim}{M} = (\pounds_\tau \underset{\sim}{M})\Delta\tau$ of $\underset{\sim}{M}$ relative to Lie transport by fiducial observers; cf. Figure 2. If $\underset{\sim}{M}$ and $\mathcal{A}$ were both attached to (i.e., Lie transported by) fiducial observers, then $\underset{\sim}{M} \cdot d\underset{\sim}{\Sigma}$ would be a 3-volume attached to them, and $\theta\underset{\sim}{M} \cdot d\underset{\sim}{\Sigma}$ would be the time rate of change of this 3-volume due to the fiducial expansion θ; the second term accounts for this change. The third term accounts for the displacement $\underset{\sim}{v}\Delta\tau$ of points on the interior of $\mathcal{A}$ relative to fiducial observers — the integral of $\underset{\sim}{\nabla} \cdot \underset{\sim}{M}$ over $(\underset{\sim}{v}\Delta\tau) \cdot d\underset{\sim}{\Sigma}$ = (volume through which $\mathcal{A}$ was displaced) can be converted by Gauss's theorem (2.22) to the difference in surface integrals between the displaced $\mathcal{A}$ and the

fiducially transported $\mathcal{A}$. The fourth term accounts for the displacement $\underset{\sim}{v}\Delta\tau$ of the boundary of $\mathcal{A}$ relative to fiducial observers, which opens up a new area element $(\underset{\sim}{v}\Delta\tau)\times d\underset{\sim}{\ell}$. Dividing the above equation by Δt, taking the limit $\Delta t \to 0$, expressing the Lie derivative in terms of the Fermi time derivative by (2.16b), and using the vector identity $\underset{\sim}{A}\cdot\underset{\sim}{B}\times\underset{\sim}{C} = \underset{\sim}{A}\times\underset{\sim}{B}\cdot\underset{\sim}{C}$, we obtain the integral identity

$$\frac{d}{dt}\int_{\mathcal{A}(t)} \underset{\sim}{M}\cdot d\underset{\sim}{\Sigma} = \int_{\mathcal{A}(t)} \alpha[D_{\tau}\underset{\sim}{M} + \tfrac{2}{3}\theta\,\underset{\sim}{M} - \underset{\sim}{\sigma}\cdot\underset{\sim}{M} + (\underset{\sim}{\nabla}\cdot\underset{\sim}{M})\underset{\sim}{v}]\cdot d\underset{\sim}{\Sigma}$$

$$+ \int_{\partial\mathcal{A}(t)} \alpha\,\underset{\sim}{M}\times\underset{\sim}{v}\cdot d\underset{\sim}{\ell} \qquad . \tag{2.26}$$

Let M be a smoothly varying vector field in spacetime; and let $\mathcal{C}(t)$ be a closed curve in $\mathcal{S}_t$ which changes in some arbitrary but smooth manner as time passes. Then between time t and t+Δt the integral of $\underset{\sim}{M}$ over $\mathcal{C}(t)$ changes by

$$\Delta\int_{\mathcal{C}(t)} \underset{\sim}{M}\cdot d\underset{\sim}{\ell} = \int_{\mathcal{C}(t)} (\alpha\Delta t)(\pounds_{\tau}\underset{\sim}{M})\cdot d\underset{\sim}{\ell}$$

$$+ \int_{\mathcal{C}(t)} 2\alpha\Delta t\ \underset{\sim}{M}\cdot(\tfrac{1}{3}\theta\,\underset{\sim}{\gamma} + \underset{\sim}{\sigma})\cdot d\underset{\sim}{\ell} + \int_{\mathcal{C}(t)} (\underset{\sim}{\nabla}\times\underset{\sim}{M})\cdot(\alpha\Delta t\ \underset{\sim}{v}\times d\underset{\sim}{\ell}) \ .$$

The first term accounts for changes of $\underset{\sim}{M}$ relative to Lie transport by fiducial observers;cf. Figure 2. If $\underset{\sim}{M}$ and $d\underset{\sim}{\ell}$ were both Lie transported by fiducial observers, then in time $\Delta\tau$ $\underset{\sim}{M}\cdot d\underset{\sim}{\ell}$ would change by $\Delta(\underset{\sim}{M}\cdot d\underset{\sim}{\ell}) = \underset{\sim}{M}\cdot(\Delta\tau\ \pounds_{\tau}\underset{\sim}{\gamma})\cdot d\underset{\sim}{\ell} = 2\alpha\Delta t\ \underset{\sim}{M}\cdot(\underset{\sim}{\sigma}+\tfrac{1}{3}\theta\,\underset{\sim}{\gamma})\cdot d\underset{\sim}{\ell}$ (Eq. 2.18b); the second term accounts for this. The third term accounts for the displacement of $\mathcal{C}(t)$ relative to fiducial observers, i.e., for the failure of $d\underset{\sim}{\ell}$ to be Lie transported; the integral of $\underset{\sim}{\nabla}\times\underset{\sim}{M}$ over the area $(\underset{\sim}{v}\Delta\tau)\times d\underset{\sim}{\ell}$ can be transformed by Stokes's theorem (2.23) into the integral of $\underset{\sim}{M}$ along the displaced $\mathcal{C}(t)$ minus

the integral along the fiducially transported $\mathcal{C}(t)$. Dividing the above equation by Δt, taking the limit $\Delta t \to 0$, expressing the Lie derivative in terms of the Fermi time derivative by (2.16b), and using $\underset{\sim}{A} \cdot \underset{\sim}{B} \times \underset{\sim}{C} = \underset{\sim}{A} \times \underset{\sim}{B} \cdot \underset{\sim}{C}$, we obtain the integral identity

$$\frac{d}{dt} \int_{\mathcal{C}(t)} \underset{\sim}{M} \cdot d\underset{\sim}{\ell} = \int_{\mathcal{C}(t)} \alpha[D_{\tau} \underset{\sim}{M} + \frac{1}{3}\theta \underset{\sim}{M} + \underset{\sim}{\sigma} \cdot \underset{\sim}{M} + (\underset{\sim}{\nabla} \times \underset{\sim}{M}) \times \underset{\sim}{v}] \cdot d\underset{\sim}{\ell} \quad . \tag{2.27}$$

3 3+1 Electrodynamics in Differential Form

3.1 ELECTROMAGNETIC QUANTITIES

The 3+1 formulation of electrodynamics involves the following quantities, which are measured by the fiducial observers in the usual manner of flat spacetime, and which therefore have the usual physical interpretation:

$$\begin{aligned}
\rho_e &= \text{charge density} && (\text{esu/cm}^3) \\
\underset{\sim}{j} &= \text{current density} && (\text{esu/cm}^3) \\
\underset{\sim}{E} &= \text{electric field} && (\text{statvolts/cm}) \\
\underset{\sim}{B} &= \text{magnetic field} && (\text{gauss}) \\
\phi &= \text{scalar potential} && (\text{statvolts}) \\
\underset{\sim}{A} &= \text{vector potential} && (\text{gauss cm, or statvolts}) \quad .
\end{aligned} \tag{3.1}$$

One can reconstruct the charge-current 4-vector J^{α}, the electromagnetic field tensor $F^{\alpha\beta}$, and the 4-vector potential $\mathcal{U}^{\alpha}$ from these 3+1 quantities, the fiducial 4-velocity U^{α}, and the 4-dimensional Levi-Civita tensor $\varepsilon_{\alpha\beta\gamma\delta}$ by regarding $\underset{\sim}{j}$, $\underset{\sim}{E}$, $\underset{\sim}{B}$, and $\underset{\sim}{A}$ as 4-vectors orthogonal to U^{α} and then computing

$$\begin{aligned}
J^{\alpha} &= \rho_e U^{\alpha} + j^{\alpha} \quad , \\
F^{\alpha\beta} &= U^{\alpha}E^{\beta} - E^{\alpha}U^{\beta} + \varepsilon^{\alpha\beta\gamma\delta} U_{\gamma} B_{\delta} \quad , \\
\mathcal{U}^{\alpha} &= \phi U^{\alpha} + A^{\alpha} \quad .
\end{aligned} \tag{3.2}$$

One can invert these relations to get

$$\rho_e = -J^\alpha U_\alpha \quad , \qquad j^\alpha = \gamma^{\alpha\beta} J_\beta \quad ,$$
$$E^\alpha = F^{\alpha\beta} U_\beta \quad , \qquad B^\alpha = -\frac{1}{2} \varepsilon^{\alpha\beta\gamma\delta} U_\beta F_{\gamma\delta} \quad , \tag{3.3}$$
$$\phi = -\mathfrak{A}^\alpha U_\alpha \quad , \qquad A^\alpha = \gamma^{\alpha\beta} \mathfrak{A}_\beta \quad .$$

3.2 MAXWELL'S EQUATIONS

Ellis (1973) has derived Maxwell's equations in the 3+1 congruence formalism from their 4-dimensional formulations $F^{\alpha\beta}{}_{;\beta} = 4\pi J^\alpha$ and $F_{[\alpha\beta;\gamma]} = 0$. We can take his 3+1 equations over into our hypersurface formalism by simply setting the fiducial rotation $\underset{\sim}{\omega}$ to zero. The result is

$$\underset{\sim}{\nabla} \cdot \underset{\sim}{E} = 4\pi\rho_e \quad , \tag{3.4a}$$

$$\underset{\sim}{\nabla} \cdot \underset{\sim}{B} = 0 \quad , \tag{3.4b}$$

$$D_\tau \underset{\sim}{E} + \frac{2}{3}\theta \underset{\sim}{E} - \underset{\sim}{\sigma} \cdot \underset{\sim}{E} = \alpha^{-1} \underset{\sim}{\nabla} \times (\alpha \underset{\sim}{B}) - 4\pi \underset{\sim}{j} \quad , \tag{3.4c}$$

$$D_\tau \underset{\sim}{B} + \frac{2}{3}\theta \underset{\sim}{B} - \underset{\sim}{\sigma} \cdot \underset{\sim}{B} = -\alpha^{-1} \underset{\sim}{\nabla} \times (\alpha \underset{\sim}{E}) \quad . \tag{3.4d}$$

Equations (3.4a,b) have the form familiar from flat-spacetime, Lorentz-frame electrodynamics. They permit one (following Hanni and Ruffini 1973; Christodoulou and Ruffini 1973; and King et al. 1975) to characterize $\underset{\sim}{E}$ and $\underset{\sim}{B}$ by electric and magnetic field lines which lie in the hypersurfaces $\mathcal{S}_t$. The magnetic field lines never end ($\underset{\sim}{\nabla} \cdot \underset{\sim}{B} = 0$); the electric field lines terminate on electric charge ($\underset{\sim}{\nabla} \cdot \underset{\sim}{E} = 4\pi\rho_e$).

Equations (3.4c,d) have a slightly different form from the corresponding flat-spacetime, Lorentz-frame equations. The differences are due to the peculiar motion of the fiducial observers (expansion θ, shear $\underset{\sim}{\sigma}$, and acceleration $\underset{\sim}{a} = \underset{\sim}{\nabla} \ln\alpha$).

Consider first equation (3.4d). If the fiducial observers were to carry a perfectly conducting medium with them, then they would never see an electric

field, and equation (3.4d) would become $D_\tau \underset{\sim}{B} + \frac{2}{3}\theta \underset{\sim}{B} - \underset{\sim}{\sigma} \cdot \underset{\sim}{B} = 0$. This is precisely the equation for the evolution of a magnetic field that is "frozen into" the conducting medium (cf. Cowling 1957 or Lichnerowicz 1967). The expansion θ of the fiducial observers moves the field lines apart with a "Hubble-type expansion rate" $\dot{\ell}/\ell = \frac{1}{3}\theta$, thereby reducing the field strength (conservation of flux), $D_\tau \underset{\sim}{B} = -\frac{2}{3}\theta \underset{\sim}{B}$. The shear $\underset{\sim}{\sigma}$ rotates the frozen-in field lines relative to parallel transport (relative to directions defined by gyroscopes), $D_\tau \underset{\sim}{B} = \underset{\sim}{\sigma} \cdot \underset{\sim}{B}$; this shearing also changes the distance between field lines and thereby changes the field strength, $D_\tau |\underset{\sim}{B}| = \sigma_{jk} B_j B_k / |\underset{\sim}{B}|$.

If the fiducial observers do not carry a perfectly conducting medium, then they can see an electric field whose curl produces a time-changing magnetic field $D_\tau \underset{\sim}{B} = -\alpha^{-1} \underset{\sim}{\nabla} \times (\alpha \underset{\sim}{E}) = -\underset{\sim}{\nabla} \times \underset{\sim}{E} - \underset{\sim}{a} \times \underset{\sim}{E}$ (right side of equation 3.4d). The lapse function α gives rise to the unfamiliar term $D_\tau \underset{\sim}{B} = -\underset{\sim}{a} \times \underset{\sim}{E}$, which has the following physical interpretation: Because the fiducial observers accelerate, they acquire in time $\Delta\tau$ a velocity $\underset{\sim}{v} = \underset{\sim}{a}\Delta\tau$ relative to their initial inertial frame. This motion, together with the electric field $\underset{\sim}{E}$ in the initial inertial frame, causes the fiducial observers to see a changed magnetic field, $\Delta \underset{\sim}{B} = -\underset{\sim}{v} \times \underset{\sim}{E} = -(\underset{\sim}{a} \times \underset{\sim}{E})\Delta\tau$.

The unfamiliar terms in equation (3.4c) have the same origin as those in equation (3.4d).

3.3 $\underset{\sim}{E}$ AND $\underset{\sim}{B}$ IN TERMS OF POTENTIALS

From the 4-vector relationship $F_{\alpha\beta} = \mathfrak{A}_{\beta;\alpha} - \mathfrak{A}_{\alpha;\beta}$ and from equations (3.2) and (3.3) one can derive the following expressions for $\underset{\sim}{E}$ and $\underset{\sim}{B}$ in terms of the scalar and vector potentials:

$$\underset{\sim}{E} = -\alpha^{-1} \underset{\sim}{\nabla}(\alpha\phi) - (D_\tau \underset{\sim}{A} + \frac{1}{3}\theta \underset{\sim}{A} + \underset{\sim}{\sigma} \cdot \underset{\sim}{A}) \quad , \tag{3.5a}$$

$$\underset{\sim}{B} = \underset{\sim}{\nabla} \times \underset{\sim}{A} \quad . \tag{3.5b}$$

When $\underset{\sim}{E}$ and $\underset{\sim}{B}$ are expressed in this manner, the two Maxwell equations (3.4b) and (3.4d) are automatically satisfied. [To verify (3.4b) is trivial; to verify (3.4d) is a somewhat lengthy calculation, making use of the identities (2.11), (2.20b), and (2.21b).]

3.4 CHARGE CONSERVATION

The 3+1 equation of charge conservation

$$D_\tau \rho_e + \rho_e \theta + \alpha^{-1} \underset{\sim}{\nabla} \cdot (\alpha \underset{\sim}{j}) = 0 \tag{3.6}$$

can be derived by a nontrivial calculation from the Maxwell equations (3.4a,c). The $\rho_e \theta$ term is the rate of decrease of ρ_e due to expansion of the fiducial congruence (volume element carried by observers gets bigger, so charge density decreases). The lapse function α gives rise to an unfamiliar term $(\alpha^{-1} \underset{\sim}{\nabla} \alpha) \cdot \underset{\sim}{j} = \underset{\sim}{a} \cdot \underset{\sim}{j}$, which is the rate at which current density $\underset{\sim}{j}$ gets Lorentz transformed into charge density ρ_e by the changing velocity of the fiducial observer.

3.5 EQUATION OF MOTION OF A CHARGED PARTICLE

Consider a particle with rest mass μ and charge q. Denote by $\underset{\sim}{v}$ its ordinary velocity, as measured in the local rest frame of the fiducial observer whom the particle is passing. Then $\underset{\sim}{v}$ and the particle's 3-momentum

$$\underset{\sim}{p} \equiv \mu \Gamma \underset{\sim}{v} \qquad , \qquad \Gamma \equiv (1 - \underset{\sim}{v}^2)^{-1/2} \tag{3.7}$$

are 3-vectors lying in $\mathcal{S}_t$. The 4-dimensional equation of motion for a charged particle, when rewritten in 3+1 form, says

$$(D_\tau + \underset{\sim}{v} \cdot \underset{\sim}{\nabla}) \underset{\sim}{p} = -(\mu \Gamma \underset{\sim}{a} + \underset{\sim}{\sigma} \cdot \underset{\sim}{p} + \tfrac{1}{3} \theta \underset{\sim}{p}) + q(\underset{\sim}{E} + \underset{\sim}{v} \times \underset{\sim}{B}) \quad . \tag{3.8}$$

Here $(D_\tau + \underset{\sim}{v} \cdot \underset{\sim}{\nabla}) \underset{\sim}{p}$ is the "convective derivative" of $\underset{\sim}{p}$ along the particle's world

line — it is the rate of change of $\underset{\sim}{p}$ with respect to (i) Fermi transport from the particle's initial position in $\mathcal{S}_t$, along the observer's world line to $\mathcal{S}_{t+\Delta\tau/\alpha}$ [the D_τ part of (3.8)], followed by (ii) spatial parallel transport, in $\mathcal{S}_{t+\Delta\tau/\alpha}$, along $\underset{\sim}{v}\Delta\tau$ to the particle's new position.

The term $-(\mu\Gamma\underset{\sim}{a} + \underset{\sim}{\sigma}\cdot\underset{\sim}{p} + \frac{1}{3}\theta\,\underset{\sim}{p})$ on the right-hand side of equation (3.8) is an "inertial force" to compensate for the fact that the fiducial observers at the old and new positions of the particle have a relative velocity $\Delta\underset{\sim}{v} = (\underset{\sim}{a} + \underset{\sim}{\sigma}\cdot\underset{\sim}{v} + \frac{1}{3}\theta\,\underset{\sim}{v})\,\Delta\tau$ as seen by inertial observers. The term $q(\underset{\sim}{E} + \underset{\sim}{v}\times\underset{\sim}{B})$ is the usual Lorentz force in 3+1 notation.

3.6 CONSERVATION OF ENERGY AND MOMENTUM FOR ELECTROMAGNETIC FIELD AND A CONTINUOUS MEDIUM

Let $T^{\alpha\beta}$ be the stress-energy tensor of the electromagnetic field and/or of a continuous medium with which it interacts. Denote by ε the mass-energy density, by $\underset{\sim}{S}$ the energy flux, and by $\underset{\sim}{W}$ the stress tensor — all as measured in the fiducial reference frame:

$$\varepsilon = T^{\mu\nu}\,U_\mu U_\nu \quad , \qquad S^\alpha = -\gamma^\alpha{}_\mu\, T^{\mu\nu}\,U_\nu \quad , \qquad W^{\alpha\beta} = \gamma^\alpha{}_\mu\, T^{\mu\nu}\,\gamma^\beta{}_\nu \ . \tag{3.9}$$

For the electromagnetic field

$$\begin{aligned} &\varepsilon = \frac{1}{8\pi}\,(\underset{\sim}{E}^2 + \underset{\sim}{B}^2) \quad , \qquad \underset{\sim}{S} = \frac{1}{4\pi}\,\underset{\sim}{E}\times\underset{\sim}{B} \ , \\ &\underset{\sim}{W} = \frac{1}{4\pi}\left[-(\underset{\sim}{E}\otimes\underset{\sim}{E} + \underset{\sim}{B}\otimes\underset{\sim}{B}) + \frac{1}{2}\,(\underset{\sim}{E}^2 + \underset{\sim}{B}^2)\underset{\sim}{\gamma}\right] \ . \end{aligned} \tag{3.10}$$

For a perfect fluid with rest-frame density of mass-energy ρ and pressure p and with velocity $\underset{\sim}{v}$ as measured by fiducial observers

$$\begin{aligned} &\varepsilon = \Gamma^2(\rho + p\underset{\sim}{v}^2) \quad , \qquad \underset{\sim}{S} = (\rho + p)\Gamma^2\underset{\sim}{v} \quad , \\ &\underset{\sim}{W} = (\rho + p)\Gamma^2\underset{\sim}{v}\otimes\underset{\sim}{v} + p\underset{\sim}{\gamma} \ , \qquad \Gamma \equiv (1 - \underset{\sim}{v}^2)^{-1/2} \ . \end{aligned} \tag{3.11}$$

The 3+1 split of the law of energy-momentum conservation $T^{\alpha\beta}{}_{;\beta} = 0$ has been worked out and applied in a variety of contexts by workers in numerical relativity; see, e.g., York (1979); Smarr, Taubes, and Wilson (1980); Wilson (1977). We record here in our notation York's (1979) general form of the law of energy conservation $U_\mu T^{\mu\nu}{}_{;\nu} = 0$:

$$D_\tau \varepsilon + \theta\varepsilon + \alpha^{-2}\underset{\sim}{\nabla}\cdot(\alpha^2\underset{\sim}{S}) + W^{jk}(\sigma_{jk} + \tfrac{1}{3}\theta\,\gamma_{jk}) = 0 \quad , \tag{3.12}$$

and his general form of the law of momentum conservation (force balance) $\gamma^\alpha{}_\mu\, T^{\mu\nu}{}_{;\nu} = 0$:

$$D_\tau \underset{\sim}{S} + \tfrac{4}{3}\theta\underset{\sim}{S} + \underset{\sim}{\sigma}\cdot\underset{\sim}{S} + \varepsilon\underset{\sim}{a} + \alpha^{-1}\underset{\sim}{\nabla}\cdot(\alpha\underset{\sim}{W}) = 0 \quad , \tag{3.13}$$

cf., York's equations (40) and (41). Here ε, $\underset{\sim}{S}$, and $\underset{\sim}{W}$ contain all forms of energy, momentum, and stress.

The analogous equations describing the energy and momentum transfer from matter to electromagnetic fields, $U_\mu\, T^{\mu\nu}_{EM\,;\nu} = -U_\mu\, F^{\mu\nu}\, J_\nu$ and $\gamma^\alpha{}_\mu\, T^{\mu\nu}_{EM\,;\nu} = -\gamma^\alpha{}_\mu\, F^{\mu\nu}\, J_\nu$, have the 3+1 form

$$D_\tau \varepsilon + \theta\varepsilon + \alpha^{-2}\underset{\sim}{\nabla}\cdot(\alpha^2\underset{\sim}{S}) + W^{jk}(\sigma_{jk} + \tfrac{1}{3}\theta\,\gamma_{jk}) = -\underset{\sim}{j}\cdot\underset{\sim}{E} \quad , \tag{3.14}$$

$$D_\tau \underset{\sim}{S} + \tfrac{4}{3}\theta\underset{\sim}{S} + \underset{\sim}{\sigma}\cdot\underset{\sim}{S} + \varepsilon\underset{\sim}{a} + \alpha^{-1}\underset{\sim}{\nabla}\cdot(\alpha\underset{\sim}{W}) = -(\rho_e\underset{\sim}{E} + \underset{\sim}{j}\times\underset{\sim}{B}) \quad . \tag{3.15}$$

Here ε, $\underset{\sim}{S}$, and $\underset{\sim}{W}$ are the electromagnetic energy density, momentum density and stress (equations 3.10).

4 3+1 Electrodynamics in Integral Form

As in flat spacetime, so also in curved spacetime, one can use integral identities to rewrite in integral form the differential Maxwell equations (3.4) and the law of charge conservation (3.6).

Gauss's law for electric flux follows from $\underset{\sim}{\nabla}\cdot\underset{\sim}{E} = 4\pi\rho_e$ and Gauss's integral identity (2.22). It says that the total electric flux through a closed

2-surface $\partial\mathcal{V}$ lying in a fiducial hypersurface $\mathcal{S}$ is equal to 4π times the total charge enclosed

$$\int_{\partial\mathcal{V}} \underset{\sim}{E} \cdot d\underset{\sim}{\Sigma} = 4\pi \int_{\mathcal{V}} \rho_e \, dV \quad . \tag{4.1}$$

Similarly, Gauss's law for magnetic flux, which is equivalent to $\underset{\sim}{\nabla} \cdot \underset{\sim}{B} = 0$, says that the total flux through any closed 2-surface in $\mathcal{S}$ must vanish,

$$\int_{\partial\mathcal{V}} \underset{\sim}{B} \cdot d\underset{\sim}{\Sigma} = 0 \quad . \tag{4.2}$$

Faraday's law of magnetic induction can be derived by applying the integral identity (2.26) to the Maxwell equation (3.4d), and by then replacing $\underset{\sim}{\nabla} \cdot \underset{\sim}{B}$ by zero and using Stokes's law (2.23) to rewrite the surface integral of $\underset{\sim}{\nabla} \times (\alpha \underset{\sim}{E})$. The result is

$$\int_{\partial\mathcal{A}(t)} \alpha(\underset{\sim}{E} + \underset{\sim}{v} \times \underset{\sim}{B}) \cdot d\underset{\sim}{\ell} = -\frac{d}{dt} \int_{\mathcal{A}(t)} \underset{\sim}{B} \cdot d\underset{\sim}{\Sigma} \quad . \tag{4.3}$$

Here $\mathcal{A}(t)$ is a 2-surface lying in $\mathcal{S}_t$; $\partial\mathcal{A}(t)$ is the closed boundary curve of $\mathcal{A}(t)$, and $\underset{\sim}{v}$ is the velocity of a point on the boundary curve as measured by the fiducial observer whom it is passing. As in flat spacetime, so also here, Faraday's law says that the time changing magnetic flux through a curve $\partial\mathcal{A}$ generates on EMF around the curve. The derivative of the flux in this case is with respect to global time t (the only universally defined time parameter, and therefore the only kind of time with respect to which one can differentiate outside the flux integral). The EMF is the integral around the curve $\partial\mathcal{A}$ of the electromagnetic force $\underset{\sim}{E} + \underset{\sim}{v} \times \underset{\sim}{B}$ acting on a unit charge which moves with the curve, multiplied by $\alpha = d\tau/dt$ to convert the force into a "rate of change of momentum $\underset{\sim}{p}$ with respect to global time t" instead of "with respect to fiducial proper time τ".

Ampere's law can be derived by applying the integral identity (2.26) to the Maxwell equation (3.4c), and by then replacing $\underset{\sim}{\nabla} \cdot \underset{\sim}{E}$ with $4\pi\rho_e$ and using Stokes's

law (2.23) to rewrite the surface integral of $\nabla \times (\alpha \underset{\sim}{B})$. The result is

$$\int_{\partial \mathcal{A}(t)} \alpha(\underset{\sim}{B} - \underset{\sim}{v} \times \underset{\sim}{E}) \cdot d\underset{\sim}{\ell} = \frac{d}{dt} \int_{\mathcal{A}(t)} \underset{\sim}{E} \cdot d\underset{\sim}{\Sigma} + 4\pi \int_{\mathcal{A}(t)} \alpha(\underset{\sim}{j} - \rho_e \underset{\sim}{v}) \cdot d\underset{\sim}{\Sigma} \quad . \tag{4.4}$$

The left side and the first term on the right are identical to Faraday's law (4.3) plus a "duality transformation" $\underset{\sim}{E} \to \underset{\sim}{B}$, $\underset{\sim}{B} \to -\underset{\sim}{E}$. The last term is 4π times the rate per unit global time that charge crosses the moving area $\mathcal{A}(t)$. [Note: $\underset{\sim}{v}$ is the velocity of a point on $\mathcal{A}(t)$ as measured by fiducial observers.]

The integral law of charge conservation can be derived by integrating the differential conservation law (3.6) over $\mathcal{V}(t)$ and by then using the integral identities (2.25) and (2.22). The result is

$$\frac{d}{dt} \int_{\mathcal{V}(t)} \rho_e dV = - \int_{\partial \mathcal{V}(t)} \alpha(\underset{\sim}{j} - \rho_e \underset{\sim}{v}) \cdot d\underset{\sim}{\Sigma} \quad . \tag{4.5}$$

Here $\mathcal{V}(t)$ is a 3-volume lying in $\mathcal{S}_t$; $\partial \mathcal{V}(t)$ is the closed 2-surface boundary of $\mathcal{V}(t)$, and $\underset{\sim}{v}$ is the velocity of a point on the boundary 2-surface as measured by the fiducial observer whom it is passing. The left side of this conservation law is the rate of increase, per unit global time t, of the charge in $\mathcal{V}(t)$. The right side is the rate, per unit global time t, at which charge flows in through the moving boundary of $\mathcal{V}(t)$.

5 3+1 Electrodynamics Outside a Stationary Black Hole

5.1 THE ZAMO REFERENCE FRAMES AND THE CHOICE OF GLOBAL TIME

We now specialize to the spacetime region $\mathcal{E}$ outside a stationary, axisymmetric black hole: $\mathcal{E}$ extends from the hole's absolute event horizon $\mathcal{H}$ out to spatial and null infinity. We require that the spacetime geometry of $\mathcal{E}$ be stationary and axisymmetric. It will be the Kerr geometry if the hole's gravity is far stronger than the gravity due to external matter. Otherwise, the

external matter will deform the geometry away from that of Kerr.

The theory of stationary, axisymmetric black holes is reviewed by Carter (1979). We adopt his notation $\mathbf{k}$ and $\mathbf{m}$ for the mutually commuting Killing vector fields which generate invariant "time translations" and invariant "rotations about the axis of symmetry". Far from the hole $\mathbf{k}^2 \to -1$ and $\mathbf{m}^2 \to$ (distance from axis of symmetry)^2. Inside the hole's ergosphere $\mathbf{k}$ is spacelike, but the Killing vector

$$\boldsymbol{\ell} \equiv \mathbf{k} + \Omega^H \mathbf{m} \tag{5.1}$$

(where Ω^H is the hole's angular velocity) is timelike. As one approaches the horizon, $\boldsymbol{\ell}$ becomes tangent to the horizon's null-geodesic generators.

We shall require that our fiducial congruence, hypersurfaces, and global time parameter mesh with the hole's stationary exterior geometry in the following senses: (i) The fiducial congruence completely covers the exterior region $\mathcal{E}$. (ii) Each fiducial observer moves along a Killing direction, so that he sees a forever unchanging spacetime geometry in his neighborhood. (iii) The hypersurfaces of simultaneity all have identical spatial geometries. (iv) Far from the hole the global time parameter t becomes equal to proper time τ as measured by the fiducial observers.

These four demands fix the fiducial congruence, hypersurfaces, and global time parameter uniquely (up to the addition of a constant to t): The fiducial observers are the "zero-angular-momentum observers" (ZAMOs) of Bardeen, Press, and Teukolsky (1973). Their 4-velocities can be expressed in terms of the Killing vectors $\mathbf{k}$ and $\mathbf{m}$ as

$$\mathbf{U} = \alpha^{-1}(\mathbf{k} + \omega\mathbf{m}) \quad , \tag{5.2}$$

where ω is the ZAMO angular velocity

$$\omega = -\mathbf{k}\cdot\mathbf{m}/\mathbf{m}^2 \quad , \tag{5.3}$$

and where α, the lapse function, can be expressed as

$$\alpha = [-\mathbf{k}^2 + (\mathbf{k}\cdot\mathbf{m})^2/\mathbf{m}^2]^{1/2} \quad . \tag{5.4}$$

The rotational Killing vector $\mathbf{m}$ is orthogonal to $\mathbf{U}$ and thus lies in the fiducial hypersurfaces $\mathcal{S}_t$ and can be regarded as a spatial vector $\underset{\sim}{m}$.

For the Schwarzschild geometry of a nonrotating black hole the global time parameter t is equal to the standard Schwarzschild time coordinate t (MTW chapter 31). For the Kerr geometry, t is the Boyer-Lindquist time coordinate (MTW chapter 33).

The congruence of Killing trajectories generated by $\mathbf{k}$ threads its way from one hypersurface $\mathcal{S}_t$ to the next and the next in a non-orthogonal manner. The equations of black-hole electrodynamics will take on a particularly simple form if we express them in terms of the time derivative $\pounds_t$ along this "shifting Killing congruence", rather than in terms of the Fermi time derivative D_τ along the fiducial world lines. To make $\pounds_t$ differentiate along $\mathbf{k} = \alpha\mathbf{U} - \omega\mathbf{m}$ we must choose as our shift vector

$$\underset{\sim}{\beta} = -\omega\underset{\sim}{m} \quad . \tag{5.5}$$

The magnitude, $|\underset{\sim}{\beta}|/\alpha$, of the ordinary velocity associated with this shift vector will be greater than the speed of light near the black hole, and less far from the hole. With this choice of shift vector, the 3+1 splits of the Killing equations $k_{(\alpha;\beta)} = 0$ and $m_{(\alpha;\beta)} = 0$ along with the mutual commutivity of $\mathbf{k}$ and $\mathbf{m}$, imply the following

$$\pounds_t\alpha = \pounds_t\omega = 0 \quad , \tag{5.6a}$$

$$\underset{\sim}{m}\cdot\underset{\sim}{\nabla}\alpha = \underset{\sim}{m}\cdot\underset{\sim}{\nabla}\omega = 0 \quad , \tag{5.6b}$$

$$\pounds_t\underset{\sim}{m} = 0 \quad , \tag{5.6c}$$

$$m_{j|k} + m_{k|j} = 0 \quad , \tag{5.6d}$$

$$\pounds_t \gamma_{jk} = 0 \quad , \tag{5.6e}$$

$$\theta = 0 \quad , \tag{5.6f}$$

$$\underset{\sim}{\sigma} = \frac{1}{2}\alpha^{-1}\,[\underset{\sim}{m} \otimes (\underset{\sim}{\nabla}\omega) + (\underset{\sim}{\nabla}\omega) \otimes \underset{\sim}{m}] \quad . \tag{5.6g}$$

Equations (5.5) and (5.6b,f,g), together with (2.16b,c), imply the following relationship between the fiducial observers' Fermi time derivative and the Lie time derivative $\pounds_t$ along $\mathbf{k}$:

$$D_T \underset{\sim}{M} = \alpha^{-1}[\pounds_t \underset{\sim}{M} + \omega \pounds_{\underset{\sim}{m}} \underset{\sim}{M} + \frac{1}{2}\,(\underset{\sim}{m} \times \underset{\sim}{\nabla}\omega) \times \underset{\sim}{M}] \quad . \tag{5.7}$$

Because our hypersurfaces $\mathcal{S}_t$ all have the same spatial geometry, and because our time derivatives $\pounds_t$ act along Killing trajectories, we can now abandon the spacetime viewpoint of relativity and return to the Galilean-Newtonian viewpoint that physics occurs in an absolute 3-dimensional space $\mathcal{S}$. As in Galilean-Newtonian physics there is a universal time parameter t which marks the evolution of fields and particles in $\mathcal{S}$; but t is no longer united with $\mathcal{S}$ in a 4-dimensional spacetime structure. We shall adopt this Galilean-Newtonian viewpoint in Paper II; but for the remainder of Paper I we shall retain the spacetime viewpoint, using it as a tool in deriving further features of the 3+1 formalism.

5.2 ELECTRODYNAMIC EQUATIONS

The Maxwell equations (3.4) can be brought into the following form by use of equations (5.6f,g) and (5.7)

$$\nabla \cdot \mathbf{E} = 4\pi\rho_e \quad , \tag{5.8a}$$

$$\nabla \cdot \mathbf{B} = 0 \quad , \tag{5.8b}$$

$$\mathcal{L}_t \mathbf{E} + \omega \pounds_{\mathbf{m}} \mathbf{E} - (\mathbf{E} \cdot \nabla\omega)\mathbf{m} = \nabla \times (\alpha \mathbf{B}) - 4\pi\alpha \mathbf{j} \quad , \tag{5.8c}$$

$$\mathcal{L}_t \mathbf{B} + \omega \pounds_{\mathbf{m}} \mathbf{B} - (\mathbf{B} \cdot \nabla\omega)\mathbf{m} = -\nabla \times (\alpha \mathbf{E}) \quad . \tag{5.8d}$$

Expressions (3.5) for $\mathbf{E}$ and $\mathbf{B}$ in terms of the scalar and vector potentials similarly can be brought into the form

$$\mathbf{E} = \alpha^{-1}(\nabla A_0 + \omega \nabla A_\varphi) - \alpha^{-1}(\mathcal{L}_t \mathbf{A} + \omega \pounds_{\mathbf{m}} \mathbf{A}) \quad , \tag{5.9a}$$

$$\mathbf{B} = \nabla \times \mathbf{A} \quad , \tag{5.9b}$$

where

$$A_\varphi \equiv \mathbf{A} \cdot \mathbf{m} \quad , \tag{5.10a}$$

$$A_0 \equiv -\alpha\phi - \omega A_\varphi = (\text{4-vector potential } \mathcal{A}) \cdot \mathbf{k} \quad . \tag{5.10b}$$

(The notation A_φ and A_0 is motivated by the fact that one will often use coordinate systems in which $\mathbf{m} = \partial/\partial\varphi$ and $\mathbf{k} = \partial/\partial t$.)

The law of charge conservation (3.6) can be rewritten, using expressions (2.16a), (5.5), and (5.6f), as

$$\mathcal{L}_t \rho_e + \omega \mathbf{m} \cdot \nabla \rho_e + \nabla \cdot (\alpha \mathbf{j}) = 0 \quad . \tag{5.11}$$

Equations (5.8) - (5.11) will simplify considerably if the electromagnetic field is stationary and axisymmetric. Then all terms involving $\mathcal{L}_t$, $\pounds_{\mathbf{m}}$, and $\mathbf{m} \cdot \nabla$ will vanish.

The equation of motion (3.8) for a test particle acted on by the electromagnetic field becomes, upon using expressions (2.4), (5.6f,g), and (5.7),

$$[\mathcal{L}_t + (\alpha \underset{\sim}{v} + \omega \underset{\sim}{m}) \cdot \nabla] \underset{\sim}{p} = \omega(\underset{\sim}{p} \cdot \nabla)\underset{\sim}{m} - (\underset{\sim}{p} \cdot \underset{\sim}{m})\nabla\omega - \mu\Gamma\nabla\alpha + \alpha q(\underset{\sim}{E} + \underset{\sim}{v} \times \underset{\sim}{B}) \quad . \tag{5.12}$$

Here μ and q are the particle's rest mass and charge; $\underset{\sim}{v}$ is its velocity as measured by the ZAMOs; $\alpha\underset{\sim}{v} + \omega\underset{\sim}{m}$ is its velocity, on a per unit global time basis d/dt, with respect to the Killing trajectories of $\mathbf{k}$; and $\underset{\sim}{p} = \mu\Gamma\underset{\sim}{v} = \mu\underset{\sim}{v}(1 - \underset{\sim}{v}^2)^{-1/2}$ is its momentum as measured by the ZAMOs.

The differential laws of energy conservation (3.12) and (3.14) for an electromagnetic field and/or a continuous medium become, upon using expressions (2.16a), (5.5), and (5.6f,g),

$$\begin{aligned} \mathcal{L}_t \varepsilon + \omega \underset{\sim}{m} \cdot \nabla\varepsilon + \alpha^{-1}\nabla \cdot (\alpha^2 \underset{\sim}{S}) + \underset{\sim}{m} \cdot \underset{\sim}{W} \cdot \nabla\omega &= 0 \quad \text{if all stress-energy is included in } \varepsilon, \underset{\sim}{S}, \underset{\sim}{W} \\ &= -\alpha \underset{\sim}{j} \cdot \underset{\sim}{E} \quad \text{if only electromagnetic stress-energy is included;} \end{aligned} \tag{5.13}$$

and the laws of momentum conservation (3.13) and (3.15) become, upon using (2.4), (5.6f,g), and (5.7),

$$\begin{aligned} \mathcal{L}_t \underset{\sim}{S} + \omega \mathcal{L}_{\underset{\sim}{m}} \underset{\sim}{S} + (\underset{\sim}{S} \cdot \underset{\sim}{m})\nabla\omega + \varepsilon\nabla\alpha + \nabla \cdot (\alpha \underset{\sim}{W}) &= 0 \quad \text{all included} \\ &= -\alpha(\rho_e \underset{\sim}{E} + \underset{\sim}{j} \times \underset{\sim}{B}) \quad \text{only electromagnetism included .} \end{aligned} \tag{5.14}$$

These differential equations cannot be converted into integral conservation laws. However, there do exist integral conservation laws associated with two special combinations of these equations — combinations associated with the two Killing vector fields $\mathbf{k}$ and $\mathbf{m}$. Associated with $\mathbf{k}$ is a conserved "redshifted energy" or "energy at infinity" with energy density $\varepsilon_E = T^{\mu\nu}k_\mu U_\nu$, i.e. [cf. equations (5.2), (3.9), (3.10)]

$$\begin{aligned} \varepsilon_E &= \alpha\varepsilon + \omega \underset{\sim}{S} \cdot \underset{\sim}{m} \quad \text{in general} \\ &= \frac{\alpha}{8\pi}(\underset{\sim}{E}^2 + \underset{\sim}{B}^2) + \frac{\omega}{4\pi}(\underset{\sim}{E} \times \underset{\sim}{B}) \cdot \underset{\sim}{m} \quad \text{for electromagnetism ,} \end{aligned} \tag{5.15a}$$

and with energy flux $S_E^\alpha = -\gamma^\alpha{}_\mu T^{\mu\nu} k_\nu$, i.e.

$$\begin{aligned} \underset{\sim}{S}_E &= \alpha \underset{\sim}{S} + \omega \underset{\sim}{W} \cdot \underset{\sim}{m} \qquad \text{in general} \\ &= \frac{1}{4\pi}\left[\alpha \underset{\sim}{E} \times \underset{\sim}{B} - \omega(\underset{\sim}{E}\cdot\underset{\sim}{m})\underset{\sim}{E} - \omega(\underset{\sim}{B}\cdot\underset{\sim}{m})\underset{\sim}{B} + \frac{1}{2}\omega(\underset{\sim}{E}^2 + \underset{\sim}{B}^2)\underset{\sim}{m}\right] \quad \text{for electromagnetism.} \end{aligned} \tag{5.15b}$$

Associated with $\underset{\sim}{m}$ is a conserved "angular momentum about the hole's symmetry axis" with density $\varepsilon_L = -T^{\mu\nu} m_\mu U_\nu$, i.e. [cf. equations (3.9) and (3.10)]

$$\begin{aligned} \varepsilon_L &= \underset{\sim}{S}\cdot\underset{\sim}{m} \qquad \text{in general} \\ &= \frac{1}{4\pi}(\underset{\sim}{E}\times\underset{\sim}{B})\cdot\underset{\sim}{m} \qquad \text{for electromagnetism,} \end{aligned} \tag{5.16a}$$

and with flux $S_L^\alpha = +\gamma^\alpha{}_\mu T^{\mu\nu} m_\nu$, i.e.

$$\begin{aligned} \underset{\sim}{S}_L &= \underset{\sim}{W}\cdot\underset{\sim}{m} \qquad \text{in general} \\ &= \frac{1}{4\pi}\left[-(\underset{\sim}{E}\cdot\underset{\sim}{m})\underset{\sim}{E} - (\underset{\sim}{B}\cdot\underset{\sim}{m})\underset{\sim}{B} + \frac{1}{2}(\underset{\sim}{E}^2 + \underset{\sim}{B}^2)\underset{\sim}{m}\right] \qquad \text{for electromagnetism.} \end{aligned} \tag{5.16b}$$

The differential and integral conservation laws for redshifted energy and for angular momentum have the same form as those for electric charge [equations (5.11) and (4.5)]:

$$\begin{aligned} &\pounds_t \varepsilon_E + \omega \underset{\sim}{m}\cdot\underset{\sim}{\nabla}\varepsilon_E + \underset{\sim}{\nabla}\cdot(\alpha \underset{\sim}{S}_E) = 0 \qquad \text{if all stress-energy is included in } \varepsilon_E, \underset{\sim}{S}_E \\ &\quad = -\alpha^2 \underset{\sim}{j}\cdot\underset{\sim}{E} - \alpha\omega(\rho_e \underset{\sim}{E} + \underset{\sim}{j}\times\underset{\sim}{B})\cdot\underset{\sim}{m} \qquad \text{if only electromagnetic stress-energy is included,} \end{aligned} \tag{5.17a}$$

$$\begin{aligned} &\pounds_t \varepsilon_L + \omega \underset{\sim}{m}\cdot\underset{\sim}{\nabla}\varepsilon_L + \underset{\sim}{\nabla}\cdot(\alpha \underset{\sim}{S}_L) = 0 \qquad \text{all included} \\ &\quad = -\alpha(\rho_e \underset{\sim}{E} + \underset{\sim}{j}\times\underset{\sim}{B})\cdot\underset{\sim}{m} \qquad \text{only electromagnetism included;} \end{aligned} \tag{5.17b}$$

$$\begin{aligned} &\frac{d}{dt}\int_{\mathcal{V}(t)} \varepsilon_E dV + \int_{\partial\mathcal{V}(t)} \alpha(\underset{\sim}{S}_E - \varepsilon_E \underset{\sim}{v})\cdot d\underset{\sim}{\Sigma} = 0 \qquad \text{all included} \\ &\quad = -\int_{\mathcal{V}(t)} [\alpha^2 \underset{\sim}{j}\cdot\underset{\sim}{E} + \alpha\omega(\rho_e \underset{\sim}{E} + \underset{\sim}{j}\times\underset{\sim}{B})\cdot\underset{\sim}{m}] dV \qquad \text{only electromagnetism included,} \end{aligned} \tag{5.18a}$$

$$\frac{d}{dt}\int_{\mathcal{V}(t)} \varepsilon_L dV + \int_{\partial\mathcal{V}(t)} \alpha(\underset{\sim}{S}_L - \varepsilon_L \underset{\sim}{v}) \cdot d\underset{\sim}{\Sigma} = 0 \quad \text{all included}$$

$$= -\int_{\mathcal{V}(t)} \alpha(\rho_e \underset{\sim}{E} + \underset{\sim}{j} \times \underset{\sim}{B}) \cdot \underset{\sim}{m}\, dV \quad \text{only electromagnetism included .} \tag{5.18b}$$

The integral formulations of Maxwell's equations [Gauss's laws (4.1) and (4.2), Faraday's law (4.3), Ampere's law (4.4), and charge conservation (4.5)] do not simplify when we specialize to stationary, axially symmetric spacetimes.

5.3 SPACETIME STRUCTURE NEAR THE HORIZON

Our foliation of hypersurfaces becomes pathological near the horizon of the black hole. The pathology can be understood most clearly in the simple case of a nonrotating Schwarzschild black hole with gravitational radius 2M (MTW chapter 31). Figure 4 is a spacetime diagram for the hole's exterior $\mathcal{E}$ ($r/2M > 1$) and interior ($r/2M < 1$) in ingoing Eddington-Finkelstein coordinates $\tilde{t}$ and r (Box 31.2 of MTW). The key feature of this coordinate system, for our purposes, is the fact that it is well behaved everywhere except at the $r = 0$ singularity; all the metric coefficients in the line element

$$ds^2 = -d\tilde{t}^2 + dr^2 + (2M/r)(d\tilde{t} + dr)^2 + r^2(d\theta^2 + \sin^2\theta\, d\varphi^2) \tag{5.19}$$

are of order unity outside, on, and near the horizon $\mathcal{H}$ ($r = 2M$). The light cones tilt near the horizon (light trapping), but do not squash down to slivers.

Our global time parameter t in Eddington-Finkelstein coordinates is given by

$$t = \tilde{t} - 2M \ln (r/2M - 1) \quad . \tag{5.20}$$

Curves of constant t (our hypersurfaces of simultaneity $\mathcal{S}_t$) are plotted in Figure 4. Note that our hypersurfaces sink deep into the past as they

approach the horizon $\mathscr{H}$ ($r = 2M$). This is a manifestation of the very slow rate at which our fiducial proper time τ marches forward near the horizon

$$d\tau/dt = \alpha = (1 - 2M/r)^{1/2} \to 0 \quad \text{at } \mathscr{H} \quad , \tag{5.21}$$

and it is characteristic of all black-hole spacetimes, not just Schwarzschild.

Suppose that one (mathematically) approaches the horizon $r = 2M$ by moving inward along a fixed hypersurface of simultaneity $\mathcal{S}_t$. In principle, one will then explore the entire past history of the spacetime region just above the horizon. For a 10^8 solar mass hole ($2M = 3 \times 10^8$km) one will see, plastered into the region between $r - 2M = 100$ microns and $r - 2M = 2$ microns, the near-horizon electromagnetic field structure laid down there $\Delta\tilde{t} = 10$ to 11 hours ago. Far beneath this, at $r - 2M = 2 \times 10^{-18}$ cm to 4×10^{-20} cm, one will see the structure characteristic of $\Delta\tilde{t} = 20$ to 21 hours ago. These structures will be layered down one after another like ancient sediment deposits on the bottom of the sea.

In view of this multilayered structure, how can we define the "limits of $\underset{\sim}{E}$ and $\underset{\sim}{B}$ as one approaches the horizon"? In principle, we can choose any layer we wish as the horizon limit. We need only note which part of the horizon (which $\tilde{t}$) is near the layer chosen, and announce our results as the limiting horizon fields at that specific moment of $\tilde{t}$ time.

In practice, the 3+1 formalism of this paper will probably be useful only when the external electromagnetic field evolves very slowly compared to $2M \simeq (17 \text{ minutes}) \cdot (M/10^8 M_\odot)$ ["quasi-stationary" evolution]. In this case the horizon structure being laid down now (in $\tilde{t}$ time) will extend so deep [to $r - 2M \lesssim 10^{-18}$cm if the evolution timescale is $\Delta\tilde{t} \gtrsim (20 \text{ hours}) \cdot (M/10^8 M_\odot)$] that previous structures can be totally ignored. One can pretend that the present structure extends all the way in to $r = 2M$.

Although the above discussion is couched in the language, formulae, and numbers of the Schwarzschild geometry, its qualitative features will be the same for any stationary, axially symmetric hole.

In the generic case, as one approaches the horizon $\mathcal{H}$, one sees the lapse function go to zero and the fiducial (ZAMO) congruence become null

$$\left.\begin{aligned} &\alpha = (d\tau/dt)_{\text{along congruence}} \to 0 \\ &\omega \to \Omega^H = (\text{angular velocity of hole}) \\ &\alpha \mathbf{U} \to \boldsymbol{\ell} = \mathbf{k} + \Omega^H \mathbf{m} = \begin{pmatrix}\text{tangent to null} \\ \text{generator of } \mathcal{H}\end{pmatrix} \end{aligned}\right\} \quad \text{at } \mathcal{H} \ . \tag{5.22a}$$

One can show, using the formulas on pages 251 and 252 of Bardeen (1973), that near the horizon the magnitude $a \equiv |\underset{\sim}{a}|$ of the acceleration of the fiducial ZAMO congruence behaves as

$$\alpha a \equiv \alpha |\underset{\sim}{a}| = \kappa + O(\alpha^2) \to \kappa \text{ at } \mathcal{H} \ . \tag{5.22b}$$

Here κ is the "surface gravity" of the hole. Since $\alpha \to 0$, a must become infinite on $\mathcal{H}$: the ZAMO observers near the horizon must accelerate like hell to avoid falling into the hole. The unit spatial vector along $\underset{\sim}{a}$

$$\underset{\sim}{n} \equiv \underset{\sim}{a}/a \ , \tag{5.23}$$

when viewed as a 4-vector $\mathbf{n}$, collapses into the 4-velocity $\mathbf{U}$ as one approaches the horizon:

$$\alpha \mathbf{n} \text{ and } \alpha \mathbf{U} \text{ both} \to \boldsymbol{\ell} \quad \text{at } \mathcal{H} \ . \tag{5.24}$$

One can take, as a pair of well-behaved basis vectors in the $\mathbf{n} \wedge \mathbf{U}$ 2-flats, $\alpha \mathbf{U}$ and any vector of the form

$$\boldsymbol{\xi} \equiv (1/\alpha)(\boldsymbol{U} - \boldsymbol{n}) + (\text{const})\,\alpha\boldsymbol{U} \quad . \tag{5.25}$$

[That $\boldsymbol{\xi}$ is finite at $\mathscr{H}$ follows from (i) the finiteness of $\alpha\boldsymbol{U} = \boldsymbol{\ell}$ at $\mathscr{H}$, (ii) the fact that $(1/\alpha)(\boldsymbol{U}-\boldsymbol{n})$ is null, and (iii) the fact that $(1/\alpha)(\boldsymbol{U}-\boldsymbol{n})\cdot\boldsymbol{\ell} = -1$ at $\mathscr{H}$.] At the horizon $\alpha\boldsymbol{U} = \boldsymbol{\ell}$ is tangent to $\mathscr{H}$, while $\boldsymbol{\xi}$ points inward through $\mathscr{H}$ (cf. Figure 4). It is convenient to fix the constant in the definition (5.25) of $\boldsymbol{\xi}$ so that

$$\tilde{t}_{,\mu}\,\xi^{\mu} = 0 \tag{5.26}$$

(i.e., $\boldsymbol{\xi}$ lies in the 3-surfaces of constant $\tilde{t}$), where

$$\tilde{t} \equiv t + \kappa^{-1} \ln \alpha \quad . \tag{5.27}$$

One can verify that the scalar field $\tilde{t}$ has finite derivatives along $\boldsymbol{\ell}$ and along $\boldsymbol{\xi}$ at $\mathscr{H}$, and thus is well behaved there. This $\tilde{t}$ is the generic analog of the Eddington-Finkelstein $\tilde{t}$ (equation 5.20). For generic black holes, as for Schwarzschild black holes, all physical quantities must approach well-behaved limits as one approaches the horizon along $\boldsymbol{\xi}$. Formally, we define

"$\to$" means "becomes equal to, as one approaches the horizon along a curve to which $\boldsymbol{\xi}$ is tangent — i.e., along a curve of constant $\tilde{t}$ in the $\boldsymbol{n}\wedge\boldsymbol{U}$ plane". (5.28)

Near the horizon one can introduce spacetime coordinates t, φ, α, and λ with these properties: $\partial/\partial t \equiv \boldsymbol{k}$; $\partial/\partial\varphi \equiv \boldsymbol{m}$; α is the lapse function and is therefore equal to zero everywhere on the horizon; and λ measures proper distance along the horizon from the rotation axis down towards the equator. In an immediate neighborhood of the horizon the spacetime line element will read

$$ds^2 = -\alpha^2\,dt^2 + \varpi^2(d\varphi - \Omega^H dt)^2 + \kappa^{-2}\,d\alpha^2 + d\lambda^2 \tag{5.29a}$$

where

$\alpha = 0$ at horizon , κ = (surface gravity) = constant , (5.29b)

$\varpi \equiv |\underset{\sim}{m}|$ is a function of λ , Ω^H = (angular velocity of hole) = constant .

The spatial geometry of the fiducial hypersurface $\mathcal{S}_t$ near $\mathcal{H}$ is

$$ds^2 = \varpi^2 \, d\varphi^2 + \kappa^{-2} \, d\alpha^2 + d\lambda^2 \quad ; \tag{5.30}$$

and the 2-geometry of $\mathcal{H}$ is

$$ds^2 = \varpi^2 \, d\varphi^2 + d\lambda^2 \quad . \tag{5.31}$$

The fiducial observers (ZAMOs) near $\mathcal{H}$ move with angular velocity $\omega = \Omega^H$:

$\varphi = \Omega^H t$, λ = const , α = const is a fiducial world line near $\mathcal{H}$. (5.32)

5.4 BOUNDARY CONDITIONS ON THE ELECTRIC AND MAGNETIC FIELDS AT THE HORIZON

Znajek (1976,1978b) and Damour (1978,1979,1980) have constructed a beautiful theory of electromagnetic boundary conditions at horizons of black holes; see Carter (1979) for an excellent review. In this section we translate that theory into our 3+1 language.

Znajek and Damour define electric and magnetic fields that live in the horizon by

$$E^H_\alpha = F_{\alpha\beta} \, \ell^\beta \, , \quad B^H_\alpha = -{}^*F_{\alpha\beta} \, \ell^\beta \quad . \tag{5.33}$$

Here $F_{\alpha\beta}$ is the electromagnetic field tensor and ${}^*F_{\alpha\beta}$ is its dual. For comparison, the electric and magnetic fields of our 3+1 formalism are $E_\alpha = F_{\alpha\beta}U^\beta$, $B_\alpha = -{}^*F_{\alpha\beta}U^\beta$. Equation (5.22a) reveals the relationship between the two types of fields:

$$\left.\begin{aligned} \alpha \underset{\sim}{E} &\to \underset{\sim}{E}^{H} \\ \alpha \underset{\sim}{B} &\to \underset{\sim}{B}^{H} \end{aligned}\right\} \text{ on } \mathscr{H} \ . \tag{5.34}$$

Here $\underset{\sim}{E}$, $\underset{\sim}{B}$, $\underset{\sim}{E}^{H}$, and $\underset{\sim}{B}^{H}$ are viewed as spatial vectors lying in the hypersurfaces of simultaneity $\mathcal{S}_t$; as one approaches the horizon, these hypersurfaces become null and coincide with $\mathscr{H}$ itself, which is why $\alpha\underset{\sim}{E}$ and $\alpha\underset{\sim}{B}$ become vectors ($\underset{\sim}{E}^{H}$ and $\underset{\sim}{B}^{H}$) lying in $\mathscr{H}$.

Fiducial observers near the horizon can split their electric and magnetic fields into parts $\underset{\sim\|}{E}$ and $\underset{\sim\|}{B}$ parallel to the horizon, and parts $E_\perp$ and $B_\perp$ perpendicular to the horizon (i.e., along their acceleration direction $\underset{\sim}{n}$):

$$\underset{\sim}{E} = \underset{\sim\|}{E} + E_\perp \underset{\sim}{n} \ , \qquad \underset{\sim}{B} = \underset{\sim\|}{B} + B_\perp \underset{\sim}{n} \ . \tag{5.35}$$

Similarly, the horizon fields can be split into components $\underset{\sim\|}{E}^{H}$ and $\underset{\sim\|}{B}^{H}$ which lie in surfaces of constant $\tilde{t} = t + \kappa^{-1} \ln \alpha$, and components $E_\perp^H$ and $B_\perp^H$ which are orthogonal to these surfaces (i.e., which point along the null generator $\underset{\sim}{\ell}$):

$$\underset{\sim}{E}^{H} = \underset{\sim\|}{E}^{H} + E_\perp^H \underset{\sim}{\ell} \ , \quad \underset{\sim}{B}^{H} = \underset{\sim\|}{B}^{H} + B_\perp^H \underset{\sim}{\ell} \ . \tag{5.36}$$

Equations (5.34) and (5.24) reveal the relationship between these decompositions:

$$\alpha \underset{\sim\|}{E} \to \underset{\sim\|}{E}^{H} \ , \quad \alpha \underset{\sim\|}{B} \to \underset{\sim\|}{B}^{H} \ , \tag{5.37a}$$

$$E_\perp \to E_\perp^H \ , \quad B_\perp \to B_\perp^H \ . \tag{5.37b}$$

Notice that the tangential fields $\underset{\sim\|}{E}$ and $\underset{\sim\|}{B}$ diverge as one approaches the horizon ($\alpha \to 0$), but the radial fields remain finite. Physically this comes about because the ZAMOs near the horizon are moving outward at nearly the speed of light relative to physically more reasonable infalling observers, who see finite fields at the horizon. This motion converts the tangential fields,

whatever they may be in physically reasonable frames, into inward propagating plane waves as seen by the ZAMOs. By pursuing this line of reasoning one can derive the following plane-wave relationship between $\underset{\sim}{E}_{\parallel}$ and $\underset{\sim}{B}_{\parallel}$:

$$|\underset{\sim}{E}_{\parallel} - \underset{\sim}{n} \times \underset{\sim}{B}_{\parallel}| \text{ goes to zero proportionally to } \alpha \text{ at } \mathscr{H} \quad . \tag{5.38}$$

Hajicek (1973, 1974) and Hanni and Ruffini (1973) have introduced the concept of surface density of electric charge on the horizon

$$\sigma^H \equiv (1/4\pi) E^H_{\perp} \quad . \tag{5.39}$$

This charge does not really exist physically on the horizon; rather, it is the charge per unit area which would precisely terminate the perpendicular electric field lines $E_{\perp}\underset{\sim}{n}$ at the horizon. If one pretends that this charge really exists, then one can ignore the actual fate of the electric field lines inside the horizon.

Damour (1978) has pursued this viewpoint further: He introduces a (fictitious) surface current density $\underset{\sim}{\mathscr{J}}^H$ (charge per unit time $\tilde{t}$ crossing a unit length perpendicular to $\underset{\sim}{\mathscr{J}}^H$), which is perfectly contrived to "complete the circuit" of all currents $\underset{\sim}{j}$ entering and leaving the horizon. Damour goes on to show that the hole behaves as though it had a surface resistivity

$$R^H \equiv 4\pi = 377 \text{ ohms} \tag{5.40}$$

(first inferred by Znajek (1976,1978b) in a different manner), in the sense that

$$\underset{\sim}{\mathscr{J}}^H = \underset{\sim}{E}^H_{\parallel} / R^H \quad . \tag{5.41}$$

Damour's properties of the surface charge and current, reexpressed in our 3+1 language, are the following:

$$E_{\perp} \to 4\pi\sigma^{H} \quad \text{at } \mathscr{H} \quad , \tag{5.42}$$

[Gauss's law: normal component of electric field is 4π times horizon's surface charge density; derivable from (5.37b) and (5.39).]

$$\alpha \underset{\sim}{B}_{\parallel} \to \underset{\sim}{B}^{H} = 4\pi \underset{\sim}{\mathcal{J}}^{H} \times \underset{\sim}{n} \quad \text{at} \quad \mathscr{H} \quad , \tag{5.43}$$

[Ampere's law: tangential magnetic field $\alpha \underset{\sim}{B}_{\parallel}$ is produced by surface current; derivable from (5.38), (5.37a), (5.40), and (5.41).]

$$\alpha \underset{\sim}{j}\cdot\underset{\sim}{n} \to -{}^{(2)}\underset{\sim}{\nabla}\cdot\underset{\sim}{\mathcal{J}}^{H} - \frac{d}{d\tilde{t}}\sigma^{H} \quad \text{at } \mathscr{H} \, . \tag{5.44}$$

[Charge conservation: $\alpha \underset{\sim}{j}\cdot\underset{\sim}{n}$ is the charge emerging from the horizon per unit area of horizon and per unit of global time t (or $\tilde{t}$); $(d/d\tilde{t})\sigma^{H} \equiv \sigma^{H}{}_{,\mu}\,\ell^{\mu}$ is the rate of change of the surface charge density with respect to global time; and ${}^{(2)}\underset{\sim}{\nabla}\cdot\underset{\sim}{\mathcal{J}}^{H}$ is the divergence of the surface current — the divergence ${}^{(2)}\underset{\sim}{\nabla}$ being taken with respect to the intrinsic 2-geometry of a $\tilde{t}$ = constant slice through $\mathscr{H}$. This law of charge conservation can be derived by projecting the Maxwell equation (3.4c) along $\underset{\sim}{n}$, and by invoking $D_{\tau\underset{\sim}{n}} = -\underset{\sim}{\sigma}\cdot\underset{\sim}{n}$ together with the horizon's Gauss and Ampere laws (5.42) and (5.43).]

Equations (5.42) - (5.44) allow one to regard the horizon as a thin surface with finite electrical conductivity, surrounding a rather peculiar interior: The interior cannot support any charges ρ_e or currents $\underset{\sim}{j}$ or perpendicular electric fields $E_{\perp}$ or tangential magnetic fields $\underset{\sim}{B}_{\parallel}$, but it can support tangential electric fields $\underset{\sim}{E}_{\parallel}$ and perpendicular magnetic fields $B_{\perp}$. As a consequence, the horizon is forced to acquire just the right surface charge density σ^{H} and current density $\underset{\sim}{\mathcal{J}}^{H}$ to (i) satisfy Ohm's law (equation 5.41), (ii) complete the circuit of external currents (equation 5.44), (iii) annul $E_{\perp}$ (equation 5.42), and (iv) annul $\underset{\sim}{B}_{\parallel}$ (equation 5.43); but the horizon permits $\underset{\sim}{E}_{\parallel}$ and $B_{\perp}$ to extend into the hole's interior. This description of a black hole is due to Damour (1978) and Carter (1979).

Znajek (1978b) describes the horizon in a somewhat different manner from this: He endows it with magnetic charge as well as electric charge, and with very high volume conductivities for both magnetic current and electric current. The resulting charges and currents annul all external quantities ($\underset{\sim}{E}_{\parallel}$, $E_{\perp}$, $\underset{\sim}{B}_{\parallel}$, $B_{\perp}$, ρ_e, $\underset{\sim}{j}$) in a thin skin just below the horizon. Znajek's description has the beauty and advantage of treating $\underset{\sim}{E}$ and $\underset{\sim}{B}$ on equal footings and of not attributing peculiar properties to the hole's interior. Nevertheless, we have adopted the Damour-Carter description instead of Znajek's because we want a formalism which so far as possible meshes with one's flat-spacetime, laboratory experience, where magnetic monopoles are nonexistent.

Since the hypersurfaces $\mathcal{S}_t$ do not extend inside the horizon, Gauss's law $\int_{\partial\mathcal{V}} \underset{\sim}{B} \cdot d\underset{\sim}{\Sigma} = 0$ [which relies on $\mathcal{V}$ lying entirely in $\mathcal{S}_t$] cannot be applied to 2-surfaces $\partial\mathcal{V}$ that enclose the horizon. On the other hand, Faraday's law (4.3) can be applied to such 2-surfaces [with $\mathcal{A}(t) = \partial\mathcal{V}$, $\partial\mathcal{A}(t) = 0$]. It says that

$$\frac{d}{dt} \int_{\partial\mathcal{V}(t)} \underset{\sim}{B} \cdot d\underset{\sim}{\Sigma} = 0 \tag{5.45}$$

for any 2-surface $\partial\mathcal{V}(t)$ enclosing the horizon — i.e., the total magnetic flux down the hole can never change. If the hole was created in the big bang, it conceivably could have been born with nonzero total magnetic flux; but if it was created by the collapse of a star, its total flux would have to be zero.

Because Damour's fictitious surface current and charge densities satisfy Maxwell's equations in the way described above, we are guaranteed that they will also lead, in the usual manner, to an electromagnetic torque on the horizon, $(\sigma^H \underset{\sim}{E}^H_{\parallel} + \underset{\sim}{\ell}^H \times \underset{\perp\sim}{B}^H \underset{\sim}{n}) \cdot \underset{\sim}{m}$, which precisely equals the flux of electromagnetic angular momentum down the hole, and a Joule heating $\underset{\sim}{E}^H_{\parallel} \cdot \underset{\sim}{\ell}^H$ of the horizon which precisely equals the hole's temperature times its rate of increase of entropy [Znajek (1978b), Damour (1978), Carter (1979)]. Specifically, the inward flux of angular momentum $-\underset{\sim}{S}_L \cdot \underset{\sim}{n}$ (equation 5.16b), when multiplied by $\alpha = d\tau/dt$ to convert to a

"per unit global time" basis, and when combined with Gauss's law (5.42) and Ampere's law (5.43), becomes

$$-\alpha\, \underset{\sim}{S}_L \cdot \underset{\sim}{n} \to \frac{d(\text{angular momentum of hole})}{d(\text{area of horizon})\, dt} \equiv \frac{dL^H}{d\Sigma^H dt}$$

$$= (\sigma^H \underset{\sim}{E}^H_{\parallel} + \underset{\sim}{\mathcal{J}}^H \times B^H_{\perp} \underset{\sim}{n}) \cdot \underset{\sim}{m} \quad . \tag{5.46}$$

Similarly, the inward flux of redshifted energy, $-\underset{\sim}{S}_E \cdot \underset{\sim}{n}$ (equation 5.15b), when multiplied by α to convert to "per unit global time", and when combined with Gauss's law (5.42) and Ampere's law (5.43), and with $\omega \to \Omega^H$, becomes

$$-\alpha\, \underset{\sim}{S}_E \cdot \underset{\sim}{n} \to \frac{d(\text{mass of hole})}{d(\text{area of horizon})\, dt} \equiv \frac{dM^H}{d\Sigma^H dt}$$

$$= \underset{\sim}{E}^H_{\parallel} \cdot \underset{\sim}{\mathcal{J}}^H + \Omega^H(\sigma^H \underset{\sim}{E}^H_{\parallel} + \underset{\sim}{\mathcal{J}}^H \times B^H_{\perp} \underset{\sim}{n}) \cdot \underset{\sim}{m} \quad . \tag{5.47}$$

Finally, combining expressions (5.46) and (5.47) with the first law of thermodynamics $dM^H = \Omega^H dL^H + \Theta^H dS^H$ where $\Theta^H = (\hbar/2\pi k)\kappa$ is the black-hole temperature and S^H is its entropy (Hawking 1976) we obtain the Joule-heating relation

$$\Theta^H \frac{dS^H}{d\Sigma^H dt} = \frac{dM^H}{d\Sigma^H dt} - \Omega^H \frac{dL^H}{d\Sigma^H dt} = \underset{\sim}{\mathcal{J}}^H \cdot \underset{\sim}{E}^H_{\parallel} \quad . \tag{5.48}$$

See Znajek (1978b), Damour (1978, 1979, 1980), and Carter (1979) for the original derivations and discussions of these relations in the 4-dimensional language.

6 Explicit Solutions of the Maxwell Equations

Since 1972 relativity theorists have put much effort into analytic solutions of Maxwell's equations for stationary, axially symmetric electromagnetic fields in black-hole spacetimes; and Wilson (1977) has initiated numerical studies of nonstationary fields in the magnetohydrodynamic approximation. This

work has been motivated in large measure by Ruffini's (1973) early recognition that electrodynamic phenomena around black holes will have important astrophysical consequences. Ruffini (1979) reviews many of the studies that have been made.

The published analytic solutions include: the electric field of a point charge at rest in the Schwarzschild geometry [solution in closed form by Copson (1928) and Linet (1976); solution as a multipole expansion by Cohen and Wald (1971); field lines plotted by Hanni and Ruffini (1973); force of hole on particle studied by Smith and Will (1980)]; the electric and magnetic fields of a point charge at rest on the symmetry axis of a Kerr black hole [Misra (1977), Léauté (1977), Linet (1979)]; the electric and magnetic fields of charged current loops around Kerr black holes [Petterson (1975), Chitre and Vishveshwara (1975), and Linet (1979) for loop in equatorial plane; Znajek (1978a) for loop out of equatorial plane]; the distortion of a uniform magnetic field by the gravity of a black hole [Ginzburg (1964) for formulas, and Hanni and Ruffini (1976) for pictures in the Schwarzschild case; Wald (1974) for Kerr hole; Znajek (1977) for Kerr hole with external magnetic field in a state of slow rotation; King and Lasota (1977) for Kerr hole with the field oblique to the axis of rotation]; and a magnetohydrodynamic solution, in the limit of very weak magnetic field, for the magnetic field dragged onto a Kerr hole by a geodesically moving, charged fluid (Ruffini and Wilson 1975).

Though none of these analytic solutions were written in 3+1 language, they can all be translated easily into that language. We give two examples. In these examples we use units in which the speed of light c and Newton's gravitational constant G are both equal to unity.

6.1 POINT CHARGE AT REST OUTSIDE A SCHWARZSCHILD HOLE

For a Schwarzschild hole the spatial geometry, lapse, and fiducial angular velocity are

$$ds^2 = \frac{dr^2}{1 - 2M/r} + r^2(d\theta^2 + \sin^2\theta\, d\varphi^2) \quad , \tag{6.1a}$$

$$\alpha = (1 - 2M/r)^{1/2} \quad , \qquad \omega = 0 \quad . \tag{6.1b}$$

For a point charge q at rest at r = b, θ = 0 Copson (1928) as corrected by Linet (1976) gives the potentials

$$A_0 = -\frac{q}{br}\frac{(r-M)(b-M) - M^2\cos\theta}{[(r-M)^2 + (b-M)^2 - M^2 - 2(r-M)(b-M)\cos\theta + M^2\cos^2\theta]^{1/2}} - \frac{qM}{br} \quad ,$$

$$\underset{\sim}{A} = A_\varphi = 0 \quad . \tag{6.2}$$

The electric field $\underset{\sim}{E} = \alpha^{-1}\underset{\sim}{\nabla} A_0$ (equation 5.9a), in terms of physical basis vectors $\underset{\sim}{e}_{\hat{r}} = (1-2M/r)^{1/2}\,\partial/\partial r$ and $\underset{\sim}{e}_{\hat{\theta}} = r^{-1}\,\partial/\partial\theta$, is

$$\underset{\sim}{E} = \frac{q}{br^2}\left\{M\left[1 - \frac{b-M+M\cos\theta}{D}\right] + \frac{r[(r-M)(b-M) - M^2\cos\theta]\,[r - M - (b-M)\cos\theta]}{D^3}\right\}\underset{\sim}{e}_{\hat{r}}$$

$$+ \frac{q(b-2M)(1-2M/r)^{1/2}\sin\theta}{D^3}\,\underset{\sim}{e}_{\hat{\theta}} \quad , \tag{6.3a}$$

where

$$D \equiv [(r-M)^2 + (b-M)^2 - M^2 - 2(r-M)(b-M)\cos\theta + M^2\cos^2\theta]^{1/2} \quad . \tag{6.3b}$$

The electric field lines intersect the horizon r = 2M orthogonally, producing a surface charge density

$$\sigma^H = \frac{q[M(1+\cos^2\theta) - 2(b-M)\cos\theta]}{8\pi b[b-M(1+\cos\theta)]^2} \tag{6.4}$$

but no surface current. The total induced surface charge is zero. Hanni and

Ruffini (1973) plot the field lines.

6.2 KERR HOLE IMMERSED IN A UNIFORM MAGNETIC FIELD

For a Kerr hole the spatial geometry, lapse, fiducial angular velocity, and angular Killing vector are

$$ds^2 = (\rho^2/\Delta)dr^2 + \rho^2 d\theta^2 + (A\sin^2\theta/\rho^2)d\varphi^2 \quad , \tag{6.5a}$$

$$\rho^2 \equiv r^2 + a^2\cos^2\theta \ , \quad \Delta = r^2 - 2Mr + a^2 \ , \quad A = (r^2 + a^2)^2 - \Delta a^2\sin^2\theta \ ;$$

$$\alpha = (\rho^2\Delta/A)^{1/2} \ ; \tag{6.5b}$$

$$\omega = 2aMr/A \ ; \tag{6.5c}$$

$$\underset{\sim}{m} = \partial/\partial\varphi \quad . \tag{6.5d}$$

Here a is the angular momentum per unit mass of the black hole, and should not be confused with the acceleration of the fiducial congruence. Wald (1974) derives the 4-vector potential $\mathfrak{A}^\alpha = \frac{1}{2} B_o(m^\alpha + 2ak^\alpha)$ for a source-free magnetic field which is asymptotically uniform with strength B_o far from the hole. From equations (3.3) and (5.10a,b) we compute the corresponding 3+1 potentials

$$A_0 = -B_o[a\alpha^2 + \omega \underset{\sim}{m}^2(1/2 - a\omega)] \ , \tag{6.6a}$$

$$A_\varphi = B_o(1/2 - a\omega)\underset{\sim}{m}^2 \ , \tag{6.6b}$$

$$\underset{\sim}{A} = B_o(1/2 - a\omega)\underset{\sim}{m} \quad . \tag{6.6c}$$

From equations (5.9a,b) we derive the magnetic and electric fields, which reside in the Kerr spatial geometry (6.5a)

$$\underset{\sim}{B} = \frac{B_o}{2\rho \sin\theta}\left(\frac{\Delta}{A}\right)^{1/2}\left[\frac{\partial X}{\partial\theta}\frac{\partial}{\partial r} - \frac{\partial X}{\partial r}\frac{\partial}{\partial\theta}\right] \tag{6.7a}$$

where $X \equiv (\sin^2\theta/\rho^2)(A - 4a^2Mr)$,

$$\underset{\sim}{E} = \frac{-B_o a A^{1/2}}{\rho^3}\left\{\Delta^{1/2}\left[\frac{\partial(\alpha^2)}{\partial r} + \frac{M\sin^2\theta}{\rho^2}(A - 4a^2Mr)\frac{\partial}{\partial r}\left(\frac{r}{A}\right)\right]\frac{\partial}{\partial r}\right.$$
$$\left. + \Delta^{-1/2}\left[\frac{\partial(\alpha^2)}{\partial\theta} + \frac{Mr\sin^2\theta}{\rho^2}(A - 4a^2Mr)\frac{\partial}{\partial\theta}\left(\frac{1}{A}\right)\right]\frac{\partial}{\partial\theta}\right\} \quad . \tag{6.7b}$$

The electric field is induced by the hole's dragging of inertial frames: note that $\underset{\sim}{E} = 0$ if $a = 0$. The 2-geometry of the horizon ($\Delta = 0$) is

$$ds^2 = (r_+^2 + a^2\cos^2\theta)d\theta^2 + \frac{(r_+^2 + a^2)^2\sin^2\theta}{r_+^2 + a^2\cos^2\theta}d\varphi^2 \quad , \tag{6.8}$$

where $r_+ \equiv M + (M^2 - a^2)^{1/2}$ is the radius of the horizon. The magnetic and electric fields and the charge and current densities on this horizon are

$$\underset{\sim}{B}^H_{\parallel} = \underset{\sim}{E}^H_{\parallel} = \mathcal{J}^H = 0 \quad , \tag{6.9a}$$

$$B^H_{\perp} = \frac{4B_o Mr_+^2(r_+ - M)\cos\theta}{(r_+^2 + a^2\cos^2\theta)^2} \quad , \tag{6.9b}$$

$$E^H_{\perp} = 4\pi\sigma^H = -\frac{B_o a(r_+ - M)}{r_+^2 + a^2\cos^2\theta}(1 + \cos^2\theta) \quad .$$

In this example the absence of tangential fields and currents at the horizon implies that no torque acts to slow the horizon's rotation. If the external magnetic field were inclined obliquely to the rotation axis instead of aligned with it, a slowing torque would act; cf. King and Lasota (1977).

ACKNOWLEDGMENTS

For helpful discussions and correspondence about the history of research on 3+1 splits we thank George Ellis, Larry Smarr, and James York; for a helpful critique of this manuscript we thank Roman Znajek.

REFERENCES

Arnowitt, R., Deser, S., & Misner, C. W., 1960a. Phys. Rev., 120, 313.

Arnowitt, R., Deser, S., & Misner, C. W., 1960b. Phys. Rev., 120, 321.

Arnowitt, R., Deser, S., & Misner, C. W., 1962. In Gravitation: An Introduction to Current Research, p. 227, ed. Witten, L., Wiley, New York.

Bardeen, J. M., 1973. In Black Holes, p. 241, ed. DeWitt, C. & DeWitt, B. S., Gordon & Breach, New York.

Bardeen, J. M., Press, W. H., & Teukolsky, S. A., 1973. Astrophys. J., 178, 347.

Blandford, R. D. & Znajek, R. L., 1977. Mon. Not. R. astr. Soc., 179, 433.

Carter, B., 1979. In General Relativity, an Einstein Centenary Survey, p. 294, ed. Hawking, S. W. & Israel, W., Cambridge University Press, Cambridge.

Cattaneo, C., 1959. Annali Matematica Pura ed Applicata, 48, 361.

Chitre, D. M. & Vishveshwara, C. V., 1975. Phys. Rev. D, 12, 1538.

Christodoulou, D. & Ruffini, R., 1973. In Black Holes, p. R151, ed. DeWitt, C. & DeWitt, B. S., Gordon & Breach, New York.

Cohen, J. & Wald, R., 1971. J. Math. Phys., 12, 1845.

Copson, E. T., 1928. Proc. R. Soc. London, Ser. A, 118, 184.

Cowling, T. G., 1957. Magnetohydrodynamics, Interscience, New York.

Damour, T., 1978. Phys. Rev. D, 18, 3598.

Damour, T., 1979. Unpublished these de doctorat d'etat, l'Universite Pierre et Marie Curie, Paris.

Damour, T., 1980. In Proceedings of Second Marcel Grossman Meeting on General Relativity, ed. Ruffini, R., North Holland, Amsterdam.

Ellis, G.F.R., 1971. In General Relativity and Cosmology, proceedings of Course 47 of the International School of Physics "Enrico Fermi," p. 104, ed. Sachs, R., Academic Press, New York.

Ellis, G. F. R., 1973. In Cargèse Lectures in Physics, Vol. 6, p. 1, ed. Schatzman, E., Gordon & Breach, New York.

Estabrook, F. B. & Wahlquist, H. D., 1964. J. Math. Phys., 5, 1629.

Ginzburg, V. L., 1964. Doklady Akad. Nauk SSSR, 156, 43; English translation in Sov. Phys.—Doklady, 9, 329.

Goldreich, P. & Julian, W. H., 1969. Astrophys. J., 157, 869.

Hajicek, P., 1973. Commun. Math. Phys., 34, 37 and 53.

Hajicek, P., 1974. Commun. Math. Phys., 36, 305.

Hanni, R. S. & Ruffini, R., 1973. Phys. Rev. D., 8, 3259.

Hanni, R. S. & Ruffini, R., 1976. Lettre al Nuovo Cimento, 15, 189.

Hawking, S. W., 1976. Phys. Rev. D, 13, 191.

King, A. R. & Lasota, J. P., 1977. Astr. Astrophys., 58, 175.

King, A. R., Lasota, J. P., & Kundt, W., 1975. Phys. Rev. D, 12, 3037.

Landau, L. D. & Lifshitz, E. M., 1941. Teoriya Polya, Nauka, Moscow, §82; English translation of a recent edition: The Classical Theory of Fields, 1975, Pergamon Press, New York, §84.

Léauté, B., 1977. Ann. Inst. Henri Poincaré, 27, 167.

Lichnerowicz, A., 1944. J. Math. Pures Appl., 23, 37.

Lichnerowicz, A., 1967. Relativistic Hydrodynamics and Magnetohydrodynamics, Benjamin, New York.

Linet, B., 1976. J. Phys. A., 9, 1081.

Linet, B., 1979. J. Phys. A., 12, 839.

Macdonald, D. & Thorne, K. S., 1981. Mon. Not. R. astr. Soc., submitted. Cited in text as Paper II.

Mestel, L., Phillips, P., & Wang, Y. M., 1979. Mon. Not. R. astr. Soc., 188, 385.

Misner, C. W., Thorne, K. S., & Wheeler, J. A., 1973. Gravitation, W. H. Freeman, San Francisco. Cited in text as MTW.

Misner, C. W. & Wheeler, J. A., 1957. Ann. Phys., 2, 525; especially pp. 578-584.

Misra, R., 1977. Prog. Theor. Phys., 57, 694.

Petterson, J. A., 1975. Phys. Rev. D, 12, 2218.

Ruffini, R., 1973. In Black Holes, p. 451, ed. DeWitt, C. & DeWitt, B. S., Gordon & Breach, New York.

Ruffini, R., 1979. In Relativity, Quanta, and Cosmology in the Development of the Scientific Thought of Albert Einstein, p. 599, ed. De Finis, F., Johnson Reprint, New York.

Ruffini, R. & Wilson, J. R., 1975. Phys. Rev. D, 12, 2959.

Schild, A., 1967. In Relativity Theory and Astrophysics, Vol. I. Relativity and Cosmology, p. 1, ed. Ehlers, J., American Mathematical Society, Providence, Rhode Island.

Smarr, L., Taubes, C., & Wilson, J. R., 1980. In Essays in General Relativity, A Festschrift for Abraham Taub, p. 157, ed. Tipler, F., Academic Press, New York.

Smarr, L. & York, J. W., Jr., 1978. Phys. Rev. D, 17, 2529.

Smith, A. G. & Will, C. M., 1980. Phys. Rev. D, 22, 1276.

Stachel, J., 1969. Acta Phys. Polon., 35, 689.

Wald, R. M., 1974. Phys. Rev. D, 10, 1680.

Wilson, J. R., 1977. In Proceedings of First Marcel Grossman Meeting on General Relativity, p. 393, ed. Ruffini, R., North-Holland, Amsterdam.

York, J. W., Jr., 1979. In Sources of Gravitational Radiation, p. 83, ed. Smarr, L., Cambridge University Press, Cambridge.

Zel'dovich, Ya. B. & Novikov, I. D., 1971. Relativistic Astrophysics, Vol. 1, Stars and Relativity, University of Chicago Press, Chicago.

Zel'manov, A. L., 1956. Doklady Akad. Nauk SSSR, 107, 805.

Zel'manov, A. L., 1959. In Trudy Shestovo Soveshchaniya po Voprosam Kosmogonii (Proceedings of the Sixth Conference on Problems of Cosmogony), p. 144, Moscow.

Zel'manov, A. L., 1973. Doklady Akad. Nauk SSSR, 209, 822; English translation in Sov. Phys.—Doklady, 18, 231.

Znajek, R. L., 1976. Unpublished PhD thesis, University of Cambridge.

Znajek, R. L., 1977. Mon. Not. R. astr. Soc., 179, 457.

Znajek, R. L., 1978a. Mon. Not. R. astr. Soc., 182. 639.

Znajek, R. L., 1978b. Mon. Not. R. astr. Soc., 185, 833.

FIGURE CAPTIONS

Figure 1. The world lines of fiducial observers with 4-velocities $\mathbf{U}$, and the spacelike hypersurfaces of simultaneity $\mathcal{S}_t$ which are orthogonal to the fiducial world lines.

Figure 2. The Fermi-Walker time derivative $D_{\tau}\underset{\sim}{M}$, Lie time derivative $\mathcal{D}_{\tau}\underset{\sim}{M}$, and shifting time derivative $\mathcal{L}_{t}\underset{\sim}{M}$ of a spatial vector $\underset{\sim}{M}$. The two hypersurfaces are separated by global time Δt, and fiducial observer A sees them separated by proper time $\Delta\tau = \alpha\Delta t$.

In the upper diagram observer A carries with himself a gyroscope, applying an acceleration $\underset{\sim}{a}$ at its center of mass to keep it moving with him. He orients the gyroscope along the direction of $\underset{\sim}{M}$ at time t, and he attaches a rod to the gyroscope with precisely the same length as $\underset{\sim}{M}$. After proper time lapse $\Delta\tau = \alpha\Delta t$ the rod is located along the dashed arrow. The difference between $\underset{\sim}{M}$ and this dashed arrow is $(D_{\tau}\underset{\sim}{M})\Delta\tau$.

At time t in the upper diagram the tail of $\underset{\sim}{M}$ sits on fiducial observer A and the tip on fiducial observer B. After proper time lapse $\Delta\tau = \alpha\Delta t$ the tail is still on A but the tip has been displaced away from B. Its vector displacement is $(\mathcal{D}_{\tau}\underset{\sim}{M})\Delta\tau$.

The lower diagram shows trajectories a and b of the shifting congruence. The velocity of a trajectory relative to fiducial observer A is $d(\underset{\sim}{\text{proper distance}})/d\tau = \underset{\sim}{\beta}/\alpha$. At time t the tail of $\underset{\sim}{M}$ sits on trajectory a and the tip on trajectory b. After global time lapse Δt the tail is still on a but the tip has been displaced away from b. Its vector displacement is $(\mathcal{L}_{t}\underset{\sim}{M})\Delta t$.

Figure 3. A curve $\mathcal{C}(t)$, lying in the hypersurface $\mathcal{S}_t$, changes in some arbitrary manner as time t passes. A point labeled 1 moves with velocity $\underset{\sim}{v}$ as measured by a fiducial observer near it. During proper time $\Delta\tau = \alpha\Delta t$ point 1 gets displaced by $\underset{\sim}{v}\Delta\tau$ relative to the fiducial observer.

Figure 4. The hypersurfaces of simultaneity S_t around a Schwarzschild black hole, as viewed in Eddington-Finkelstein coordinates (MTW Box 31.2). Plotted upward is the Eddington-Finkelstein time coordinate $\tilde{t}$, which is related to the Schwarzschild time and radial coordinates by $\tilde{t} = t + 2M \ln(r/2M - 1)$. Plotted horizontally is the Eddington-Finkelstein radial coordinate r, which is identical to the Schwarzschild radial coordinate. The curves shown are our fiducial hypersurfaces S_t, and the cones are the radial light cones as given by the metric (5.19).

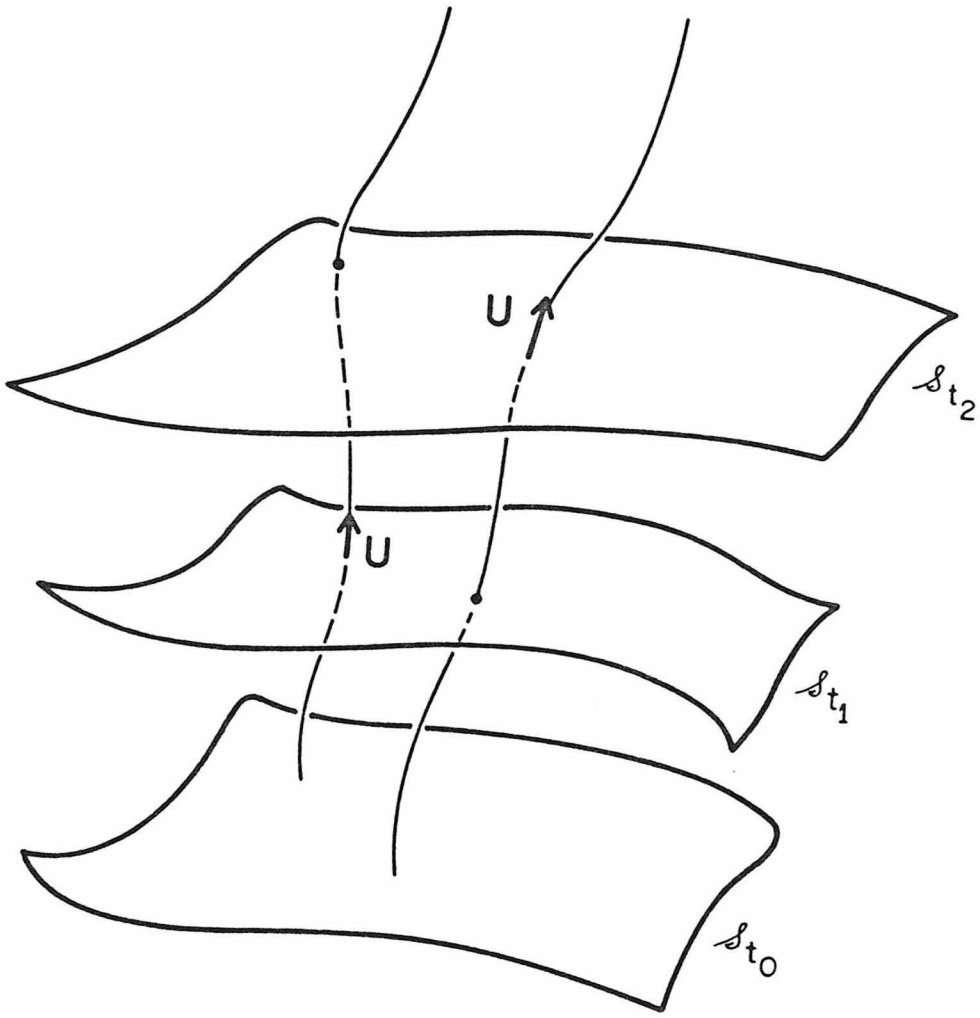

Fig. 1

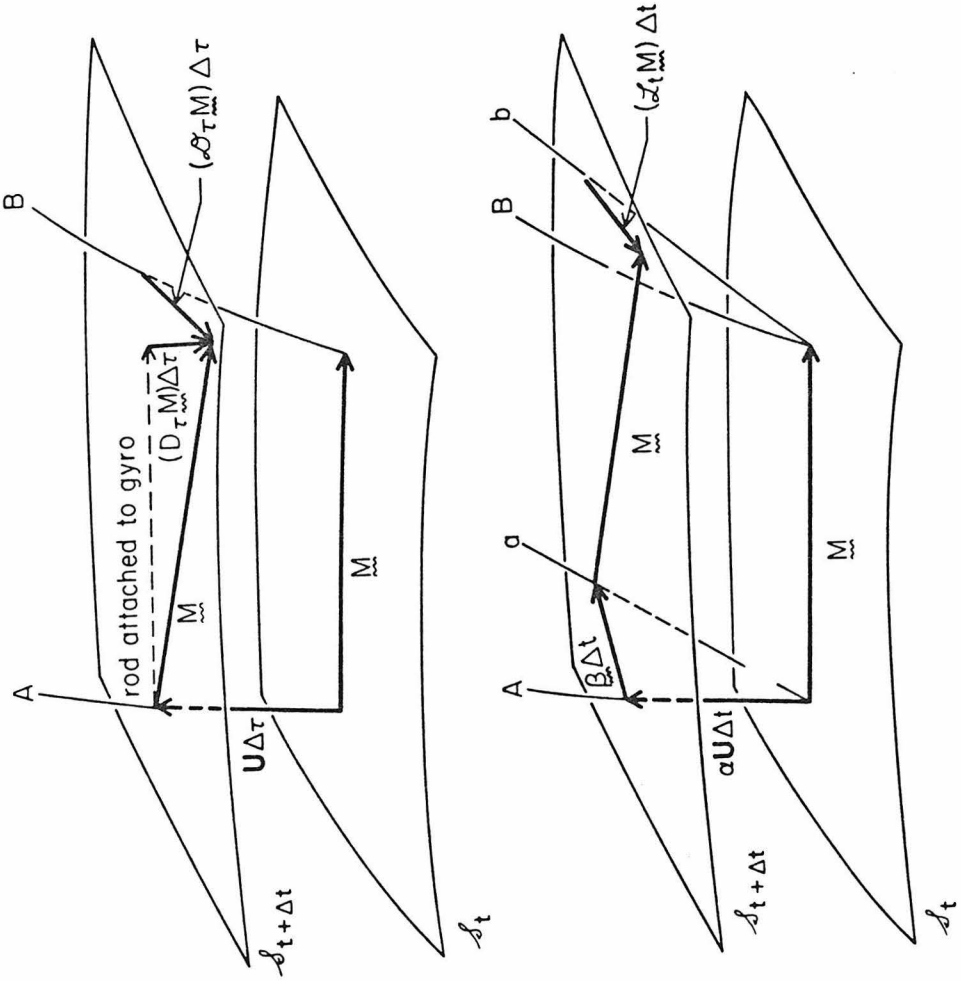
A
B
rod attached to gyro
$(D_\tau \underline{\underline{M}})\Delta\tau$
$(\omega_\tau \underline{\underline{M}})\Delta\tau$
$\underline{\underline{M}}$
$U\Delta\tau$
$\underline{\underline{M}}$
$\mathcal{S}_{t+\Delta t}$
$\mathcal{S}_t$
A
B
b
$(\alpha_t \underline{\underline{M}})\Delta t$
a
$\beta\Delta t$
$\underline{\underline{M}}$
$\alpha U\Delta t$
$\underline{\underline{M}}$
$\mathcal{S}_{t+\Delta t}$
$\mathcal{S}_t$

Fig. 2

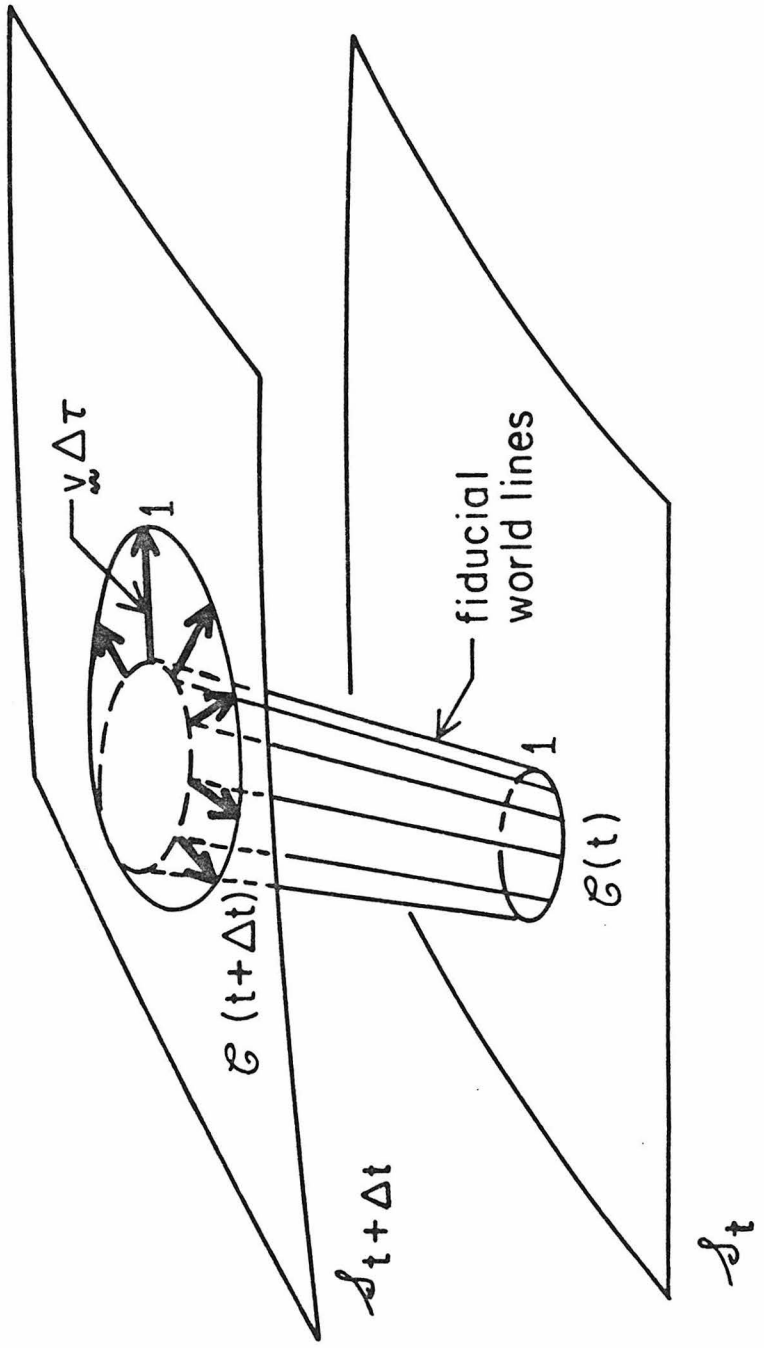
$v\Delta\tau$
1
fiducial
world lines
1
$\mathcal{C}(t+\Delta t)$
$\mathcal{C}(t)$
$\mathcal{S}_{t+\Delta t}$
$\mathcal{S}_t$

Fig. 3

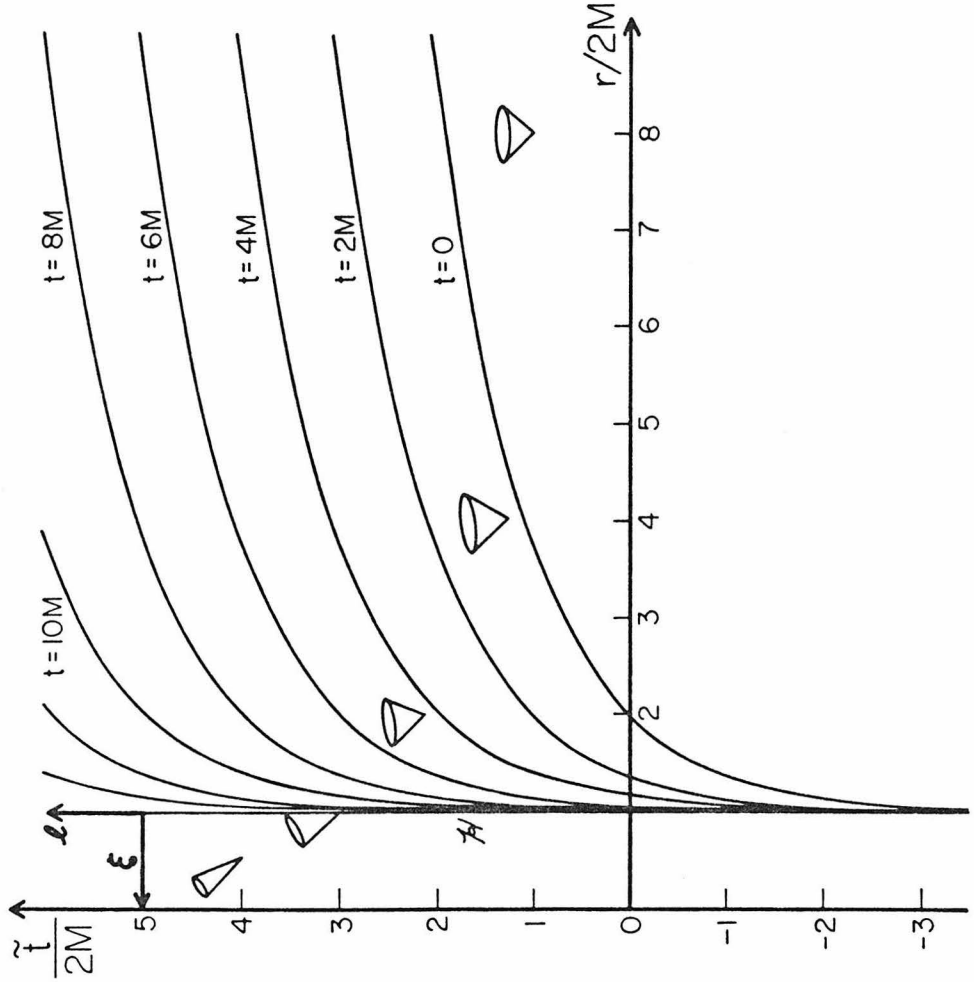

Fig. 4

CHAPTER III

OAP-616

BLACK-HOLE ELECTRODYNAMICS: AN ABSOLUTE-SPACE/UNIVERSAL-TIME FORMULATION*

DOUGLAS MACDONALD and KIP S. THORNE
W. K. Kellogg Radiation Laboratory
California Institute of Technology, Pasadena, California 91125

ABSTRACT

This paper reformulates and extends the Blandford-Znajek theory of a stationary, axisymmetric magnetosphere anchored in a black hole and in its accretion disk. Such a magnetosphere should transfer much of the rotational energy of the hole and orbital energy of the disk into an intense flux of electromagnetic energy — which in turn might be the energizer for quasars and active galactic nuclei.

Our reformulation of the theory attempts to make it accessible to plasma astrophysicists who have little experience with general relativity. This is done by replacing the relativist's "unified spacetime" viewpoint with an equivalent Galilean-type "absolute-space-plus-universal-time" viewpoint, and by replacing the electromagnetic field tensor $F_{\mu\nu}$ with electric and magnetic fields $\underset{\sim}{E}$ and $\underset{\sim}{B}$ that reside in the absolute space outside the black hole. The resulting formalism resembles the theory of axisymmetric pulsar magnetospheres; and it will, we hope, permit a fairly easy transfer of physical intuition and results from the pulsar problem to the black-hole problem.

The Blandford-Znajek theory focussed primarily on force-free regions of the magnetosphere. This paper, in addition to recasting the force-free theory in new language, extends it to encompass regions that are degenerate ($\underset{\sim}{E} \cdot \underset{\sim}{B} = 0$) but not force-free, and regions that are neither degenerate nor force-free. Blandford and Znajek showed that the magnetospheric structure in the force-free region is determined by a general relativistic "stream differential equation". This paper presents an action principle for the stream equation, it elucidates the boundary conditions that one must pose on the stream function ψ, and it shows that ψ and the poloidal magnetic field distribute themselves over the hole's horizon in such a manner as to extremize the horizon's electromagnetic surface energy.

This paper also constructs a general relativistic version of DC electronic circuit theory and uses it to elucidate the flows of electric current and of electromagnetic power in the magnetosphere. The circuit-theory analysis, and independently a torque-balance analysis, suggests that those magnetic field lines which thread the hole will be dragged into rotation with roughly half the angular velocity of the hole — and, consequently, that the hole will deliver to the magnetosphere the maximum electromagnetic power permitted by the horizon strengths of the magnetic fields.

---

*Supported in part by the National Science Foundation [AST79-22012].

ONE OF THE ORANGE AID PREPRINT SERIES
IN NUCLEAR, ATOMIC & THEORETICAL ASTROPHYSICS

March 1981

1 Introduction

Within one year after the discovery of pulsars (Hewish et al. 1968) it became evident that they are rotating neutron stars, and that the rotational energy is transmitted to radiating particles by a strong magnetic field embedded in the star (Gold 1968, Pacini 1968). During the subsequent year Goldreich & Julian (1969) laid the foundations for the theory of this "pulsar electrodynamics"; and during the decade since then scores of outstanding researchers have explored many different variants of the theory (see, e.g. the review by Arons 1979).

Quasars were discovered four years before pulsars (Schmidt 1963), and almost immediately a number of astrophysicists proposed that they might be energized by black holes (Robinson et al. 1965). However, a fully viable and compelling mechanism by which black holes can energize quasars was not found until 1976, thirteen years after the quasar discovery (Blandford 1976, Lovelace 1976, Harrison 1976). The long delay in finding this mechanism is surprising, since the mechanism is essentially the same as in the pulsar case: Magnetic fields, embedded in a rotating black hole and a surrounding accretion disk, transmit rotational and orbital energy to distant, radiating particles. Equally surprising is the fact that scores of theorists have not, since 1976, explored many different variants of the theory of "black-hole and accretion-disk electrodynamics." (For the modest amount of work that has been done, see Blandford & Znajek 1977; Znajek 1977, 1978b; Lovelace et al. 1979).

Why has the theory of black-hole and accretion-disk electrodynamics developed so slowly? We think a significant factor is the arena of curved 4-dimensional spacetime in which crucial parts of the theory must reside. Many astrophysicists feel uncomfortable in curved spacetime, even when the subject

they are exploring, electrodynamics, is totally familiar.

Relativity theorists are largely responsible for the astrophysicists' discomfort. The relativist prefers to think about physics in a geometric, frame-independent way, representing the electromagnetic field by the tensor $\mathbf{F}$, a 4-dimensional geometric object. The astrophysicist, on the other hand, would prefer to split this tensor into a 3-dimensional electric field $\underset{\sim}{E}$ and magnetic field $\underset{\sim}{B}$, sacrificing the general covariance of the theory for the insight to be gained from a comparison with the well-developed flat-spacetime theory of pulsar electrodynamics.

Moreover, the relativist likes to regard spacetime as a global, 4-dimensional manifold, free of any global reference frames. In calculating, he may introduce a local reference frame here, a different local frame there, a third one elsewhere, and flit back and forth from frame to frame as suits his convenience. The astrophysicist is apt to be uncomfortable with this slippery mode of study. His intuition is based largely on the Galilean-Newtonian viewpoint, in which physics occurs in a fixed, absolute 3-dimensional space with an associated universal reference frame, and events are demarked by the passage of a universal time. This absolute-space/universal-time viewpoint has given the astrophysicist a firm foundation on which to develop a vast lore of insights into pulsar electrodynamics and other astrophysical problems.

The relativist's slippery viewpoint is essential when spacetime is highly dynamical; and it has been enormously powerful in studies of cosmological singularities and of dynamically evolving black holes. However, its track record in treating black-hole electrodynamics had not been good.

Fortunately, in stationary, curved spacetimes such as those outside most astrophysical black holes, one can reformulate electrodynamics in terms of an

absolute but curved 3-dimensional space and a universal time. The variables in this reformulation are those familiar from flat-space electrodynamics: electric and magnetic fields $\underset{\sim}{E}$ and $\underset{\sim}{B}$, charge density ρ_e, and current density $\underset{\sim}{j}$. We present and utilize that reformulation in this paper, with the hope that it may catalyze pulsar-experienced astrophysicists to begin research on black-hole electrodynamics and to bring to bear on this topic their lore about the "axisymmetric pulsar problem" (e.g. Mestel, Phillips & Wang 1979).

Our absolute-space/universal-time formulation of stationary general relativity has deep roots in the "3+1 hypersurface formulations" of dynamical relativity, which are used nowadays by numerical relativists; and those 3+1 formulations in turn have deep roots in the Hamiltonian formulation of geometrodynamics, which was introduced in the 1950's as a tool for quantizing general relativity. We describe those roots in an accompanying paper (Thorne & Macdonald 1980, cited henceforth as Paper I); and, more important, we there use the 3+1 formulations of general relativity to derive the absolute-space/universal-time formalism of this paper.

In this paper we present without derivation the absolute-space/universal-time formalism, restricted to the space outside a rotating, axially symmetric black hole. We then use that formalism to derive the basic equations governing black-hole accretion disks and their magnetospheres.

More specifically, the remainder of this paper does the following: Section 2 presents without derivation the absolute-space/universal-time formulation of general relativity outside stationary black holes. Subsection 2.1 focusses on the mathematical structure of the formalism and its physical interpretation. Subsection 2.2 focusses (i) on the equations of electrodynamics; (ii) on the local laws of energy balance and force balance (first law of thermodynamics, and Euler or Navier-Stokes equations for an arbitrary continuous medium and

for the electromagnetic field); and (iii) on the global laws of conservation of angular momentum and "redshifted energy." Subsection 2.3 presents the Znajek (1978)-Damour (1978) theory of boundary conditions at the black hole's horizon, reformulated in our language of absolute space. Derivations of these results are to be found in Paper I.

Section 3 uses the absolute-space formalism of Section 2 to give an overview of black-hole and accretion-disk electrodynamics. More specifically, Faraday's law is used to describe the manner in which an accretion disk dynamically squeezes magnetic field lines onto a black hole and holds them there (Fig. 1). The discussion is fully dynamical; it does not require stationarity or axial symmetry of the accretion disk or its magnetic field.

The remainder of the paper, Sections 4-7, develops the theory of a stationary, axially symmetric magnetosphere. Sections 4, 5, and 6 develop the fundamental magnetosphere equations with successively increasing degrees of specialization; and then Section 7 shows how to put together a coherent magnetosphere model based on those equations.

The general equations for a stationary, axisymmetric magnetosphere are developed in Section 4. Section 5 imposes the constraint that the electromagnetic field be degenerate, $\underset{\sim}{E} \cdot \underset{\sim}{B} = 0$, and derives the consequences of degeneracy for the magnetosphere equations. Section 6 imposes, in addition to degeneracy, the constraint that the fields and currents be force-free, $\rho_e \underset{\sim}{E} + (\underset{\sim}{j}/c) \times \underset{\sim}{B} = 0$, and derives the consequences of force-freeness. Subsections 4.1, 5.1, and 6.1 focus on regions of the magnetosphere outside the black hole's horizon; subsections 4.2, 5.2, and 6.2 present the boundary conditions at the horizon for the unspecialized case, the degenerate case, and the degenerate force-free case, respectively. Subsection 6.3 presents action principles for the magnetosphere structure in force-free regions and for the distribution of the magnetic field on the horizon.

The magnetosphere theory for force-free regions has been developed previously by Blandford & Znajek (1977) using the usual 4-dimensional spacetime formulation of general relativity; and the general 4-dimensional theory of boundary conditions has been developed by Znajek (1977, 1978b) and Damour (1978). Our versions of these theories are isomorphic to theirs; we merely rewrite them in our absolute-space language, and extend them to include non-force-free regions of the magnetosphere.

Our general magnetosphere equations can act as a foundation for a plethora of different magnetosphere models. The details of a model will depend on the detailed assumptions made about the behavior of the plasma and charged particles in the non-force-free regions; and those details are left unspecified in our equations. Section 7 sketches various aspects of global magnetosphere models which are independent of the detailed assumptions about the non-force-free regions. Section 7 makes only the mild constraining assumptions that the fields in the disk are degenerate, that just outside the disk and hole there is a force-free region, and that beyond the force-free region is a non-degenerate, non-force-free region, the acceleration region, where the magnetosphere's rotation-induced power output is deposited into charged particles (cf. Fig. 2). Subsection 7.1 presents an overview of this assumed global magnetosphere structure.

Subsection 7.2 analyzes the balance that must exist between the torques exerted at one end of a magnetic flux tube by the hole or disk, and at the other end by charged particles in the acceleration region. This torque balance determines the angular velocity Ω^F of the flux tube; and, in the case of tubes threading the disk (but not those threading the hole), it also determines the current flowing in the force-free region of the magnetosphere. Subsection 7.2 also describes the rotation-induced power flow from disk and

hole to acceleration region, and presents an argument (generalized from pulsar theory) which suggests that torque balance on flux tubes threading the hole will lead to a flux-tube angular velocity roughly half that of the hole $\Omega^F \simeq \Omega^H/2$ ——and will thereby lead to optimal power output.

Subsection 7.3 develops a quantitative version of a DC circuit analysis of power flow through the force-free region, which was proposed qualitatively by Znajek (1978) and Blandford (1979). This analysis shows that the angular velocity Ω^F of a flux tube threading the horizon is determined by the ratio of impedances across the tube in the horizon, ΔZ^H, and in the acceleration region, ΔZ^A: $\Omega^F/(\Omega^H - \Omega^F) = \Delta Z^A/\Delta Z^H$ where Ω^H is the hole's angular velocity. The standard circuit-theory condition for optimal power flow, (load impedance) $\equiv \Delta Z^A$ = (source impedance) $\equiv \Delta Z^H$, agrees with the torque-balance condition for optimal power flow, $\Omega^F = \Omega^H/2$. Estimates of the impedance of the acceleration region (e.g. Lovelace et al. 1979) suggest that this impedance matching may be roughly achieved in Nature.

Subsection 7.4 discusses the mathematical structure of the problem of constructing a precise model for the force-free region. Roughly speaking, one must specify at the interface with the disk and acceleration regions the normal components of the magnetic field and electric current, and the angular velocity of the field lines. One does not specify any boundary conditions at all on the black-hole horizon. One then solves a single nonlinear partial differential equation——the relativistic stream equation of Blandford & Znajek (1977)——subject to these boundary conditions; and from the resulting stream function ψ, one computes the electric and magnetic fields and the current and charge densities throughout the force-free region and on the horizon. The resulting fields and currents will automatically satisfy the Znajek-Damour boundary conditions at the horizon.

Subsection 7.5 proves that a magnetic field loop cannot exist in the stationary, force-free region with both its feet anchored in the horizon. Presum-

ably such a loop, if formed, will annihilate itself on a timescale Δt of the order of the light travel time across the loop.

Because the mathematical details of Sections 2, 4, 5, and 6 may seem formidable at first sight (actually they are not because they closely mirror flat-space axisymmetric pulsar theory), readers may find it helpful to peruse the astrophysical sections of the paper (Sections 3 and 7) before going on to a more detailed reading.

Throughout this paper we use cgs and gaussian units ($\underset{\sim}{B}$ measured in Gauss, $\underset{\sim}{E}$ in statvolts per centimeter); and we use the terminology "equation (I,2.4)" to denote "equation (2.4) of Paper I (Thorne & Macdonald 1981)".

2 The Absolute-Space Formulation of Black-Hole Physics

2.1 THE MATHEMATICS OF ABSOLUTE SPACE

In the standard 4-dimensional spacetime formalism of general relativity, a stationary axisymmetric black hole is characterized by the spacetime geometry

$$ds^2 = -\alpha^2 c^2 dt^2 + \varpi^2 (d\phi - \omega dt)^2 + e^{2\mu_1} dr^2 + e^{2\mu_2} d\theta^2 \tag{2.1}$$

(see, e.g. Carter 1979, Bardeen 1973). Here the metric coefficients α, ϖ, ω, μ_1, and μ_2 are functions of r and θ, and c is the speed of light.

In our absolute-space formalism, the hole is characterized instead by an absolute 3-dimensional space with curved geometry

$$\begin{aligned} ds^2 &= \gamma_{jk}\, dx^j\, dx^k \\ &= \varpi^2 d\phi^2 + e^{2\mu_1} dr^2 + e^{2\mu_2} d\theta^2 \qquad \text{in above coordinates.} \end{aligned} \tag{2.2}$$

We denote by $\underset{\sim}{\nabla}\underset{\sim}{A}$ (components $A_{j|k}$) the gradient (covariant derivative) of a vector $\underset{\sim}{A}$ in this absolute space. The axial symmetry of the space is embodied

in the fact that ϖ, μ_1, and μ_2 are independent of ϕ — or, more abstractly, in the fact that $\underset{\sim}{m} = \varpi^2 \underset{\sim}{\nabla} \phi$ is a Killing vector field

$$\underset{\sim}{m} = \varpi^2 \underset{\sim}{\nabla} \phi \quad , \qquad m_{j|k} + m_{k|j} = 0 \quad . \tag{2.3}$$

Note that ϖ is the length of this Killing vector

$$\varpi \equiv |\underset{\sim}{m}| \ ; \tag{2.4}$$

i.e., $2\pi\varpi$ is the circumference of the circle of constant radius and latitude, (r,θ) = constant, to which $\underset{\sim}{m}$ is tangent. We shall call such circles "$\underset{\sim}{m}$-loops," and we shall call ϖ the "cylindrical radius" of an $\underset{\sim}{m}$-loop.

Going hand in hand with our absolute space is an absolute global time t [equal to the time coordinate t of the 4-dimensional spacetime metric (2.1)]. A vector field $\underset{\sim}{A}$ in absolute space can evolve with time: $\underset{\sim}{A} = \underset{\sim}{A}(\underset{\sim}{x},t)$. Its time derivative at fixed absolute-space location will be denoted

$$\dot{\underset{\sim}{A}} = \partial \underset{\sim}{A}/\partial t \quad , \qquad \dot{A}^j = \partial A^j/\partial t \quad . \tag{2.5}$$

[In the "3+1" formalism of paper I this derivative is denoted $\pounds_{t\sim} \underset{\sim}{A}$ (equations I,2.15 and I,5.5); it is the "Lie derivative" of $\underset{\sim}{A}$ along the spacetime Killing vector field $\mathbf{k} = \partial/\partial t$.]

Living in our absolute space is a family of fiducial observers called "zero-angular-momentum observers", or ZAMOs (Bardeen, Press & Teukolsky 1973). In our absolute-space formalism all the laws of physics are formulated in terms of physical quantities (observables) measured by the ZAMOs. For example, a particle with charge q and velocity $\underset{\sim}{v}$ as measured by the ZAMOs, moving through electric and magnetic fields $\underset{\sim}{E}$ and $\underset{\sim}{B}$ as measured by the ZAMOs, experiences a Lorentz force $q[\underset{\sim}{E} + (\underset{\sim}{v}/c) \times \underset{\sim}{B}]$; see Section 2.2.

If the black hole is nonrotating, then the ZAMOs are at rest relative to absolute space. However, rotation of the hole drags the ZAMOs into toroidal motion along $\underset{\sim}{m}$-loops; their angular velocity relative to absolute space is

$$(d\phi/dt)_{\text{of ZAMO rest frame}} = \omega \quad . \tag{2.6}$$

This ZAMO angular velocity ω is the same quantity that appears in the spacetime metric (2.1). When one adopts the 4-dimensional spacetime viewpoint (which we do not), one discovers that, despite the toroidal ZAMO motion $d\phi/dt = \omega$, the ZAMO world lines are orthogonal to the 3-dimensional hypersurfaces of constant time t — i.e., orthogonal to our absolute space; cf. equation (2.1). Thus, our absolute space at time t is regarded by the ZAMOs as a space of constant time in their local Lorentz frames.

If the black hole did not gravitate, the clock carried by a ZAMO would read absolute global time t. However, the gravity of the hole produces a gravitational redshift of ZAMO clocks; their lapse of proper time $d\tau$ is related to the lapse of global time dt by:

$$(d\tau/dt)_{\text{of ZAMO clock}} = \alpha \quad . \tag{2.7}$$

Here α, the "lapse function", is the same quantity that appears in the spacetime metric (2.1). The gravitational acceleration $\underset{\sim}{g}$ measured by a gravimeter carried by a ZAMO (which is the negative of the acceleration $\underset{\sim}{a}$ measured by his accelerometers) is (equation I,2.4)

$$\underset{\sim}{g} = -\underset{\sim}{a} = -c^2 \underset{\sim}{\nabla} \ln \alpha \quad . \tag{2.8}$$

Because absolute space is axially symmetric, the ZAMO angular velocity ω, the lapse function α, and the cylindrical radius function ϖ are all

constant on $\underset{\sim}{m}$-loops

$$\underset{\sim}{m}\cdot\underset{\sim}{\nabla}\omega = d\omega/d\phi = 0\ , \quad \underset{\sim}{m}\cdot\underset{\sim}{\nabla}\alpha = d\alpha/d\phi = 0\ , \quad \underset{\sim}{m}\cdot\underset{\sim}{\nabla}\varpi = d\varpi/d\phi = 0. \tag{2.9}$$

The horizon $\mathcal{H}$ of the black hole is the two-dimensional surface of infinite gravitational redshift, $\alpha = 0$. Everywhere on $\mathcal{H}$ the ZAMOs are dragged into motion with the uniform angular velocity Ω^H of the black hole (equations I,5.22a):

$$\alpha \to 0\ , \quad \omega \to \Omega^H \quad \text{at horizon } \mathcal{H}\ . \tag{2.10}$$

ZAMOs at the horizon feel an infinitely strong gravitational acceleration $\underset{\sim}{g}$. However, if one multiplies $\underset{\sim}{g}$ by $\alpha = d\tau/dt$ to convert the acceleration from a "per unit ZAMO proper time" basis to a "per unit global time" basis, one obtains a finite result (equation I,5.22b or page 252 of Bardeen 1973):

$$\alpha\underset{\sim}{g} \to -\kappa\underset{\sim}{n} \quad \text{at } \mathcal{H}\ . \tag{2.11}$$

Here $\underset{\sim}{n}$ is a unit vector pointing orthogonally out of $\mathcal{H}$, and κ is the "surface gravity" of the hole. (κ and Ω^H are both constant over $\mathcal{H}$, see e.g. Carter 1979). In calculations very near $\mathcal{H}$ it is useful to introduce a coordinate system (α,λ,ϕ) where $\lambda \equiv$ (proper distance along $\mathcal{H}$ from the north pole toward the equator). In this coordinate system the metric of absolute space reads (equation I,5.30)

$$ds^2 = (c^2/\kappa)^2\, d\alpha^2 + d\lambda^2 + \varpi^2\, d\phi^2 \quad \text{near } \mathcal{H}\ , \tag{2.12a}$$

and unit vectors along the "toroidal" (i.e., ϕ) direction, the "poloidal" (i.e., λ) direction, and the "normal" (i.e., α) direction are—in the notation of modern differential geometers—

$$\underset{\sim}{e}_{\hat{\phi}} = \frac{1}{\varpi}\frac{\partial}{\partial\phi} = \frac{1}{\varpi}\underset{\sim}{m} \quad , \quad \underset{\sim}{e}_{\hat{\lambda}} = \frac{\partial}{\partial\lambda} \quad , \quad \underset{\sim}{n} = \frac{\kappa}{c^2}\frac{\partial}{\partial\alpha} \quad . \tag{2.12b}$$

Observers freely falling into the hole move at the speed of light c relative to the infinitely accelerated ZAMOs at the horizon:

$$\frac{ds}{d\tau} = -\frac{(c^2/\kappa)\,d\alpha}{\alpha\,dt} = c \quad ;$$

consequently, they move along trajectories

$$\alpha = \text{const.} \times \exp(-\kappa t/c) \quad \text{near } \mathcal{H} \quad . \tag{2.13}$$

Because the infalling observers are physically nonpathological, all physical quantities which they measure must approach well-behaved limits along their trajectories. These limits are defined mathematically by

" $\longrightarrow$ " means "approaches, as one approaches the horizon along a time-evolving trajectory $\alpha = \text{const.} \times \exp(-\kappa t/c)$." (2.14)

(For further discussion see Section 5.3 of Paper I.)

For the special case of a nonrotating Schwarzschild black hole of mass M and a Schwarzschild spatial coordinate system, the quantities appearing in the above discussion are:

$$ds^2 = (1 - 2GM/c^2r)^{-1}\,dr^2 + r^2d\theta^2 + r^2\sin^2\theta\;d\phi^2 \quad ;$$

$$\alpha = (1 - 2GM/c^2r)^{1/2} \quad , \quad \omega = 0 \quad , \quad \varpi = r\sin\theta;$$

$$\underset{\sim}{g} = -\frac{GM/r^2}{(1 - 2GM/c^2r)^{1/2}}\,\underset{\sim}{e}_{\hat{r}} \quad \text{with } \underset{\sim}{e}_{\hat{r}} \equiv \left(1 - \frac{2GM}{c^2r}\right)^{1/2}\frac{\partial}{\partial r} = \text{(unit radial vector)}; \tag{2.15}$$

$\mathcal{H}$ is at $r = 2GM/c^2$; there $\kappa = c^4/4GM$, $\Omega^H = 0$, $\underset{\sim}{n} = \underset{\sim}{e}_{\hat{r}}$;

$$\lambda = (2GM/c^2)\theta \quad \text{near } \mathcal{H} \quad ;$$

$$\alpha = \text{const.} \times \exp(-\kappa t/c) \iff r - 2M = \text{const.} \times \exp(-c^3t/2GM)$$

for freely falling observers near $\mathcal{H}$.

Here G is Newton's gravitational constant.

For the special case of a rotating Kerr black hole of mass M and angular momentum per unit mass $a \equiv L^H/Mc$, and a Boyer-Lindquist spatial coordinate system:

$$ds^2 = (\rho^2/\Delta)dr^2 + \rho^2 d\theta^2 + (A \sin^2\theta/\rho^2)d\phi^2 \quad ,$$

$$\rho^2 \equiv r^2 + a^2\cos^2\theta \quad , \quad \Delta \equiv r^2 - 2GMr/c^2 + a^2 \quad , \quad A \equiv (r^2+a^2)^2 - a^2\Delta \sin^2\theta \ ;$$

$$\alpha = (\rho^2\Delta/A)^{1/2} \quad , \quad \omega = 2aGMr/cA \quad , \quad \varpi = (A/\rho^2)^{1/2}\sin\theta \ ;$$

$$\underset{\sim}{g} = -\frac{c^2 A}{2\rho^3\Delta}\left[\Delta^{1/2}\frac{\partial}{\partial r}\left(\frac{\rho^2\Delta}{A}\right)\underset{\sim}{e}_{\hat{r}} + \frac{\partial}{\partial\theta}\left(\frac{\rho^2\Delta}{A}\right)\underset{\sim}{e}_{\hat{\theta}}\right]$$

with $\underset{\sim}{e}_{\hat{r}} \equiv (\Delta^{1/2}/\rho)\,\partial/\partial r$ and $\underset{\sim}{e}_{\hat{\theta}} \equiv (1/\rho)\,\partial/\partial\theta$ unit vectors ;

$\mathcal{H}$ is at $r = r_+ \equiv GM/c^2 + [(GM/c^2)^2 - a^2]^{1/2}$;

$$\text{At } \mathcal{H}, \ \kappa = c^4(r_+ - GM/c^2)/2GMr_+ \ , \ \Omega^H = c^3 a/2GMr_+ \ , \ \underset{\sim}{n} = \underset{\sim}{e}_{\hat{r}} \ ; \qquad (2.16)$$

$$\lambda = \int_0^\theta (r_+^2 + a^2\cos^2\theta)^{1/2} d\theta = (r_+^2 + a^2)^{1/2}\, E[\theta, \ a/(r_+^2 + a^2)^{1/2}] \text{ near } \mathcal{H} \ ,$$

with E ≡ (elliptic integral of the second kind) ;

$$\alpha = \text{const.} \times \exp(-\kappa t/c) \iff r - r_+ = \text{const.} \times \exp[-c^3 t(r_+ - GM/c^2)/GMr_+]$$

for freely falling observers near $\mathcal{H}$.

Our absolute-space formalism is also applicable to stationary, axially symmetric black holes whose spatial metric γ_{jk}, lapse function α, and ZAMO angular velocity ω are modified away from Kerr by the gravitational effects of surrounding matter.

2.2 ELECTRODYNAMICS IN ABSOLUTE SPACE

When studying electrodynamic phenomena around black holes we deal with the electric field $\underset{\sim}{E}$, the magnetic field $\underset{\sim}{B}$, the electric charge density ρ_e,

and the current density $\underset{\sim}{j}$, all as measured by the ZAMOs. In terms of these quantities, Maxwell's equations are (equations I,5.8)

$$\underset{\sim}{\nabla} \cdot \underset{\sim}{E} = 4\pi \rho_e \quad , \tag{2.17a}$$

$$\underset{\sim}{\nabla} \cdot \underset{\sim}{B} = 0 \quad , \tag{2.17b}$$

$$\underset{\sim}{\nabla} \times (\alpha \underset{\sim}{B}) = 4\pi\alpha \underset{\sim}{j}/c + (1/c)[\dot{\underset{\sim}{E}} + \omega \pounds_{\underset{\sim}{m}} \underset{\sim}{E} - (\underset{\sim}{E} \cdot \underset{\sim}{\nabla}\omega)\underset{\sim}{m}] \quad , \tag{2.17c}$$

$$\underset{\sim}{\nabla} \times (\alpha \underset{\sim}{E}) = -(1/c)[\dot{\underset{\sim}{B}} + \omega \pounds_{\underset{\sim}{m}} \underset{\sim}{B} - (\underset{\sim}{B} \cdot \underset{\sim}{\nabla}\omega)\underset{\sim}{m}] \quad . \tag{2.17d}$$

Here $\pounds_{\underset{\sim}{m}} \underset{\sim}{E}$ is the "Lie derivative" of $\underset{\sim}{E}$ along the toroidal Killing vector $\underset{\sim}{m}$

$$\pounds_{\underset{\sim}{m}} \underset{\sim}{E} \equiv (\underset{\sim}{m} \cdot \underset{\sim}{\nabla})\underset{\sim}{E} - (\underset{\sim}{E} \cdot \underset{\sim}{\nabla})\underset{\sim}{m} \quad . \tag{2.18}$$

Notice that the unfamiliar expression in square brackets

$$\dot{\underset{\sim}{E}} + \omega \pounds_{\underset{\sim}{m}} \underset{\sim}{E} - (\underset{\sim}{E} \cdot \underset{\sim}{\nabla}\omega)\underset{\sim}{m} = \partial \underset{\sim}{E}/\partial t + \pounds_{\omega \underset{\sim}{m}} \underset{\sim}{E} \tag{2.19}$$

is just the "Lie-type" time derivative, moving with the ZAMOs ($d\underset{\sim}{x}/dt = \omega \underset{\sim}{m}$), of the electric field. When the electric and magnetic fields are stationary and axisymmetric, the terms $\dot{\underset{\sim}{E}}$, $\pounds_{\underset{\sim}{m}} \underset{\sim}{E}$, $\dot{\underset{\sim}{B}}$, and $\pounds_{\underset{\sim}{m}} \underset{\sim}{B}$ will vanish. Notice also that the lapse function α is introduced to convert the curl and current terms in (2.17) over to the same "per unit global time t" basis as the time derivative terms. The fields $\alpha \underset{\sim}{E}$ and $\alpha \underset{\sim}{B}$, which we shall meet extensively below, are the electric and magnetic fields measured by ZAMOs, if the ZAMOs use global time t rather than ZAMO proper time τ in computing the rate of change of momenta:

$$(d\underset{\sim}{p}/dt)_{\text{Lorentz force}} = \alpha\,(d\underset{\sim}{p}/d\tau) = q(\alpha \underset{\sim}{E} + \underset{\sim}{v} \times \alpha \underset{\sim}{B}) \quad .$$

The four Maxwell equations (2.17) can be reexpressed in integral form (equations I,4.1 - I,4.4)

$$\int_{\partial \mathcal{V}} \underset{\sim}{E} \cdot d\underset{\sim}{\Sigma} = 4\pi \int_{\mathcal{V}} \rho_e \, dV \qquad \text{(Gauss's law for } \underset{\sim}{E}) \quad , \tag{2.20a}$$

$$\int_{\partial \mathcal{V}} \underset{\sim}{B} \cdot d\underset{\sim}{\Sigma} = 0 \qquad \text{(Gauss's law for } \underset{\sim}{B}) \quad , \tag{2.20b}$$

$$\int_{\partial\mathcal{A}(t)} \alpha(\underset{\sim}{B} - \frac{1}{c}\underset{\sim}{v}\times\underset{\sim}{E})\cdot d\underset{\sim}{\ell} = \frac{1}{c}\frac{d}{dt}\int_{\mathcal{A}(t)} \underset{\sim}{E}\cdot d\underset{\sim}{\Sigma} + \frac{4\pi}{c}\int_{\mathcal{A}(t)} \alpha(\underset{\sim}{j} - \rho_e\underset{\sim}{v})\cdot d\underset{\sim}{\Sigma}$$

(Ampere's law) , (2.20c)

$$\int_{\partial\mathcal{A}(t)} \alpha(\underset{\sim}{E}+\frac{1}{c}\underset{\sim}{v}\times\underset{\sim}{B})\cdot d\underset{\sim}{\ell} = -\frac{1}{c}\frac{d}{dt}\int_{\mathcal{A}(t)} \underset{\sim}{B}\cdot d\underset{\sim}{\Sigma}$$ (Faraday's law) . (2.20d)

Here $\mathcal{V}$ is any 3-dimensional volume entirely outside the horizon and $\partial\mathcal{V}$ is its 2-dimensional boundary; dV = d(proper volume) and $d\underset{\sim}{\Sigma}$ = (outward pointing unit normal to $\partial\mathcal{V}$)d(proper area). Also $\mathcal{A}(t)$ is any 2-dimensional surface entirely outside the horizon and $\partial\mathcal{A}(t)$ is its boundary curve; $d\underset{\sim}{\ell}$ = d(proper distance along boundary curve); and the orientations of $d\underset{\sim}{\Sigma}$ and $d\underset{\sim}{\ell}$ must be chosen in accordance with the right-hand rule. Finally, $\underset{\sim}{v}$ is the physical velocity

$$\underset{\sim}{v} = \left[\frac{d(\text{proper distance})}{d\tau}\right]_{\text{relative to ZAMOs}}$$ (2.21a)

of a point on $\mathcal{A}(t)$ or $\partial\mathcal{A}(t)$, relative to and as measured by the ZAMOs. (Thus

$$\alpha\underset{\sim}{v} + \omega\underset{\sim}{m} = \left[\frac{d(\text{proper distance})}{dt}\right]_{\text{relative to absolute space}}$$ (2.21b)

is the velocity, per unit global time, relative to absolute space.)

The Maxwell equations (2.17) imply the differential law of charge conservation (equation I,5.11)

$$\partial\rho_e/\partial t + \omega\underset{\sim}{m}\cdot\underset{\sim}{\nabla}\rho_e + \underset{\sim}{\nabla}\cdot(\alpha\underset{\sim}{j}) = 0 \quad .$$ (2.22)

Note that $\partial/\partial t + \omega\underset{\sim}{m}\cdot\underset{\sim}{\nabla}$ is the global time derivative along the ZAMO

trajectories (where ρ_e and $\underset{\sim}{j}$ are measured), and the factor α converts $\underset{\sim}{j}$ over from "charge per unit area per unit proper time τ" to "charge per unit area per unit global time t." The integral formulation of this law of charge conservation is (equation I,4.5)

$$\frac{d}{dt}\int_{\mathcal{V}(t)} \rho_e \, dV = -\int_{\partial\mathcal{V}(t)} \alpha(\underset{\sim}{j} - \rho_e \underset{\sim}{v}) \cdot d\underset{\sim}{\Sigma} \quad . \tag{2.23}$$

The electric and magnetic fields can be derived from a scalar potential A_0 and a vector potential $\underset{\sim}{A}$ (equations I,5.9)

$$\underset{\sim}{E} = \alpha^{-1}[\underset{\sim}{\nabla} A_0 + (\omega/c)\underset{\sim}{\nabla} A_\phi] - (\alpha c)^{-1}(\dot{\underset{\sim}{A}} + \omega \pounds_{\underset{\sim}{m}} \underset{\sim}{A}) \tag{2.24a}$$

where $A_\phi \equiv \underset{\sim}{A} \cdot \underset{\sim}{m}$,

$$\underset{\sim}{B} = \underset{\sim}{\nabla} \times \underset{\sim}{A} \quad . \tag{2.24b}$$

When these expressions are used, the source-free Maxwell equations (2.17b,d) are automatically satisfied.

A test particle of charge q and rest mass μ, moving through absolute space, obeys the equation of motion (equation I,5.12)

$$\alpha^{-1}[\partial/\partial t + (\alpha \underset{\sim}{v} + \omega \underset{\sim}{m}) \cdot \underset{\sim}{\nabla}]\underset{\sim}{p} =$$

$$= \mu\Gamma \underset{\sim}{g} + \alpha^{-1}[\omega(\underset{\sim}{p} \cdot \underset{\sim}{\nabla})\underset{\sim}{m} - (\underset{\sim}{p} \cdot \underset{\sim}{m})\underset{\sim}{\nabla}\omega] + q[\underset{\sim}{E} + (\underset{\sim}{v}/c) \times \underset{\sim}{B}] \quad . \tag{2.25}$$

Here $\underset{\sim}{v}$ is the particle's physical velocity relative to the ZAMOs (Eq. 2.21); $\mu\Gamma$ is its mass-energy, and $\underset{\sim}{p}$ its momentum as measured by the ZAMOs

$$\Gamma \equiv \left(1 - \frac{\underset{\sim}{v}^2}{c^2}\right)^{-1/2} \quad , \qquad \underset{\sim}{p} = \mu\Gamma \underset{\sim}{v} \quad ; \tag{2.26}$$

$\alpha^{-1}[\partial/\partial t + (\alpha \underset{\sim}{v} + \omega \underset{\sim}{m}) \cdot \underset{\sim}{\nabla}]$ is the ZAMO proper time derivative moving with the

particle; $\mu\Gamma\,\underset{\sim}{g}$ is the "gravitational acceleration" of the hole on the particle; $\alpha^{-1}[\omega(\underset{\sim}{p}\cdot\nabla)\underset{\sim}{m} - (\underset{\sim}{p}\cdot\underset{\sim}{m})\nabla\omega]$ is the "frame-dragging" force of the hole's rotation on the particle; and $q[\underset{\sim}{E} + (\underset{\sim}{v}/c)\times\underset{\sim}{B}]$ is the Lorentz force.

The ZAMOs will characterize the electromagnetic field and/or any continuous medium present by

$\varepsilon \equiv$ (total mass-energy density, erg/cm^3, as measured by ZAMOs) ,

$\underset{\sim}{S} \equiv$ (total flux of energy, erg/cm^{2}sec, as measured by ZAMOs) ,

$\underset{\sim}{W} \equiv$ (stress tensor, dyne/cm^2, as measured by ZAMOs). (2.27)

In terms of these we can also define densities and fluxes of "redshifted energy" (also often called "energy-at-infinity"), and of "angular momentum about the hole's symmetry axis" (equations I,5.15 and I,5.16)

$$\varepsilon_E \equiv \alpha\varepsilon + \omega\underset{\sim}{S}\cdot\underset{\sim}{m}/c^2 \quad , \qquad \underset{\sim}{S}_E \equiv \alpha\underset{\sim}{S} + \omega\underset{\sim}{W}\cdot\underset{\sim}{m} \quad , \tag{2.28a}$$

$$\varepsilon_L \equiv \underset{\sim}{S}\cdot\underset{\sim}{m}/c^2 \quad , \qquad \underset{\sim}{S}_L \equiv \underset{\sim}{W}\cdot\underset{\sim}{m} \quad . \tag{2.28b}$$

For the electromagnetic field

$$\varepsilon = (1/8\pi)(\underset{\sim}{E}^2 + \underset{\sim}{B}^2) \quad , \qquad \underset{\sim}{S} = (c/4\pi)(\underset{\sim}{E}\times\underset{\sim}{B}) \quad , \tag{2.29a}$$

$$\underset{\sim}{W} = (1/4\pi)[-(\underset{\sim}{E}\otimes\underset{\sim}{E} + \underset{\sim}{B}\otimes\underset{\sim}{B}) + \tfrac{1}{2}(\underset{\sim}{E}^2 + \underset{\sim}{B}^2)\underset{\sim}{\gamma}] \ ; \tag{2.29b}$$

$$\varepsilon_E = (\alpha/8\pi)(\underset{\sim}{E}^2 + \underset{\sim}{B}^2) + (\omega/4\pi c)(\underset{\sim}{E}\times\underset{\sim}{B})\cdot\underset{\sim}{m} \quad , \tag{2.30a}$$

$$\underset{\sim}{S}_E = (1/4\pi)[\alpha c\,\underset{\sim}{E}\times\underset{\sim}{B} - \omega(\underset{\sim}{E}\cdot\underset{\sim}{m})\underset{\sim}{E} - \omega(\underset{\sim}{B}\cdot\underset{\sim}{m})\underset{\sim}{B} - \tfrac{1}{2}\omega(\underset{\sim}{E}^2 + \underset{\sim}{B}^2)\underset{\sim}{m}] \ ; \tag{2.30b}$$

$$\varepsilon_L = (1/4\pi c)(\underset{\sim}{E}\times\underset{\sim}{B})\cdot\underset{\sim}{m} \quad , \tag{2.31a}$$

$$\underset{\sim}{S}_L = (1/4\pi)[-(\underset{\sim}{E}\cdot\underset{\sim}{m})\underset{\sim}{E} - (\underset{\sim}{B}\cdot\underset{\sim}{m})\underset{\sim}{B} + \tfrac{1}{2}(\underset{\sim}{E}^2 + \underset{\sim}{B}^2)\underset{\sim}{m}] \quad . \tag{2.31b}$$

For a perfect fluid with density of mass-energy ρ (erg/cm^3) and pressure p (dyne/cm^2) as measured in its own rest frame, and with velocity $\underset{\sim}{v}$ as measured by the ZAMOs,

$$\varepsilon = \Gamma^2(\rho + p\underset{\sim}{v}^2/c^2) \quad , \qquad \underset{\sim}{S} = (\rho + p)\Gamma^2\underset{\sim}{v} \quad , \tag{2.32a}$$

$$\underset{\sim}{W} = (1/c^2)(\rho + p)\Gamma^2\ \underset{\sim}{v}\otimes\underset{\sim}{v} + p\underset{\sim}{\gamma} \quad , \quad \Gamma \equiv (1 - \underset{\sim}{v}^2/c^2)^{-1/2} \quad . \tag{2.32b}$$

The law of local energy balance as formulated by the ZAMOs is (equation I,5.13)

$$\alpha^{-1}[\partial/\partial t + \omega\underset{\sim}{m}\cdot\underset{\sim}{\nabla}]\varepsilon + \alpha^{-2}\underset{\sim}{\nabla}\cdot(\alpha^2\underset{\sim}{S}) + \alpha^{-1}\underset{\sim}{m}\cdot\underset{\sim}{W}\cdot\underset{\sim}{\nabla}\omega$$

$$= 0 \quad \text{if all forms of energy and stress are included in } \varepsilon,\ \underset{\sim}{S},\ \underset{\sim}{W}$$

$$= -\underset{\sim}{j}\cdot\underset{\sim}{E} \quad \text{if only electromagnetic contributions are included in } \varepsilon,\ \underset{\sim}{S},\ \underset{\sim}{W}. \tag{2.33a}$$

(The third term on the left side of the equation is caused by the shear of the ZAMO trajectories relative to each other.) The law of local momentum balance (force balance) as formulated by the ZAMOs is (equation I,5.14)

$$\alpha^{-1}[\partial/\partial t + \omega\pounds_{\underset{\sim}{m}}]\underset{\sim}{S} + \alpha^{-1}(\underset{\sim}{S}\cdot\underset{\sim}{m})\underset{\sim}{\nabla}\omega - \varepsilon\underset{\sim}{g} + c^2\alpha^{-1}\underset{\sim}{\nabla}\cdot(\alpha\underset{\sim}{W})$$

$$= 0 \quad \text{if all stress and energy are included in } \underset{\sim}{S} \text{ and } \underset{\sim}{W}$$

$$= -c^2[\rho_e\underset{\sim}{E} + (\underset{\sim}{j}/c)\times\underset{\sim}{B}] \quad \text{if only electromagnetism is included.} \tag{2.33b}$$

(The test-particle equation of motion (2.25) can be derived in the usual way from this general force-balance equation.) From the laws of energy balance and force balance one can derive differential and integral conservation laws for redshifted energy and for angular momentum (equations I,5.17 and I,5.18)

$$\alpha^{-1}(\partial/\partial t + \omega \underset{\sim}{m} \cdot \underset{\sim}{\nabla})\varepsilon_E + \alpha^{-1}\underset{\sim}{\nabla} \cdot (\alpha \underset{\sim}{S}_E) = 0 \qquad \text{if all included}$$

$$= -\alpha \underset{\sim}{j} \cdot \underset{\sim}{E} - \omega[\rho_e \underset{\sim}{E} + (\underset{\sim}{j}/c) \times \underset{\sim}{B}] \cdot \underset{\sim}{m} \qquad \text{if only electromagnetism,} \tag{2.34a}$$

$$\alpha^{-1}(\partial/\partial t + \omega \underset{\sim}{m} \cdot \underset{\sim}{\nabla})\varepsilon_L + \alpha^{-1}\underset{\sim}{\nabla} \cdot (\alpha \underset{\sim}{S}_L) = 0 \qquad \text{if all included}$$

$$= -[\rho_e \underset{\sim}{E} + (\underset{\sim}{j}/c) \times \underset{\sim}{B}] \cdot \underset{\sim}{m} \qquad \text{if only electromagnetism;} \tag{2.34b}$$

$$\frac{d}{dt}\int_{\mathcal{V}(t)} \varepsilon_E \, dV + \int_{\partial\mathcal{V}(t)} \alpha(\underset{\sim}{S}_E - \varepsilon_E \underset{\sim}{v}) \cdot d\underset{\sim}{\Sigma} = 0 \qquad \text{if all included}$$

$$= -\int_{\mathcal{V}(t)} \{\alpha^2 \underset{\sim}{j} \cdot \underset{\sim}{E} + \alpha\omega[\rho_e \underset{\sim}{E} + (\underset{\sim}{j}/c) \times \underset{\sim}{B}] \cdot \underset{\sim}{m}\} dV \quad \text{if only electromagnetism,} \tag{2.35a}$$

$$\frac{d}{dt}\int_{\mathcal{V}(t)} \varepsilon_L \, dV + \int_{\partial\mathcal{V}(t)} \alpha(\underset{\sim}{S}_L - \varepsilon_L \underset{\sim}{v}) \cdot d\underset{\sim}{\Sigma} = 0 \qquad \text{if all included}$$

$$= -\int_{\mathcal{V}(t)} \alpha[\rho_e \underset{\sim}{E} + (\underset{\sim}{j}/c) \times \underset{\sim}{B}] \cdot \underset{\sim}{m} \, dV \qquad \text{if only electromagnetism.} \tag{2.35b}$$

Far from the black hole space becomes flat, the lapse function α becomes unity, the ZAMO angular velocity ω goes to zero; and, consequently, our formalism reduces to standard flat-space physics in a global Lorentz frame—the rest frame of the hole. In the asymptotically flat region redshifted energy reduces to ordinary, every-day energy.

2.3 BOUNDARY CONDITIONS AT THE HORIZON

Znajek (1978b) and Damour (1978) have developed an elegant formalism for studying the boundary conditions at the horizon by defining surface charge and current densities lying in the horizon. (For a beautiful review of this work

see Carter 1979.) This formalism can be expressed naturally in the language of absolute space and universal time, where the horizon is just the two-dimensional surface $\alpha = 0$ (see Section 5.4 of Paper I). The horizon's charge density

$$\sigma^H = (\text{charge per unit area on } \mathcal{H}) \tag{2.36}$$

and current density

$$\underset{\sim}{\mathcal{J}}^H = \begin{pmatrix}\text{charge crossing a unit length perpendicular} \\ \text{to } \underset{\sim}{\mathcal{J}}^H \text{ on } \mathcal{H}, \text{ per unit global time } t\end{pmatrix} \tag{2.37}$$

have these properties: (i) σ^H terminates all electric flux that intersects the horizon (equation I,5.42)

$$\underset{\sim}{E} \cdot \underset{\sim}{n} \equiv E_{\perp} \longrightarrow 4\pi\sigma^H \qquad \text{(Gauss's law at } \mathcal{H}), \tag{2.38}$$

(where $\underset{\sim}{n}$ is the unit outward normal to the horizon and "$\longrightarrow$" means "approaches as one approaches the horizon in the manner of equation 2.14"); (ii) $\underset{\sim}{\mathcal{J}}^H$ completes the circuit of all electric currents that intersect the horizon (equation I,5.44)

$$\alpha \underset{\sim}{j} \cdot \underset{\sim}{n} \longrightarrow - \partial\sigma^H/\partial t - {}^{(2)}\underset{\sim}{\nabla} \cdot \underset{\sim}{\mathcal{J}}^H \qquad \text{(charge conservation at } \mathcal{H}), \tag{2.39}$$

(where ${}^{(2)}\underset{\sim}{\nabla} \cdot \underset{\sim}{\mathcal{J}}^H$ is the two-dimensional divergence of the surface current in the 2-dimensional geometry of the horizon); (iii) $\underset{\sim}{\mathcal{J}}^H$ terminates all tangential magnetic fields at the horizon (equation I,5.43)

$$\alpha \underset{\sim}{B}_{\parallel} \longrightarrow \underset{\sim}{B}^H \equiv (4\pi/c)\underset{\sim}{\mathcal{J}}^H \times \underset{\sim}{n} \qquad \text{(Ampere's law at } \mathcal{H}) \tag{2.40}$$

(where $\underset{\sim}{B}_{\parallel}$ is the component of the magnetic field tangential to the horizon, and $\alpha \underset{\sim}{B}_{\parallel}$ is this tangential field converted over to a "per unit global time" basis); (iv) the horizon has a surface resistivity

$$R^H = 4\pi/c = 377 \text{ ohms} \tag{2.41}$$

in the sense that (equations I,5.41 and I,5.37a)

$$\alpha \underset{\sim}{E}_{\|} \longrightarrow \underset{\sim}{E}^H \equiv R^H \underset{\sim}{\mathcal{J}}^H \qquad \text{(Ohm's law in } \mathcal{H}\text{)} \qquad (2.42)$$

(where $\underset{\sim}{E}_{\|}$ is the component of the electric field tangential to the horizon and $\alpha\underset{\sim}{E}_{\|}$ is this tangential field converted to a "per unit global time" basis). [Note that the "horizon fields" $\underset{\sim}{E}^H$ and $\underset{\sim}{B}^H$ of this paper are the same as the $\underset{\sim}{E}^H_{\|}$ and $\underset{\sim}{B}^H_{\|}$ of Paper I — i.e., in passing from Paper I to this paper we have deleted the null components $E^H_{\perp\underset{\sim}{\ell}}$ and $B^H_{\perp\underset{\sim}{\ell}}$ from $\underset{\sim}{E}^H$ and $\underset{\sim}{B}^H$ (equation I,5.36).]

Because $\underset{\sim}{E}^H$ and $\underset{\sim}{B}^H$ must be finite and because $\alpha \to 0$ at $\mathcal{H}$, the tangential fields $\underset{\sim}{E}_{\|}$ and $\underset{\sim}{B}_{\|}$ can diverge at $\mathcal{H}$ as $1/\alpha$. By contrast, the normal fields $B_\perp \equiv \underset{\sim}{B}\cdot\underset{\sim}{n}$ and $E_\perp \equiv \underset{\sim}{E}\cdot\underset{\sim}{n}$ must be finite (Section 5.4 of Paper I). The fact that R^H is an impedance equal to that of free space at the end of an open waveguide, together with Ohm's law (2.42) and Ampere's law (2.40), guarantees that the electromagnetic field looks to ZAMOs near the horizon like an infinitely blue shifted, ingoing electromagnetic plane wave:

$$E_\perp \text{ and } B_\perp \text{ finite at } \mathcal{H} \quad , \qquad (2.43a)$$

$$\underset{\sim}{E}_{\|} \text{ and } \underset{\sim}{B}_{\|} \text{ diverge as } 1/\alpha \text{ at } \mathcal{H} \quad , \qquad (2.43b)$$

$$\left|\underset{\sim}{E}_{\|} - \underset{\sim}{n}\times\underset{\sim}{B}_{\|}\right| \text{ goes to zero as } \alpha \text{ at } \mathcal{H} \, . \qquad (2.43c)$$

[A derivation of the rate at which $\left|\underset{\sim}{E}_{\|} - \underset{\sim}{n}\times\underset{\sim}{B}_{\|}\right|$ goes to zero is sketched in the paragraph preceding equation (I,5.38).]

The electromagnetic field produces a torque per unit area on the hole's horizon given by (cf. equations 2.31b, 2.38, 2.40, 2.42; also I,5.46)

$$-\alpha\underset{\sim}{S}_L\cdot\underset{\sim}{n} \longrightarrow \frac{d(\text{angular momentum of hole})}{d(\text{area of horizon})\,dt} \equiv \frac{dL^H}{d\Sigma^H dt}$$

$$= [\sigma^H\underset{\sim}{E}^H + (\underset{\sim}{\mathcal{J}}^H/c)\times\underset{\sim}{B}_\perp]\cdot\underset{\sim}{m} \, . \qquad (2.44)$$

Here $\underset{\sim}{B}_\perp \equiv B_\perp \underset{\sim}{n}$ is the component of $\underset{\sim}{B}$ perpendicular to $\mathcal{H}$. The fields also increase the hole's entropy by Joule heating (equation I,5.48)

$$\Theta^H \frac{dS^H}{d\Sigma^H dt} = \underset{\sim}{\mathcal{J}}^H \cdot \underset{\sim}{E}^H \quad , \tag{2.45}$$

where $\Theta^H = (\hbar/2\pi kc)\kappa$ is the hole's temperature and $S^H = (c^3 k/4\hbar G) \times$ (area of horizon) is its entropy (Hawking 1976). Here k is Boltzmann's constant and $\hbar$ is Planck's constant. Finally, the fields increase the hole's mass at a rate given by the thermodynamic law $dM^H c^2 = \Omega^H dL^H + \Theta^H dS^H$ — and given equally well by the relation $dM^H c^2 =$ d(redshifted energy entering the hole)

$$-\alpha \underset{\sim}{S}_E \cdot \underset{\sim}{n} \longrightarrow \frac{dM^H c^2}{d\Sigma^H dt} \equiv -\frac{dP^H}{d\Sigma^H} = \frac{\Omega^H dL^H + \Theta^H dS^H}{d\Sigma^H dt}$$

$$= \Omega^H [\sigma^H \underset{\sim}{E}^H + (\underset{\sim}{\mathcal{J}}^H/c) \times \underset{\sim}{B}_\perp] \cdot \underset{\sim}{m} + \underset{\sim}{E}^H \cdot \underset{\sim}{\mathcal{J}}^H \quad . \tag{2.46}$$

(cf. equations 2.10, 2.30b, 2.38, 2.40, 2.42; also 2.44, 2.45; also I,5.47). Here $dP/d\Sigma^H$ is the redshifted energy per unit time t per unit area (i.e., the redshifted power per unit area) flowing out of the hole.

3 Overview of Black-Hole and Accretion-Disk Electrodynamics

Consider a black hole surrounded by an accretion disk in which a magnetic field is embedded (Fig. 1). Initially make no simplifying assumptions about the disk and its magnetosphere: Let them evolve dynamically; let them have no axial symmetry; admit the possibility that the fields near the hole may be so strong that classical electromagnetic theory must be replaced by quantum electrodynamics, and so tangled that the field lines slip through the disk's plasma and reconnect. On the other hand, insist that far from the hole the field be weak enough to

be described classically, and that in the equatorial plane far from the hole the field be frozen into the disk's plasma (perfect magnetohydrodynamic approximation).

We can get insight into the structure and evolution of the magnetic field by applying our curved-space Faraday law (2.20d) to the 2-dimensional surface $\mathcal{A}$ shown in Figure 1. The boundary $\partial\mathcal{A}$ of this surface is an $\underset{\sim}{m}$-loop (circle of constant r and θ) in the equatorial plane, at a sufficiently large radius for the field to be frozen in and classical. The surface $\mathcal{A}$ stretches upward from this anchoring curve and over the hole's north pole like a circus tent — remaining always at a sufficiently large radius for classical theory to apply, and remaining everywhere axially symmetric. Require that $\mathcal{A}$ be fixed in space — or, equivalently since $\mathcal{A}$ is axially symmetric, that it be attached to and move toroidally with the ZAMOs.

Faraday's law (2.20d), applied to $\mathcal{A}$ and $\partial\mathcal{A}$, says

$$d\Phi_{\mathcal{A}}/dt = -c \int_{\partial\mathcal{A}} \alpha \underset{\sim}{E} \cdot d\underset{\sim}{\ell} \quad , \tag{3.1}$$

where $\Phi_{\mathcal{A}}$ is the magnetic flux crossing $\mathcal{A}$. The EMF on the right-hand side can be reexpressed in terms of the magnetic field $\underset{\sim}{B}$ by invoking the freezing-in condition

$$\underset{\sim}{E} + (\underset{\sim}{v}/c) \times \underset{\sim}{B} = 0 \qquad \text{in the disk at } \partial\mathcal{A} \quad , \tag{3.2}$$

where $\underset{\sim}{v}$ is the velocity of the disk's plasma as measured by the ZAMOs:

$$d\Phi_{\mathcal{A}}/dt = \int_{\partial\mathcal{A}} \alpha \underset{\sim}{v} \times \underset{\sim}{B} \cdot d\underset{\sim}{\ell} \quad . \tag{3.3}$$

The right-hand side has an obvious physical interpretation as the rate (per unit global time t) at which the plasma carries magnetic flux inward across

$\partial\mathcal{A}$. Thus, magnetic flux is conserved in time; the flux across $\mathcal{A}$ can increase or decrease only as a result of field lines being physically transported inward or outward across $\partial\mathcal{A}$.

Consider, now, the fate of the magnetic field lines being transported in toward the hole by the accretion disk's plasma: As the plasma reaches the inner edge of the disk and then spirals down the hole, it becomes causally disconnected from the field lines it was transporting. This does not liberate the transported field, however. Our flux conservation law guarantees that the field lines, though disconnected from their sources, cannot escape. They are squeezed inward and are forced to thread the hole by the Maxwell pressure of surrounding field lines, which in turn are anchored in the disk. (An exception is a field line such as b in Fig. 1, which will annihilate itself once the disk has deposited both its feet onto the hole; see Section 7.5.) If the disk's conductivity were suddenly turned off, the field anchored in it would suddenly fly away, releasing its Maxwell pressure from the field lines threading the hole. The hole's gravity has little power to hold the threading field; with the Maxwell pressures gone it would quickly disperse as well ["Price's theorem"; Price (1972)].

In the remainder of this paper we shall assume that an accretion-disk-plus-magnetic-field structure like that in Figure 1 has been set up, and that the electric and magnetic fields are weak enough for classical electrodynamics to be a good approximation. We shall assume, further, that the disk and its fields have settled down into a stationary, axisymmetric state. In the next three sections, we shall consider the electrodynamic equations for successively more specialized field configurations. Section 4 considers situations where the electromagnetic field is stationary and axisymmetric, but not otherwise special; section 5 specializes to the case where the field is degenerate; and section 6 specializes still further to the case where the field is force-free.

In section 7 these three cases are put together into a coherent model of the fields in the disk and its magnetosphere.

4 Stationary, Axisymmetric Electrodynamics

4.1 OUTSIDE THE HORIZON

We now specialize the electrodynamic equations of section 2 to fields and charge-current distributions that are stationary and axisymmetric:

$$\partial \underset{\sim}{F}/\partial t \equiv \dot{\underset{\sim}{F}} = 0 \quad , \qquad \pounds_{\underset{\sim}{m}} \underset{\sim}{F} = 0 \qquad \text{for all vector fields, } \underset{\sim}{F} \ ,$$
$$\partial f/\partial t \equiv \dot{f} = 0 \quad , \qquad \underset{\sim}{m}\cdot\nabla f = 0 \qquad \text{for all scalar fields, } f \ . \tag{4.1}$$

This specialization simplifies the theory so much that the electric field $\underset{\sim}{E}$, the magnetic field $\underset{\sim}{B}$, the charge density ρ_e, and the current density $\underset{\sim}{j}$ can all be derived from three freely-specifiable scalar potentials. (Put differently: given stationary, axisymmetric distributions of ρ_e and $\underset{\sim}{j}$ satisfying charge conservation $\nabla\cdot(\alpha\underset{\sim}{j}) = 0$, the 3 independent functions in ρ_e and $\underset{\sim}{j}$ determine via Maxwell's equations 3 independent potentials, from which $\underset{\sim}{E}$ and $\underset{\sim}{B}$ can be computed by differentiation.)

We shall choose as our potentials A_0, the electrical potential of equation (2.24a); I, the total current passing downward through an $\underset{\sim}{m}$-loop; and ψ, the total magnetic flux passing upward through an $\underset{\sim}{m}$-loop. To define I and ψ more precisely, let $\underset{\sim}{x}$ be a location in absolute space at which they are to be evaluated, let $\partial\mathcal{A}$ be the $\underset{\sim}{m}$-loop passing through $\underset{\sim}{x}$, and let $\mathcal{A}$ be any surface bounded by $\partial\mathcal{A}$ and not intersecting the horizon. Then

$$I(\underset{\sim}{x}) \equiv -\int_{\mathcal{A}} \alpha\underset{\sim}{j}\cdot d\underset{\sim}{\Sigma} = -\,(\text{current through } \partial\mathcal{A}) \ , \tag{4.2a}$$

$$\psi(\underset{\sim}{x}) \equiv \int_{\mathcal{A}} \underset{\sim}{B}\cdot d\underset{\sim}{\Sigma} = (\text{magnetic flux through } \partial\mathcal{A}) \ , \tag{4.2b}$$

where the orientation of $d\underset{\sim}{\Sigma}$ is chosen "upward" rather than "downward" (i.e., along the direction of the hole's angular momentum vector rather than opposed to it). The integrals in equations (4.2) do not depend on the choice made for $\mathcal{A}$, as long as it is outside the horizon. Charge conservation (2.23), together with stationarity (including stationarity of the total charge on the horizon $\mathcal{H}$) guarantees that $I(\underset{\sim}{x})$ is independent of our choice of the integration area $\mathcal{A}$ (including whether it passes over the hole or under the hole). The magnetic Gauss law (2.20b) similarly guarantees that $\psi(\underset{\sim}{x})$ is independent of our choice of $\mathcal{A}$. (If the total magnetic flux entering the hole were nonzero, $\psi(\underset{\sim}{x})$ would be different depending on whether $\mathcal{A}$ passed over the hole or under it. However, the only way that any hole's total flux can be nonzero is by the hole having been so created in the big bang; see equation (I,5.45). We exclude this by fiat, and thereby deal with a $\psi(\underset{\sim}{x})$ which is uniquely defined everywhere outside the horizon.)

The magnetic flux $\psi(\underset{\sim}{x})$ is simply related to the component $A_\phi \equiv \underset{\sim}{A}\cdot\underset{\sim}{m}$ of the vector potential $\underset{\sim}{A}$: By integrating $\underset{\sim}{B} = \underset{\sim}{\nabla}\times\underset{\sim}{A}$ over the surface $\mathcal{A}$ and then using Stokes's theorem (I,2.23) to convert to an integral around $\partial\mathcal{A}$ we find

$$\psi(\underset{\sim}{x}) = \int_{\mathcal{A}} \underset{\sim}{B}\cdot d\underset{\sim}{\Sigma} = \int_{\mathcal{A}} (\underset{\sim}{\nabla}\times\underset{\sim}{A})\cdot d\underset{\sim}{\Sigma} = \int_{\partial\mathcal{A}} \underset{\sim}{A}\cdot d\underset{\sim}{\ell}$$

$$= 2\pi A_\phi \quad . \tag{4.3}$$

In contrast to other authors (Scharlemann & Wagoner 1973, Blandford & Znajek 1977), we prefer to use ψ as our potential rather than A_ϕ because of its simple physical interpretation.

When expressing $\underset{\sim}{E}$ and $\underset{\sim}{B}$ in terms of A_0, I, ψ, we shall break them into their "toroidal" parts (parts along the toroidal direction $\underset{\sim}{m}$) and their "poloidal" parts (parts orthogonal to $\underset{\sim}{m}$):

$$\underset{\sim}{E} \equiv \underset{\sim}{E}^T + \underset{\sim}{E}^P \quad , \qquad \underset{\sim}{E}^T \equiv \varpi^{-2}(\underset{\sim}{E} \cdot \underset{\sim}{m})\underset{\sim}{m} \quad ; \tag{4.4a}$$

$$\underset{\sim}{B} \equiv \underset{\sim}{B}^T + \underset{\sim}{B}^P \quad , \qquad \underset{\sim}{B}^T \equiv \varpi^{-2}(\underset{\sim}{B} \cdot \underset{\sim}{m})\underset{\sim}{m} \quad . \tag{4.4b}$$

Because the magnetic flux ψ through an $\underset{\sim}{m}$-loop is constant in time (stationarity), the EMF around the loop must be zero (Faraday's law 2.20d), and consequently the toroidal electric field must vanish

$$\underset{\sim}{E}^T = 0 \quad , \qquad \underset{\sim}{E} \text{ is pure poloidal.} \tag{4.5}$$

Axisymmetry of $\underset{\sim}{B}$ ($\pounds_{\underset{\sim}{m}} \underset{\sim}{B} = 0$, equation 2.18) guarantees that $\underset{\sim}{\nabla} \cdot \underset{\sim}{B}^T = 0$; this, together with $\underset{\sim}{\nabla} \cdot \underset{\sim}{B} = 0$, guarantees that

$$\underset{\sim}{\nabla} \cdot \underset{\sim}{B}^T = 0 = \underset{\sim}{\nabla} \cdot \underset{\sim}{B}^P \; ; \tag{4.6}$$

i.e., the toroidal magnetic field and the poloidal magnetic field can be characterized separately by field lines that never end.

The general expression (2.24a) for $\underset{\sim}{E}$ in terms of A_0 and $\underset{\sim}{A}$, together with stationarity, axisymmetry, and $A_\phi = \psi/2\pi$, implies the following expression for the electric field in terms of A_0 and ψ

$$\underset{\sim}{E} = \frac{1}{\alpha}\left(\underset{\sim}{\nabla} A_0 + \frac{\omega}{2\pi c}\underset{\sim}{\nabla}\psi\right) \quad . \tag{4.7}$$

Ampere's law (2.20c) applied to an $\underset{\sim}{m}$-loop $\partial\mathcal{A}$ gives us the following expression for the toroidal magnetic field in terms of the current I through $\partial\mathcal{A}$

$$\underset{\sim}{B}^T = -\frac{2I}{\alpha\varpi^2 c}\underset{\sim}{m} \quad . \tag{4.8}$$

If we move our field point $\underset{\sim}{x}$ by $d\underset{\sim}{x}$ and thereby also move the $\underset{\sim}{m}$-loop passing through it, we change the flux $\psi(\underset{\sim}{x})$ by $d\psi = \underset{\sim}{\nabla}\psi \cdot d\underset{\sim}{x} = (d\underset{\sim}{x} \times 2\pi\underset{\sim}{m}) \cdot \underset{\sim}{B} = (2\pi\underset{\sim}{m} \times \underset{\sim}{B}) \cdot d\underset{\sim}{x}$. This fact permits us to write $\underset{\sim}{B}^P$ (the part of $\underset{\sim}{B}$ orthogonal

to $\underset{\sim}{m}$) as

$$\nabla\psi = 2\pi \underset{\sim}{m} \times \underset{\sim}{B}^P , \qquad \underset{\sim}{B}^P = -\frac{\underset{\sim}{m} \times \nabla\psi}{2\pi\varpi^2} \quad . \tag{4.9}$$

This expression can also be derived from $\underset{\sim}{B} = \nabla \times \underset{\sim}{A}$, together with $\psi/2\pi = A_\phi = \underset{\sim}{A} \cdot \underset{\sim}{m}$, and $\underset{\sim}{m} \times \underset{\sim}{B} = \underset{\sim}{m} \times \underset{\sim}{B}^P$. (Note that the same argument enables us to write similar expressions

$$\nabla I = -2\pi \underset{\sim}{m} \times (\alpha \underset{\sim}{j}^P), \qquad \alpha \underset{\sim}{j}^P = \frac{\underset{\sim}{m} \times \nabla I}{2\pi\varpi^2} \quad . \tag{4.10a}$$

for the poloidal part of the current density $\underset{\sim}{j}^P$ in terms of its flux, the current I.) Using equations (2.17a,c), (4.7), (4.8), (4.9), and (2.3) we can express the toroidal part of $\underset{\sim}{j}$ and the charge density ρ_e in the forms

$$4\pi j^T \equiv 4\pi \underset{\sim}{j}^T \cdot \frac{\underset{\sim}{m}}{\varpi} = -\frac{c\varpi}{\alpha} \nabla \cdot \left(\frac{\alpha \nabla\psi}{2\pi\varpi^2} \right) + \frac{\varpi}{\alpha^2} \nabla\omega \cdot \left(\nabla A_0 + \frac{\omega \nabla\psi}{2\pi c} \right) \quad , \tag{4.10b}$$

$$4\pi\rho_e = \nabla \cdot \left[\frac{1}{\alpha} \left(\nabla A_0 + \frac{\omega \nabla\psi}{2\pi c} \right) \right] \quad . \tag{4.10c}$$

One can regard equations (4.10) either as formulae for computing ρ_e and $\underset{\sim}{j}$ from specified potentials ψ, I, A_0, or as differential equations for ψ, I, A_0 in terms of their sources, ρ_e, j^T, and a divergence-free $\alpha \underset{\sim}{j}^P$.

[Petterson (1975), as corrected and extended by Znajek (1978a), gives a general multipole expansion for vacuum, stationary, axisymmetric solutions of Maxwell's equations in Kerr spacetime. The absence of sources means that there are only two independent scalar potentials in his formalism, which he calls A_t and A_ϕ (equal to our A_0 and $\psi/2\pi$, respectively). The vacuum solutions found by Petterson and Znajek may be used to construct the Green's function of any problem containing no poloidal sources, e.g. a toroidal current loop, but they may not be used in situations where $\underset{\sim}{j}^P$ and I are nonzero. Linet (1979) presents a procedure by which the field of any stationary,

axisymmetric charge and current distribution in Kerr spacetime can be constructed using Debye potentials. His procedure is consistent with ours, although expressed in very different language.]

The flow of electromagnetic angular momentum and redshifted energy in the magnetosphere is described by the poloidal parts of the flux vectors $\underset{\sim}{S}_L$ and $\underset{\sim}{S}_E$. Equation (2.31b) for the flux of angular momentum, together with $\underset{\sim}{E}^T = 0$, implies

$$\underset{\sim}{S}_L^P = -(\varpi/4\pi)\,|\underset{\sim}{B}^T|\underset{\sim}{B}^P = (I/2\pi\alpha c)\,\underset{\sim}{B}^P \quad . \tag{4.11}$$

Thus, angular momentum flows poloidally along magnetic field lines; there is no angular momentum flow unless currents also flow; and the angular momentum will flow outward (away from disk and hole) only if the current I through an $\underset{\sim}{m}$-loop flows in a direction opposite to that of the poloidal field (i.e., $I > 0$ if $\underset{\sim}{B}^P$ points upward; $I < 0$ if $\underset{\sim}{B}^P$ points downward). The torque per unit volume of the electric and magnetic fields on the matter (equation 2.34b) is

$$\begin{pmatrix}\text{Torque per}\\ \text{unit volume}\end{pmatrix} = -\frac{1}{\alpha}\,\underset{\sim}{\nabla}\cdot(\alpha\underset{\sim}{S}_L^P) = (\underset{\sim}{j}/c)\times\underset{\sim}{B}\cdot\underset{\sim}{m} \quad . \tag{4.12}$$

Equation (2.30b) for the flux of redshifted energy, together with the facts $\underset{\sim}{E}^T = 0$ and $\underset{\sim}{E}^P \times \underset{\sim}{B}^P$ = (a purely toroidal vector), implies

$$\begin{aligned}\underset{\sim}{S}_E^P &= (\alpha c/4\pi)(\underset{\sim}{E}\times\underset{\sim}{B}^T) + \omega\,\underset{\sim}{S}_L^P \\ &= \frac{I}{2\pi}\left(\frac{\omega}{\alpha c}\,\underset{\sim}{B}^P - \frac{\underset{\sim}{E}\times\underset{\sim}{m}}{\varpi^2}\right) \quad .\end{aligned} \tag{4.13}$$

Thus, the poloidal flow of redshifted energy is in part orthogonal to $\underset{\sim}{E}$ and in part along $\underset{\sim}{B}^P$; and there is no flow at all unless poloidal currents are present ($I \neq 0$). The rate at which electromagnetic fields transfer redshifted energy to matter (equation 2.34a) is

$$\left(\begin{array}{l}\text{rate, per unit } \tau \text{ time, that} \\ \text{redshifted energy is fed} \\ \text{into a unit volume of matter}\end{array}\right) = -\frac{1}{\alpha}\,\underset{\sim}{\nabla}\cdot(\alpha \underset{\sim}{S}^P_E)$$

$$= \alpha \underset{\sim}{j}\cdot\underset{\sim}{E} + (\omega/c)\,\underset{\sim}{j}\times\underset{\sim}{B}\cdot\underset{\sim}{m} \quad . \tag{4.14}$$

4.2 BOUNDARY CONDITIONS AT THE HORIZON

In the black hole's horizon the vanishing of the toroidal electric field, together with Ohm's law (2.42), Ampere's law (2.40), and expression (4.8) for $\underset{\sim}{B}^T$, implies

$$\underset{\sim}{\mathcal{J}}^H = \frac{I}{2\pi\varpi}\,\underset{\sim}{e}_{\hat{\lambda}} \quad , \qquad \underset{\sim}{E}^H = \frac{2I}{\varpi c}\,\underset{\sim}{e}_{\hat{\lambda}} \quad , \qquad \underset{\sim}{B}^H = -\frac{2I}{\varpi c}\,\underset{\sim}{e}_{\hat{\phi}} \quad . \tag{4.15}$$

Here we have used the horizon basis vectors of equation (2.12b). Note that the horizon current and electric field are purely poloidal, while the horizon magnetic field is purely toroidal. Note also that $\underset{\sim}{\mathcal{J}}^H = (I/2\pi\varpi)\underset{\sim}{e}_{\hat{\lambda}}$, at some "observation point" on the horizon, is precisely the surface current required to sink the total current I flowing into $\mathcal{H}$ north of the observation point.

The precise vanishing of the toroidal electric field, together with the horizon boundary condition $|\underset{\sim}{E}_{\parallel} - \underset{\sim}{n}\times\underset{\sim}{B}_{\parallel}| = 0(\alpha)$ at $\mathcal{H}$, implies that the poloidal magnetic field as measured by the ZAMOs intersects the horizon orthogonally

$$\underset{\sim}{B}^P \longrightarrow \underset{\sim}{B}_{\perp} + (\text{a parallel component that dies out as } \alpha) \quad . \tag{4.16a}$$

The toroidal magnetic field, of course, diverges as $1/\alpha$ (equations 2.40 and (4.15):

$$\alpha \underset{\sim}{B}^{T} \longrightarrow \underset{\sim}{B}^{H} = -(2I/\varpi c)\, \underset{\sim}{e}_{\hat{\phi}} \quad . \tag{4.16b}$$

Boundary condition (4.16b) is automatically satisfied by our expression (4.8) for $\underset{\sim}{B}^{T}$ in terms of the potential I, but condition (4.16a) is satisfied only if the potential ψ of equation (4.9) has the limiting form, in the coordinates of equation (2.12a),

$$\psi = \psi_0(\lambda) + O(\alpha^2) \qquad \text{near } \mathcal{H} \quad . \tag{4.17}$$

The tangential component of the (purely poloidal) electric field measured by the ZAMOs diverges at the horizon as $1/\alpha$ (equations 2.42 and 4.15)

$$\alpha \underset{\sim\|}{E} \longrightarrow \underset{\sim}{E}^{H} = (2I/\varpi c)\, \underset{\sim}{e}_{\hat{\lambda}} \quad , \tag{4.18a}$$

while the perpendicular component remains finite (Gauss's law 2.38)

$$\underset{\sim\perp}{E} \longrightarrow 4\pi\sigma^{H}\, \underset{\sim}{n} \quad . \tag{4.18b}$$

These boundary conditions are compatible with expression (4.7) for $\underset{\sim}{E}$ in terms of the potentials A_0 and ψ only if A_0 has the limiting form near the horizon,

$$A_0 = -\frac{\Omega^H}{2\pi c}\,\psi + \left[\int_0^{\lambda} \frac{2I}{\varpi c}\, d\lambda\right]_{\alpha=0} + O(\alpha^2) \quad . \tag{4.19}$$

The hole's surface charge σ^H and $E_\perp = 4\pi\sigma^H$ are determined by the $O(\alpha^2)$ part of A_0 and ψ, whereas $B_\perp$ is determined by $\psi_0(\lambda)$.

The torque of stationary, axisymmetric electromagnetic fields on a unit area of the horizon (equation 2.44) is

$$-\alpha \underset{\sim L}{S} \cdot \underset{\sim}{n} \longrightarrow \frac{dL^H}{d\Sigma^H dt} = \frac{1}{c}\,(\underset{\sim}{\mathcal{J}}^H \times \underset{\sim\perp}{B}) \cdot \underset{\sim}{m} = -\frac{IB_\perp}{2\pi c} \quad ; \tag{4.20}$$

the Joule heating rate per unit area (equation 2.45) is

$$\Theta^H \frac{dS^H}{d\Sigma^H dt} = \underset{\sim}{\mathcal{J}}^H \cdot \underset{\sim}{E}^H = \frac{1}{\pi c}\left(\frac{I}{\varpi}\right)^2 \quad ; \tag{4.21}$$

and the rate per unit area that redshifted energy flows into the hole, increasing its mass (equation 2.46), is

$$-\alpha \underset{\sim}{S}_E \cdot \underset{\sim}{n} \longrightarrow \frac{dM^H c^2}{d\Sigma^H dt} = -\frac{dP^H}{d\Sigma^H} = \frac{\Omega^H}{c}\underset{\sim}{m} \cdot (\underset{\sim}{\mathcal{J}}^H \times \underset{\sim}{B}_\perp) + \underset{\sim}{\mathcal{J}}^H \cdot \underset{\sim}{E}^H$$

$$= -\frac{\Omega^H I B_\perp}{2\pi c} + \frac{1}{\pi c}\left(\frac{I}{\varpi}\right)^2 \quad . \tag{4.22}$$

In equation (4.20) we see that the hole loses angular momentum when I and $B_\perp$ have the same sign, which is consistent with equation (4.11).

5 Degenerate, Stationary, Axisymmetric Electrodynamics

5.1 OUTSIDE THE HORIZON

In regions of space where

$$|\underset{\sim}{E} \cdot \underset{\sim}{B}| << |\underset{\sim}{B}^2 - \underset{\sim}{E}^2| \tag{5.1a}$$

it is reasonable to make the simplifying approximation that the fields are "degenerate"

$$\underset{\sim}{E} \cdot \underset{\sim}{B} = 0 \quad . \tag{5.1b}$$

The degeneracy approximation is justified in a wide range of physical situations, most notably in the presence of a plasma with electrical conductivity so high that the electric field vanishes in the plasma rest frame and the magnetic field is thereby frozen into the plasma. See, e.g. Carter (1979) for a thorough relativistic discussion. For our stationary axisymmetric magnetosphere, degeneracy, together with the fact that $\underset{\sim}{E}$ is purely poloidal, guarantees the existence of a toroidal vector

$$\underset{\sim}{v}^F \equiv \alpha^{-1}(\Omega^F - \omega)\,\underset{\sim}{m} \tag{5.2}$$

such that

$$\underset{\sim}{E} = -(\underset{\sim}{v}^F/c) \times \underset{\sim}{B}^P = -\frac{(\Omega^F - \omega)}{2\pi\alpha c}\,\underset{\sim}{\nabla}\psi \tag{5.3}$$

(cf. equation 4.9). One can interpret $\underset{\sim}{v}^F$ as the physical velocity of the magnetic field lines relative to the ZAMOs; note that nothing constrains $\underset{\sim}{v}^F$ to be less than the speed of light. Any observer who moves with the magnetic field lines, i.e., with velocity $\underset{\sim}{v}^F$, sees a vanishing electric field $\underset{\sim}{E}' = [1 - (\underset{\sim}{v}^F)^2/c^2]^{-1/2}\,[\underset{\sim}{E} + (\underset{\sim}{v}^F/c) \times \underset{\sim}{B}] = 0$. The nonzero electric field $\underset{\sim}{E}$ seen by the ZAMOs is entirely induced by the motion of the magnetic field. Note that just as ω is the angular velocity $d\phi/dt$ of the ZAMOs relative to absolute space, so the Ω^F in equation (5.2) is the angular velocity $d\phi/dt$ of the magnetic field lines relative to absolute space.

Each magnetic field line must rotate with constant angular velocity--i.e., Ω^F must be constant along field lines

$$\underset{\sim}{B}^P \cdot \underset{\sim}{\nabla}\Omega^F = 0 \quad ; \tag{5.4}$$

otherwise the magnetic field would "wind itself up" in violation of stationarity. The mathematical proof of this "isorotation law" is carried out by setting $\dot{\underset{\sim}{B}} = 0$ in Maxwell's evolution law (2.17d) for $\underset{\sim}{B}$, imposing in addition axisymmetry and expression (5.3) for $\underset{\sim}{E}$ in terms of ψ, invoking $\underset{\sim}{\nabla} \times \underset{\sim}{\nabla}\psi = 0$, and then reexpressing $\underset{\sim}{\nabla}\psi$ in terms of $\underset{\sim}{B}^P$ by equation (4.9). The original, nonrelativistic version of the isorotation law (5.4) is due to Ferraro (1937); and the relativistic version is due to Blandford and Znajek (1977) for force-free magnetospheres, and due to Carter (1979) for degenerate magnetospheres.

In studying the electromagnetic field structure, it is useful to think not only in terms of poloidal magnetic field lines, but also in terms of the axially symmetric field surfaces obtained by moving the poloidal field lines around the axis of symmetry along $\underset{\sim}{m}$-loops. These axially symmetric field surfaces can be labeled by the flux ψ, since ψ is obviously constant on them. Since $\underset{\sim}{B}^P \cdot \underset{\sim}{\nabla}\Omega^F = 0$ (isorotation) and $\underset{\sim}{m} \cdot \underset{\sim}{\nabla}\Omega^F = 0$ (axial symmetry), Ω^F is also constant on the magnetic surfaces—which means that we can regard Ω^F as a function of ψ, $\Omega^F(\psi)$. From equations (5.3) and (4.7) we see that in the degenerate region A_0 is also a function of ψ, as is A_ϕ (equation 4.3):

$$dA_0/d\psi = -\Omega^F/2\pi c \quad , \qquad dA_\phi/d\psi = 1/2\pi \quad . \tag{5.5}$$

In the general stationary axisymmetric case a full solution of Maxwell's equations $(\underset{\sim}{E},\underset{\sim}{B},\rho_e,\underset{\sim}{j})$ was generated by three independent and freely specifiable scalar fields, I, ψ, and A_0. When degeneracy is also imposed, a full solution is generated by two freely specifiable scalar fields I and ψ, plus one function, $\Omega^F(\psi)$. The electric field $\underset{\sim}{E}$ is computed from expression (5.3), the toroidal and poloidal magnetic fields $\underset{\sim}{B}^T$ and $\underset{\sim}{B}^P$ from (4.8) and (4.9), and the charge and current densities ρ_e and $\underset{\sim}{j}$ from the Maxwell equations (2.17a,c). The resulting expressions for ρ_e and $\underset{\sim}{j}$ are equations (4.10), specialized to the case $\underset{\sim}{\nabla}A_0 = -(\Omega^F/2\pi c)\underset{\sim}{\nabla}\psi$:

$$\alpha \underset{\sim}{j}^P = \frac{\underset{\sim}{m} \times \underset{\sim}{\nabla} I}{2\pi \varpi^2} \quad , \tag{5.6a}$$

$$8\pi^2 j^T = -\frac{c\varpi}{\alpha}\underset{\sim}{\nabla}\cdot\left(\frac{\alpha}{\varpi^2}\underset{\sim}{\nabla}\psi\right) + \frac{\varpi}{\alpha^2 c}(\Omega^F - \omega)\underset{\sim}{\nabla}\psi\cdot\underset{\sim}{\nabla}(\Omega^F - \omega)$$

$$- \frac{\varpi}{\alpha^2 c}(\Omega^F - \omega)\frac{d\Omega^F}{d\psi}(\underset{\sim}{\nabla}\psi)^2 \quad , \tag{5.6b}$$

$$8\pi^2 \rho_e = -\underset{\sim}{\nabla}\cdot\left[\left(\frac{\Omega^F - \omega}{\alpha c}\right)\underset{\sim}{\nabla}\psi\right] \quad . \tag{5.6c}$$

Notice that the divergence-free $\alpha \underset{\sim}{j}^P$ is still determined by I alone, while j^T and ρ_e are both determined by ψ and $\Omega^F(\psi)$. Thus ρ_e and j^T are not independent. The charge density and toroidal current must carefully adjust themselves in degenerate regions (e.g. in regions where there is a highly conducting plasma) so as to keep $\underset{\sim}{E} \cdot \underset{\sim}{B} = 0$.

Degeneracy simplifies expression (4.13) for the poloidal flux of redshifted energy. Using equations (5.2), (5.3), and (4.11), we make it read

$$\underset{\sim}{S}_E^P = \Omega^F \underset{\sim}{S}_L^P = -\Omega^F (\varpi/4\pi) \; |\underset{\sim}{B}^T| \underset{\sim}{B}^P$$

$$= \Omega^F (I/2\pi\alpha c) \; \underset{\sim}{B}^P \quad . \tag{5.7}$$

Similarly, the rate at which the fields deposit redshifted energy in matter (equation 4.14) simplifies to

$$\begin{pmatrix}\text{rate, per unit } \tau \text{ time, that}\\ \text{redshifted energy is fed}\\ \text{into a unit volume of matter}\end{pmatrix} = -\frac{1}{\alpha} \underset{\sim}{\nabla} \cdot (\alpha \underset{\sim}{S}_E^P)$$

$$= \Omega^F \begin{pmatrix}\text{torque per unit}\\ \text{volume of electromag-}\\ \text{netic fields on matter}\end{pmatrix} = -\frac{\Omega^F}{\alpha} \underset{\sim}{\nabla} \cdot (\alpha \underset{\sim}{S}_L^P) \tag{5.8}$$

$$= (\Omega^F/c)(\underset{\sim}{j} \times \underset{\sim}{B}) \cdot \underset{\sim}{m} \quad .$$

Thus, angular momentum and redshifted energy both flow along poloidal magnetic field lines, and their ratio everywhere satisfies the "energy-angular momentum relation" $dE = \Omega^F dL$.

5.2 BOUNDARY CONDITIONS AT THE HORIZON

Degeneracy tightens up and simplifies the boundary conditions at the horizon. All the boundary conditions of Section 4.2 remain valid, but they are now augmented by the new constraint (equations 5.2, 5.3, 2.10, 2.42, and 4.16a)

$$\underset{\sim}{E}^H = -\frac{1}{c} (\Omega^F - \Omega^H) \underset{\sim}{m} \times \underset{\sim}{B}_\perp \quad . \tag{5.9}$$

This constraint, together with our old expression (4.18a) for $\underset{\sim}{E}^H$, implies that

$$I = \frac{1}{2}\,(\Omega^H - \Omega^F)\varpi^2 B_\perp \qquad \text{at } \mathcal{H} \quad , \tag{5.10}$$

and combined with expression (4.9) for $\underset{\sim}{B}_\perp = \underset{\sim}{B}^P$, it says that the potentials ψ and I cannot be specified freely at the horizon; they must in fact be related by

$$I = (\Omega^H - \Omega^F)(\varpi/4\pi)\; d\psi_0/d\lambda \qquad \text{on } \mathcal{H}\,, \tag{5.11}$$

where $\psi_0(\lambda)$ is the horizon value of ψ (equation 4.17).

Condition (5.9) simplifies expressions (4.20) - (4.22) for the torque, dissipation, and mass increase on the horizon:

$$-\alpha \underset{\sim}{S}_L \cdot \underset{\sim}{n} \longrightarrow \frac{dL^H}{d\Sigma^H dt} = \frac{(\Omega^F - \Omega^H)}{4\pi c}\,(\varpi B_\perp)^2 \quad , \tag{5.12}$$

$$\frac{\Theta^H dS^H}{d\Sigma^H dt} = \frac{(\Omega^F - \Omega^H)^2}{4\pi c}\,(\varpi B_\perp)^2 \quad , \tag{5.13}$$

$$-\alpha \underset{\sim}{S}_E \cdot \underset{\sim}{n} \longrightarrow \frac{dM^H c^2}{d\Sigma^H dt} = -\frac{dP^H}{d\Sigma^H} = \frac{\Omega^F(\Omega^F - \Omega^H)}{4\pi c}\,(\varpi B_\perp)^2 \tag{5.14}$$

$$= \Omega^F \frac{dL^H}{d\Sigma^H dt} \quad .$$

Notice that in the horizon, as outside it, degeneracy enforces the energy-angular-momentum relation $dM^H c^2 = \Omega^F dL^H$.

The above boundary conditions at the horizon for a degenerate magnetosphere are identical to those for a force-free magnetosphere (see Section 6.2 below). They were first derived for the force-free case by Znajek (1977) and Blandford & Znajek (1977).

6 Force-Free, Stationary, Axisymmetric Electrodynamics

6.1 OUTSIDE THE HORIZON

Consider a region of the magnetosphere where large amounts of plasma are freely available, and where the plasma has adjusted its charge and current densities to make $|\underset{\sim}{E}\cdot\underset{\sim}{B}| \ll |\underset{\sim}{B}^2 - \underset{\sim}{E}^2|$. If the inertial and gravitational forces on the plasma are small enough compared to the inertia of the electromagnetic field, the plasma will be unable to exert significant force on the field, i.e. it will further adjust itself so that

$$|\underset{\sim}{E}\cdot\underset{\sim}{B}| \ll |\underset{\sim}{B}^2 - \underset{\sim}{E}^2|, \qquad |\rho_e \underset{\sim}{E} + (\underset{\sim}{j}/c)\times\underset{\sim}{B}| \ll |\underset{\sim}{j}/c||\underset{\sim}{B}| \quad . \tag{6.1a}$$

In such regions we shall approximate the fields as precisely degenerate and force-free

$$\underset{\sim}{E}\cdot\underset{\sim}{B} = 0, \qquad \rho_e\underset{\sim}{E} + (\underset{\sim}{j}/c)\times\underset{\sim}{B} = 0 \quad . \tag{6.1b}$$

Note that precise force-freeness implies precise degeneracy. The relativistic theory of degenerate, force-free, stationary, axisymmetric electrodynamics has been developed previously by Blandford & Znajek (1977). The formulas which follow are simply a rewrite of their formalism in our "absolute space/universal time" language.

When the constraint of force-freeness is added to the constraint of degeneracy, the formalism of Section 5 is thereby tightened: No longer are the "potentials" I and ψ independent scalar fields; now I, like Ω^F, must be constant on magnetic field surfaces and therefore must be a function of ψ. To see this, note that because $\underset{\sim}{E}$ is pure poloidal, force-freeness (6.1b) implies that $(\underset{\sim}{j}\times\underset{\sim}{B})^T \equiv \underset{\sim}{j}^P\times\underset{\sim}{B}^P$ must vanish, which means that the poloidal

part of the current $\underset{\sim}{j}^P$ is everywhere parallel to the poloidal part of the magnetic field $\underset{\sim}{B}^P$, which in turn means that $\underset{\sim}{\nabla}\psi = 2\pi m \times \underset{\sim}{B}^P$ (equation 4.9) and $\underset{\sim}{\nabla} I = -2\pi m \times (\alpha \underset{\sim}{j}^P)$ (equation 4.10a) are parallel, which in turn means that surfaces of constant I and ψ coincide; I is a function of ψ. Moreover, from $\underset{\sim}{\nabla} I = -2\pi m \times (\alpha \underset{\sim}{j}^P)$ and $\underset{\sim}{\nabla}\psi = 2\pi m \times \underset{\sim}{B}^P$ we can read off the proportionality constant relating $\underset{\sim}{j}^P$ to $\underset{\sim}{B}^P$:

$$\underset{\sim}{j}^P = (-\alpha^{-1} dI/d\psi)\, \underset{\sim}{B}^P \quad . \tag{6.2}$$

Combining this with force-freeness $\rho_e \underset{\sim}{E} + (\underset{\sim}{j}/c) \times \underset{\sim}{B} = 0$ and the expression $\underset{\sim}{E} = -(\underset{\sim}{v}^F/c) \times \underset{\sim}{B}$ we see that the full current density (poloidal plus toroidal) is

$$\underset{\sim}{j} = \rho_e \underset{\sim}{v}^F - (\alpha^{-1} dI/d\psi)\, \underset{\sim}{B} \quad . \tag{6.3}$$

In general, stationary, axisymmetric regions there were three freely specifiable scalar fields in the most general solution of Maxwell's equations: ψ, I, and A_0 — or, alternatively, ρ_e, j^T, and the divergence-free $\alpha \underset{\sim}{j}^P$. When degeneracy was imposed, the charges were forced to distribute themselves in a special manner so as to keep $\underset{\sim}{E} \cdot \underset{\sim}{B} = 0$ — and this reduced the number of freely specifiable scalar fields from 3 to 2: ψ and I, or j^T and the divergence-free $\alpha \underset{\sim}{j}^P$. Now, as we impose force-freeness, we suddenly reduce the number of freely specifiable scalar fields from 2 to 0: The degeneracy relationship (5.6b,c) between ρ_e and j^T is compatible with their force-free relationship $j^T = \rho_e(\Omega^F - \omega)\varpi/\alpha + (\alpha^{-1} dI/d\psi)(2I/\alpha\varpi c)$ [equation (6.3) with B^T replaced by (4.8)] if and only if the potential ψ satisfies the partial differential equation

$$\underset{\sim}{\nabla} \cdot \left\{ \frac{\alpha}{\varpi^2} \left[1 - \frac{(\Omega^F - \omega)^2 \varpi^2}{\alpha^2 c^2} \right] \underset{\sim}{\nabla}\psi \right\} + \frac{(\Omega^F - \omega)}{\alpha c^2} \frac{d\Omega^F}{d\psi} (\underset{\sim}{\nabla}\psi)^2 + \frac{16\pi^2}{\alpha \varpi^2 c^2} I \frac{dI}{d\psi} = 0 \, . \tag{6.4}$$

The general force-free solution of Maxwell's equations is obtained by selecting a solution ψ, $\Omega^F(\psi)$, $I(\psi)$ of this equation, then computing $\underset{\sim}{E}$ from (5.3), $\underset{\sim}{B}$ from (4.8) and (4.9), and ρ_e and $\underset{\sim}{j}$ from (5.6).

Following Newtonian practice, we call ψ the "stream function" and equation (6.4) the "stream equation", because the poloidal current and the poloidal magnetic field both point along "stream lines" of ψ, i.e., along poloidal lines of constant ψ. Our general relativistic stream equation (6.4) agrees with that derived, in very different notation, in the pioneering paper of Blandford & Znajek (1977).

In the force-free region the fluxes of angular momentum and redshifted energy carried by the electromagnetic field are conserved

$$\underset{\sim}{\nabla} \cdot \left(\alpha \underset{\sim}{S}^P_E\right) = \underset{\sim}{\nabla} \cdot \left(\alpha \underset{\sim}{S}^P_L\right) = 0 \tag{6.5}$$

(equations 5.8). The angular momentum and redshifted energy flow without loss along the poloidal magnetic field lines.

6.2 BOUNDARY CONDITIONS AT THE HORIZON

Because the horizon fields are degenerate, $\underset{\sim}{E}^H \cdot \underset{\sim}{B}^H = 0$, but not force-free, $\sigma^H \underset{\sim}{E}^H + (\underset{\sim}{\mathcal{J}}^H/c) \times \underset{\sim}{B}_\perp \neq 0$, the boundary conditions at the horizon are unchanged when we constrain the degenerate exterior fields ($\underset{\sim}{E} \cdot \underset{\sim}{B} = 0$) to be force-free [$\rho_e \underset{\sim}{E} + (\underset{\sim}{j}/c) \times \underset{\sim}{B} = 0$]. The boundary conditions remain as described in Section 5.2.

However, it is important to examine the relationship between the stream equation (6.4) and the unchanged boundary conditions on ψ, $I(\psi)$, and $\Omega^F(\psi)$

$$\psi = \psi_0(\lambda) + O(\alpha^2) \qquad \text{near } \mathcal{H} , \tag{6.6a}$$

$$4\pi I = (\Omega^H - \Omega^F)\varpi \, d\psi_0/d\lambda \qquad \text{at } \mathcal{H} , \tag{6.6b}$$

(equations 4.17 and 5.11). In the neighborhood of the horizon, and in the coordinate system of equation (2.12a), the stream equation (6.4) can be put in the form

$$\frac{\kappa^2}{c^4}(\Omega^F-\Omega^H)^2\alpha\frac{\partial}{\partial\alpha}\left(\frac{1}{\alpha}\frac{\partial\psi}{\partial\alpha}\right)+\left(\frac{1}{2\varpi^2\partial\psi/\partial\lambda}\right)\frac{\partial}{\partial\lambda}\left\{\left[(\Omega^F-\Omega^H)\varpi\frac{\partial\psi}{\partial\lambda}\right]^2-(4\pi I)^2\right\}$$

$$+\ [\text{coefficients of } O(\alpha)]\times[\text{derivatives of }\psi] \qquad (6.7)$$

$$+\ [\text{coefficients of order unity}]\times[\partial\psi/\partial\alpha] \;=\; 0\ .$$

Notice that if ψ is finite at the horizon, then this stream equation requires that $\psi=\psi_0(\lambda)+O(\alpha^2\ln\alpha)+O(\alpha^2)$ at $\mathcal{H}$. If, moreover, ψ and I are well behaved on the axis of symmetry ($\psi\propto\varpi^2$ and $I\propto\varpi^2$), then this stream equation says that the absence of $O(\alpha^2\ln\alpha)$ terms from ψ is equivalent to the demand that $4\pi I=\pm(\Omega^H-\Omega^F)\varpi\,d\psi_0/d\lambda$. Roman Znajek points out to us that the choice of sign (+ versus -) corresponds to a choice of the direction of the Poynting flux at the horizon (in versus out) and thence to a choice of whether the horizon is a future horizon (black hole) or a past horizon (white hole).

Thus, <u>physically well-behaved solutions of the stream equation</u> [solutions with ψ finite and no $O(\alpha^2\ln\alpha)$ terms at $\mathcal{H}$] <u>automatically satisfy the boundary conditions (6.6)--except for a possible sign error in (6.6b)</u>. In Section 7.4 we shall use this fact to elucidate the global structure of the force-free region of a magnetosphere, and to formulate the problem of constructing solutions for the force-free region.

6.3 ACTION PRINCIPLES FOR STREAM FUNCTION

In the force-free region we can regard the stream function ψ as governed either by the stream equation (6.4) or (equivalently) by an action principle. The action to be extremized is

$$\mathcal{I}=\int_{\mathcal{V}}(1/8\pi)[(\underset{\sim}{B}^P)^2-(\underset{\sim}{B}^T)^2-(\underset{\sim}{E})^2]\alpha\,dV \qquad . \qquad (6.8a)$$

Here $\mathcal{V}$ is the region of integration (which must be force-free); and $\underset{\sim}{B}^P$, $\underset{\sim}{B}^T$, $\underset{\sim}{E}$ are to be expressed in terms of ψ, I, and Ω^F via equations (4.9), (4.8), and (5.3), yielding

$$\mathcal{I} = \int_{\mathcal{V}} \frac{1}{8\pi}\left\{\left[1 - \frac{(\Omega^F - \omega)^2 \varpi^2}{\alpha^2 c^2}\right]\left(\frac{\nabla\psi}{2\pi\varpi}\right)^2 - \left(\frac{2I}{\alpha\varpi c}\right)^2\right\}\alpha\, dV \quad . \tag{6.8b}$$

In this action $dV \equiv (\det \|\gamma_{jk}\|)^{1/2}\, dx^1 dx^2 dx^3$ is the proper volume element of absolute space; α, ω, and ϖ are known functions of x^1, x^2, x^3 describing the black hole; and I and Ω^F are to be specified as explicit functions of ψ before the variation. The variation of ψ in this action leads to

$$\delta\mathcal{I} = -\frac{1}{16\pi^3}\int_{\mathcal{V}} \delta\psi[\text{left-hand side of stream equation (6.4)}]\, dV$$
$$+ \frac{1}{16\pi^3}\int_{\partial\mathcal{V}} \delta\psi\, \frac{\alpha}{\varpi^2}\left[1 - \frac{(\Omega^F - \omega)^2\varpi^2}{\alpha^2 c^2}\right]\underset{\sim}{\nabla}\psi \cdot d\underset{\sim}{\Sigma} \quad . \tag{6.8c}$$

Thus, so long as the region of integration is bounded away from the horizon ($\alpha > 0$ throughout $\mathcal{V}$ and $\partial\mathcal{V}$), the appropriate boundary conditions on ψ are:

At each point on $\partial\mathcal{V}$
either specify an arbitrary but smoothly changing value of ψ ($\delta\psi = 0$)
or specify that $\underset{\sim}{\nabla}\psi$ be parallel to $\partial\mathcal{V}$ ($\underset{\sim}{\nabla}\psi \cdot d\underset{\sim}{\Sigma} = 0$). (6.8d)

If ψ and $\underset{\sim}{\nabla}\psi$ are thus specified on $\partial\mathcal{V}$, the functions ψ which extremize $\mathcal{I}$ ($\delta\mathcal{I} = 0$) will be precisely the solutions of the stream equation.

If the region of integration $\mathcal{V}$ is bounded in part by the black hole's horizon $\mathcal{H}$ ($\alpha = 0$), then the action (6.8a,b) is infinite [$(\underset{\sim}{B}^T)^2$ and $(\underset{\sim}{E})^2$ both diverge as $1/\alpha^2$, so $\mathcal{I}$ diverges as $\ln\alpha$]. This defect can be repaired by a renormalization of the action:

$$\mathcal{I}' = \text{LIM}\left\{\int_{\mathcal{V}} (1/8\pi)[(\underset{\sim}{B}^P)^2 - (\underset{\sim}{B}^T)^2 - (\underset{\sim}{E})^2]\,\alpha\, dV\right.$$
$$\left. - (c^2/\kappa)\ln\alpha \int_{\mathcal{H}\cap\partial\mathcal{V}} (1/8\pi)[(\underset{\sim}{B}^H)^2 + (\underset{\sim}{E}^H)^2]\, d\Sigma\right\} \quad . \tag{6.9a}$$

Here and below "LIM" means "take the limit as the boundary $\partial\mathcal{V}$ approaches the

horizon $\mathcal{H}$, i.e. as $\alpha \to 0$ on $\mathcal{H} \cap \partial\mathcal{V}$;" also, $\underset{\sim}{B}^H = \mathrm{LIM}(\alpha \underset{\sim}{B}^T)$ and $\underset{\sim}{E}^H = \mathrm{LIM}(\alpha \underset{\sim}{E}_{\|})$ are the horizon fields (cf. equations 4.16b and 4.18a). When $\underset{\sim}{B}^P$, $\underset{\sim}{B}^T$, and $\underset{\sim}{E}$ are expressed in terms of ψ, I, and Ω^F via equations (4.9), (4.8), and (5.3), this renormalized action becomes

$$\mathcal{I}' = \mathrm{LIM}\left[\frac{1}{8\pi}\int_{\mathcal{V}}\left\{\left[1 - \frac{(\Omega^F - \omega)^2\varpi^2}{\alpha^2 c^2}\right]\left(\frac{\nabla\psi}{2\pi\varpi}\right)^2 - \left(\frac{2I}{\alpha\varpi c}\right)^2\right\}\alpha\, dV \right.$$
$$\left. - \frac{\ln\alpha}{8\pi\kappa}\int_{\mathcal{H}\cap\partial\mathcal{V}}\left\{\frac{(\Omega^F - \Omega^H)^2}{4\pi^2}\left(\frac{d\psi}{d\lambda}\right)^2 + \left(\frac{2I}{\varpi}\right)^2\right\}\varpi\, d\phi\, d\lambda\right] \quad . \tag{6.9b}$$

Here we have used the coordinates of equation (2.12a) for the horizon surface integral. The variation of ψ in this action, with I and Ω^F taken to be fixed functions of ψ as before, yields

$$\delta\mathcal{I}' = \mathrm{LIM}\left[-\frac{1}{16\pi^3}\int_{\mathcal{V}}\delta\psi[\text{left-hand side of stream equation (6.4)}]\, dV\right.$$
$$+ \frac{1}{16\pi^3}\int_{\partial\mathcal{V}}\delta\psi\,\frac{\alpha}{\varpi^2}\left[1 - \frac{(\Omega^F - \omega)^2\varpi^2}{\alpha^2 c^2}\right]\underset{\sim}{\nabla}\psi \cdot d\underset{\sim}{\Sigma}$$
$$- \frac{\ln\alpha}{32\pi^3\kappa}\int_{\mathcal{H}\cap\partial\mathcal{V}}\left(\frac{\delta\psi}{\varpi\, d\psi/d\lambda}\right)\frac{d}{d\lambda}\left\{(4\pi I)^2 - \left[\varpi(\Omega^F - \Omega^H)\frac{d\psi}{d\lambda}\right]^2\right\} d\varphi d\lambda$$
$$\left. - \frac{\ln\alpha}{16\pi^3\kappa}\int_{\partial(\mathcal{H}\cap\partial\mathcal{V})}\delta\psi[\varpi(\Omega^F - \Omega^H)^2\,\frac{d\psi}{d\lambda}]\, d\phi\right] \quad . \tag{6.9c}$$

Thus, the appropriate boundary conditions on ψ are:

At each point on $\mathcal{H} \cap \partial\mathcal{V}$

specify ψ as a fixed solution of the differential equation $4\pi I = (\Omega^H - \Omega^F)\varpi\, d\psi/d\lambda$ [equation (6.6b)] (so $\delta\psi = 0$).

At each point of $\partial\mathcal{V}$ that is not part of $\mathcal{H}$

either specify an arbitrarily but smoothly changing value of ψ ($\delta\psi = 0$), or specify that $\underset{\sim}{\nabla}\psi$ be parallel to $\partial\mathcal{V}$ ($\underset{\sim}{\nabla}\psi \cdot d\underset{\sim}{\Sigma} = 0$). \tag{6.9d}

The functions ψ which extremize $\mathcal{I}'$ subject to these constraints are precisely

the solutions of the stream equation.

The two action principles (6.8) and (6.9) are generalizations to black holes of the flat-space, pulsar-magnetosphere action principle of Scharlemann & Wagoner (1973). A third action principle, one without a pulsar analog, governs the distribution of magnetic field on the horizon:

Suppose that just outside the horizon the magnetosphere is force free. Let the total magnetic flux through the horizon, between the poles and equator, be specified [i.e. let $\psi_0 = 0$ at the north and south poles, and $\psi_0 = \psi_E$ at the equator be fixed]. Specify, moreover, for each poloidal field line, its angular velocity Ω^F and the current I inside it [i.e., let the functions $\Omega^F(\psi_0)$ and $I(\psi_0)$ be fixed]. Then <u>the poloidal magnetic field lines will distribute themselves over the horizon in such a manner as to extremize the horizon's total surface energy of tangential electromagnetic field</u>

$$\mathcal{E} = \int_{\mathcal{H}} (1/8\pi)[(\underset{\sim}{B}^H)^2 + (\underset{\sim}{E}^H)^2]\, d\Sigma$$

$$= \int_{\mathcal{H}} \frac{1}{8\pi c^2}\left[\frac{(\Omega^F - \Omega^H)^2}{4\pi^2}\left(\frac{d\psi_0}{d\lambda}\right)^2 + \left(\frac{2I}{\varpi}\right)^2\right]\varpi\, d\phi\, d\lambda \quad . \tag{6.10}$$

In fact, the Euler-Lagrange equation for the action principle $\delta\mathcal{E} = 0$ is identical to the near-horizon form (6.7) of the stream equation

$$\frac{1}{\varpi d\psi_0/d\lambda}\frac{d}{d\lambda}\left\{\left[(\Omega^F - \Omega^H)\varpi\frac{d\psi_0}{d\lambda}\right]^2 - (4\pi I)^2\right\} = 0 \ ; \tag{6.11}$$

and this equation is satisfied by the "true" magnetic field distribution [$4\pi I = (\Omega^H - \Omega^F)\varpi\, d\psi_0/d\lambda$; equation (6.6b)]. In Section 7.4 we shall discuss further the manner in which this action principle and equation (6.6b) govern the horizon's field.

Roman Znajek (private communication) points out to us that the action $\mathcal{E}$ is not merely extremized by the horizon's poloidal field configuration; it is actually minimized: the second variation of expression (6.10), evaluated at the extremal configuration (6.11), is

$$\delta^2\mathcal{E} = \int_{\mathcal{H}} \frac{(\Omega^F - \Omega^H)^2}{32\pi^3 c^2} \left[\frac{d}{d\lambda}\,\delta\psi_o - \delta\psi_o \frac{d}{d\lambda}\,\ell n \left(\varpi \frac{d\psi_o}{d\lambda}\right)\right]^2 \varpi\, d\phi\, d\lambda \quad , \tag{6.12}$$

which is positive semidefinite. Znajek goes on to point out that, after the action $\mathcal{E}$ has been extremized and one has found that $\underset{\sim}{B}^H = \underset{\sim}{E}^H$, then $\mathcal{E} = (1/c) \times$ (rate of Joule heating of the horizon). In an alternative description of the horizon (Section 5.4 of Paper I), Znajek (1978b) has attributed the horizon's Joule heating to a combination of electric current and magnetic current. In this description $\mathcal{E}$ is $(1/c) \times$ (rate of Joule heating) even before minimization—which means that the horizon's rate of entropy production is minimized by its equilibrium distribution of poloidal flux, a result reminiscent of "Prigogine's Principle" (cf. Kittel 1958).

7. Global Model of Stationary Magnetosphere

7.1 OVERVIEW

We now use the results of Sections 4, 5, and 6 to elucidate features of the Blandford-Znajek (1977) model for the power sources of quasars and active galactic nuclei.

We assume that the black hole, the accretion disk, and their magnetosphere have settled down into a stationary state that is axisymmetric about the hole's rotation axis and reflection symmetric in the hole's equatorial plane, and that has the qualitative character of Fig. 1. We assume, further, that the plasma in the disk is a sufficiently good conductor that, although the field lines might slip through it a bit, nevertheless the fields are degenerate ($|\underset{\sim}{E}\cdot\underset{\sim}{B}| \ll |\underset{\sim}{B}^2 - \underset{\sim}{E}^2|$). We shall idealize them as perfectly degenerate, $\underset{\sim}{E}\cdot\underset{\sim}{B} = 0$, but not as force-free: The inertia of the disk's plasma is absolutely crucial for containing the magnetic field. Without it the field would fly away. This degenerate, non-force-free region (which also includes the horizon) is marked "D" in Fig. 2.

Following Blandford (1976) and Blandford & Znajek (1977), we assume further that just outside the disk and hole the plasma becomes sufficiently rarified that it no longer exerts significant force on the magnetic field—but it is still sufficiently dense to provide the charged particles needed for degeneracy and force-freeness:

$$|\underset{\sim}{E}\cdot\underset{\sim}{B}| \ll \underset{\sim}{B}^2 - \underset{\sim}{E}^2 , \qquad |\rho_e\underset{\sim}{E} + (\underset{\sim}{j}/c)\times\underset{\sim}{B}| \ll |\underset{\sim}{j}/c||\underset{\sim}{B}|.$$

As discussed by Blandford (1976), on field lines threading the disk the necessary charged particles are likely extracted from the disk by the Goldreich-Julian (1969) mechanism: a component of $\underset{\sim}{E}$ along $\underset{\sim}{B}$, which is so weak as to constitute a negligible violation of our force-free, degenerate assumption, pulls the charges out of the disk. However, magnetic field lines that thread the hole must get their charges and currents in some other manner. Blandford & Znajek (1977) argue that they come from the Ruderman-Sutherland (1975)

"spark-gap" process, a cascade production of electron-positron pairs in the force-free region—a production induced indirectly by a component of $\underset{\sim}{E}$ along $\underset{\sim}{B}$, which again is so weak as to constitute a negligible violation of force-freeness and degeneracy. We shall assume that by these processes, or some others, the necessary charged particles are supplied and the region marked "FF" in Fig. 2 becomes force-free. This region might extend through the annulus between the disk and the horizon, if the plasma there is tenuous enough for force-freeness to be established. We shall idealize the FF region as being precisely degenerate and force-free $[\underset{\sim}{E} \cdot \underset{\sim}{B} = 0, \quad \rho_e \underset{\sim}{E} + (j/c) \times \underset{\sim}{B} = 0]$.

Outside the FF region, where the magnetic field becomes weak and where it may be dragging charges into rotation at nearly the speed of light, the inertia of the charged particles begins to make itself felt. In this region, marked "A" in Fig. 2, the field loses both its degeneracy and force-freeness, and it presumably uses its energy to accelerate charged particles and (hopefully) to form charged-particle beams. Blandford (1976), Lovelace (1976), and Lovelace et al. (1979) have speculated extensively about the physics which occurs in this acceleration region. For our purposes the only important point (assumption) is that all the power being transported outward through the FF region by DC electromagnetic fields somehow gets transferred to charged particles—and subsequently perhaps into radiation—in the A region.

7.2 GLOBAL ENERGY AND ANGULAR MOMENTUM BALANCE

Each magnetic field line in the D and FF regions rotates rigidly, dragged around by the hole's rotation and the disk's orbital motion. In the A region, where particle inertia is strong, degeneracy breaks down and the concept of field-line angular velocity Ω^F ceases to be a useful one. [If one defines Ω^F so as to account, by $\underset{\sim}{B}$-field motion, for the component of $\underset{\sim}{E}$ orthogonal to $\underset{\sim}{B}$ (analogue of equation 5.3), one finds that in the A region Ω^F is no longer constant along field lines.] Nevertheless, the fields in the A region continue to transport energy and angular momentum.

Consider an annular tube of magnetic flux $\Delta\psi$ intersecting the hole (flux tube "a" in Fig. 3). The horizon exerts a net torque

$$-\frac{d\Delta L^H}{dt} = -\frac{1}{c}\,(\underset{\sim}{\mathcal{J}}^H \times \underset{\sim}{n}\Delta\psi)\cdot\underset{\sim}{m} = \frac{(\Omega^H-\Omega^F)}{4\pi c}\varpi^2 B_\perp \Delta\psi \tag{7.1}$$

on this flux tube (equations 4.20 and 5.12); and with this torque it transmits a redshifted power (equation 5.14)

$$\Delta P = -\Omega^F \frac{d\Delta L^H}{dt} = \frac{\Omega^F(\Omega^H-\Omega^F)}{4\pi c}\,\varpi^2 B_\perp \Delta\psi \tag{7.2}$$

up the flux tube and into the FF region. The torque (7.1) and power (7.2) are transmitted loss-free along the flux tube (equations 5.7 and 6.5) through the entire thickness of the FF region and into the A region. In the A region the angular momentum continues to flow along the flux tube (equation 4.11), where it gradually gets deposited into charged particles (equation 4.12)

$$\begin{aligned}\frac{d\Delta L^A}{dt} &= \frac{1}{c}\int_{\text{flux tube in A}} \alpha \underset{\sim}{j}\times\underset{\sim}{B}\cdot\underset{\sim}{m}\,dV \\ &= -\frac{d\Delta L^H}{dt}\quad .\end{aligned} \tag{7.3}$$

The power, by contrast, flows away from the flux tube into adjoining regions of space (equation 4.13), where it presumably also gets deposited in charged particles (equation 4.14).

The total power output from the flux tube, expression (7.2) (which was derived by Blandford & Znajek), depends critically on the tube's angular velocity Ω^F. That angular velocity is determined by torque balance along the flux tube between the hole and the A region (equations 7.1 and 7.3). If the particles in the A region of the tube have enormous inertia, they will drag the tube down to $\Omega^F \ll \Omega^H$, and the power transmitted will be very small (equation 7.2). If the particles have very little inertia, the tube will be dragged up

to $\Omega^F \simeq \Omega^H$, and once again the power transmitted will be very small. From this viewpoint it might appear to be a miracle if the charged particles conspired with the hole so as to have just the right amount of inertia to make $\Omega^F \sim \Omega^H/2$ and thereby produce large power output. Nevertheless, such a miracle may well occur, according to the following variant of a classic Goldreich-Julian (1969) argument for pulsars.

Near the black hole, magnetic field lines rotate backward relative to ZAMOs with velocities $\underset{\sim}{v}^F = -(\Omega^H - \Omega^F)\underset{\sim}{m}/\alpha$ which greatly exceed the speed of light ($\alpha \to 0$ at $\mathcal{H}$). Far from the hole and away from the symmetry axis ($\alpha \to 1$, $\omega \to 0$, ϖ large), field lines rotate forward relative to ZAMOs with velocities $\underset{\sim}{v}^F = \Omega^F \underset{\sim}{m}$ which also greatly exceed the speed of light. A charged particle that is constrained to move along a magnetic field line can move, relative to ZAMOs, more slowly than the field line. Near the hole it does this by sliding down the field line toward the horizon; far from the hole it does it by sliding out the field line. However, there is a minimum possible speed with which the particle can slide if it is to stay on the field line:

$$v_{min} = \frac{v^F}{\left[1 + (\underset{\sim}{B}^T)^2/(\underset{\sim}{B}^P)^2\right]^{1/2}} \quad . \tag{7.4}$$

The boundary condition $I = \frac{1}{2}(\Omega^H - \Omega^F)\varpi^2 B_\perp$ (equation 5.10) at the horizon is perfectly designed to make this minimum sliding velocity equal to the speed of light (cf. equations 4.8, 4.16a, 5.2): charged particles slide along field lines into the horizon at precisely the speed of light relative to ZAMOs. Far from the hole, v_{min} will be of order c if and only if $\Omega^F \simeq \Omega^H/2$:

$$v^F \simeq \Omega^F \varpi, \quad B^T \simeq 2I/\varpi c \simeq (1/\varpi c)\left[(\Omega^H - \Omega^F)\varpi^2 B_\perp\right]_{\text{at } \mathcal{H}} \simeq (\Omega^H - \Omega^F)\psi/\pi c\varpi,$$

$$B^P = |\underset{\sim}{\nabla}\psi|/2\pi\varpi \simeq \psi/\pi\varpi^2, \quad v_{min} \simeq c\Omega^F/(\Omega^H - \Omega^F) \ .$$

Thus, if $\Omega^F << \Omega^H/2$, particles can easily slide along the field lines more slowly

than light near the boundary of the FF and A regions; and perhaps this will lead to small particle inertia in the A region and thereby to a spinning up of the field toward $\Omega^F \simeq \Omega^H/2$. On the other hand, if $(\Omega^H - \Omega^F) << \Omega^H/2$, charged particles will be unable to achieve $v_{min} >> c$ at large radii; they will be thrown off the field lines, and they may well exert a back-reaction torque on the field lines sufficient to drive Ω^F back down near $\Omega^H/2$.

Of course, this argument is speculative. The analogous argument in the case of pulsars (where Ω^F is fixed but I is adjustable and determines v_{min}) is highly controversial even today, a dozen years after the Goldreich-Julian work (see, e.g. Mestel, Phillips & Wang 1979, Arons 1979).

Turn attention now to field lines which thread the disk. For simplicity, assume that the disk is reflection symmetric, and restrict attention to the region above the equatorial plane. As in the case of the hole, consider an annular tube of magnetic flux which threads the disk (flux tube "b" in Fig. 3). Let Ω^D be the angular velocity of the disk's plasma inside this tube (appropriately averaged vertically if necessary). The field lines in the tube will rotate slightly more slowly than Ω^D, due to drag on the tube in the A region; this velocity difference will induce in the rest frame of the disk plasma a radial electric field proportional to $(\Omega^D - \Omega^F)B^P$, which in turn will drive a radial current $j \propto (\Omega^D - \Omega^F)B^P/(\text{resistivity})$ that will interact with $\underset{\sim}{B}^P$ to produce a torque on the flux tube

$$-\frac{d\Delta L^D}{dt} = \left(\frac{\Omega^D - \Omega^F}{4\pi^2 c^2}\right)\frac{\Delta\psi}{\Delta Z^D}\,\Delta\psi \quad . \tag{7.5}$$

Here ΔZ^D is the total electrical resistance (impedance) in the disk, north of the equator, between the inner surface of the flux tube and the outer surface. (For further details about ΔZ^D see the next section.) This net torque will be transmitted,

loss-free, through the FF region where it is described by equation (5.7)

$$-\frac{d\Delta L^D}{dt} = (I/2\pi c)\,\Delta\psi \quad , \tag{7.6}$$

and into the A region where it will act on charged particles in the flux tube (equation 4.12)

$$-\frac{d\Delta L^D}{dt} = \frac{d\Delta L^A}{dt} = \frac{1}{c}\int_{\text{flux tube in A}} \alpha \underset{\sim}{j} \times \underset{\sim}{B} \cdot \underset{\sim}{m}\, dV \quad . \tag{7.7}$$

Associated with this torque is the redshifted power (equation 5.8)

$$\Delta P = \Omega^F \frac{d\Delta L^A}{dt} = \Omega^F\left(\frac{I}{2\pi c}\right)\Delta\psi \quad , \tag{7.8}$$

which the magnetic flux tube extracts from the disk and transfers to charged particles in the A region.

Torque balance, i.e. equality of expressions (7.5), (7.6), (7.7), determines both Ω^F (the tube's angular velocity) and I (the current flowing in the disk across the tube) in terms of $\Delta\psi$ (the magnetic flux in the tube), Ω^D (the disk's angular velocity at the foot of the tube), ΔZ^D (the disk's impedance across the tube), and $-d\Delta L^A/dt$ (the torque of the acceleration-region plasma on the tube). Typically, the disk impedance ΔZ^D will be very small (high conductivity), and the field lines will therefore be locked into the disk, $\Omega^F \simeq \Omega^D$.

Our variant of the Goldreich-Julian argument suggests that the torque in the A region might regulate itself so as to make $v_{min} \simeq c$, and thereby (equations 4.8 and 5.2)

$$I \simeq I_{crit} = \Omega^F\psi/2\pi \quad . \tag{7.9}$$

These conditions of self regulation ($\Omega^F \simeq \Omega^H/2$ and thence $I \simeq \Omega^F\psi/2\pi$ for lines threading the hole; $I \simeq \Omega^F\psi/2\pi$ for lines threading the disk) lead to astrophysically interesting power outputs from both disk and hole (Blandford 1976, Blandford & Znajek 1977, Blandford 1979): For a black hole of mass $M \simeq 10^8 M_\odot$ rotating at $\Omega^H \simeq 1$ radian / 1000 sec ("a/M" near unity), onto which an accretion disk has deposited a 10^4 Gauss magnetic field, the power outputs from the hole and the disk will both be roughly 10^{44} erg/sec.

7.3 CIRCUIT ANALYSIS OF POWER FLOW

Znajek (1978b) and Blandford (1979) have described the above model, semi-quantitatively, in terms of a circuit analogy. Blandford says: "The massive black hole behaves like a battery with an EMF of up to 10^{21} Volts and an internal resistance of about 30 ohms. When a current flows, the power dissipated within the horizon, manifest as an increase in the irreducible mass [i.e., entropy], is comparable with that dissipated in particle acceleration etc. in the far field." In this section we shall give a mathematically precise version of this description.

We begin by defining the potential drop $\Delta V^{\mathcal{C}}$ along any curve segment $\mathcal{C}$ in absolute space:

$$\Delta V^{\mathcal{C}} \equiv \int_{\mathcal{C}} \alpha \underset{\sim}{E} \cdot d\underset{\sim}{\ell} \quad . \tag{7.10}$$

The factor α converts the forces produced by the electric field $\underset{\sim}{E}$ from a "per unit proper time d/dτ" basis to a "per unit global time d/dt" basis. Without the α, we would be unable to use Faraday's law (2.20d) to deduce the potential drop around a circuit; and without it the total current $I' = \int \alpha \underset{\sim}{j} \cdot d\underset{\sim}{\Sigma}$ = (charge per unit global time t), flowing in a thin magnetic-

free wire at rest relative to the ZAMOs, could not be expressed simply as $I' = \Delta V/R$ with R the resistance of the wire as measured in flat space. The α in expression (7.10) is required to balance the α in I' and to thereby make standard circuit theory valid in the presence of gravity. (We use a prime on I' merely to distinguish it from the potential I of our magnetosphere theory.)

We can compute the total potential drop around any closed curve $\mathcal{C}$ from Faraday's law (2.20d). Obviously, the total drop must be independent of the state of motion of the curve—and, in fact, the two magnetic terms in Faraday's law conspire to make this so (see Section 2.5 of Paper I). For purposes of computation, assume that the curve is at rest in invariant space, so its shape and size are unchanging; and for application to our magnetosphere assume that the magnetic field is time independent, $\dot{\underset{\sim}{B}} = 0$. Then the time derivative of the flux through the curve vanishes, the velocity of the curve relative to the ZAMOs is $\underset{\sim}{v} = -\underset{\sim}{\omega m}/\alpha$, and Faraday's law becomes

$$\Delta V^{\mathcal{C}} = (1/c) \oint_{\mathcal{C}} (\underset{\sim}{\omega m} \times \underset{\sim}{B}) \cdot d\underset{\sim}{\ell} \quad . \tag{7.11}$$

Thus, the interaction of a stationary magnetic field, $\dot{\underset{\sim}{B}} = 0$, with the hole's dragging of inertial frames (i.e., with its "gravitomagnetic field") produces an EMF around closed curves. Using our stationary, axisymmetric magnetosphere equation (4.9), we can rewrite this EMF in terms of the flux potential

$$\Delta V^{\mathcal{C}} = (1/c) \oint (\omega/2\pi) \underset{\sim}{\nabla} \psi \cdot d\underset{\sim}{\ell} \quad . \tag{7.12}$$

[Note: This could have been derived more quickly, but perhaps with less physical clarity, from equations (7.10) and (4.7).]

Figure 4 shows several electric equipotential surfaces (surfaces orthogonal to $\alpha\underset{\sim}{E}$, i.e., surfaces made up of curves along which $\Delta V = 0$). Consider the neighboring equipotentials labeled 1 and 2, which intersect the

horizon. In the D and FF regions these equipotentials coincide with the walls of the inner magnetic flux tube of Fig. 3 ($\underset{\sim}{E}$ is orthogonal to the flux tube walls due to degeneracy, so there is no potential drop ΔV along any curve lying entirely in a flux tube wall). However, the equipotentials separate from the flux tube walls in region A, where degeneracy breaks down. In fact, the equipotentials must eventually close upon themselves, as shown, in order for spatial infinity to remain at zero potential. Everywhere in the FF region currents are constrained to flow in the equipotential surfaces ($\underset{\sim}{j} \cdot \underset{\sim}{E} = 0$); no current can cross them. However, in the horizon (a D region) current flows from the north polar region, across equipotentials, toward the equator. The total current crossing our two equipotential surfaces 1 and 2 in the horizon is I, where I is the current "potential" of previous sections evaluated at the feet of the equipotential surfaces. By stationarity, this same total current I must flow back across surfaces 2 and 1 in the A region. (We assume that 2 and 1 are close enough together that the poloidal current between them in the FF region is negligible.)

In the horizon, with its surface resistivity $R^H = 4\pi/c = 377$ ohms, the current crossing from surface 1 to surface 2 encounters a total resistance

$$\Delta Z^H = R^H \frac{\text{(distance from 1 to 2)}}{\text{(circumference across which I flows)}} = R^H \frac{\Delta\lambda}{2\pi\varpi}$$

$$= R^H \frac{\Delta\psi}{4\pi^2\varpi^2 B_\perp} \quad . \tag{7.13}$$

Here $\Delta\psi$, as in the last section, is the total magnetic flux in the tube between 1 and 2. The potential drop in the horizon between 1 and 2 is, of course,

$$\Delta V^H = I\Delta Z^H \quad , \tag{7.14a}$$

and it can be expressed equally well from equation (5.3) and $\alpha\underset{\sim}{E} \to \underset{\sim}{E}^H$, as

$$\Delta V^H = \int_1^2 \underset{\sim}{E}^H \cdot d\underset{\sim}{\ell} = (\Omega^H - \Omega^F)\ \Delta\psi/2\pi c \quad . \tag{7.14b}$$

We assume for pedagogical purposes (and because it is likely true) that the entire A region is far enough from the hole that $\omega << \Omega^H$ there; and we therefore approximate ω as zero in A. Then equation (7.11) guarantees that in the A region the potential drop ΔV^A between surfaces 2 and 1 is independent of where one computes it—near the symmetry axis, or at 15° latitude, or.... . This unique potential drop can be thought of as produced by a resistance ΔZ^A to the flow of the current I:

$$\Delta V^A = I\Delta Z^A \quad . \tag{7.15a}$$

An alternative expression for the potential drop, derivable by integration at the interface between the A and FF regions where expression (5.3) for $\underset{\sim}{E}$ is valid, is

$$\Delta V^A = \int_2^1 \alpha\underset{\sim}{E} \cdot d\underset{\sim}{\ell} = \Omega^F\ \Delta\psi/2\pi c \quad . \tag{7.15b}$$

The sum of the potential drops in the horizon $\mathcal{H}$ (equations 7.14) and in region A (equations 7.15) is equal to the total EMF around a closed curve that passes along $\mathcal{H}$ from 1 to 2, then up 2 poloidally into region A, then from 2 to 1, then poloidally down 1 to its starting point at $\mathcal{H}$. This total closed-loop EMF can be evaluated from equation (7.12), where the only nonzero contribution comes from $\mathcal{H}$ (because $\omega = 0$ in A and $\underset{\sim}{\nabla}\psi \cdot d\underset{\sim}{\ell} = 0$ in the FF portions of 1 and 2). The result is

$$\Delta V^H + \Delta V^A = \text{EMF} = \Omega^H\ \Delta\psi/2\pi c \quad . \tag{7.16}$$

Equations (7.14)-(7.16) for the potential drops and equation (7.13) for the horizon resistance are the foundations for our circuit-theory analysis of power flow.

The ratio of the potential drops in the acceleration region and horizon, as computed from equations (7.14) and (7.15), is

$$\frac{\Delta V^A}{\Delta V^H} = \frac{\Delta Z^A}{\Delta Z^H} = \frac{\Omega^F}{\Omega^H - \Omega^F} \quad ; \tag{7.17}$$

the total current as computed from (7.16), (7.17), and (7.13) is

$$I = \frac{EMF}{\Delta Z^A + \Delta Z^H} = \frac{1}{2}(\Omega^H - \Omega^F)\,\varpi^2 B_\perp \quad ; \tag{7.18}$$

the total power transmitted to the A region as computed from (7.18), (7.17), and (7.13) is

$$\Delta P = \Delta Z^A I^2 = \frac{\Omega^F(\Omega^H - \Omega^F)}{4\pi c}\,\varpi^2 B_\perp\,\Delta\psi \quad ; \tag{7.19}$$

and the power dissipated in the horizon is

$$\Theta^H \frac{d\Delta S^H}{dt} = \Delta Z^H I^2 = \frac{(\Omega^H - \Omega^F)^2}{4\pi c}\,\varpi^2 B_\perp\,\Delta\psi \quad . \tag{7.20}$$

(The right-hand sides of equations (7.18)-(7.20) are all evaluated at the feet of the equipotentials in the horizon.)

Note that our circuit analysis produces the same result for the power output as was obtained from the torque-balance analysis of the last section (cf. equations 7.2 and 7.19). It also reproduces the standard horizon boundary condition on I (cf. equations 7.18 and 5.10). In addition, it gives new insight into the determination of the field line

angular velocity: Ω^F is determined by the ratio of the resistance of the acceleration region to the resistance of the horizon (equation 7.17). And the condition of maximum power output, $\Omega^F = \Omega^H/2$, corresponds precisely to the standard circuit-theory condition: the impedance ΔZ^A of the load should equal the impedance ΔZ^H of the power source. Moreover, as in our torque-balance discussion so also here, there is reason to suspect that the optimal power output will be approximately achieved in nature: Lovelace et al. (1979) argue that the complex processes occurring in region A are likely to produce a total impedance between widely separated equipotentials of $\sim$25 ohms. Between our neighboring surfaces the impedance will be smaller than this by $\sim$(thickness of flux tube)/(distance to symmetry axis) $\sim \Delta\lambda/\varpi$. Comparison with (7.13) shows

$$\Delta Z^H = (R^H/2\pi)(\Delta\lambda/\varpi) \sim (60 \text{ ohms})(\Delta\lambda/\varpi)$$

$$\Delta Z^A \sim (25 \text{ ohms})(\Delta\lambda/\varpi) \quad , \tag{7.21}$$

i.e., rough impedance matching. This conclusion, that the impedances will roughly match and therefore the power output will be roughly optimal, is due to Blandford (1979).

A circuit analysis can also be developed for a neighboring pair of equipotentials threading the upper half of the disk. A current I flows, in the upper half disk, between the equipotential surfaces 3 and 4 of Fig. 4. This current produces a potential drop between surfaces 3 and 4 given by

$$I\Delta Z^D = \int_3^4 \alpha[\underset{\sim}{E} + (\underset{\sim}{v}^D/c) \times \underset{\sim}{B}] \cdot d\underset{\sim}{\ell} = \Delta V^D + (\Omega^D - \omega^D)\,\Delta\psi/2\pi c \quad . \tag{7.22}$$

(One can regard this as defining the disk impedance ΔZ^D between surfaces 3 and 4.) Here $\underset{\sim}{v}^D = (\Omega^D - \omega^D)\underset{\sim}{m}/\alpha$ is the disk's orbital velocity relative to ZAMOs, and the integral is performed in the equatorial plane where the ZAMO angular

velocity is $\omega \equiv \omega^D$. The current I flows back from equipotential 4 to equipotential 3 in region A, where it produces a potential drop

$$\Delta V^A = I\Delta Z^A = \Omega^F \Delta\psi/2\pi c \tag{7.23}$$

(equation 7.15). The total EMF around the loop is

$$\Delta V^D + \Delta V^A = \text{EMF} = \omega^D \Delta\psi/2\pi c \tag{7.24}$$

(equation 7.12). Combining equations (7.22)-(7.24) we obtain

$$\frac{\Delta Z^A}{\Delta Z^D} = \frac{\Omega^F}{\Omega^D - \Omega^F} \quad , \tag{7.25}$$

$$I = \Omega^F \frac{\Delta\psi}{2\pi c\ \Delta Z^A} = (\Omega^D - \Omega^F) \frac{\Delta\psi}{2\pi c\ \Delta Z^D} \quad , \tag{7.26}$$

$$\Delta P = I^2 \Delta Z^A = \Omega^F \left(\frac{I}{2\pi c}\right) \Delta\psi \quad . \tag{7.27}$$

As for field lines threading the hole, so also here, the field line angular velocity Ω^F is determined by the ratio of acceleration-region impedance to disk impedance. If the disk impedance is very low, the disk will lock the field lines to itself, $\Omega^F \simeq \Omega^D$. Once Ω^F is fixed, the current I is determined by the A-region impedance.

7.4 CONSTRUCTION OF A MODEL FOR THE FORCE-FREE REGION

The details of the disk and of the acceleration region are highly dependent on ill-understood plasma physics. Not so the force-free region and the horizon. They can be modeled with considerable confidence (as Blandford & Znajek emphasize)—except for uncertain boundary conditions at the interface with the disk and the A-region. In this section we summarize the

mathematical structure of the problem of modeling the force-free (FF) region.

A poloidal slice through the FF region is shown in Fig. 5. It is bounded by the horizon (labeled $\mathcal{H}$), the symmetry axis (labeled $\mathcal{S}$), and the boundaries with the disk and acceleration region (both labeled $\mathcal{B}$). Except at the end of this section, we shall regard the disk as extending all the way in to the horizon's equator. A solution for all details of the FF region and the horizon is generated by the stream function ψ and the two subsidiary functions $I(\psi)$ and $\Omega^F(\psi)$. Once $I(\psi)$, $\Omega^F(\psi)$, and suitable boundary conditions are specified, ψ is computed by solving the partial differential stream equation (6.4) or, equivalently, by extremizing the action (6.9).

The boundary conditions on ψ are determined by the poloidal magnetic field distribution at the boundary. (Recall: ψ is the flux through $\underset{\sim}{m}$-loops; $\underset{\sim}{B}^P = -\underset{\sim}{m} \times \underset{\sim}{\nabla}\psi/2\pi\varpi^2$.) To avoid unphysical singularities on the symmetry axis $\mathcal{S}$, one must set $\psi = 0$ there and $\psi \propto \varpi^2$ on $\mathcal{B}$ near $\mathcal{S}$; but otherwise there are no constraints of principle on ψ:

$$\psi = 0 \quad \text{on } \mathcal{S}\,, \qquad \psi \propto \varpi^2 \text{ as } \varpi \to 0 \quad \text{on } \mathcal{B}\,,$$
$$\psi \text{ otherwise arbitrary on } \mathcal{B}\,. \tag{7.28a}$$

As one moves away from the symmetry axis along $\mathcal{B}$, one is free to make ψ increase for a while, then decrease and even go negative, then increase again and oscillate. Such complicated behavior will lead, when solving the stream equation, to magnetic field loops going out through $\mathcal{B}$ and then returning in various places, and to neutral points of field reversal. But, of course, one would prefer to choose ψ on $\mathcal{B}$ to match as closely as possible boundary fields from realistic models of the disk and acceleration regions.

One must also specify $I(\psi)$ and $\Omega^F(\psi)$ on the boundary, subject to one non-obvious constraint

$$dI/d\psi = (\Omega^H - \Omega^F)/2\pi \quad \text{at the intersection of } \mathcal{B} \text{ and } \mathcal{S} \tag{7.28b}$$

(see below), and several obvious ones

$$I = 0 \quad \text{on } \mathcal{S} \ , \qquad I \propto \varpi^2 \quad \text{as } \varpi \to 0 \quad \text{on } \mathcal{B} \ ,$$

$$\Omega^F = \text{constant on } \mathcal{S} \ , \tag{7.28c}$$

I and Ω^F otherwise arbitrary on $\mathcal{B}$, except that they must be functions of ψ in the sense not that every point with the same ψ has the same I and Ω^F, but rather that points with the same (ψ, I, Ω^F) come in pairs so distributed that one can topologically draw non-crossing lines of force connecting them.

Of course, in practice one will try to choose I and Ω^F in accord with the physical conditions of the last two sections: Ω^F determined by Ω^H or Ω^D and by the relative A-region and D-region impedances; I determined by Ω^F and the A-region impedance, $I = \Omega^F \Delta\psi / (2\pi c \ \Delta Z^A)$ (equation 7.26).

One need not be concerned about any boundary conditions on the horizon. The stream differential equation, when it is solved, will automatically enforce the two horizon boundary conditions

$$\psi = \psi_0(\lambda) + O(\alpha^2) \qquad \text{near } \mathcal{H} \ , \tag{7.29a}$$

$$4\pi I = (\Omega^H - \Omega^F)\varpi \, d\psi_0/d\lambda \quad \text{on } \mathcal{H} \ , \tag{7.29b}$$

except for a possible sign error in (7.29b) (cf. Section 6.2). The boundary condition (7.28b) is designed in part to ensure that, at least near the symmetry axis, the sign starts out correct. If a solution of the stream equation produces an incorrect sign reversal at a null point of the magnetic field

($d\psi_0/d\lambda = 0$) further along the horizon—an unlikely occurrence—then one must discard the solution as unphysical.

It is instructive to see how the stream equation distributes the poloidal magnetic field $B_\perp = (2\pi\varpi)^{-1}\, d\psi_0/d\lambda$ over the horizon. It distributes the field in such a manner as to extremize the horizon's electromagnetic surface energy (6.10), or equivalently in accordance with the ordinary differential equation (7.29b). Rewrite this equation as

$$d\psi_0/G(\psi_0) = d\lambda/\varpi(\lambda) \tag{7.30}$$

where $\varpi(\lambda)$ is a known function determined by the surface geometry of the horizon, and

$$G(\psi_0) \equiv \frac{4\pi I(\psi_0)}{\Omega^H - \Omega^F(\psi_0)} \tag{7.31}$$

is a known function determined by the choice of boundary conditions moving outward from the symmetry axis $\mathcal{S}$ along $\mathcal{B}$. In the limit as one approaches the symmetry axis, smoothness of the horizon requires $\varpi = \lambda$, and our (previously unexplained) constraint (7.28b) on the boundary data guarantees $G = 2\psi$, which in turn guarantees that the solution of the differential equation (7.30) has the well-behaved form

$$\psi = \pi\lambda^2 B_{\perp 0} \quad \text{as } \lambda \to 0 \ . \tag{7.32}$$

The integration constant $B_{\perp 0}$ is the poloidal magnetic field strength on the symmetry axis of the horizon. Imagine integrating the differential equation (7.29b) along the horizon from pole toward equator, beginning with some trial value of $B_{\perp 0}$. Unless that trial value is chosen very carefully, upon reaching the intersection of $\mathcal{H}$ with $\mathcal{B}$, one will have a value of ψ which does not match the chosen boundary value there. Obtaining the right match

can be regarded as an eigenvalue problem for $B_{\perp 0}$. Presumably, by solving the stream differential equation (6.4) subject to the boundary conditions (7.28) on $\mathcal{S}$ and $\mathcal{B}$, one automatically also solves the eigenvalue problem for $B_{\perp 0}$ and obtains a unique physically well-behaved solution on all of the horizon and throughout the force-free region.

However, we do not claim to have proved rigorously that there will always exist a solution to the stream equation with boundary conditions of the specified type, nor that when such a solution exists it will be unique.

The above formulation of the boundary-value problem is appropriate to situations where the magnetic field is firmly anchored in the disk all the way in to the horizon, so that it is appropriate to specify ψ on $\mathcal{B}$ all the way in to $\mathcal{B}$'s intersection with $\mathcal{H}$. When, instead, there is a force-free gap between the disk and the horizon, one must modify the boundary-value problem. The boundaries then have the form of Fig. 6, which is the same as Fig. 5 except for the presence of a force-free equatorial boundary segment $\mathcal{F}$. Since field lines passing through $\mathcal{F}$ are force free everywhere except in the distant acceleration region A, they presumably will be anchored in A and will thus have zero angular velocity $\Omega^F = 0$ and will carry zero torque, $\underset{\sim}{S}^P_L = (I/2\pi\alpha c)\underset{\sim}{B}^P = 0$ (equation 5.7). This means that the boundary values ψ, $\Omega^F(\psi)$, and $I(\psi)$ must be chosen such that

$$\Omega^F = I = 0 \quad \text{everywhere on } \mathcal{F} \quad . \tag{7.33a}$$

By contrast with the boundaries $\mathcal{S}$ and $\mathcal{B}$, one should not explicitly specify the distribution of ψ on $\mathcal{F}$; rather, reflection symmetry dictates that one specify

$$\underset{\sim}{\nabla}\psi \quad \text{parallel to } \mathcal{F} \text{ everywhere on } \mathcal{F} \quad . \tag{7.33b}$$

However, the values of ψ will be fixed at the inner and outer edges of $\mathcal{F}$, i.e., at the intersections with $\mathcal{A}$ and $\mathcal{B}$:

$$\psi \quad \text{fixed at } \mathcal{A}\cap\mathcal{F} \quad \text{and } \mathcal{B}\cap\mathcal{F} \quad \text{as those values for which } \Omega^{F}(\psi) \text{ and } I(\psi) \text{ start departing from zero.} \tag{7.33c}$$

Boundary values ψ, $I(\psi)$, $\Omega^{F}(\psi)$ chosen in accord with equations (7.28) and (7.33) lead to a well-posed action principle (6.9) for the stream function ψ in the FF region—an action principle whose Euler-Lagrange equation is the stream differential equation (6.4).

7.5 ABSENCE OF MAGNETIC LOOPS THREADING THE HORIZON

In Section 3 we mentioned that a looped field line such as b in Figure 1, with one foot on the horizon $\mathcal{H}$ and the other anchored in the disk, will annihilate itself once the disk has deposited the loop's second foot onto $\mathcal{H}$. Presumably the annihilation will occur on a timescale Δt roughly equal to the light travel time across the loop. (This is what one would compute from the flat-space theory of the diffusion of magnetic field lines through a medium with surface resistivity $R^H = 377$ ohms.) However, we shall not attempt here a relativistic derivation of this timescale. Rather, we shall content ourselves with a formal proof that the annihilation must occur—i.e. that a poloidal magnetic field loop $\mathcal{L}_o$ of the form shown in Figure 7 cannot exist in the force-free region of a stationary axisymmetric magnetosphere. For simplicity of proof we presume that the topology of the poloidal field inside $\mathcal{L}_o$ is as shown in Figure 7: a series of simple nested loops with the magnetic field in the same direction on each loop (no neutral points). The reader can generalize the proof.

The first step in our proof is to show that on each loop inside $\mathcal{L}_o$ $\Omega^F = \Omega^H$ and $I = 0$. This follows from torque balance. Conserved angular momentum travels along each loop, outward from $\mathcal{H}$ at one foot and back into $\mathcal{H}$ at the other. But because Ω^F is constant along a loop, the direction of the angular momentum flow must be the same at both feet (outward if $\Omega^F < \Omega^H$; inward if $\Omega^F > \Omega^H$; equation 7.1). This is possible only if there is no flow of angular momentum at all, i.e. only if $\Omega^F = \Omega^H$ (equation 7.1), which means in turn that $I = 0$ (equation 5.11).

Because $\Omega^F = \Omega^H$ and $I = 0$ throughout the interior of $\mathcal{L}_o$, the stream equation (6.4) is there a perfect divergence. Integrating it over the interior of $\mathcal{L}_o$ and converting to a surface integral by Gauss's theorem, and noting that the contribution from $\mathcal{H}$ vanishes because $\Omega^F - \omega = \Omega^H - \omega = O(\alpha^2)$ and $\alpha \to 0$ at $\mathcal{H}$ (see pp. 251-252 of Bardeen 1973), we obtain

$$\int_{\mathcal{L}_o} (\alpha/\varpi^2)\,[1 - (v^F/c)^2]\,\underset{\sim}{\nabla}\psi \cdot d\underset{\sim}{\Sigma} = 0 \ , \qquad (7.34)$$

$v^F = (\Omega^H - \omega)\,\varpi/\alpha$ = (linear velocity of field line relative to ZAMOs).

Note that because $\mathcal{L}_o$ is a surface of constant flux, $\underset{\sim}{\nabla}\psi$ is parallel to $d\underset{\sim}{\Sigma}$; and because of our assumed simple loop topology (Fig. 7), $\underset{\sim}{\nabla}\psi \cdot d\underset{\sim}{\Sigma}$ has a constant sign (positive or negative) everywhere on $\mathcal{L}_o$. Shown dashed in Figure 7 is the "velocity of light" surface on which $v^F = c$. If $\mathcal{L}_o$ lies entirely inside that surface, then $v^F < c$ everywhere on $\mathcal{L}_o$, and (7.34) then demands that $\underset{\sim}{\nabla}\psi \cdot d\underset{\sim}{\Sigma} = 0$ everywhere on $\mathcal{L}_o$, which in turn means that $\underset{\sim}{\nabla}\psi = 0$ and hence $\underset{\sim}{B}^P = 0$ everywhere on $\mathcal{L}_o$. Thus, there is no field at all, much less any field line, on $\mathcal{L}_o$—and the same holds true for all loops inside $\mathcal{L}_o$.

If $\mathcal{L}_o$ pierces through the velocity-of-light surface (the case shown in Figure 7), then integrate the stream equation separately over the shaded and unshaded parts of the interior of $\mathcal{L}_o$, convert to surface integrals, note that the integrals over $\mathcal{H}$ and over the velocity-of-light surface vanish, and thereby conclude that (7.34) holds separately for the shaded ($v^F < c$) and unshaded ($v^F > c$) parts of $\mathcal{L}_o$. This means, again, that $\underset{\sim}{\nabla}\psi \cdot d\underset{\sim}{\Sigma} = 0$ everywhere on $\mathcal{L}_o$, which means that there is no poloidal magnetic field at all, much less any field line, on $\mathcal{L}_o$—and the same holds true for all loops inside $\mathcal{L}_o$.

Thus, a loop of the form $\mathcal{L}_o$ cannot exist in the force-free region—though it can exist if part of the loop exits from the force-free region, e.g. into the disk.

8. Conclusion

In this paper we have tried to focus exclusively on those aspects of black-hole electrodynamics which are independent of the complexities and uncertainties of realistic plasma physics. As a result, we have ignored the most important features of the theory: the processes by which the flowing electromagnetic power gets deposited into charged particles in the acceleration region, and the details of the resulting particle motions. However, we think and hope that our formalism can serve as a foundation for detailed studies of these phenomena and of other aspects of black-hole magnetospheres.

We thank Roger Blandford for several very helpful discussions, and Roman Znajek and Chris McKee for helpful critiques of our manuscript.

REFERENCES

Arons, J., 1979. Space Sci. Rev., 24, 437.

Bardeen, J. M., 1973. In Black Holes, p. 241, eds. Dewitt, C. & Dewitt, B.S., Gordon & Breach, New York.

Bardeen, J. M., Press, W. H., & Teukolsky, S. A., 1973. Astrophys. J., 178, 347.

Blandford, R. D., 1976. Mon. Not. R. astr. Soc., 176, 465.

Blandford, R. D., 1979. In Active Galactic Nuclei, p. 241, eds. Hazard, C. & Mitton, S., Cambridge University Press, Cambridge.

Blandford, R. D. & Znajek, R. L., 1977. Mon. Not. R. astr. Soc., 179, 433.

Carter, B., 1979. In General Relativity, An Einstein Centenary Survey, p. 294, eds. Hawking, S. W. & Israel, W., Cambridge University Press, Cambridge.

Damour, T., 1978. Phys. Rev. D, 18, 3598.

Ferraro, V.C.A., 1937. Mon. Not. R. astr. Soc., 97, 458.

Gold, T., 1968. Nature, 218, 731.

Goldreich, P. & Julian, W. H., 1969. Astrophys. J., 157, 869.

Harrison, E. R., 1976. Nature, 264, 525.

Hawking, S. W., 1976. Phys. Rev. D, 13, 191.

Hewish, A., Bell, S. J., Pilkington, J.D.H., Scott, P. F., & Collins, R. A., 1968. Nature, 217, 709.

Kittel, C., 1958. Elementary Statistical Physics, John Wiley & Sons, New York, Section 35.

Linet, B., 1979. J. Phys. A, 12, 839.

Lovelace, R.V.E., 1976. Nature, 262, 649.

Lovelace, R.V.E., MacAuslan, J., & Burns, M., 1979. In Proceedings of La Jolla Institute Workshop on Particle Acceleration Mechanisms in Astrophysics, American Institute of Physics, New York.

Mestel, L., Phillips, P., & Wang, Y. M., 1979. Mon. Not. R. astr. Soc., 188, 385.

Pacini, F., 1968. Nature, 219, 145.

Petterson, J. A., 1975. Phys. Rev. D, 12, 2218.

Price, R. H., 1972. Phys. Rev. D, 5, 2439.

Robinson, I., Schild, A., & Schücking, E., eds., 1965. Quasistellar Sources and Gravitational Collapse, University of Chicago Press, Chicago.

Ruderman, M. & Sutherland, P. G., 1975. Astrophys. J., 196, 51.

Scharlemann, E. T. & Wagoner, R. V., 1973. Astrophys. J., 182, 951.

Schmidt, M., 1963. Nature, 197, 1040.

Thorne, K. S. & Macdonald, D. A., 1981. Mon. Not. R. astr. Soc., submitted. Cited in text as Paper I.

Znajek, R. L., 1977. Mon. Not. R. astr. Soc., 179, 457.

Znajek, R. L., 1978a. Mon. Not. R. astr. Soc., 182, 639.

Znajek, R. L., 1978b. Mon. Not. R. astr. Soc., 185, 833.

FIGURE CAPTIONS

Fig. 1 Accretion disk around a black hole, with magnetic field lines threading it. Although the disk is shown thin, nothing anywhere in our analysis constrains it to be so. The surface $\mathcal{A}$ and its boundary $\partial\mathcal{A}$ are used in the mathematical discussion of magnetic flux conservation in section 3.

Fig. 2 Cross section through space at constant azimuth ϕ showing three types of regions where we make three different assumptions about the structure of the electromagnetic field. In region FF the field is force free; in region D (which includes the disk and the horizon) it is degenerate but not force free; in region A ("acceleration region") it is neither degenerate nor force free. The boundaries between the FF, D, and A regions are shown as dashed lines. Although the disk is drawn fairly thin, it might well be so thick as to reach up and intersect the acceleration region A.

Fig. 3 Annular magnetic flux tubes (dashed lines) used in the text's discussion of torque balance and power flow. Two annular flux tubes are shown. The inner tube (labeled "a") intersects the hole. The outer tube (labeled "b") intersects the disk. Magnetic field lines on the inner face of each tube are characterized by some value ψ of the flux parameter; those on the outer face are characterized by $\psi + \Delta\psi$, where $\Delta\psi$ is the total magnetic flux in the annular tube.

Fig. 4 Cross section showing several electric equipotential surfaces (solid lines, labeled 1, 2, 3, and 4) and several curves along which poloidal current flows (dotted curves labeled $\underset{\sim}{j}$). The degenerate, force free, and acceleration regions are marked D, FF, and A as in Fig. 2. In the D and FF regions the equipotential surfaces coincide with the walls of

the magnetic flux tubes of Fig. 3, but in the A region they deviate from the flux tubes and close up on themselves. In the FF region the current flows along equipotential surfaces, but in the D and A regions it can flow across them.

Fig. 5 Poloidal diagram of the force-free region FF and its boundaries $\mathcal{S}$, $\mathcal{B}$, and $\mathcal{H}$ as used in Section 7.4 in formulating initial value data for solutions of the stream equation.

Fig. 6 Poloidal diagram of the force-free region FF and its boundaries for situations where there is a force-free equatorial gap $\mathcal{G}$ between disk and horizon.

Fig. 7 Diagram used in the proof that poloidal magnetic field loops such as $\mathcal{L}_o$ cannot exist in the force-free region of a stationary, axisymmetric magnetosphere.

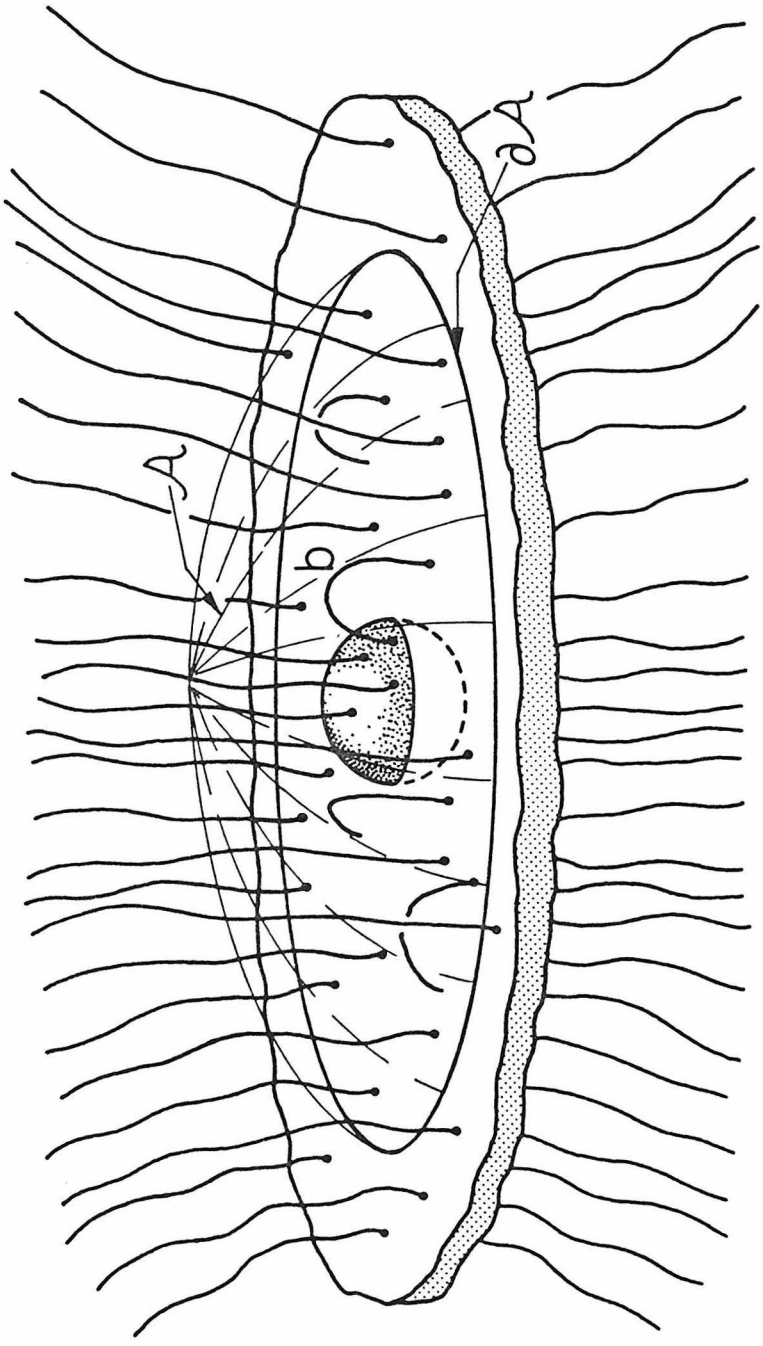

Fig. 1

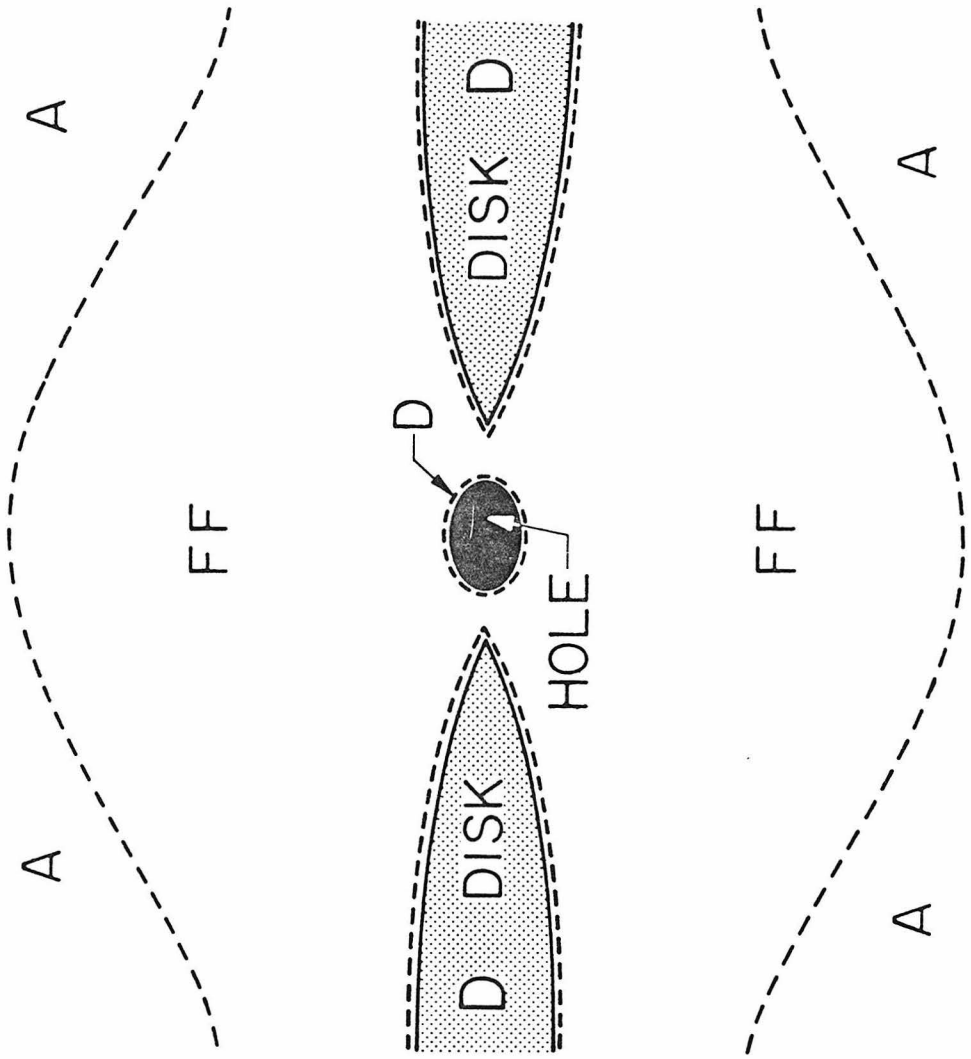

Fig. 2

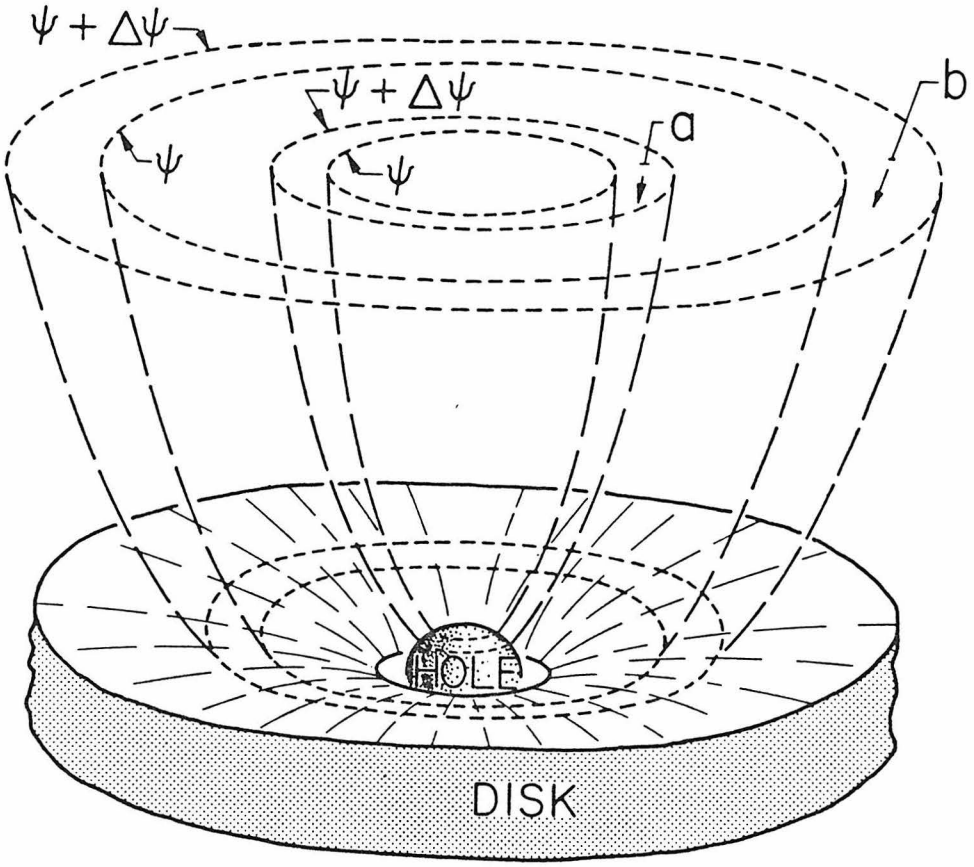

Fig. 3

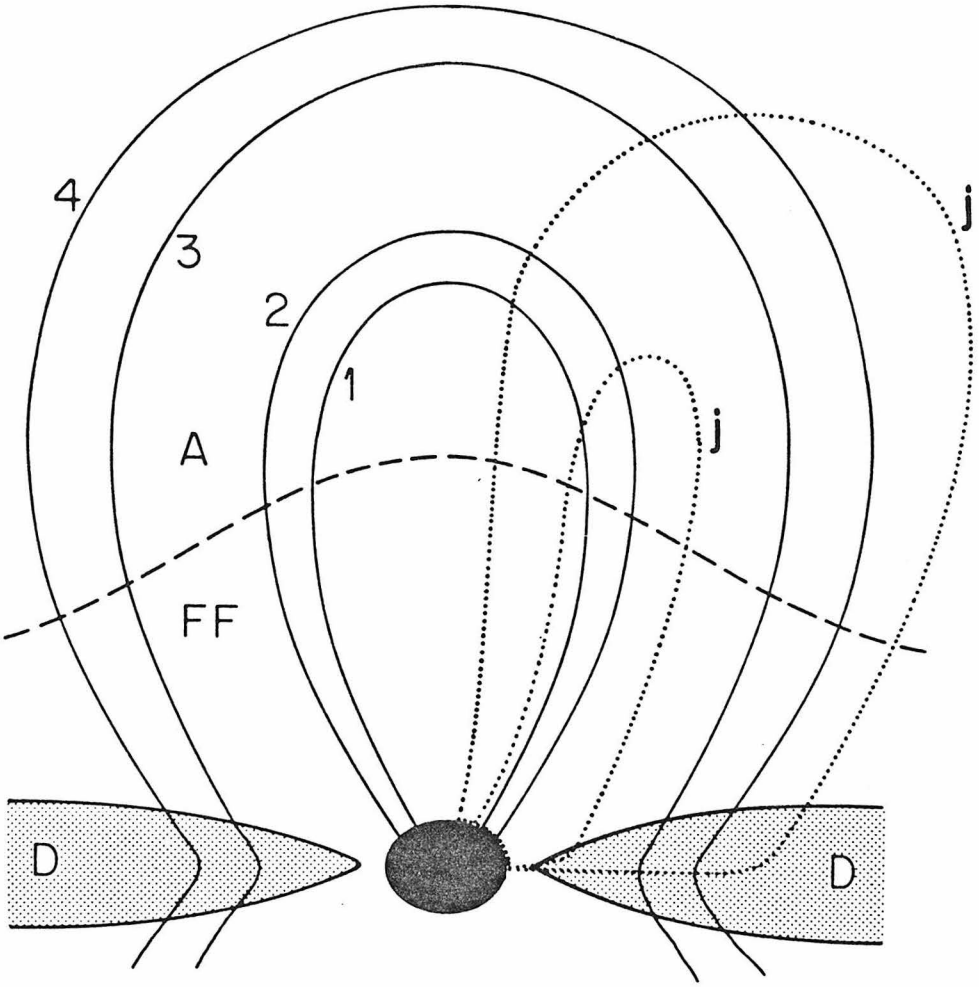

Fig. 4

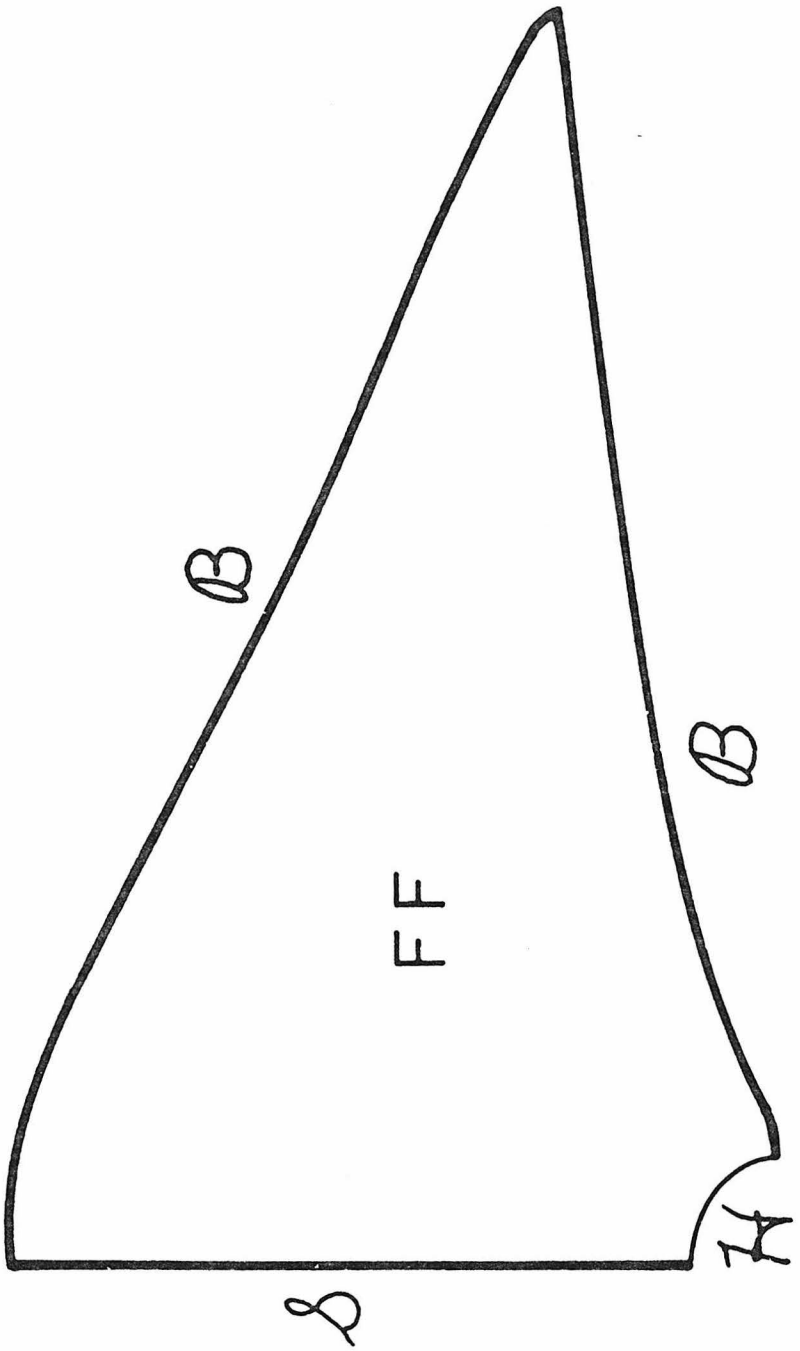

Fig. 5

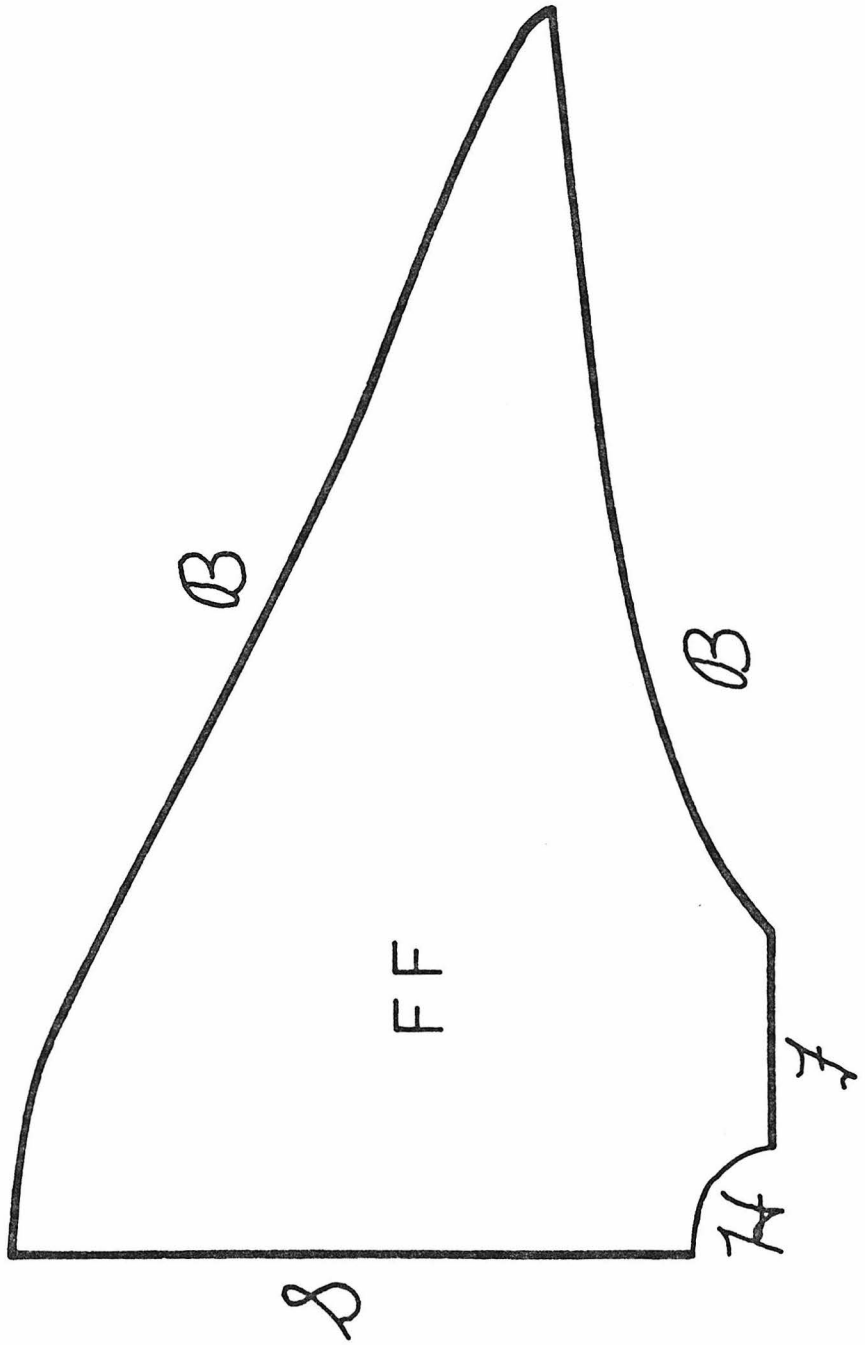

Fig. 6

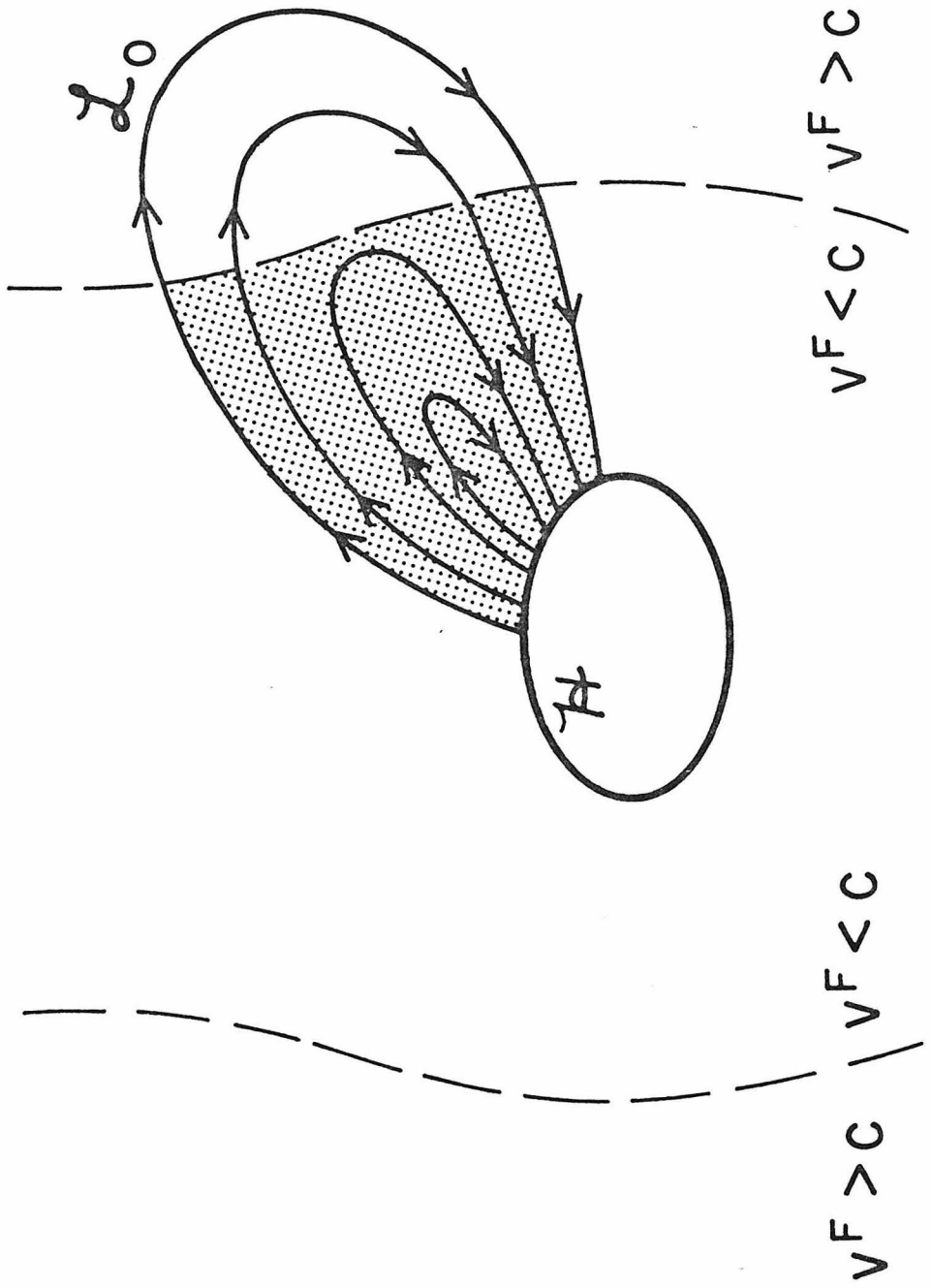

Fig. 7

CHAPTER IV

NUMERICAL MODELS OF BLACK-HOLE MAGNETOSPHERES*

Douglas A. Macdonald

W. K. Kellogg Radiation Laboratory

California Institute of Technology, Pasadena, California 91125

ABSTRACT

This paper develops numerical models of stationary, axisymmetric, force-free black-hole magnetospheres, based on the theory originally developed by Blandford & Znajek and reformulated and extended by Macdonald & Thorne. The structure of such a magnetosphere is determined by a single scalar "stream function" satisfying a nonlinear, second-order partial differential "stream equation" on a region bounded by the black-hole horizon, the accretion disk, and an outer boundary beyond which the force-free condition breaks down. The stream equation is solved numerically, using an iterative relaxation method, for three different poloidal magnetic field configurations: (1) (roughly) radial magnetic field; (2) (roughly) uniform magnetic field; and (3) (roughly) paraboloidal magnetic field. The second and third cases also include a force-free gap between the inner edge of the disk and the horizon, with which the horizon may exchange magnetic flux. For the chosen boundary conditions, it is found that the poloidal field structure

* Supported in part by the National Science Foundation [AST82-14126]

does not change greatly as the field is spun up.

1 Introduction

The mechanism behind the enormous power outputs of quasars and active galactic nuclei has been a subject of lively speculation since their discovery twenty years ago. The idea that black holes may play a role was recognized within months of the discovery of the first quasar, but it was not until relatively recently that realistic models were proposed for the direct extraction of energy from black holes (Blandford 1976, Lovelace 1976, Harrison 1976, Blandford & Znajek 1977). These models have in common the assumption of a supermassive ($\sim 10^8 M_\odot$), stationary, axisymmetric black hole, surrounded by an accretion disk that holds a strong ($\sim 10^4$ Gauss) magnetic field on the hole. A toroidal component of the field extracts the rotational energy of the hole and disk and transfers it to accelerated charged particles, which form a jet carrying the energy to the observed double lobed structures. In some variants of these models, the direction of the jet is determined by the spin axis of the black hole, whose large inertia is responsible for the long-term stability of the linear structure of the jet.

In the Blandford-Znajek model, it is assumed that there exists a region near the horizon where the magnetic field is sufficiently strong, and the plasma sufficiently tenuous, that the plasma exerts no force on the magnetic field. The only role of the plasma in the magnetosphere is to provide the charge and current sources for the field. The field entirely dominates the dynamics, dragging the plasma whither it will. The mathematical expression of this force-free approximation is the vanishing of the Lorentz force density: $\rho_e \mathbf{E} + \mathbf{j} \times \mathbf{B} = 0$. On the other hand, in the non-force-free disk the plasma has so much inertia that it determines the dynamics of the field lines which thread it and are locked into it by its very high electrical conductivity. This point is crucial to the entire model, since it is the disk, not the hole's gravity, that holds the magnetic field on the

hole.

Znajek (1978) and Damour (1978) have shown that, in its interactions with the electromagnetic field, the horizon behaves as if it were an ordinary body with a surface conductivity of $R^H = 4\pi = 377$ ohms. The field lines thus may slip through the horizon; but as they do, it exerts a torque on them. The angular momentum and mechanical energy thereby extracted from the hole are transmitted along the field lines without loss until they reach a region where the force-free approximation breaks down. In this non-force-free "acceleration" region, the energy and angular momentum presumably are transferred to charged particles. The possible mechanisms operating in this acceleration region have been investigated by Blandford (1976), Lovelace (1976), Lovelace *et al.* (1979) and Phinney (1983).

The Blandford-Znajek theory of black-hole magnetospheres was recast in a 3 + 1 language by Macdonald & Thorne (1982) (Paper II in this series) using a formalism developed by Thorne & Macdonald (1982) (Paper I). This paper (Paper III) extends that work by constructing numerical models of stationary, axisymmetric, force-free black-hole magnetospheres. Section 2.1 presents without proof the equations of black-hole magnetospheres derived in Macdonald & Thorne (1982) and describes the prescription to be used in generating the numerical models. The procedure used consists of taking known, static, vacuum solutions of Maxwell's equations in Schwarzschild spacetime and "spinning up" both the hole and the field to obtain the desired force-free solutions in Kerr spacetime. Section 2.2 briefly describes the numerical methods used in constructing the models.

Section 3 describes the details of three specific models. Section 3.1 presents a problem in which the magnetic field lines all thread the horizon and in which the initial field, before spinup, is precisely radial. Section 3.2 considers

a model in which the initial field structure is that of a uniform magnetic field; it also allows the possibility of a force-free gap between the inner edge of the disk and the horizon, with which the horizon may exchange magnetic flux. Section 3.3 describes a model in which the initial field structure is paraboloidal, and also includes a force-free gap.

Throughout this paper, units are used in which the speed of light c and Newton's gravitational constant G are equal to unity. Electromagnetic quantities are expressed in cgs units.

2 Equations of magnetosphere models

2.1 THEORY OF FORCE-FREE BLACK-HOLE MAGNETOSPHERES

This paper treats the topic of black-hole magnetospheres from the viewpoint of the absolute-space/universal-time formalism derived in Macdonald & Thorne (1982) (Paper II). The 3 + 1 notation used there and in this paper is derived and discussed in detail in Thorne & Macdonald (1982) (Paper I); only the fundamentals of it will be reviewed here.

In the absolute-space formalism, a stationary, axisymmetric black-hole spacetime is characterized not by the usual four-dimensional spacetime metric, but rather by an absolute three-geometry

$$dS^2 = e^{2\mu_1}dr^2 + e^{2\mu_2}d\theta^2 + \varpi^2 d\varphi^2 \quad , \tag{2.1}$$

and an associated universal time t. Stationarity means that all quantities are independent of time t; axisymmetry means that they are independent of φ.

The laws of electromagnetism in the absolute-space formalism are couched in terms of the fields measured by a particular family of fiducial observers: the zero-angular-momentum-observers, or ZAMOs, of Bardeen, Press & Teukolsky (1973). Two scalar functions characterize this congruence of observers: their

angular velocity ω defined by

$$\omega \equiv (d\varphi / dt)_{\text{of ZAMO rest frame}} , \tag{2.2}$$

and their "gravitational redshift factor" (also called "lapse function") α defined by

$$\alpha \equiv \frac{d(\text{proper time of ZAMO})}{dt} . \tag{2.3}$$

The functions α and ω together can be thought of as making up the "time-time" and "time-space" parts of the four-dimensional metric of which equation (2.1) is the "space-space" part. The stationarity and axisymmetry of the spacetime require that the functions α, ω, ϖ, μ_1 and μ_2 be independent of t and φ, i.e. be functions of r and θ only.

The structure of a force-free black-hole magnetosphere is determined by a single scalar *stream function* $\psi(r,\theta)$ and two functions of ψ: $\Omega^F(\psi)$ and $I(\psi)$. In terms of these functions, the poloidal and toroidal components of the electric and magnetic fields seen by the ZAMOs are

$$\begin{aligned} \mathbf{E}^P &= -\frac{(\Omega^F - \omega)}{2\pi\alpha}\nabla\psi \ , \ \mathbf{E}^T = 0 \ , \\ \mathbf{B}^P &= \frac{\nabla\psi\times\mathbf{e}_{\hat{\varphi}}}{2\pi\varpi} \ , \ \mathbf{B}^T = -\frac{2I}{\alpha\varpi}\mathbf{e}_{\hat{\varphi}} \ , \end{aligned} \tag{2.4}$$

where ∇ is the gradient (covariant derivative) operator in absolute three-dimensional space and $\mathbf{e}_{\hat{\varphi}}$ is the unit vector in the φ direction. Mathematically, the stream function ψ is equal to 2π times the toroidal component A_φ of the vector potential. Physically, ψ at a point (r_o, θ_o) is equal (by Faraday's law) to the total magnetic flux upward through the azimuthal loop $(r = r_o, \theta = \theta_o)$. Similarly, $I(r_o, \theta_o)$ may be shown to be the total current downward through the same loop. The quantity $\Omega^F(\psi)$ may be interpreted as the angular velocity of the

magnetic field lines relative to absolute space since an observer moving with angular velocity $d\varphi/dt = \Omega^F$ relative to absolute space, i.e. with physical velocity $\mathbf{v}^F \equiv \alpha^{-1}(\Omega^F - \omega)\varpi\mathbf{e}_{\hat{\varphi}}$ as measured by ZAMOs, will see a vanishing electric field $\mathbf{E}' = \gamma[\mathbf{E} + \mathbf{v}^F \times \mathbf{B}] = 0$.

The stream function satisfies a nonlinear, second-order partial differential *stream equation* which was first derived in four-dimensional spacetime language by Blandford & Znajek (1977). In 3 + 1 form it is

$$\nabla\cdot\left\{\frac{\alpha}{\varpi^2}\left[1 - \frac{(\Omega^F - \omega)^2\varpi^2}{\alpha^2}\right]\nabla\psi\right\} + \frac{(\Omega^F - \omega)}{\alpha}\frac{d\Omega^F}{d\psi}(\nabla\psi)^2 + \frac{16\pi^2}{\alpha\varpi^2} I \frac{dI}{d\psi} = 0 \quad . \qquad (2.5)$$

In order to construct a force-free magnetosphere model, one solves equation (2.5) subject to boundary conditions at the borders of the force-free region to be described below.

All of the solutions to be described in this paper will be carried out on a region of the Kerr black-hole spacetime. The lapse function α, ZAMO angular velocity ω, and three-metric of this spacetime in Boyer-Lindquist coordinates (t, r, θ, φ) are

$$\alpha = \sqrt{\frac{\rho^2\Delta}{A}} \quad ,$$

$$\omega = \frac{2aMr}{A} \quad , \qquad (2.6)$$

$$ds^2 = \frac{\rho^2}{\Delta}dr^2 + \rho^2 d\theta^2 + \frac{A\sin^2\theta}{\rho^2}d\varphi^2 \quad ,$$

where M is the mass of the black hole and a is its angular momentum per unit

mass, and where

$$\rho^2 \equiv r^2 + a^2\cos^2\theta \quad ,$$

$$\Delta \equiv r^2 - 2Mr + a^2 \quad ,$$

$$A \equiv (r^2 + a^2)^2 - a^2\Delta\sin^2\theta \quad , \tag{2.7}$$

$$\varpi^2 = \frac{A\sin^2\theta}{\rho^2} \quad .$$

The horizon is located at $r = r_+ \equiv M + \sqrt{M^2 - a^2}$, where $\Delta = a = 0$.

A poloidal slice of the force-free region is shown in Fig. 1. Its inner boundary is at the horizon $\mathscr{H}$ ($r = r_+$), and its outer boundary $\mathscr{B}$ is at some radius $r = R$. Beyond this outer boundary, the force-free condition is presumed to break down, and the electromagnetic field energy is transferred to charged particles; the region beyond the outer boundary is therefore called the acceleration region. In a realistic physical model, the acceleration region would likely be far enough from the hole that both its Keplerian orbital angular velocity and the ZAMO angular velocity ω would be negligible. The models considered here will not all satisfy the condition $R \gg r_+$ (generally R will be taken to be about $5r_+$), but for the sake of simplicity and since the phenomena of greatest interest occur near the horizon and the disk, the angular velocity of the acceleration region will be assumed to be zero. The boundary $\mathscr{S}$ is the axis of symmetry $\theta = 0$. The boundary in the equatorial plane at $\theta = 90°$ is made up of two disjoint regions: a "disk" region $\mathscr{D}$ where the magnetic fields are assumed anchored into the highly conducting plasma of an accretion disk, and a "gap" region $\mathscr{G}$ between the horizon and the inner edge of the disk, through which the force-free magnetic fields extend unimpeded. In some of the models discussed in this paper, $\mathscr{G}$ will be assumed to be nonexistent and the disk will be taken to

extend all the way in to the horizon. In numerical integrations of equation (2.5), it is sufficient to consider just the region shown, thanks to axial symmetry and reflection symmetry about the equatorial plane.

The boundary conditions to be applied on the various regions of the boundary in solving equation (2.5) will now be described: The requirements on the stream function ψ are

$$\mathscr{S} : \quad \psi = 0 \tag{2.8a}$$

$$\mathscr{B} : \quad \psi \text{ a fixed function of position, which is arbitrary except that } \psi \propto \varpi^2 \text{ as } \varpi \to 0 \text{ on } \mathscr{B} \tag{2.8b}$$

$$\mathscr{D} : \quad \psi \text{ a fixed but arbitrary function of position} \tag{2.8c}$$

$$\mathscr{G} : \quad \nabla\psi \propto \mathbf{e}_{\hat{r}} \tag{2.8d}$$

$$\mathscr{H} : \quad \frac{d\psi}{d\theta} = \frac{4\pi I(\psi)}{\Omega^H - \Omega^F(\psi)} \frac{r_+^2 + a^2\cos^2\theta}{(r_+^2 + a^2)\sin\theta} \ . \tag{2.8e}$$

Here Ω^H, the angular velocity of the horizon, is the limit of the ZAMO angular velocity ω at the horizon. The restrictions on ψ at $\mathscr{S}$ and $\mathscr{B}$ are enforced to prevent unphysical singularities in the poloidal magnetic field on the symmetry axis; and the condition at $\mathscr{G}$ guarantees that the magnetic field lines will be vertical in the force-free gap. The boundary condition on $\mathscr{H}$ was first derived by Znajek (1977), and was shown by Macdonald & Thorne (1982) to be the condition of minimal ohmic dissipation in the horizon. The meaning of "arbitrary" in the above context is somewhat restricted; in order for equation (2.5) to have a solution in the interior of the force-free region, the assumed boundary values on $\mathscr{B}$ and $\mathscr{D}$ must be consistent in the sense that points of equal ψ on the

boundary can be joined through the interior by non-crossing lines of force.

The boundary conditions on the functions $\Omega^F(\psi)$ and $I(\psi)$ are

$$\mathscr{S}: \quad \Omega^F = \text{constant} \; ; \; I = 0 \tag{2.9a}$$

$$\mathscr{B}: \quad \Omega^F \text{ and } I \text{ arbitrary except (1) } I \propto \varpi^2 \text{ as } \varpi \to 0 \text{ on } \mathscr{B} \tag{2.9b}$$
$$(2)\; dI/d\psi = (\Omega^H - \Omega^F)/2\pi \text{ at } \mathscr{S} \cap \mathscr{B}$$

$$\mathscr{D}: \quad \Omega^F \text{ and } I \text{ arbitrary} \tag{2.9c}$$

$$\mathscr{G}: \quad \Omega^F = 0 \; ; \; I = 0 \tag{2.9d}$$

$$\mathscr{H}: \quad \Omega^F \text{ and } I \text{ arbitrary} \quad . \tag{2.9e}$$

Here again the conditions on $\mathscr{S}$ and $\mathscr{B}$ are required to prevent unphysical singularities on the symmetry axis. The conditions on $\mathscr{G}$ arise because field lines passing through the gap are anchored at both ends in the acceleration region and will thus share its angular velocity (zero) and will have no toroidal component ($I \propto B^T$ by equation 2.4).

The wide arbitrariness in the choice of boundary conditions on ψ allows a wide variety of solutions in the interior of the force-free region. One may choose boundary conditions to yield arbitrarily complex structures such as magnetic field loops embedded in the disk or in the boundary of the acceleration region. There is no basis for ruling out these complex structures on physical grounds; a magnetic field being dragged in toward a black hole by an accretion disk might be expected to have a tangled and chaotic structure since the high conductivity of the disk will not allow the field loops to slip through the plasma and annihilate themselves. On the other hand, the horizon has a relatively high surface resistivity: $R^H = 4\pi = 377$ ohms, as shown by Znajek (1978) and Damour (1978); any

field loop embedded in it will annihilate itself on a timescale of the order of the light-travel time across the loop. The structure of the horizon field determined by equation (2.8e) will thus generally be simpler and more uniform than the structure of the field threading the disk; the horizon can therefore be thought of as "cleaning" the field carried onto it by the disk (cf. section 7.5 of Paper II; also Thorne *et al.* 1984).

Notwithstanding the allowed freedom in the choice of boundary conditions, it is not desirable for the purposes of the present paper to assume boundary conditions which lead to complex field structures. The phenomenon of greatest interest is the behavior of the magnetic field as the black hole is spun up, i.e. as Ω^H is increased from zero. To isolate this behavior from the effects of variations in other parameters of the problem and peculiarities in their form, it is convenient to fix the boundary conditions in as simple a manner as possible while the hole is spun up. Another consideration favoring simplicity is that the numerical solutions derived here will all be derived by spinning up static, vacuum magnetic field solutions in the Schwarzschild metric, so the assumed forms of $\Omega^F(\psi)$ and $I(\psi)$ must satisfy the horizon boundary condition (2.8e) in the limit that I, Ω^F and Ω^H approach zero; that is, the boundary functions must be chosen so that the ratio $I(\psi)/[\Omega^H - \Omega^F(\psi)]$ approaches $\sin\theta(d\psi/d\theta)$ as $a \to 0$ in order for equation (2.8e) to be satisfied.

One may obtain some guidance in choosing the functional forms of $\Omega^F(\psi)$ and $I(\psi)$ by considering the arguments contained in section 7 of Paper II. There a precise analogy is drawn between the force-free magnetosphere and a DC circuit, and it is shown that the angular velocity Ω^F of a magnetic flux tube is determined by the ratio of the impedances across the tube at its two ends. In order to make this idea quantitative, one defines a function Z^A, considered as a function of ψ, as the total resistance of the acceleration region between field

lines which intersect it at some fixed latitude θ_o, and field lines labelled by ψ. (The constant θ_o is introduced to avoid the infinite values which would appear if the impedance were defined from the axis, but it will not enter into physical equations since Z^A will always appear as a differentiated quantity.) Similar functions $Z^H(\psi)$ and $Z^D(\psi)$ may be defined for the horizon and the disk, respectively. The horizon impedance Z^H has a fairly simple functional form; for a Schwarzschild hole, it is calculated by multiplying the horizon's surface resistivity $R^H = 4\pi$ by the meridional distance $r d\theta$ and dividing by the cross sectional length $2\pi\varpi = 2\pi r \sin\theta$, then integrating over θ:

$$Z^H = \int_{\theta_o}^{\theta} \frac{2 d\theta'}{\sin\theta'} = 2 \ln \frac{\tan\theta/2}{\tan\theta_o/2} \quad . \tag{2.10}$$

The disk and acceleration-region impedances in general will have a more complicated form than this since their resistivities will depend on the characteristics of the matter of which they are composed.

The field-line angular velocity is determined on lines threading the horizon by

$$\frac{\Omega^F(\psi)}{\Omega^H - \Omega^F(\psi)} = \frac{dZ^A(\psi)}{dZ^H(\psi)} \quad , \tag{2.11a}$$

and on lines threading the disk by

$$\frac{\Omega^F(\psi)}{\Omega^D - \Omega^F(\psi)} = \frac{dZ^A(\psi)}{dZ^D(\psi)} \quad . \tag{2.11b}$$

Blandford & Znajek (1977), Lovelace *et al.* (1979), Macdonald & Thorne (1982) and Phinney (1983) give models and arguments suggesting that the ratio $dZ^A(\psi)/dZ^H(\psi)$ should be roughly unity, which implies that $\Omega^F \approx \Omega^H/2$; i.e. the angular velocities of field lines threading the hole are half that of the hole.

Blandford & Znajek show that this is the condition for extraction of maximum power by a given magnetic-field distribution on the hole. On the other hand, the ratio $dZ^A(\psi)/dZ^D(\psi)$ should be very large because of the large conductivity of the plasma making up the disk; equation (2.10b) then implies that $\Omega^F \approx \Omega^D$, i.e. the field lines are frozen into the disk.

The current potential $I(\psi)$ is determined by the equations

$$I^H = \frac{\Omega^H - \Omega^F}{2\pi(dZ^H/d\psi)} , \quad I^D = \frac{\Omega^F}{2\pi(dZ^A/d\psi)} , \tag{2.12}$$

for field lines threading the hole and the disk, respectively.

In accordance with the above guidelines, the field-line angular velocity Ω^F for field lines threading the hole will be chosen to equal $\Omega^H/2$ in all models constructed here. The currents will be taken to have the functional form defined by the slow-rotation limit of equations (2.12), i.e. the derivatives $dZ^H/d\psi$ and $dZ^A/d\psi$ will be figured using the ψ of the pre-spinup, Schwarzschild-spacetime solution. Since the ratio $dZ^A(\psi)/dZ^H(\psi)$ is assumed to be approximately unity, the acceleration region will be taken to have an effective surface resistivity of order unity; the impedance Z^A used in equation (2.12) to determine the current on field lines threading the disk will therefore be defined by an equation of the form $dZ^A \propto d\theta/\sin\theta$. The disk will be taken to have infinite conductivity so that the magnetic field lines are rigidly frozen into the disk and must rotate with its angular velocity.

2.2 METHODS OF NUMERICAL SOLUTION

As a first step in constructing a numerical magnetosphere model, it is convenient to rescale all quantities of interest so that they are dimensionless. This may be done using the only scale factor inherent in the problem: the mass M of

the black hole.

$$r^* \equiv r/M \ , \quad a^* \equiv a/M \ , \quad \varpi^* \equiv \varpi/M \ , \quad t^* \equiv t/M \ , \quad \omega^* \equiv \omega M \ , \quad \Omega^{F*} \equiv \Omega^F M \ ,$$

$$\Omega^{H*} \equiv \Omega^H M = a^*/2Mr^* \ , \quad r_+^* \equiv r_+/M = 1 + (1 - a^{*2})^{1/2} \ , \tag{2.13}$$

$$\mathbf{B}^* \equiv \mathbf{B}M \ , \quad \mathbf{E}^* \equiv \mathbf{E}M \ , \quad \psi^* \equiv \psi/M \ , \quad I^* \equiv I \ .$$

For a black hole of mass $M \sim 10^8 M_\odot$, surrounded by a magnetic field of strength $B \sim 10^4$ G, and with magnetospheric currents of order 10^{18} amperes, the dimensionless quantities $\mathbf{B}^*$, ψ^* and I^* will all have magnitudes of order 10^{-8}. If one reformulates all of the equations in section 2.1 in terms of the rescaled quantities (including expressing the ∇ operator in terms of r^*-derivatives), all equations precisely retain their original forms except for the replacement of non-starred by starred quantities. Thus, in the interest of notational simplicity, the stars will be dropped and all quantities will henceforth be understood to be dimensionless.

Equation (2.5) is elliptic everywhere except on the locus $(v^F)^2 = 1$ or $(\Omega^F - \omega)^2 \varpi^2 / \alpha^2 = 1$ ("velocity-of-light surface"), where it becomes a first-order equation. It is thus amenable to solution by finite-difference, point-iterative relaxation methods on a grid (see e.g. Ames 1977). The grid chosen was an $r-\theta$ coordinate grid with constant stepsizes h_r and h_θ in the respective directions. The computational molecule is shown in Fig. 2.

The gradient operators in equation (2.5) are covariant derivatives in absolute three-dimensional space. The first term in (2.5) may be expressed in terms of ordinary derivatives as

$$\nabla \cdot \left[X \nabla \psi \right] = \frac{1}{\sqrt{g}} (\sqrt{g}\, X g^{ij} \psi_{,j})_{,i} \tag{2.14}$$

$$= \frac{e^{-\mu_1 - \mu_2}}{\varpi} \left[(e^{-\mu_1 + \mu_2} X \varpi \psi_{,r})_{,r} + (e^{\mu_1 - \mu_2} X \varpi \psi_{,\theta})_{,\theta} \right] \ ,$$

where $e^{\mu_1} = \rho/\sqrt{\Delta}$, $e^{\mu_2} = \rho$ [cf. equations (2.1) and (2.6)], $X \equiv \alpha(1 - (\varpi^F)^2)/\varpi^2$, and where $\sqrt{g} \equiv \varpi e^{\mu_1 + \mu_2}$ is the square root of the determinant of the three-dimensional metric (2.1). The differential equation (2.5) may thus be written as a difference equation on the grid of Fig. 2 in the following form:

$$\frac{e^{-\mu_1-\mu_2}|_0}{\varpi_0}\left[(e^{-\mu_1+\mu_2}X\varpi)_0\,\frac{\psi_1-2\psi_0+\psi_3}{h_r^2}+(e^{-\mu_1+\mu_2}X\varpi)_{,r}|_0\,\frac{\psi_1-\psi_3}{2h_r}\right.$$

$$\left.+(e^{\mu_1-\mu_2}X\varpi)_0\,\frac{\psi_4-2\psi_0+\psi_2}{h_\theta^2}+(e^{\mu_1-\mu_2}X\varpi)_{,\theta}|_0\,\frac{\psi_4-\psi_2}{2h_\theta}\right] \qquad (2.15)$$

$$+\frac{(\Omega^F-\omega)_0}{\alpha_0}\,\frac{d\Omega^F}{d\psi}\bigg|_{\psi_0}\left[\frac{e^{-2\mu_1}|_0}{4h_r^2}(\psi_1-\psi_3)^2+\frac{e^{-2\mu_2}|_0}{4h_\theta^2}(\psi_4-\psi_2)^2\right]+\frac{16\pi^2}{\alpha_0\varpi_0^2}I(\psi_0)\,\frac{dI}{d\psi}\bigg|_{\psi_0}=0\ ,$$

where the subscripts 0–4 refer to the points labeled in Fig. 2.

Solving this equation for ψ_0 yields a prescription for an iterative relaxation scheme; in updating the array, the new value of ψ at the point 0 is calculated as a function of the old values of ψ at the surrounding points. The particular method used was a technique known as successive over-relaxation (SOR) with Gauss-Seidel iteration (see e.g. Ames 1977). In this method, the prospective correction $\psi_{0(new)} - \psi_{0(old)}$ is multiplied by a factor β $(1 \le \beta < 2)$ before being added to $\psi_{0(old)}$. The relaxation parameter β may be chosen to optimize the convergence rate: if λ is the asymptotic ratio of maximum corrections on successive iterations when $\beta = 1$, then the optimal value of β is $\beta_{SOR} = 2/(1 + \sqrt{1 - \lambda})$; this value of β produces a convergence ratio (ratio of successive maximum corrections) of $\beta_{SOR} - 1$.

One point of difficulty with the solution is that, as mentioned previously, equation (2.5) becomes a first-order equation on the velocity-of-light surface $(\mathbf{v}^F)^2 = 1$. If $0 \le \Omega^F \le \Omega^H$ (which is the condition for energy extraction), there

are actually two distinct velocity-of-light surfaces: an inner one near the horizon, within which any particle attached to the field lines must slide inward in order to avoid superluminal motion; and an outer surface, corresponding to the familiar pulsar light cylinder, beyond which particles locked to the field lines must slide outward. For a nonrotating hole and field, the inner light surface is coincident with the horizon and the outer one is at infinity.

At the light surfaces, equation (2.5) just becomes a Neumann-type boundary condition

$$|\nabla X| \frac{\partial \psi}{\partial n} + \frac{(\Omega^F - \omega)}{\alpha} \frac{d\Omega^F}{d\psi} (\nabla \psi)^2 + \frac{16\pi^2}{\alpha \varpi^2} I \frac{dI}{d\psi} = 0 , \tag{2.16}$$

where $\partial \psi / \partial n$ denotes the normal derivative of ψ at the light surface.

Considerable difficulty was encountered in finding a difference equation which was stable at the light surface. Several schemes which were tried before equation (2.15) was selected were found to produce divergences if the outer light cylinder was within the region of integration. Explicit attempts to model the Neumann boundary condition (2.16) produced more success, but the best results were obtained using the differencing scheme embodied in equation (2.15). Even this method exhibited noticeable oscillations in the solution values at lattice points which happened to lie very near the light surface (much nearer than the stepsizes h_r and h_θ); this is due to the fact that, in solving equation (2.15) for ψ_0, the quantity X, which vanishes on the the light surface, occurs in the denominator. Oscillations may occur if a particular iteration moves the light surface across a lattice point lying near it; the next iteration will then apply a correction of the opposite sign which will tend to move the light surface back across the lattice point. But the oscillations were usually small enough that equation (2.15) converged to a solution for the rotation parameter a less than about 0.75, where the criterion for successful convergence was defined by

requiring the maximum correction to decline to a value 0.001 times its value at the first iteration.

In situations where a force-free gap was assumed to exist between the horizon and the inner edge of the disk, the boundary condition (2.8d) was enforced by resetting the boundary values of ψ on the gap after each iteration in such a way as to require the field to pass through the gap vertically. After each iteration, the magnetic field would generally come out with a small but nonzero radial component at the gap; condition (2.8d) was applied by changing the values of ψ on the gap so that it once more represented a vertical field at the boundary. In general, this required adding or removing some flux from the horizon; this was accomplished by refiguring the horizon field using (2.8e) and the newly calculated value of the total flux threading the horizon.

3 Specific models

3.1 RADIAL MAGNETIC FIELD

Since the interaction of the magnetic field with the horizon is one of the major phenomena of interest, it is instructive to consider a problem in which all of the magnetic flux threads the horizon and is held on the hole by a disk extending all the way up to the horizon. This is not physically realistic; it presupposes that the disk, which carried the magnetic field onto the hole, has run out of flux threading it, and it further requires part of the disk to be inside the innermost stable circular orbit. However, this idealization allows the effects of the spinup of the horizon on the field to be seen free from the interference of effects of the disk. This model is similar to an analytic, perturbative solution for small a/M derived by Blandford & Znajek (1977).

The solutions described in this section are derived by spinning up the solution

$$\psi = \psi_o(1 - \cos\theta) \quad , \tag{3.1}$$

which satisfies the vacuum stream equation $\nabla\cdot(\alpha\nabla\psi/\varpi^2) = 0$ for zero rotation and consists of precisely radial field lines, all of which thread the horizon. (The field points into the horizon below the equator, and out of it above the equator; otherwise Gauss's magnetic law $\oint \mathbf{B}\cdot d\Sigma = 0$ could not be satisfied.)

If all of the field lines are taken to rotate with angular velocity $\Omega^F = \Omega^H/2$, then the horizon boundary condition (2.8e) implies that the current I depends on ψ as

$$I = \frac{\Omega^F\psi_o}{4\pi}\sin^2\theta = \frac{\Omega^F\psi_o}{4\pi}\left[2\,\frac{\psi}{\psi_o} - \frac{\psi^2}{\psi_o^2}\right] \tag{3.2}$$

in the zero-rotation limit. For simplicity, it will be assumed that this functional form is retained throughout the spinup of the hole. For nonzero rotation, the horizon boundary condition (2.8e) may be separated

$$\frac{\Omega^F}{4\pi}\,\frac{d\psi}{I(\psi)} = \frac{r_+^2 + a^2\cos^2\theta}{(r_+^2 + a^2)\sin\theta}\,d\theta \quad , \tag{3.3}$$

and integrated to get the horizon field $\psi^H(\theta)$

$$\psi^H(\theta) = \frac{2\psi_o}{1 + \dfrac{\sin^2\theta}{(1-\cos\theta)^2}\exp\left[-\dfrac{2a^2\cos\theta}{r_+^2 + a^2}\right]} \quad . \tag{3.4}$$

This function reduces to the form (3.1) in the limit of zero rotation; it is plotted in Fig. 3 for several different values of the rotation parameter a. It may be seen that, as the hole is spun up, the field threading the hole concentrates itself toward the pole. The effect is not dramatic however; for a nonrotating hole ($a = 0$), half the flux threads the hole north of latitude 30°, while for an extreme

Kerr hole ($a = 1$), roughly 71% of the flux threads the hole north of this latitude.

In solving this problem, the zero-rotation solution (3.1) was used as a starting solution for spinning the hole up to $a = 0.1$. After this solution converged, it was used as the initial solution for spinning the hole up to $a = 0.2$, and so on. This procedure ensured that the initial solution in the iteration was always a fairly good approximation to the desired solution; this had the advantage of guaranteeing rapid convergence as well as avoiding unwanted divergences. For a magnetosphere with radius $R \sim 10$, the hole could be spun up to about $a = 0.75$ with good convergence.

Fig. 4 shows the poloidal field structure for several representative choices of the rotation parameter a and the total magnetospheric radius R. The spinup of the hole has little effect on the poloidal field structure; the field lines for $R = 10$, $a = 0.5$ are barely distinguishable from the precisely radial field lines which exist for $a = 0$. The diagrams for the cases $R = 10$, $a = 0.66$ and $R = 100$, $a = 0.1$ are included to show the effects of the light surface, which in this case is a cylinder of approximate radius $8/a$. The effects of the oscillations mentioned in section 2.2 are discernible as slight kinks in the field lines, but it is clear that these are just numerical difficulties and that there is no physical impediment to integrating the solutions across the light surface. The solution for $R = 4$, $a = 0.9$ shows a slight focussing of the field lines toward the rotation axis.

3.2 UNIFORM MAGNETIC FIELD

The stream function for an asymptotically uniform magnetic field threading a Schwarzschild black hole in vacuum is (cf. Wald 1974, Hanni & Ruffini 1976)

$$\psi = \frac{\psi_o}{4} r^2 \sin^2\theta \quad , \tag{3.5}$$

where ψ_o is the magnetic flux threading the hole. The asymptotic strength of the magnetic field is $\psi_o / 4\pi$. The solutions described in this section are derived by spinning up this solution.

Assuming as before that all of the field lines threading the horizon rotate with angular velocity $\Omega^F = \Omega^H / 2$, the horizon boundary condition (2.8e) implies that the current potential I^H on these field lines depends on ψ as

$$I^H = \frac{\Omega^F \psi_o}{2\pi} \sin^2\theta \cos\theta = \frac{\Omega^F}{2\pi} \psi \sqrt{1 - (\psi / \psi_o)} \tag{3.6}$$

in the zero-rotation limit. This form of I implies that current flows into the horizon north of the latitude where $\psi = 2\psi_o / 3$, and out of the horizon south of this latitude. As before, it will be assumed that the functional form (3.6) holds throughout the spinup of the hole. For nonzero rotation, the horizon boundary condition (2.8e) may be separated and integrated to obtain

$$\psi^H(\theta) = \psi_o \left\{ \frac{4(1 - \cos\theta)^2 \exp[2a^2 \cos\theta / (r^2 + a^2)]}{\{\sin^2\theta + (1 - \cos\theta)^2 \exp[2a^2 \cos\theta / (r^2 + a^2)]\}^2} \right\} \sin^2\theta \quad . \tag{3.7}$$

Here, unlike in the radial-field-line problem, the quantity ψ_o is not be taken as fixed; rather, a gap region $\mathscr{G}$ is assumed to exist between the inner edge of the disk and the horizon, with which the horizon may exchange magnetic flux. The current (3.6) goes to zero at the equator of the hole so that it matches continuously to the gap boundary condition (2.9d). The function $\psi^H(\theta) / \psi_o$ is plotted in Fig. 5 for several different values of the rotation parameter a. As in the radial-field problem, the field concentrates itself toward the pole as the hole is spun up, but the effect is not dramatic.

The plasma of the disk is assumed to be moving in circular geodesic orbits; the angular velocity of these orbits is the relativistic generalization of the Keplerian angular velocity:

$$\Omega^D = 1/(r^{3/2} + a) \tag{3.8}$$

(see e.g. Bardeen 1973). The field lines embedded in it are assumed to rotate with it: $\Omega^F = \Omega^D$. The inner edge of the disk is assumed to be at a fixed value of r. Although it might have made more physical sense to choose it at the radius of the marginally stable orbit, it was deemed unnecessary to introduce this additional complication to the problem. That choice would have led to the r-coordinate radius of the gap going to zero as $a \to 1$ (which could not be accommodated by the chosen integration scheme), while its proper radius approached infinity.

The current on field lines threading the disk is determined solely by the impedance of the acceleration region according to equation (2.12). This impedance is assumed to be determined by an equation of the form $dZ^A = d\theta/\sin\theta$ at the boundary of the acceleration region, i.e. surface resistivity equals unity. Equation (2.12) then implies

$$I^D = \frac{\Omega^F \psi_o R^2}{4\pi} \sin^2\theta\cos\theta = \frac{\Omega^F}{\pi}\psi\sqrt{1 - 4\psi/\psi_0 R^2} \quad , \tag{3.9}$$

where R is the radius of the boundary of the acceleration region.

As a first step in solving this problem, the force-free gap was introduced, and the zero-rotation solution (3.5) was allowed to relax into it in accord with the boundary condition (2.8d). This caused almost no change in the field since it already passed vertically through the equatorial plane. (The small change which did occur was due to the fact that, although a precisely vertical magnetic field is an exact solution of the differential equation (2.5) with the given boundary conditions, it may differ from the exact solution of the difference equation (2.15) by terms of order h_r^2 or h_θ^2.) The disk was then spun up, and the frozen-in field with it, using the step-by-step procedure described in the last section. Lastly the

hole was spun up using the same procedure.

Fig. 6 shows the poloidal field structure for several different values of the rotation parameter a. The boundary of the acceleration region has been taken to lie at $r = 10$, and the edge of the disk has been taken to be at $r = 6$. As in the radial-field problem, the poloidal field structure is not greatly affected by the spinup of the hole. The amount of magnetic flux threading the hole was found to stay roughly constant as the hole was spun up, even though the cross sectional area of the horizon is decreasing.

3.3 PARABOLOIDAL MAGNETIC FIELD

The stream function

$$\psi = \frac{\psi_o}{4\ln 2}\left\{(r-2)(1-\cos\theta) + 2\left[2\ln 2 - (1+\cos\theta)\ln(1+\cos\theta)\right]\right\} \tag{3.10}$$

satisfies the vacuum Maxwell equations in Schwarzschild spacetime and describes an asymptotically paraboloidal magnetic field which threads both the black hole and the disk. The total flux threading the hole is ψ_o. The models described in this section are derived by spinning up this solution.

This model is of particular interest because, in contrast to the uniform-field model, the flux is concentrated on the hole, and also because the electromagnetic energy is focussed along the rotation axis, as is observed in astrophysical jets. It is also consistent with a nonrelativistic argument given by Blandford (1976) to the effect that, if the only torques acting on the disk and the hole are electromagnetic, then stationarity requires that the poloidal field strength at the disk vary inversely with radius, and thus that ψ vary directly with radius.

Unfortunately, the specialization of equation (3.10) to the horizon yields a form for $\psi^H(\theta)$ which cannot be inverted and solved analytically for θ, thus not

allowing the prescription used in the preceding two sections to be carried out. To make the problem computationally tractable, the horizon field for $a = 0$ will be chosen to be $\psi^H(\theta) = \psi_o(1 - \cos\theta)$. This form is close to that derived by restricting equation (3.10) to the horizon, differing from it by at most 22%. Diagram (a) of Fig. 7 shows the field lines for the solution (3.10), while diagram (b) shows the field lines with the new choice of horizon field; it may be seen that the new choice retains the overall paraboloidal form of the field while greatly simplifying the numerical computations.

A similar approximation must be made, for the same reason, in figuring the current on field lines threading the disk. If the flux at the surface $r = R$ of the acceleration region is approximated as $\psi^A(\theta) = (\psi_o R / 4\ln 2)(1 - \cos\theta)$, the current is

$$I^D = \frac{\Omega^F \psi_o R}{8\pi \ln 2} \sin^2\theta = \frac{\Omega^F \psi_o R}{8\pi \ln 2} \left[1 - \left[1 - \frac{4\psi \ln 2}{\psi_o R}\right]^2\right] \quad . \tag{3.11}$$

As in the two previous models, it is assumed that all field lines threading the horizon rotate with angular velocity $\Omega^F = \Omega^H / 2$, so the current on field lines threading the horizon is just given by equation (3.2) and the horizon field for the spun-up hole is given by equation (3.4) and Fig. 3. The current does not go to zero at the equator as in the uniform-field case, so a poloidal current sheet is required in the magnetosphere to support the discontinuity in the toroidal magnetic field. A force-free gap is again assumed to lie between the horizon and the inner edge of the disk. The disk is assumed to be Keplerian (equation 3.8).

The sequence of steps followed in solving this problem was the same as that used in the uniform-field case. First the force-free gap was introduced and the field was allowed to relax into it. In contrast to the uniform field case, this relaxation had a large effect on the field since the original field had kinks in it at the

disk due to the toroidal currents there. This problem therefore serves as a good test of the algorithm used for exchanging flux between the gap and the horizon. Diagram (c) of Fig. 7 shows the configuration of the field lines after the field has relaxed into the gap. The gap field is roughly vertical, but is modified somewhat from verticality by the Maxwell pressure of the surrounding field.

Next, the disk was spun up to Keplerian orbital velocity; the result of this is shown in diagram (d) of Fig. 7. Finally, the hole was spun up.

Fig 8 shows the poloidal field structure for several different values of a. Again the boundary of the acceleration region has been taken to lie at $r = 10$ and the outer edge of the force-free gap at $r = 6$. Once more it is seen that the poloidal field structure is only slightly affected by the spinup of the hole. As in the uniform-field case, the amount of flux threading the hole was found to stay roughly constant as the hole was spun up.

Acknowledgements

I thank Kip Thorne for suggesting this problem and for many helpful suggestions, and Roger Blandford for several useful discussions.

REFERENCES

Ames, W. F., 1977. *Numerical Methods for Partial Differential Equations*, Academic Press, New York.

Bardeen, J. M., 1973. In *Black Holes*, p. 215, eds. Dewitt, C. & Dewitt, B. S., Gordon & Breach, New York.

Bardeen, J. M., Press, W. H., & Teukolsky, S. A., 1973. *Astrophys. J.*, **178**, 347.

Blandford, R. D., 1976. *Mon. Not. R. astr. Soc.*, **176**, 465.

Blandford, R. D. & Znajek, R. L., 1977. *Mon. Not. R. astr. Soc.*, **179**, 433.

Damour, T., 1978. *Phys. Rev. D*, **18**, 3598.

Hanni, R. S. & Ruffini, R., 1976. *Lettere al Nuovo Cimento*, **15**, 189.

Harrison, E. R., 1976. *Nature*, **264**, 525.

Lovelace, R. V. E., 1976. *Nature*, **262**, 649.

Lovelace, R. V. E., MacAuslan, J., & Burns, M., 1979. In *Proceedings of La Jolla Institute Workshop on Particle Acceleration Mechanisms in Astrophysics*, American Institute of Physics, New York.

Macdonald, D. A. & Thorne, K. S., 1982. *Mon. Not. R. astr. Soc.*, **198**, 345.

Phinney, E. S., 1983. In *Proceedings of the Torino Workshop on Astrophysical Jets*, p. 201, eds. Ferrari, A. & Pacholczyk, A. G., D. Reidel, Dordrecht, Holland.

Thorne, K. S. & Macdonald, D. A., 1982. *Mon. Not. R. astr. Soc.*, **198**, 339 and Microfiche MN 198/1.

Thorne, Kip S., Price, Richard H., Crowley, Ronald J., Zurek, Wojciech, Suen, Wai-Mo, Redmount, Ian H., Macdonald, Douglas A., Finn, L. Sam, & Zhang, Xiao-

He, 1984. In preparation, to be submitted to *Rev. Mod. Phys.*

Wald, R. M., 1974. *Phys. Rev. D*, **10**, 1680.

Znajek, R. L., 1977. *Mon. Not. R. astr. Soc.*, **179**, 457.

Znajek, R. L., 1978. *Mon. Not. R. astr. Soc.*, **185**, 833.

FIGURE CAPTIONS

Figure 1. Poloidal diagram of the force-free region, showing its boundary segments. The inner radial boundary is the horizon $\mathscr{H}$ and the outer boundary $\mathscr{B}$ is at radius $r = R$. The boundary $\mathscr{S}$ is the axis of symmetry $\theta = 0$. The boundary in the equatorial plane at $\theta = 90°$ is made up of a "disk" region $\mathscr{D}$ where the magnetic fields are assumed anchored into the highly conducting plasma of an accretion disk, and a "gap" region $\mathscr{G}$ between the horizon and the inner edge of the disk, through which the force-free magnetic fields extend unimpeded.

Figure 2. The computational molecule used in the numerical solution of the stream equation. The grid has constant stepsizes h_r and h_θ in the r and θ directions, respectively. The labels 0–4 on the grid points are used in the finite-difference equation (2.15).

Figure 3. The horizon magnetic flux distribution ψ^H / ψ_0 for the radial-field-line problem, shown for various different values of the rotation parameter a. The same diagram applies for the paraboloidal-field problem.

Figure 4. Poloidal field diagrams for the radial-magnetic-field problem for representative choices of rotation parameter a and total magnetospheric radius R.

Figure 5. The horizon magnetic flux distribution ψ^H / ψ_0 for the uniform-field problem, shown for various different values of the rotation parameter a.

Figure 6. Poloidal field diagrams for the uniform-magnetic-field problem for representative choices of the rotation parameter a. The outer boundary of the magnetosphere is at $r = 10$ and the outer edge of the force-free gap is at $r = 6$.

Figure 7. Stages in the relaxation of the paraboloidal field before spinup of the hole. Diagram (a) shows the solution (3.10); diagram (b) shows the solution with numerically simpler horizon boundary conditions. Diagram (c) shows the field

after the force-free gap is introduced and the field is allowed to relax into it. Diagram (d) shows the field after the spinup of the disk to Keplerian angular velocity.

Figure 8. Poloidal field diagrams for the paraboloidal-magnetic-field problem for representative choices of the rotation parameter α. The outer boundary of the magnetosphere is at $r = 10$ and the outer edge of the force-free gap is at $r = 6$.

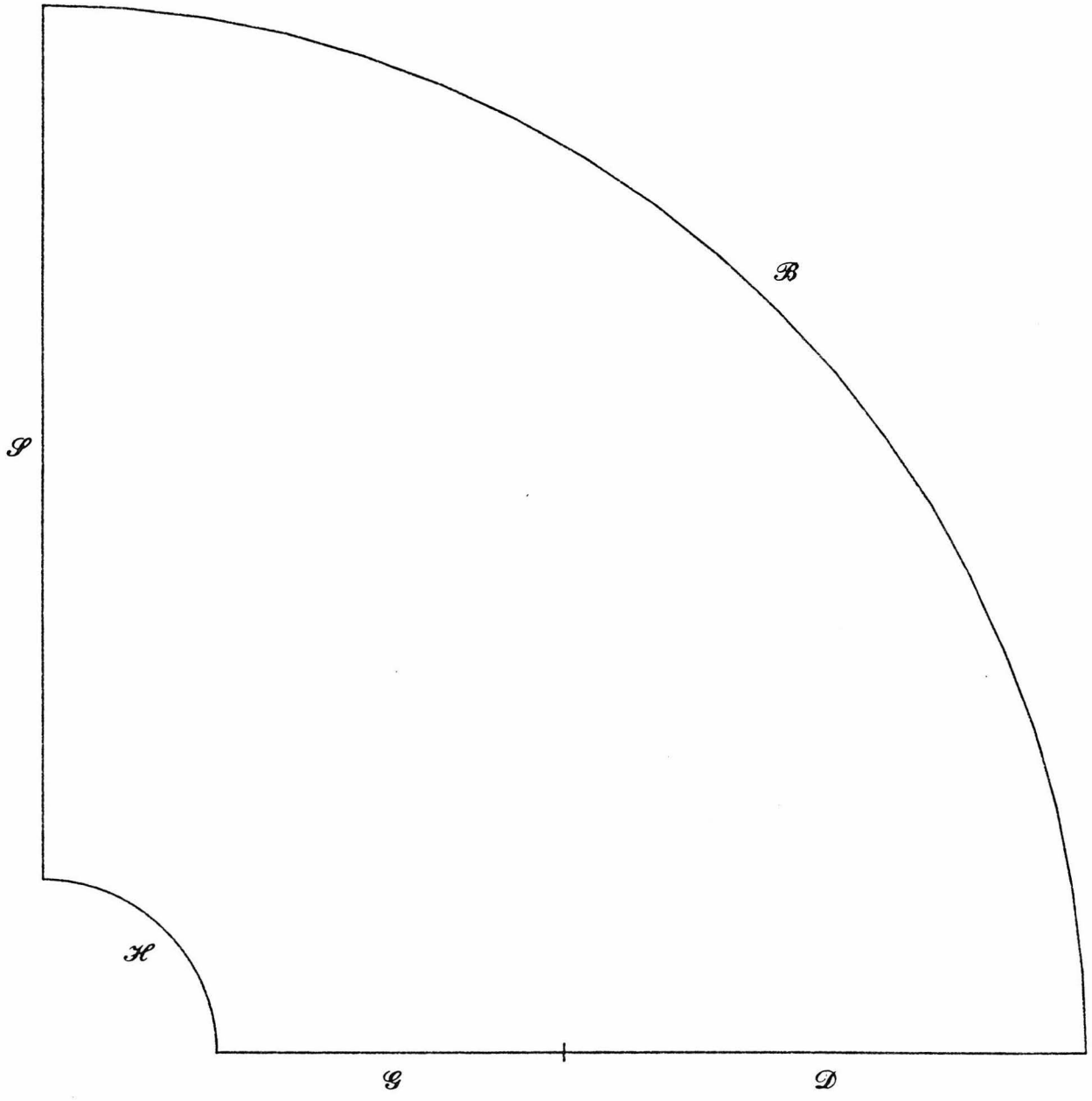

Fig. 1

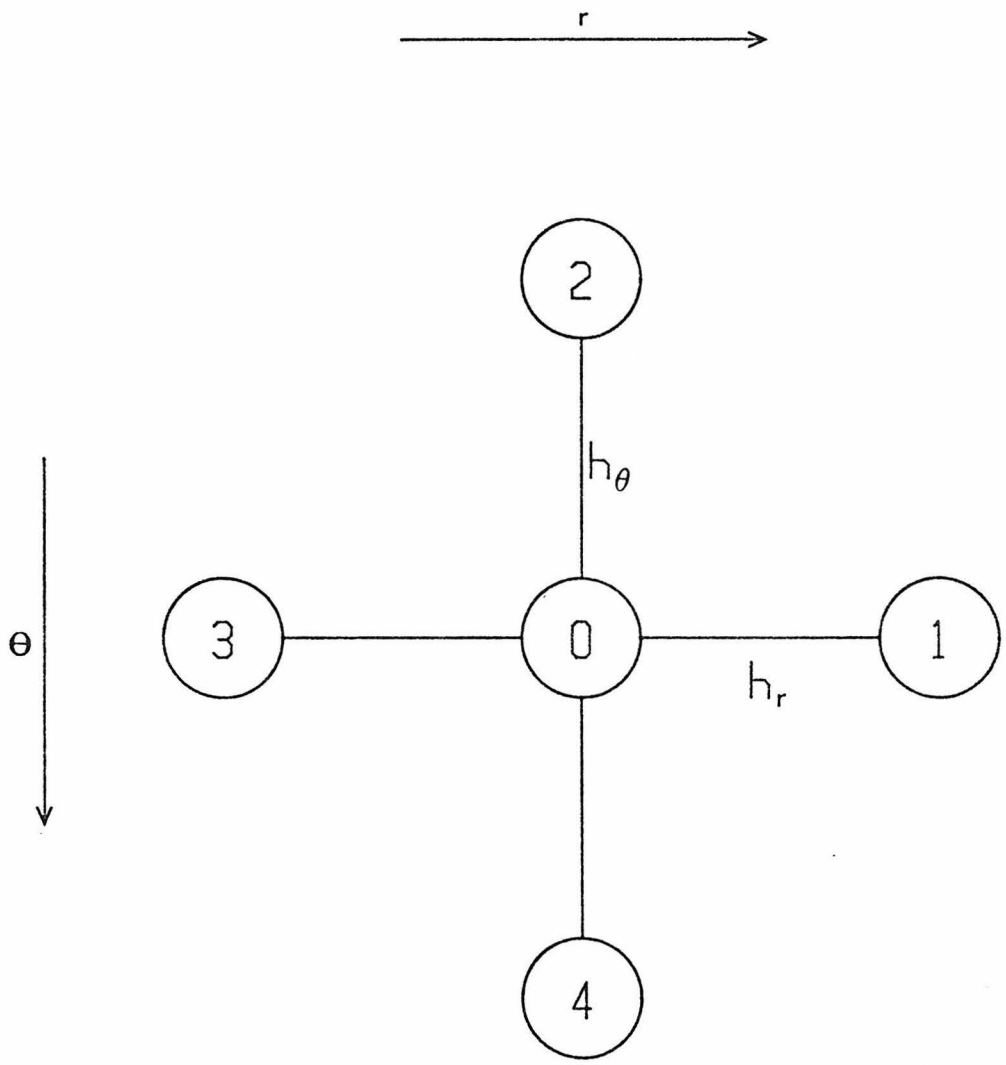

Fig. 2

Fig. 3

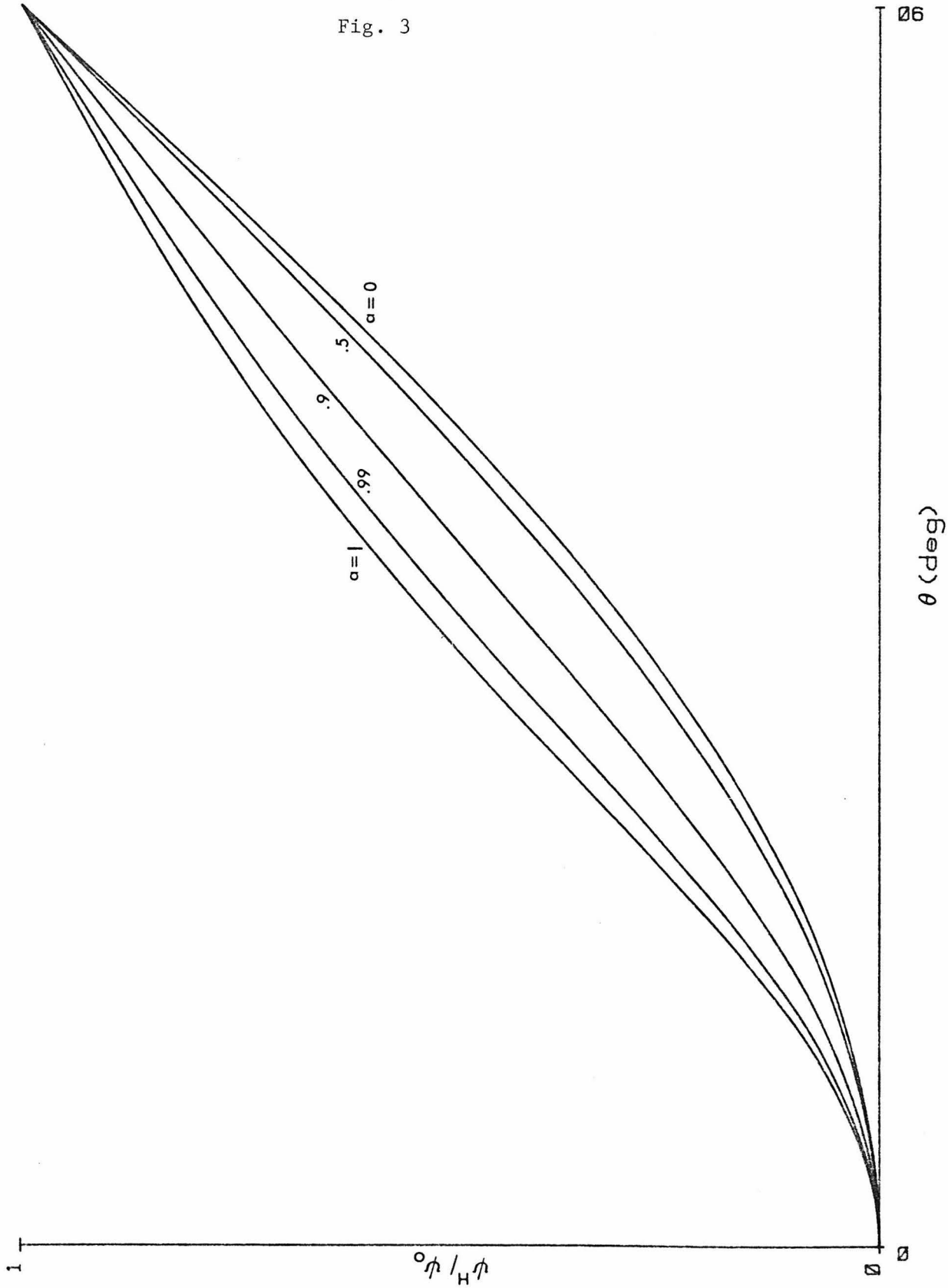

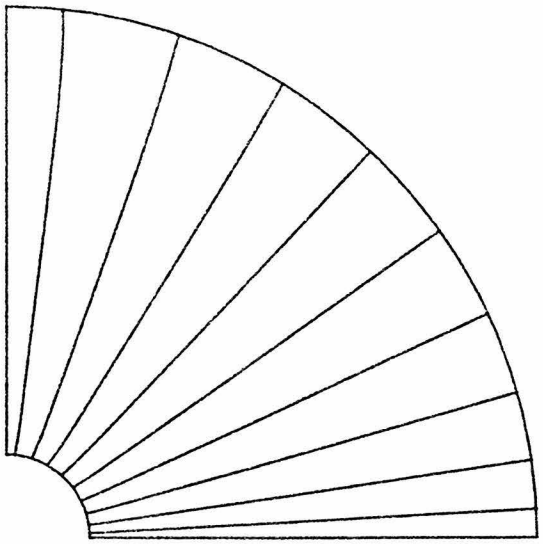

R = 10 ; a = .5

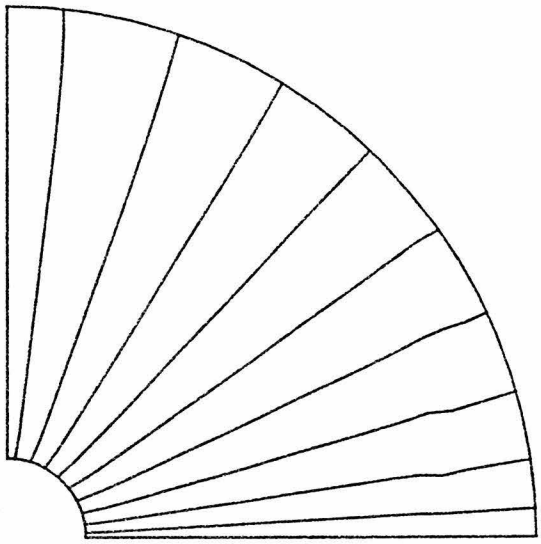

R = 10 ; a = .66

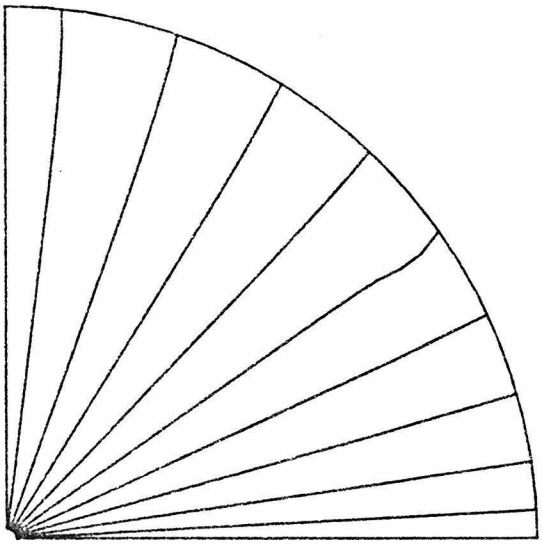

R = 100 ; a = .1

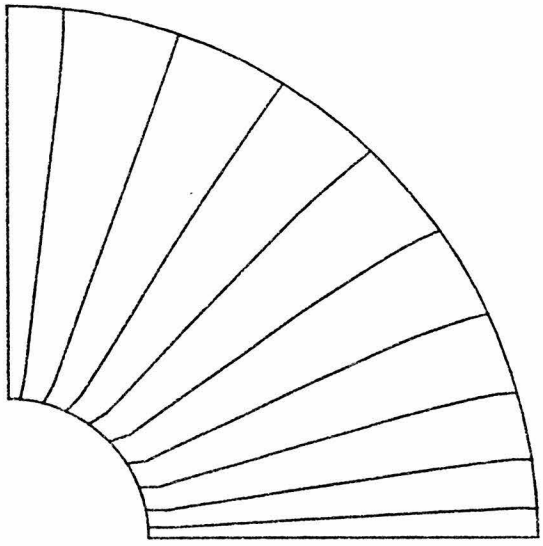

R = 4 ; a = .9

Fig. 4

Fig. 5

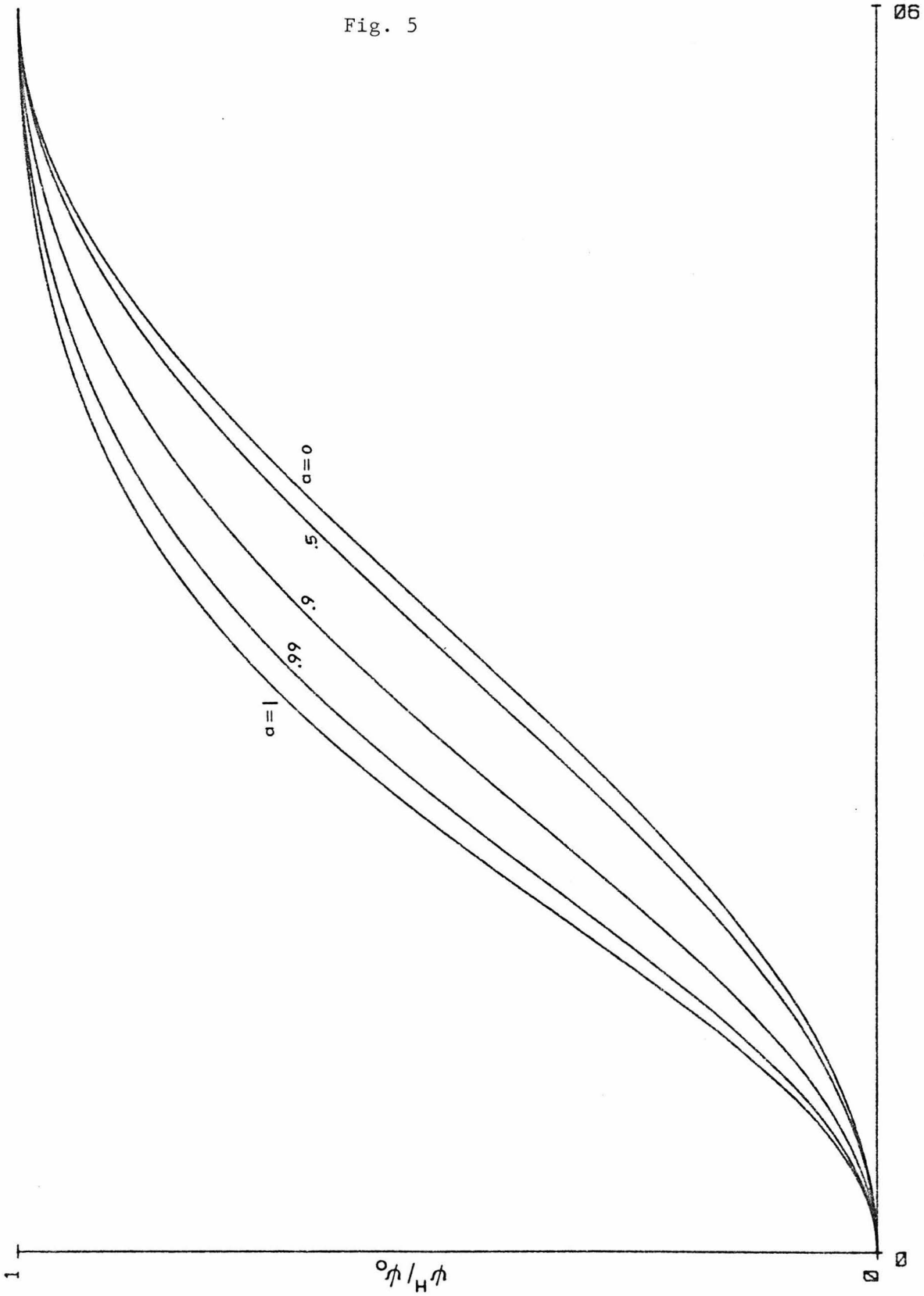

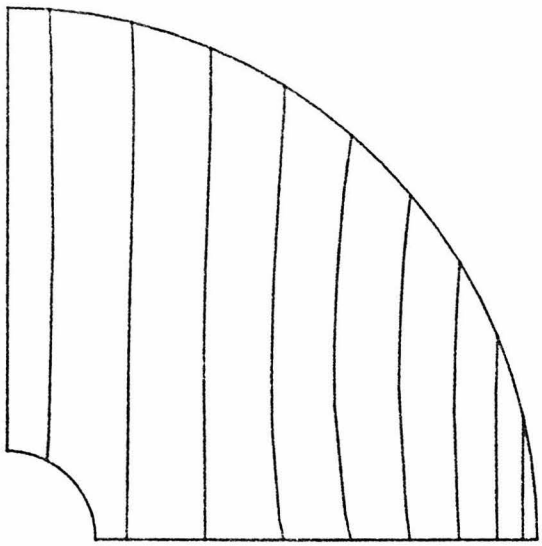

a = 0

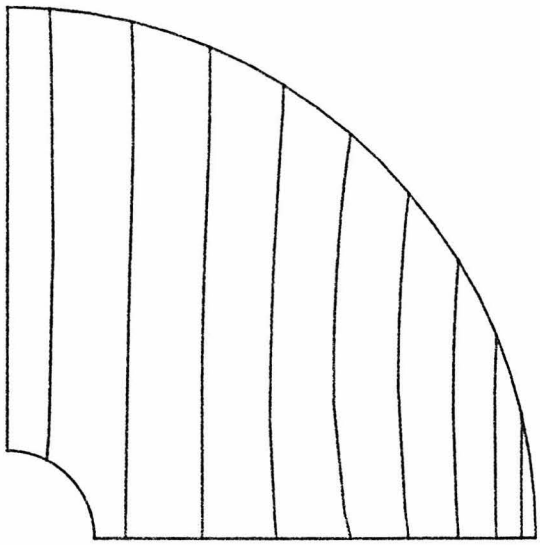

a = .1

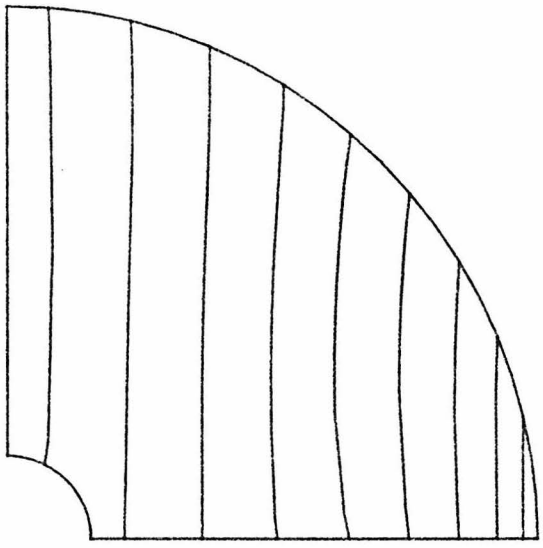

a = .5

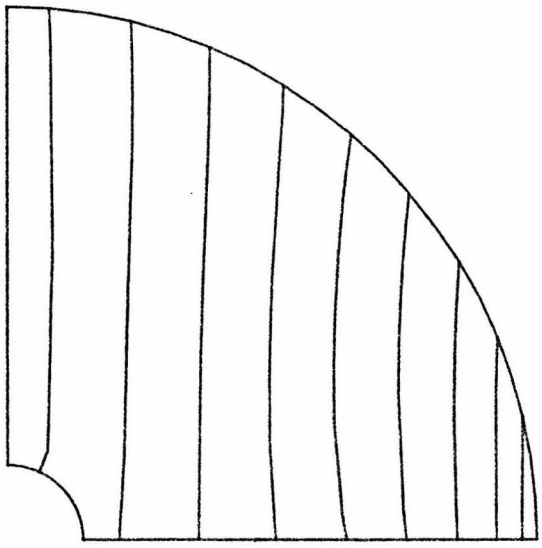

a = .75

Fig. 6

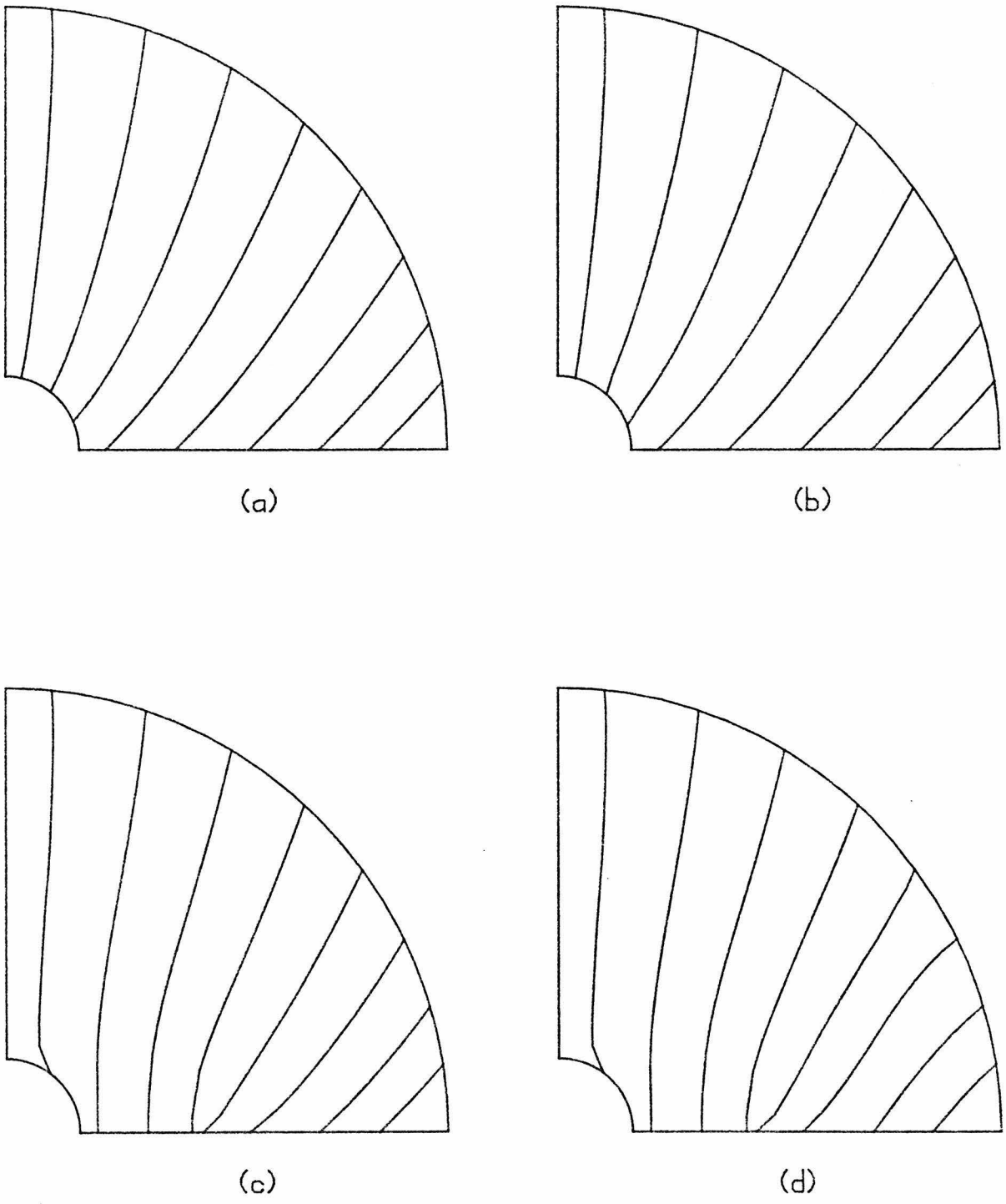

Fig. 7

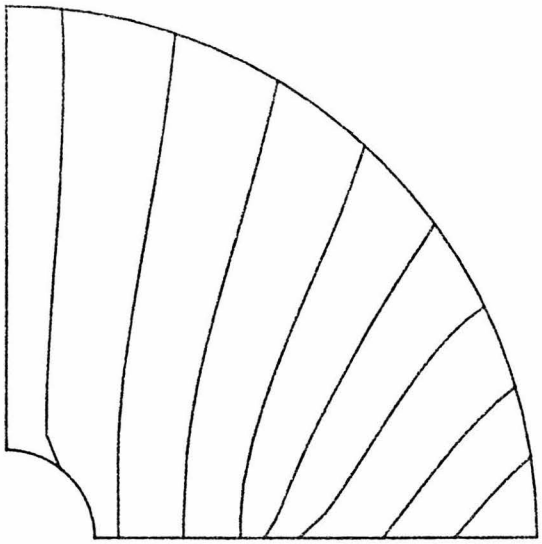

$a = .1$

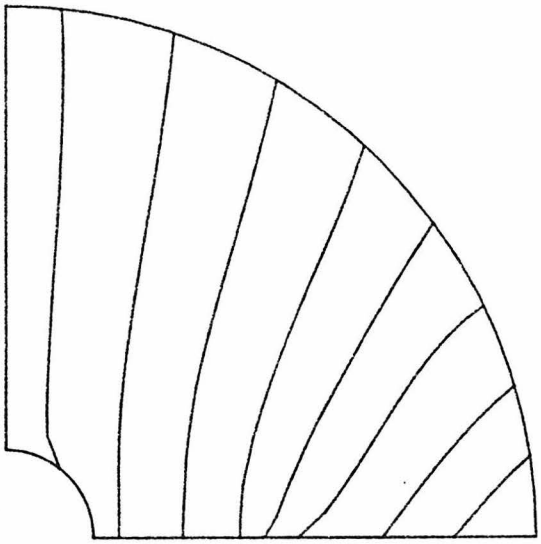

$a = .2$

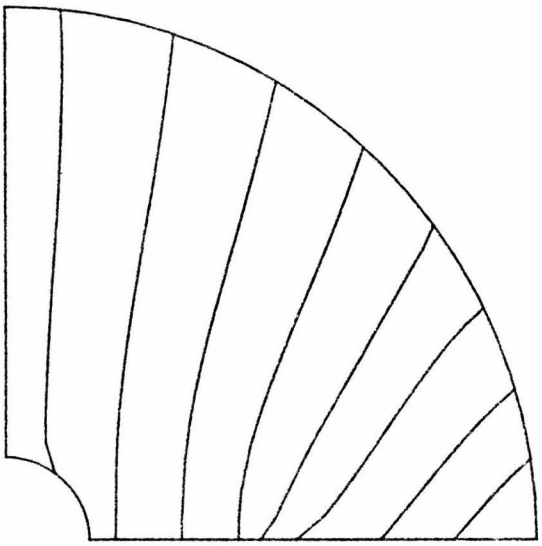

$a = .5$

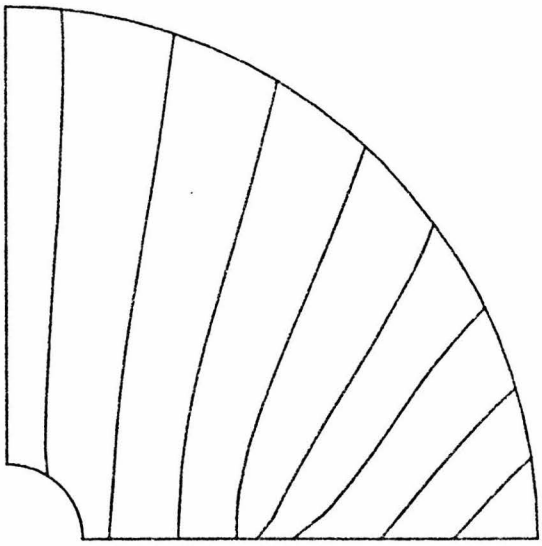

$a = .75$

Fig. 8

CHAPTER V

DYNAMICAL ELECTROMAGNETIC FIELDS NEAR BLACK-HOLE HORIZONS

Introduction

The 3 + 1 equations of electrodynamics developed in the first part of Chapter II were completely general. In the latter half of chapter II and in chapters III and IV, however, these laws were applied only to the study of stationary processes. This chapter will study in detail two simple dynamical problems meant to elucidate the behavior of electromagnetic fields in the neighborhood of the horizon and illustrate the connections between the frozen-star and membrane paradigms mentioned in the Introduction. Both of these problems involve the relaxation of a specified initial field toward a stationary final state and show explicitly the near-horizon field behavior described qualitatively in chapters I and II.

In section 5.3 of chapter II, a qualitative description of the structure of a general electromagnetic field near the horizon of a black hole was given. There it was pointed out that, due to the pathology of the constant-time hypersurfaces used in making the 3 + 1 split, i.e. the fact that they fall deep into the past as they approach the horizon (see Fig. 4 of chapter II), there is a problem in defining the boundary conditions on electromagnetic fields at the horizon. Because of this pathology, the fiducial observers of the 3 + 1 split never see any particle or part of the electromagnetic field actually cross the horizon. If the field is dynamical, they will see a layered field structure at the horizon reflecting the entire past history of the near-horizon field.

A method of circumventing this difficulty was suggested in chapter II: First one chooses a new time coordinate $\tilde{t}$ (see Fig. 4 of Chapter II), which, unlike the global time t, is well behaved at the horizon. One then defines the horizon value

of a field at global time $t = t_1$ to be its value at the intersection of the hypersurface $t = t_1$ with some $\tilde{t}$ = constant hypersurface near the point of interest on the two-dimensional horizon cross section. From the point of view of the fiducial observers, the effect of this prescription is to apply the boundary conditions on electromagnetic fields not at the true horizon, but at a *stretched horizon* displaced outward slightly from the true horizon.

The precise value of $\tilde{t}$ time to be chosen or, equivalently, the amount by which the horizon is to be stretched, was not specified in chapter II. There it was merely noted that the 3 + 1 formalism was likely to be most useful for cases of quasistatic field evolution, i.e. cases where the timescale of evolution of the field is much less than the mass M of the black hole. In such cases the stretching is trivially easy. This chapter will study two examples dynamical on timescales $\lesssim M$ and will show that even in these cases the electromagnetic solutions obtained are not sensitively dependent on the position of the stretched horizon, so long as certain criteria are met. In effect, this means that the layered fields at the horizon have no discernible influence on the fields external to the stretched horizon, so long as its location is chosen reasonably. This lack of sensitivity to the structure of the layered relic field is in accord with intuitive expectations from the membrane paradigm, which predicts the horizon to act like a body of finite conductivity in its interactions with electromagnetic fields.

Section 1 of this chapter treats the dynamical relaxation of the electric field of a charged particle falling into the horizon of Rindler spacetime. As will be explained, Rindler spacetime is a good approximation to the Schwarzschild and Kerr black-hole spacetimes in the near-horizon limit or, equivalently, in the limit as the horizon size becomes arbitrarily large. Rindler combines the kinematic properties of horizons predicted by the membrane paradigm (such as electrical conductivity) with an algebraic simplicity lacking in the black-hole

spacetimes. Thus, many of the conclusions drawn from this model may be expected also to hold for black-hole spacetimes.

Section 2 investigates the dynamical relaxation of an initially stationary but nonequilibrium magnetic field threading a Schwarzschild black hole. The magnetic field lines oscillate in a manner qualitatively similar to vibrating strings, with damping occurring only through the inner (horizon) boundary condition. The layered field structure described above manifests itself as disconnected loops of magnetic flux falling toward the horizon. The transfer of energy through the horizon is studied in detail using concepts developed in chapter II, and the dependence of the damping timescale on the parameters of the problem is investigated.

1. Dynamical Fields in Rindler Spacetime

Consider a particle in flat spacetime which is undergoing constant acceleration of magnitude g in a particular direction. By picking cylindrical Minkowski coordinates (t,ϖ,φ,z) so that the motion of the particle is along the z axis, the spacetime trajectory of the particle can easily be shown, with a proper choice of origin, to be a hyperbola

$$z^2 - t^2 = \frac{1}{g^2} \tag{1.1}$$

(see e.g. chapter 6 of Misner, Thorne & Wheeler 1973). One may define the local coordinates of a family of accelerated observers moving with the particle; these are called Rindler coordinates (T,ϖ,φ,Z), and are related to the Minkowski coordinates by

$$\left.\begin{aligned} t &= (Z + g^{-1})\sinh gT \\ z &= (Z + g^{-1})\cosh gT \end{aligned}\right\} \iff \left\{\begin{aligned} Z &= \sqrt{z^2 - t^2} - g^{-1} \\ T &= g^{-1}\tanh^{-1}(t/z) \end{aligned}\right. \tag{1.2}$$

The coordinates ϖ and φ are the same in both systems. The trajectory (1.1) of the accelerated particle in Rindler coordinates is just $Z = 0$. The spacetime line element in terms of Rindler coordinates is expressed as

$$ds^2 = -(1 + gZ)^2 dT^2 + d\varpi^2 + \varpi^2 d\varphi^2 + dZ^2 \quad . \tag{1.3}$$

Fig. 1 shows the surfaces of constant T and Z associated with the Rindler coordinate system. In Fig. 2, the trajectory $Z = 0$ of the accelerated particle is plotted as a dashed line in both the Minkowski and Rindler coordinate systems.

The Rindler coordinate patch covers only one quarter of Minkowski spacetime. Since the Rindler coordinate system is accelerated, it cannot cover all of spacetime, but must break down at a distance of order $1/g$ from the particle. The locus of this breakdown, the horizon of Rindler spacetime, is the surface $Z = -1/g$ or $z = t$. This horizon possesses all of the kinematic properties of the more familiar black-hole horizons; and most importantly for the present problem, its surface resistivity is $R^H = 4\pi = 377$ ohms.

The consideration of fields in Rindler spacetime is of interest for more than just its own sake. The near-horizon metric form for a stationary, spherically symmetric black hole may be written as (cf. equation 5.29a of chapter II)

$$ds^2 = -\alpha^2 dT^2 + \kappa^{-2} d\alpha^2 + r_G^2 [d\theta^2 + \sin^2\theta d\varphi^2] \quad . \tag{1.4}$$

where r_G is the coordinate radius of the horizon and κ is the surface gravity. If one looks just at locations near the north pole so that $\sin\theta \sim \theta$ and makes the identifications $\alpha \to 1 + gZ$, $r_G\theta \to \varpi$, $\kappa \to g$, this takes the form of equation (1.3). Therefore, the Rindler field can be considered as an approximation to the field of a spherically symmetric black hole in the limit as one approaches the horizon. [Fairly obviously, it can also be considered as an approximation to the field of a nonspherical, axisymmetric, rotating (e.g. Kerr) black hole in the near-horizon

limit at the north pole; furthermore, it is a valid approximation to Kerr away from the pole to lowest order in Z, i.e. neglecting radial variations in frame dragging.] In the Rindler approximation, $Z + 1/g$ is the proper distance from the horizon: for a Schwarzschild hole of mass M, where $r_G = 2M$, the relationship between the usual Schwarzschild radial coordinate r and the Rindler coordinate Z is

$$\int_{2M}^{r} \frac{dr}{\sqrt{1-2M/r}} \approx 4M\sqrt{1-2M/r} \quad \rightarrow \quad Z + \frac{1}{g} \ . \tag{1.5}$$

If the particle moving along the accelerated trajectory $Z = 0$ has a charge Q, it will generate an electromagnetic field. The field at an observation point O (see Fig. 1) will be generated entirely by a single point of the particle's trajectory, the retarded point R which lies at the intersection of the particle's trajectory with the past null cone of the observer point:

$$-(t - t_R)^2 + (z - z_R)^2 + \varpi^2 = 0 \quad \text{where} \quad z_R = \sqrt{g^{-2} + t_R^2} \ , \quad (t_R < t) \ . \tag{1.6}$$

Here the coordinates of the retarded point are denoted by the subscript R, while those of the observation point are not subscripted; and the formulas use Minkowski coordinates (t,ϖ,φ,z). Solving for the retarded coordinates yields

$$t_R = \frac{t\eta - z\xi}{2(z^2 - t^2)} \ , \qquad z_R = \frac{z\eta - t\xi}{2(z^2 - t^2)} \ , \tag{1.7}$$

where $\xi \equiv \sqrt{\eta^2 + 4(z^2 - t^2)/g^2} = \sqrt{(-t^2 + z^2 + \varpi^2 - g^{-2})^2 + 4\varpi^2/g^2}$ and $\eta \equiv -t^2 + z^2 + \varpi^2 + g^{-2}$.

The vector potential produced by the charge may be calculated from the standard Liénard-Wiechert potentials (see e.g. Soffel, Müller and Greiner 1980) to be

$$A^t = \frac{Q(z\eta - t\xi)}{\xi(z^2 - t^2)} \ , \qquad A^z = \frac{Q(t\eta - z\xi)}{\xi(z^2 - t^2)} \ , \tag{1.8}$$

so the physical components of the electromagnetic field are:

$$E_{\hat{\varpi}} = -\frac{\partial A^t}{\partial \varpi} = \frac{8Q\varpi z}{g^2\xi^3} \quad ,$$

$$E_{\hat{z}} = -\frac{\partial A^t}{\partial z} - \frac{\partial A^z}{\partial t} = \frac{4Q(z^2 - \varpi^2 - t^2 - g^{-2})}{g^2\xi^3} \quad , \tag{1.9}$$

$$B_{\hat{\varphi}} = -\frac{\partial A^z}{\partial \varpi} = \frac{8Q\varpi t}{g^2\xi^3} \quad .$$

If the fields are transformed to Rindler coordinates, the only nonvanishing physical components are

$$E_{\hat{\varpi}'} = \frac{8Q\varpi(Z + g^{-1})}{g^2\xi^3} \quad ,$$

$$E_{\hat{Z}'} = \frac{4Q}{g^2\xi^3}[(Z + g^{-1})^2 - \varpi^2 - g^{-2}] \quad , \tag{1.10}$$

where $\xi \equiv \sqrt{[(Z + g^{-1})^2 + \varpi^2 - g^{-2}]^2 + 4\varpi^2/g^2}$ in terms of Rindler coordinates. As might be expected, this field is stationary in the sense that it does not depend on the Rindler time T. It should also be noted that it is normal to the horizon at $Z = -g^{-1}$. The electric field lines are plotted in Fig. 3. As explained in section 5.4 of chapter II, the field lines may be considered to be terminated at the horizon by a surface charge density

$$\sigma^H = \left.\frac{E_{\hat{Z}'}}{4\pi}\right|_{Z = -1/g} = \frac{-Q}{\pi g^2(\varpi^2 + g^{-2})^2} \quad ; \tag{1.11}$$

and by integrating σ^H over the horizon, one may verify that the total charge induced on the horizon is equal to $-Q$. The horizon surface current density defined in chapter II vanishes, and there is no dissipation of energy in the horizon.

The solution (1.10) might alternatively have been derived from the solution of Linet (1976) for a point charge at rest outside a Schwarzschild black hole by applying the change of variables and the limiting process described in equation (1.5) and the preceding paragraph. Linet's solution is summarized in 3 + 1 form in section 6.1 of chapter II.

In order to consider a dynamical problem, introduce another particle of charge $-Q$ which is stationary in Minkowski coordinates at position $z = 1/2g$, so that its trajectory in Rindler coordinates is

$$Z = \frac{1}{2g\,\cosh gT} - \frac{1}{g} \quad . \tag{1.12}$$

As seen in Rindler coordinates, this particle emerges from the past horizon at $T = -\infty$, reaches a maximum distance $1/2g$ from it, and then falls into the future horizon at $T = +\infty$. In Fig. 2, the trajectory of this charge is shown as a dotted line in the two different coordinate systems. Only the infalling part of the trajectory will be considered here. The physical components of the particle's field in Minkowski coordinates are

$$E_{\hat{\varpi}} = -\frac{Q\varpi}{r^3} \quad , \qquad E_{\hat{z}} = -\frac{Q(z - g^{-1}/2)}{r^3} \quad , \tag{1.13}$$

where $r \equiv \sqrt{\varpi^2 + (z - g^{-1}/2)^2}$. In Rindler coordinates the physical components are

$$E_{\hat{\varpi}}' = -\frac{Q\varpi}{r^3}\cosh gT \quad ,$$

$$E_{\hat{Z}}' = -\frac{Q}{r^3}\left[(Z + g^{-1})\,\cosh gT - \frac{1}{2g}\right] \quad , \tag{1.14}$$

$$B_{\hat{\varphi}}' = \frac{Q\varpi}{r^3}\sinh gT \quad ,$$

where $r \equiv \sqrt{\varpi^2 + [(Z + g^{-1})\cosh gT - g^{-1}/2]^2}$ in terms of Rindler coordinates.

The definition of horizon charge and current densities in this case is trickier than in the case of the Rindler-stationary charge. In attempting to calculate them, one evaluates $E_{\hat{\varpi}}'$ and $E_{\hat{Z}}'$ at the horizon ($Z = -1/g$, $T = \infty$), which leads to indeterminate results. The reason for this is the infinite gravitational redshift at the horizon. Unlike the field of the Rindler-stationary charge, which has existed since $T = -\infty$ and therefore extends all the way down to the horizon, the field of the infalling charge has not had time (and never will) to propagate down to the horizon. To get meaningful results, it is necessary to define the charge and current densities on a "stretched" horizon at $Z = -g^{-1} + \varepsilon$, where $\varepsilon \ll g^{-1}$. By using the results of chapter II, the charge and current densities produced by the infalling charge on the stretched horizon may be shown to be

$$\sigma^H = \frac{E_{\hat{Z}}'}{4\pi}\bigg|_{Z=-g^{-1}+\varepsilon} = \frac{-Q(\varepsilon\cosh gT - g^{-1}/2)}{4\pi[\varpi^2 + (\varepsilon\cosh gT - g^{-1}/2)^2]^{3/2}}\,, \qquad (1.15a)$$

$$\mathcal{J}^H = \left[(1 + gZ)\frac{\mathbf{E}_{\|}'}{R^H}\right]_{Z=-g^{-1}+\varepsilon} = \frac{-Q\,g\,\varpi\varepsilon\cosh gT\;\mathbf{e}_{\hat{\varpi}}}{4\pi[\varpi^2 + (\varepsilon\cosh gT - g^{-1}/2)^2]^{3/2}}\,, \qquad (1.15b)$$

respectively, where $\mathbf{E}_{\|}$ is the component of E parallel to the horizon. As the particle descends toward the stretched horizon, the charge density (1.15a) becomes more and more sharply peaked at the position $\varpi = 0$ directly under the particle; the integral of σ^H over the horizon, however, remains constant at the value $Q/2$ during the descent. In the limit as the particle approaches the stretched horizon, the charge density approaches the functional form

$$\sigma^H \to \frac{Q\delta(\varpi)}{4\pi\varpi}\,. \qquad (1.16)$$

The surface current density (1.15b) feeds the growing concentration of charge at $\varpi = 0$.

In section 5.4 of chapter II, it was shown that the energy flux density through the stretched horizon is just $\mathcal{J}^H \cdot \mathbf{E}^H$, where $\mathbf{E}^H$, the horizon electric field, is the horizon limit of the quantity $(1 + gZ)\mathbf{E}_{\|}$. The energy flux may be obtained by integrating this quantity over the stretched horizon:

$$\int_{\mathcal{H}} \mathcal{J}^H \cdot \mathbf{E}^H d\Sigma = \frac{Q^2 g^2 \varepsilon^2 \cosh^2 gT}{8(\varepsilon \cosh gT - g^{-1}/2)^2} \quad . \tag{1.17}$$

The integral of this function over time, which should give the total energy absorbed by the horizon, diverges due to an infinite contribution at the point at which the particle crosses the stretched horizon. This is not unexpected, however, since the particle is assumed to be pointlike and thus has an infinite amount of energy in its near field.

In contrast to the case of the Rindler-stationary charge, only half of the field lines of the infalling charge intersect the stretched horizon; the rest escape to spatial infinity. But as the particle falls in, its field lines (even the ones that eventually escape to spatial infinity), are flattened down near the stretched horizon within an ever-widening circle of radius $\Delta\varpi \sim \varepsilon \cosh gT$ on the horizon. Therefore, if only the infalling particle existed, its entire field out to any chosen radius ϖ would ultimately seem to disappear beneath the stretched horizon; so the oppositely charged particle, stationary outside the horizon, with field given by equation (1.10), is added to "hold the field lines up" and to illustrate the approach of the field toward stationarity.

Fig. 4 shows the electric field lines resulting from the superposition of the fields (1.10) and (1.14) at several representative times. It may be seen that the effects of the field of the infalling particle rapidly vanish, and that by about $T = 6/g$, the field has very nearly settled down to the stationary form which would be produced by the Rindler charge alone. All of the effects of the infalling particle's field become flattened into a thin layer just above the horizon, the

thickness of which decreases at a rate proportional to $1/\cosh gT \sim e^{-gT}$. If the horizon is stretched slightly, i.e. moved up to $Z = -g^{-1} + \varepsilon$, all effects of the infalling charge disappear beneath it in a time of order $-g^{-1}\ln(g\varepsilon)$.

2. Relaxation of a Magnetic Field in Schwarzschild Spacetime

Consider the problem of a Schwarzschild black hole of mass M, surrounded by a perfectly conducting concentric sphere of radius $R > 2M$ into which an axially symmetric magnetic field is frozen. At time $t = 0$, the magnetic field lines are momentarily static and purely radial, pointing into the hole below the equator and out of the hole above it, as shown in Fig. 5. Immediately after time $t = 0$, this initial configuration is released and allowed to evolve dynamically in accord with the vacuum Maxwell equations — except that the field lines continue to be held fixed in the conducting sphere at radius R. We shall study the dynamical evolution of this field.

In solving this problem, we shall use the 3 + 1 formulation of electrodynamics developed in chapter II. In this formulation, the split of spacetime is characterized by two scalar fields: the lapse function α which is equal to $[-(^{(4)}\nabla t)^2]^{-1/2}$, where t is the universal time coordinate of the 3 + 1 split; and ϖ, which is the magnitude of the Killing vector corresponding to the azimuthal spatial isometry of the spacetime.

In Schwarzschild coordinates (t,r,θ,φ), where the lapse function is $\alpha = \sqrt{1-2M/r}$ and the cylindrical radius is $\varpi = r\sin\theta$, the initial electric and magnetic fields are

$$\mathbf{E} = 0 \ , \qquad \mathbf{B} = B_0\alpha\left(\frac{R}{r}\right)^2 \cos\theta \ \frac{\partial}{\partial r} = B_0\left(\frac{R}{r}\right)^2 \cos\theta \ \mathbf{e}_{\hat{r}} \ , \tag{2.1}$$

and the corresponding initial vector potential is a purely azimuthal one-form:

$$\mathbf{A} = \frac{B_o R^2}{2}\sin^2\theta \, \mathbf{d}\varphi = \frac{B_o R^2}{2r}\sin\theta \, \mathbf{e}_{\hat{\varphi}} \quad , \tag{2.2}$$

where B_o is the magnetic field strength on axis at the outer sphere.

The field lines are fixed at their outer ends because they are frozen into the perfectly conducting outer sphere, but they are free to slip through the stretched horizon since it has a finite conductivity. Qualitatively, one would expect the field lines to pull themselves into a more vertical orientation due to their tension.

The subsequent evolution of the field is governed by the inhomogeneous Maxwell equations

$$F^{\mu;\nu}{}_{;\nu} = 4\pi J^{\mu} = 0 \quad \Longrightarrow \quad A^{[\mu;\nu]}{}_{;\nu} = 0 \quad , \tag{2.3}$$

where square brackets denote antisymmetrization on indices and where the fact was used that $J^{\mu} = 0$ since the region of interest is vacuum. The divergence of the antisymmetric tensor $A^{[\mu;\nu]}$ may be written in terms of ordinary derivatives using the theorem expressed in equation (8.51c) of Misner, Thorne & Wheeler (1973):

$$\frac{1}{\sqrt{-g}}[\sqrt{-g}\, g^{\mu\alpha} g^{\nu\beta}(A_{\alpha,\beta} - A_{\beta,\alpha})]_{,\nu} = 0 \quad . \tag{2.4}$$

The symmetries of the problem allow a gauge to be chosen in which the only nonzero component of the vector potential is $A_{\varphi}(t,r,\theta)$. The properties of axisymmetry and the diagonality of the Schwarzschild metric then together imply that the only non-vacuous component of equation (2.4) is the $\mu = \varphi$ component. This component may be written in terms of the "magnetic flux function" $\psi(t,r,\theta) \equiv 2\pi A_{\varphi}(t,r,\theta)$ which, as shown in chapter III, is equal to the total

magnetic flux through the circle of constant radius and latitude (r,θ) = constant; the result is

$$-\frac{\psi_{,tt}}{1-2M/r}+\left[1-\frac{2M}{r}\right]\psi_{,rr}+\frac{2M}{r^2}\psi_{,r}+\frac{\psi_{,\theta\theta}}{r^2}-\frac{\cot\theta}{r^2}\psi_{,\theta}=0 \quad . \tag{2.5}$$

By introducing the "tortoise coordinate" r^* of Regge & Wheeler (1957) defined by

$$dr^*=\frac{dr}{1-2M/r} \quad , \qquad r^*=r+2M\ln\left(\frac{r}{2M}-1\right) \quad , \tag{2.6}$$

equation (2.5) can be put into the form

$$-\psi_{,tt}+\psi_{,r^*r^*}+\frac{1}{r^2}\left[1-\frac{2M}{r}\right]\left[\psi_{,\theta\theta}-\cot\theta\,\psi_{,\theta}\right]=0 \quad . \tag{2.7}$$

In this equation, r is to be thought of as an implicitly defined function of r^*.

The boundary condition of "no outgoing waves at the horizon" (see chapter II) requires

$$[\mathbf{E}_{\|}-\mathbf{n}\times\mathbf{B}_{\|}]_{r\to 2M}\ \to\ 0 \quad , \tag{2.8}$$

where $\mathbf{n}$ is the unit normal vector $\mathbf{e}_{\hat{r}}$ to the horizon and $\mathbf{E}_{\|}$ and $\mathbf{B}_{\|}$ are the field components tangential to the horizon. The tangential fields may be expressed in terms of the potential ψ as

$$\mathbf{E}_{\|}=-\frac{\dot{\psi}\mathbf{e}_{\hat{\varphi}}}{2\pi\alpha\varpi}=-\frac{1}{2\pi\alpha r\sin\theta}\frac{\partial\psi}{\partial t}\mathbf{e}_{\hat{\varphi}} \quad , \qquad \mathbf{B}_{\|}=\frac{[\nabla\psi\times\mathbf{e}_{\hat{\varphi}}]_{\|}}{2\pi\varpi}=-\frac{\alpha}{2\pi r\sin\theta}\frac{\partial\psi}{\partial r}\mathbf{e}_{\hat{\theta}} \quad , \tag{2.9}$$

where the overhead dot denotes time differentiation; so the horizon boundary condition (2.8) becomes

$$\left[\frac{\partial\psi}{\partial t}-\frac{\partial\psi}{\partial r^*}\right]_{r\to 2M}\ \to\ 0 \quad . \tag{2.10}$$

The initial field $\psi(0,r,\theta)\,\mathbf{d}\varphi = \pi B_o(R^2/r)\sin\theta\,\mathbf{e}_{\hat{\varphi}}$ has the angular dependence of the $l = 1, m = 0$ vector spherical harmonic (Jackson 1975) $\mathbf{X}_{1,0}(\theta,\varphi) = i\sqrt{3/8\pi}\,\sin\theta\,\mathbf{e}_{\hat{\varphi}}$; and since neither the differential equation (2.7) nor the boundary conditions mix different multipoles, the field will remain proportional to this harmonic as it evolves. It is thus convenient to separate variables by defining a new field variable $u(t,r)$:

$$\psi(t,r,\theta)\,\mathbf{d}\varphi = \pi B_o R^2 \frac{u(t,r)}{r}\sin\theta\,\mathbf{e}_{\hat{\varphi}} \implies \psi(t,r,\theta) = \pi B_o R^2 u(t,r)\sin^2\theta \quad . \tag{2.11}$$

Then the wave equation (2.7) for ψ takes the form

$$-u_{,tt} + u_{,r^*r^*} - \frac{2}{r^2}\left(1 - \frac{2M}{r}\right)u = 0 \quad . \tag{2.12}$$

This equation describes a one-dimensional wave subject to a potential $V(r^*) \equiv 2(1 - 2M/r)/r^2$. This potential goes to zero at the horizon proportionally to α^2, goes to zero as $1/r^2$ at large r, and has a global maximum at $r = 3M$: $V_{\max} = 2/(27M^2)$. The inner boundary condition (2.10) written in terms of $u(t,r)$ is just

$$\left[\frac{\partial u}{\partial t} - \frac{\partial u}{\partial r^*}\right]_{r\to 2M} \to 0 \quad . \tag{2.13}$$

which has the form of a "perfectly absorbing" boundary condition for the one-dimensional wave equation (2.12). The outer boundary condition is $u(t,R) = 1$, and the initial conditions are $u(0,r) = 1$ and $u_{,t}(0,r) = 0$.

The wave equation (2.12) was integrated numerically subject to these initial and boundary conditions, and the structure of the magnetic field lines was then reconstructed from $u(t,r)$ using the relation (2.11) and the definition of $\psi(t,r,\theta)$ as the magnetic flux function (equation 2.9). The inner boundary

condition (2.13) was applied not at the actual horizon $r^* = -\infty$, but at a slightly stretched horizon $r^* = -20M$, which corresponds to the Schwarzschild radius $r = (2 + 3.3 \times 10^{-5})M$. (Although this horizon stretching is motivated by numerical considerations, it is the same stretching as occurs in the membrane paradigm.) Representative plots of the magnetic field line structure are shown in Figs. 6 and 7 for the cases $R = 3M$ and $R = 10M$, respectively.

The qualitative behavior of the solutions, as depicted in $r-\theta$ coordinates, is that the field oscillates for a time before settling down to a final static configuration consisting of precisely vertical field lines. This static configuration could be derived directly by setting the time derivatives in equation (2.12) to zero, and solving subject to the same boundary conditions; it is the solution $\psi(r,\theta) = \pi B_0 r^2 \sin^2\theta$ found by Wald (1974) and by Hanni & Ruffini (1976).

As the field lines oscillate, they leave disconnected field-line loops such as those shown in the diagram for $t/M = 28$ in Fig. 7. These loops drop toward the horizon at the locally measured speed of light, $dr^*/dt \sim 1$ or $dr/dt \sim \alpha^2$. Thus, as described qualitatively in chapter II, the field has a layered structure at the horizon which reflects the entire past history of its evolution. However, these layered horizon fields do not affect the overall large-scale structure of the field outside the horizon; the position of the stretched horizon in the numerical integration could be moved outward considerably without changing the diagrams in Figs. 6 and 7 in any noticeable way.

The complex, multilayered nature of the near-horizon fields is illustrated graphically in Fig. 8. In the top part of this figure, the magnetic field lines are plotted on an embedding diagram for Schwarzschild spacetime, which consists of a paraboloid of revolution (see e.g. section 23.8 of Misner, Thorne & Wheeler 1973). In this part of the diagram, the Schwarzschild radial coordinate r is identified with the cylindrical coordinate measured radially outward from the

axis of symmetry of the embedding diagram, and the angular coordinate θ is identified with the cylindrical angular coordinate measured around this axis. The ignorable coordinates t and φ are suppressed. The diagrams in Figs. 6 and 7 are what one would see if one were looking down into the paraboloid along the axis of symmetry. The paraboloid of the embedding diagram is cut off at a stretched horizon which is taken to be at a radius $r = 2.15M$. (As will be explained later, this would be a poor choice of stretched horizon at which to apply the boundary condition (2.13), but it is chosen here for illustrative purposes.) In order to make the near-horizon fields visible, they are plotted on a cylinder matched to the paraboloid at the stretched horizon. In this part of the diagram, the distance along the axis, i.e. the cylindrical "z-coordinate", is identified with the tortoise coordinate r^*; and the previous identification of θ with the cylindrical angular coordinate is maintained. Plotting the near-horizon fields in this way as functions of r^* has the effect of expanding the radial scale so that the field structure is visible.

The data plotted in Fig. 8 show the field-line structure at the time $t = 92M$ for the case $R = 10M$. At this time, the field lines have sprung outward and snapped back inward four times and are beginning to spring outward for a fifth time. The relic field line loops left by each of these oscillations are visible running down the cylinder, and the partially formed loops at the top of the cylinder may be seen to connect to field lines outside the stretched horizon. The field lines are vertical in the lowermost region of the diagram due to the fact that the field was held stationary until its release at $t = 0$. As one proceeds up the cylinder, one finds successively fewer concentric loops in each set of field lines since the oscillations are dying out and fewer field lines snap back to the stretched horizon with each oscillation.

Two criteria need to be considered in choosing the position of the stretched horizon in a problem of this sort. The potential $V(r^*)$ in equation (2.12) acts as a barrier to incoming waves, partially transmitting them and partially reflecting them. Application of the "perfectly absorbing" boundary condition at the stretched horizon rather than at the true horizon is equivalent to neglecting waves reflected from the part of the potential barrier between the two horizons. Since $V(r^*)$ goes to zero proportionally to α^2 at the horizon, this approximation becomes better and better as the stretched horizon is moved inward toward the true horizon. In the problem at hand, it was found that moving the stretched horizon out to $r^* = -10M$ or $r = (2 + 4.9 \times 10^{-3})M$ made no noticeable difference in the solutions obtained. On the other hand, putting the stretched horizon at $r = 2.15M$, as was done above for illustrative purposes, should not be done in the numerical solution of the problem since $V(r^*)$ still has 41% of its maximum value there. The other condition affecting the choice of the stretched horizon is the requirement that its proper distance from the true horizon be smaller than the (global) timescale of evolution of the field, so that important features of the field are not neglected below the stretched horizon. This is certainly satisfied in the present problem for either of the choices of the stretched horizon mentioned above, since the timescale of variation of the field is of order M.

The only dissipation in this problem comes from the horizon boundary condition. If the stretched horizon had a surface resistivity of either zero or infinity, rather than presenting incoming waves with the vacuum impedance $R^H = 4\pi = 377$ ohms, the field lines would oscillate forever. The damping timescale of the oscillations is determined by the size of the horizon relative to the perfectly conducting outer sphere: for the case $R = 3M$, the field lines almost settle down to the static configuration after springing outward just once, while

for the case $R = 10M$, they oscillate many times.

The magnetohydrodynamical decay time of a field slipping through a conducting medium with surface resistivity R^H may be shown (see e.g. Cowling 1957) to be roughly equal to $4\pi L / R^H$, where L is a length comparable with the dimensions of the region where current flows. For the present problem, where $L \sim 2M$, this timescale is just $2M$, the light-travel time across the hole (which, as shown in section 7.5 of chapter III, is the approximate annihilation time for a field loop with both feet in the hole). Not all of the field lines are dissipating their vibrational energy in the hole at a particular time, however. One would therefore expect the timescale τ of the relaxation of the field lines to be roughly equal to $2M$ divided by the time-averaged fraction of field lines which thread the horizon, which is approximately $4M^2/R^2$; that is

$$\tau \sim 2M \left(\frac{R^2}{4M^2} \right) = \frac{R^2}{2M} \quad . \tag{2.14}$$

The time τ is the timescale of the loss of magnetic field energy into the hole, so it will be instructive to elaborate further on the nature of the transfer of electromagnetic energy into the hole.

Following chapter III, one may define a density ε_E and flux density $\mathbf{S}_E$ of "redshifted energy":

$$\varepsilon_E \equiv (\alpha / 8\pi) \, (\mathbf{E}^2 + \mathbf{B}^2) = \frac{\alpha}{32\pi^3 \varpi^2} \left[\frac{\dot{\psi}^2}{\alpha^2} + (\nabla\psi)^2 \right] \quad , \tag{2.15a}$$

$$\mathbf{S}_E \equiv (\alpha / 4\pi) \, \mathbf{E} \times \mathbf{B} = - \frac{\dot{\psi} \nabla\psi}{16\pi^3 \varpi^2} \quad . \tag{2.15b}$$

These satisfy the conservation law

$$\frac{d}{dt} \int_{V(t)} \varepsilon_E \, dV + \int_{\partial V(t)} \alpha \mathbf{S}_E \cdot d\Sigma = 0 \quad , \tag{2.16}$$

for any three-dimensional region $V(t)$ lying entirely exterior to the horizon and having the boundary surface $\partial V(t)$. By taking the region V to be the spherical shell between a stretched horizon $r = 2M + \varepsilon$ and the outer radius $r = R$, and integrating this relation over time, one obtains

$$E_{final} - E_{initial} = \Delta \int_V \varepsilon_E \, dV = -\int_0^\infty \left[\int_{\mathcal{H}} \alpha \mathbf{S}_E \cdot d\Sigma \right] dt \quad , \tag{2.17}$$

where the boundary integral is taken only over the stretched horizon since there is no energy flux through the perfectly conducting sphere at $r = R$. Here the area element vector $d\Sigma$ points along the outward normal to the region V and hence along the *inward* normal to the horizon.

The quantities $E_{initial}$ and E_{final} may be obtained explicitly by integrating the energy density ε_E over the region V using the initial and final fields: $\psi_i = \pi B_0 R^2 \sin^2\theta$ and $\psi_f = \pi B_0 r^2 \sin^2\theta$, respectively. The results are

$$E_{initial} = \frac{B_0^2 R^4}{12M}\left(1 - \frac{2M}{R}\right) , \qquad E_{final} = \frac{B_0^2 R^3}{6}\left(1 - \frac{2M}{R}\right) . \tag{2.18}$$

The rate of energy flow through the stretched horizon can be calculated from equations (2.11) and (2.15b) to be

$$\int_{\mathcal{H}} \alpha \mathbf{S}_E \cdot d\Sigma = \frac{B_0^2 R^4}{6}\left(\frac{\partial u}{\partial r^*}\right)^2_{\mathcal{H}} . \tag{2.19}$$

This quantity is non-negative as expected since $d\Sigma$ points along the inward normal to the horizon.

One may also derive equation (2.19) by considering the energy dissipation to be the result of ohmic losses due to the (fictitious) surface current flowing in the stretched horizon. As derived in section 5.4 of chapter II, one may define a horizon surface current density $\mathcal{J}^H$ which "closes the circuit" of external

currents entering the horizon. It satisfies an Ohm's law of the form

$$\mathcal{J}^H = \frac{\mathbf{E}^H}{R^H} = -\frac{\dot{\psi}\mathbf{e}_{\hat{\varphi}}}{8\pi^2\varpi} \quad , \tag{2.20}$$

where $R^H \equiv 4\pi$ is the horizon surface resistivity and $\mathbf{E}^H$, the horizon electric field, is defined as the horizon limit of the quantity $\alpha\mathbf{E}_{\|}$. The horizon current density is thus purely toroidal, and from equation (2.11) one may see that it varies with latitude proportionally to $\sin\theta$. Then from equation (5.47) of chapter II, the energy flux through the stretched horizon is just the ohmic heating rate

$$\int_{\mathcal{H}} \alpha \mathbf{S}_E \cdot d\Sigma = \int_{\mathcal{H}} \mathcal{J}^H \cdot \mathbf{E}^H d\Sigma \quad . \tag{2.21}$$

Using equations (2.9), (2.11) and (2.13), this may be reduced to the same form as equation (2.19).

The quantity $(\partial u / \partial r^*)^2_{\mathcal{H}}$, which by equation (2.19) is proportional to the energy flux through the stretched horizon, is plotted in Fig. 9 for the cases $R = 3M$ and $R = 10M$ and in Fig. 10 for the cases $R = 30M$ and $R = 100M$. The displacement of the first peak from the origin in these diagrams is due to the finite time required for the waves to propagate down to the stretched horizon. It has been verified numerically that the area under these curves satisfies the energy balance condition, equation (2.17), i.e.

$$E_{final} - E_{initial} = -\frac{B_0^2 R^4}{12M}\left(1 - \frac{2M}{R}\right)^2 = -\frac{B_0^2 R^4}{6}\int_0^\infty \left(\frac{\partial u}{\partial r^*}\right)^2_{\mathcal{H}} dt$$

$$\Longrightarrow \quad \int_0^\infty \left(\frac{\partial u}{\partial r^*}\right)^2_{\mathcal{H}} dt = \frac{(1 - 2M/R)^2}{2M} \quad . \tag{2.22}$$

The curves in Fig. 10 each seem to be a superposition of two oscillations of distinct periods, a fact which may be confirmed by Fourier transforming them. The period of the longer-term oscillation in each case is approximately twice the radius R of the outer shell, i.e. roughly the light-travel time across the shell. This just corresponds to the time necessary for a particular field line to spring outward and then back inward.

The period of the shorter-term oscillation in both cases is roughly equal to $10M$. This value may be justified by an argument similar to that used by Price (1971) for gravitational waves. Since the initial-value function $u(0,r)$ assumed in equation (2.12) is a constant independent of r^*, the second term in equation (2.12) is negligible for small t. The behavior of $u(t,r^*)$ for small time t will thus not be a propagating wave, but rather an oscillation characterized at each point r^* by the approximate angular frequency $\sqrt{V(r^*)}$. Since this frequency varies with r, the oscillations soon become out of phase from point to point, and the initially smooth waveform builds up Fourier components of ever shortening wavelength. Only when wavelengths of order $\Delta r^* \approx 2\pi/\sqrt{V(r^*)}$ have developed, so that the second term in equation (2.12) is of the same order of magnitude as the third, do traveling waves form. These have the approximate period

$$T \sim \frac{2\pi}{V_{\max}^{1/2}} = 3\pi\sqrt{6}\, M \sim 23\, M \quad . \tag{2.23}$$

This is the approximate period of $u(t,r)$; the energy flux curves in Figs. 9 and 10 are proportional to the squares of $\partial u/\partial r^*$, and so should have roughly half this period, or about $10M$ as observed. This argument could also be couched in terms of the gradual decay of a packet of electromagnetic waves in spiral orbits close to the unstable photon orbit at $r = 3M$, as Goebel (1972) does for gravitational waves.

Thus, the short period might be characterized as the "sticking time", during which the oscillating field lines are caught and held by the effective potential, while the long period is the natural vibration time of the field lines.

The double periodicity noticeable in Fig. 10 is not evident in the cases shown in Fig. 9 since the two periods are too close together in the $R = 10M$ case and the oscillations die out too soon in the $R = 3M$ case.

This double periodicity somewhat complicates the task of finding an "experimental" relationship between the damping timescale τ and the cavity radius R to compare with the "theoretical" relationship (2.14). The curves consist of periods of oscillation interspersed with periods of quiescence, so a good fit to an exponential decay is impossible. However, rough fits to the envelopes of the curves yield decay times which conform approximately to a power law relationship of the form $\tau/M = \beta(R/M)^{\gamma}$. The values of γ given by a least squares log-log fit ranged from 1.6 to 1.8 depending on the assumptions made in the fits to the envelopes, and the values obtained for β ranged from 0.4 to 0.6. The theoretical relationship (2.14) would predict the values $\beta = 0.5$ and $\gamma = 2$.

CONCLUSION

This chapter has presented in great detail the solutions to two simple problems involving dynamical electromagnetic fields in the neighborhood of horizons. The objective in this was not so much the problems per se, but rather the elucidation of the relationship between the frozen-star and membrane paradigms described in the Introduction.

In both problems, it was found that part of the field assumes a flattened structure near the horizon. In the Rindler-spacetime problem (particle falling through horizon), these flattened field lines are just the field necessary to connect the infalling charge to the external field lines which are approaching

stationarity. In this sense, it is similar to the flattened field in the Hanni and Ruffini (1973) solutions described at the end of the Introduction to this thesis. The flattened field in the Schwarzschild problem (vibrating field lines) is more complex in structure, consisting of disconnected infalling magnetic field loops reflecting the entire oscillatory history of the near-horizon field. But it also shows the feature, common to both problems, that the external fields are very insensitive to the form of the layered horizon fields, and thus to the precise location of the stretched horizon.

For the Schwarzschild problem, the transfer of energy through the horizon and the damping timescale were investigated, and the criteria governing the choice of the stretched horizon were discussed in detail. These criteria, although they were derived from consideration of a very specific problem, do not depend on the precise details of that model. This of course is to be desired if the concept of the stretched horizon is to have applicability beyond this limited problem.

This chapter has tried to motivate the adoption of the membrane paradigm not only as a calculational tool in solving problems, but as an aid to intuition in thinking about these problems. As was emphasized in the Introduction, there is no difference in the physical predictions of the frozen-star and membrane paradigms; they are both consequences of General Relativity and are thus mathematically equivalent. They differ solely in the aspects of the physics which they emphasize and in the array of mental pictures they present as aids to intuitive understanding of physical problems. This chapter has attempted to show that, for problems involving dynamical electromagnetic fields around black holes, the mental pictures conjured up by the membrane paradigm are much more apt for a physical description of the problem than are those conjured up by the frozen-star paradigm.

REFERENCES

Cowling, T. G., 1957. *Magnetohydrodynamics*, Interscience, New York.

Goebel, C. J., 1972. *Astrophys. J.*, **172**, L95.

Hanni, R. S. & Ruffini, R., 1973. *Phys. Rev. D*, **8**, 3259.

Hanni, R. S. & Ruffini, R., 1976. *Lettere al Nuovo Cimento*, **15**, 189.

Jackson, J. D., 1975. *Classical Electrodynamics*, 2nd ed., John Wiley & Sons, New York.

Linet, B., 1976. *J. Phys. A.*, **9**, 1081.

Misner, C. W., Thorne, K. S., & Wheeler, J. A., 1973. *Gravitation*, W. H. Freeman, San Francisco.

Press, W. H., 1971. *Astrophys. J.*, **170**, L105.

Regge, T. & Wheeler, J. A., 1957. *Phys. Rev.*, **103**, 1063.

Soffel, M., Müller, B. & Greiner, W., 1980. *Gen. Rel. Grav.*, **12**, 287.

Wald, R. M., 1974. *Phys. Rev. D*, **10**, 1680.

FIGURE CAPTIONS

Figure 1. Comparison of Rindler and Minkowski coordinate systems. Minkowski coordinates are (t,z). The Rindler coordinate surfaces Z = constant are represented by hyperbolas and the surfaces T = constant by straight lines through the origin. The geometry of source and observation points for calculation of the field of a uniformly accelerated particle is shown. The electromagnetic field at the observation point O is dependent only on the single point R of the source particle's motion, where R lies on the past null cone of O.

Figure 2. The world lines of the Minkowski-stationary (dotted line) and Rindler-stationary (dashed line) charges, as seen in Minkowski (a) and Rindler (b) coordinates. The Minkowski-stationary charge is fixed at $z = 1/2g$, while the Rindler-stationary charge is fixed at $Z = 0$. In diagram (a), the lower and upper 45° lines represent the past and future event horizons, respectively. In diagram (b), both horizons are represented by the solid vertical line $Z = -1/g$, to which the dotted line asymptotes.

Figure 3. Electric field lines of Rindler-stationary charge plotted in Rindler coordinates. In these coordinates the charge is stationary at $Z = 0$ and there is a horizon at $Z = -1/g$, where g is the acceleration relative to Minkowski space.

Figure 4. Electric field lines for two opposite charges: one stationary in Rindler coordinates, and the other stationary in Minkowski coordinates and thus falling into the horizon as described in the text. The field line diagrams are shown at Rindler-time intervals of $1/g$. By $T = 6/g$, the field geometry has become very similar to the field of the stationary charge alone, which is shown in the lower right-hand diagram.

Figure 5. Initial geometry of magnetic field lines in Schwarzschild background, shown for the case $R = 10M$. The arrows show the direction of the field. The

field lines are frozen into the outer sphere, but are free to slip through the horizon since its conductivity is finite. The tension of the field lines will tend to straighten them out.

Figure 6. Representative magnetic-field-line diagrams in the evolution of the case $R = 3M$. Since most of the field lines thread the horizon, the field settles down quickly to its final static configuration.

Figure 7. Representative magnetic-field-line diagrams in the evolution of the case $R = 10M$. Since the horizon is small relative to the outer sphere, the field lines oscillate for a long time before reaching the final static configuration. The diagrams shown cover only the first oscillation in detail, and the beginning of the second oscillation at $t/M = 28$. The last two diagrams are much further in the future and show that the oscillations have died out substantially by $t/M = 155$ and almost completely by $t/M = 500$. The kinks in the field lines for the case $t/M = 12$ are due to the grid used in the numerical integration.

Figure 8. Embedding-diagram view of the magnetic field at time $t = 92M$ for the case $R = 10M$, with the near-horizon fields expanded for visibility. In the top part of the figure, the magnetic field lines are plotted on the paraboloidal embedding diagram of Schwarzschild spacetime. The paraboloid is cut off at a stretched horizon which is taken to be at a radius $r = 2.15M$, and a cylinder is matched onto it there. In order to make the near-horizon fields visible, the distance along this cylinder is measured by the tortoise coordinate r^*. The elevation angle is 18° and the rotation angle is 45°.

At the time shown, the field lines have sprung outward and snapped back inward four times and are beginning to spring outward for a fifth time. The relic field-line loops left by each of these oscillations are visible running down the cylinder, and the partially formed loops at the top of the cylinder may be seen to connect to field lines outside the stretched horizon. In the lowermost region

of the diagram, the field lines are vertical due to the fact that the field was held stationary until its release at $t = 0$. As one proceeds up the cylinder, one finds successively fewer concentric loops in each set of field lines, since the oscillations are dying out and fewer field lines snap back to the stretched horizon with each oscillation.

Figure 9. $(\partial u / \partial r^*)^2_{\mathcal{H}}$ as a function of time for the cases $R = 3M$ and $R = 10M$. As shown in equation (2.19), this quantity is proportional to the energy flux through the horizon.

Figure 10. $(\partial u / \partial r^*)^2_{\mathcal{H}}$ as a function of time for the cases $R = 30M$ and $R = 100M$. These curves show a clear double periodicity corresponding to the two different length scales in the problem: R and M.

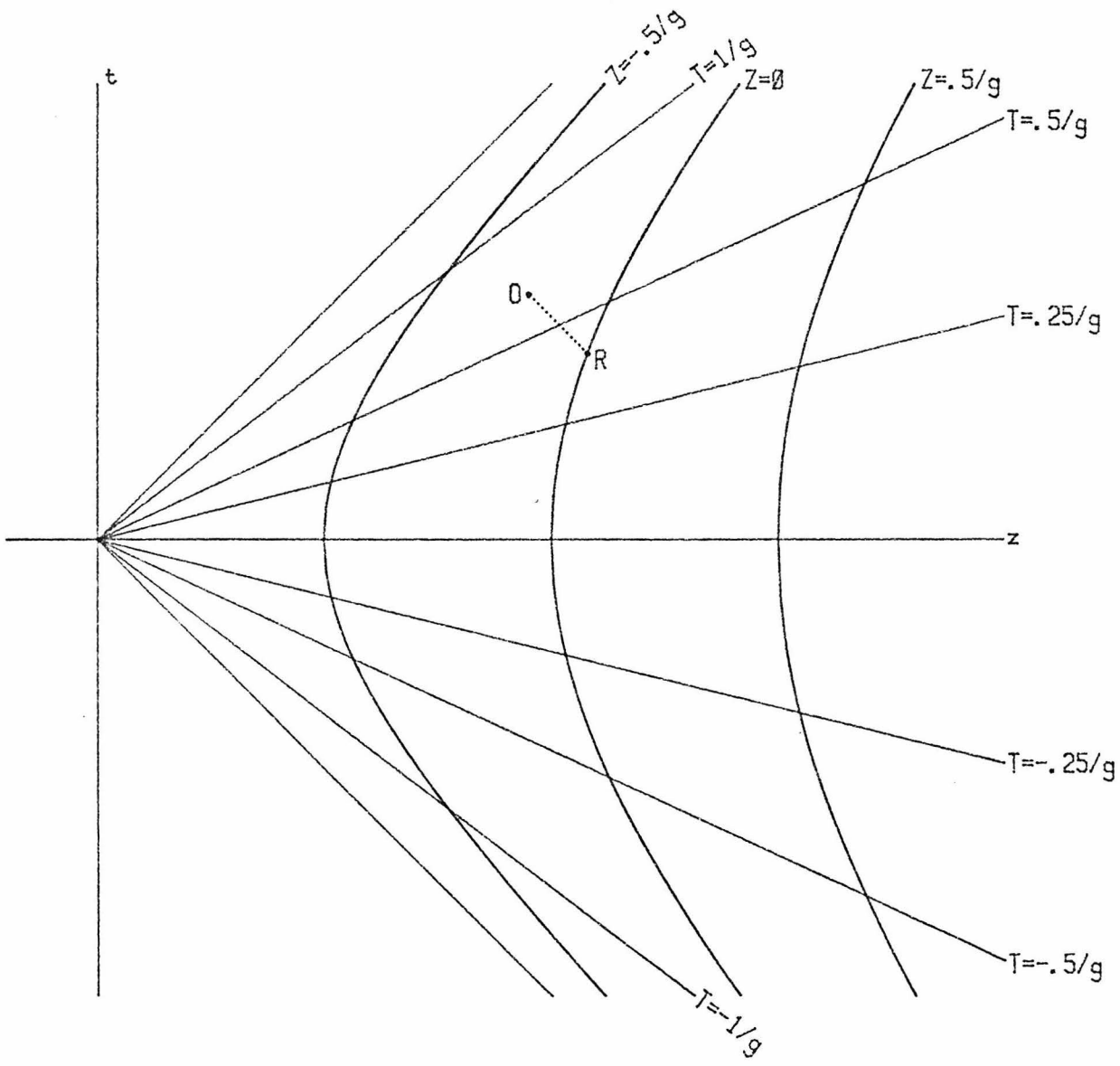

Fig. 1

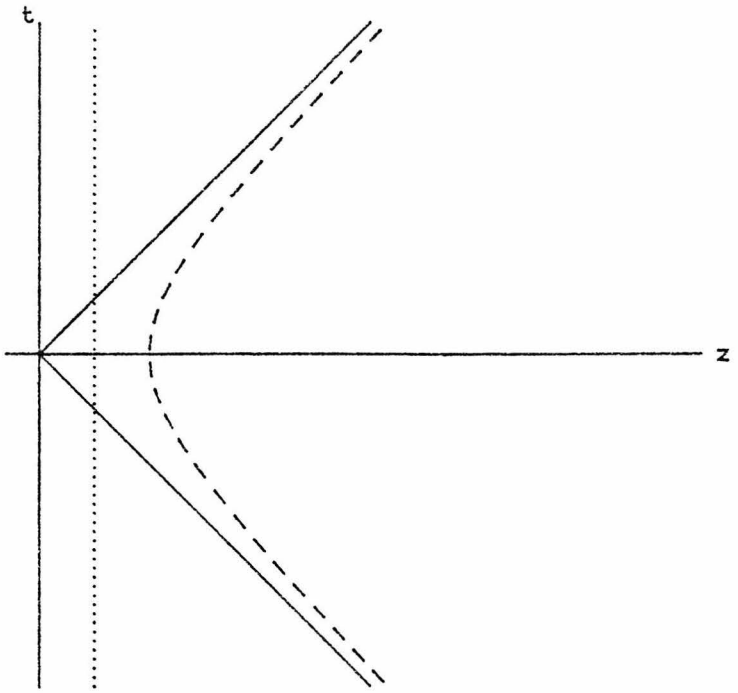

(a)

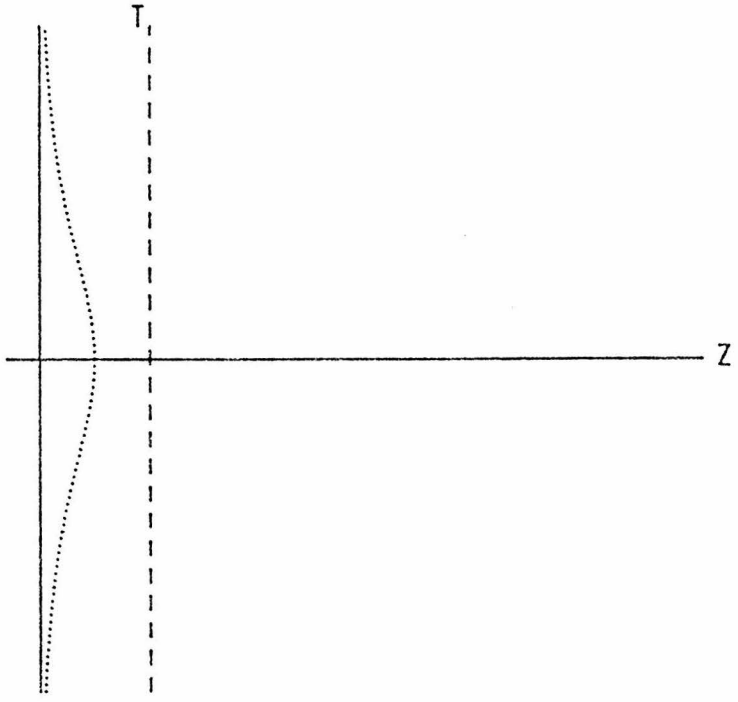

(b)

Fig. 2

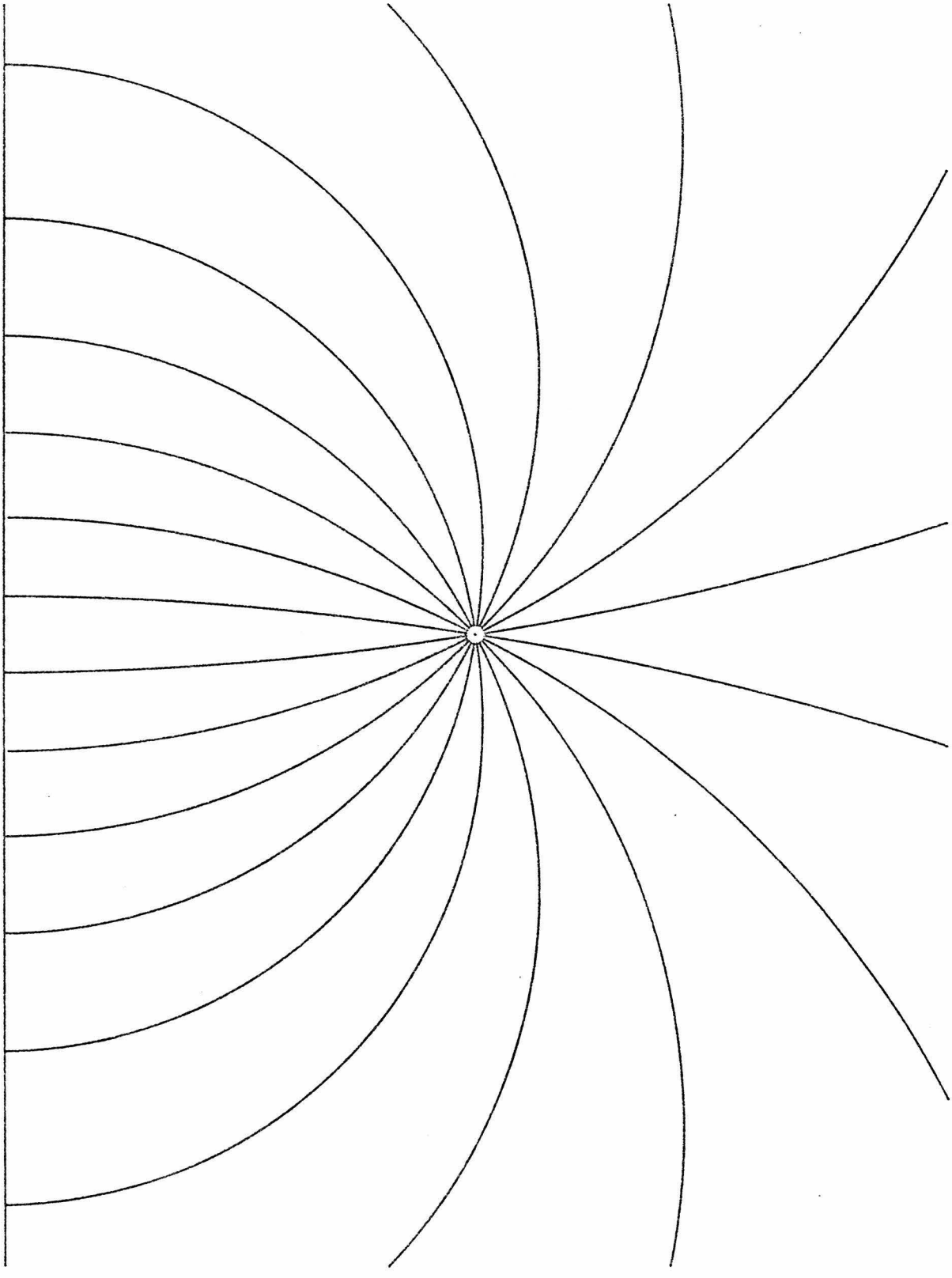

Fig. 3

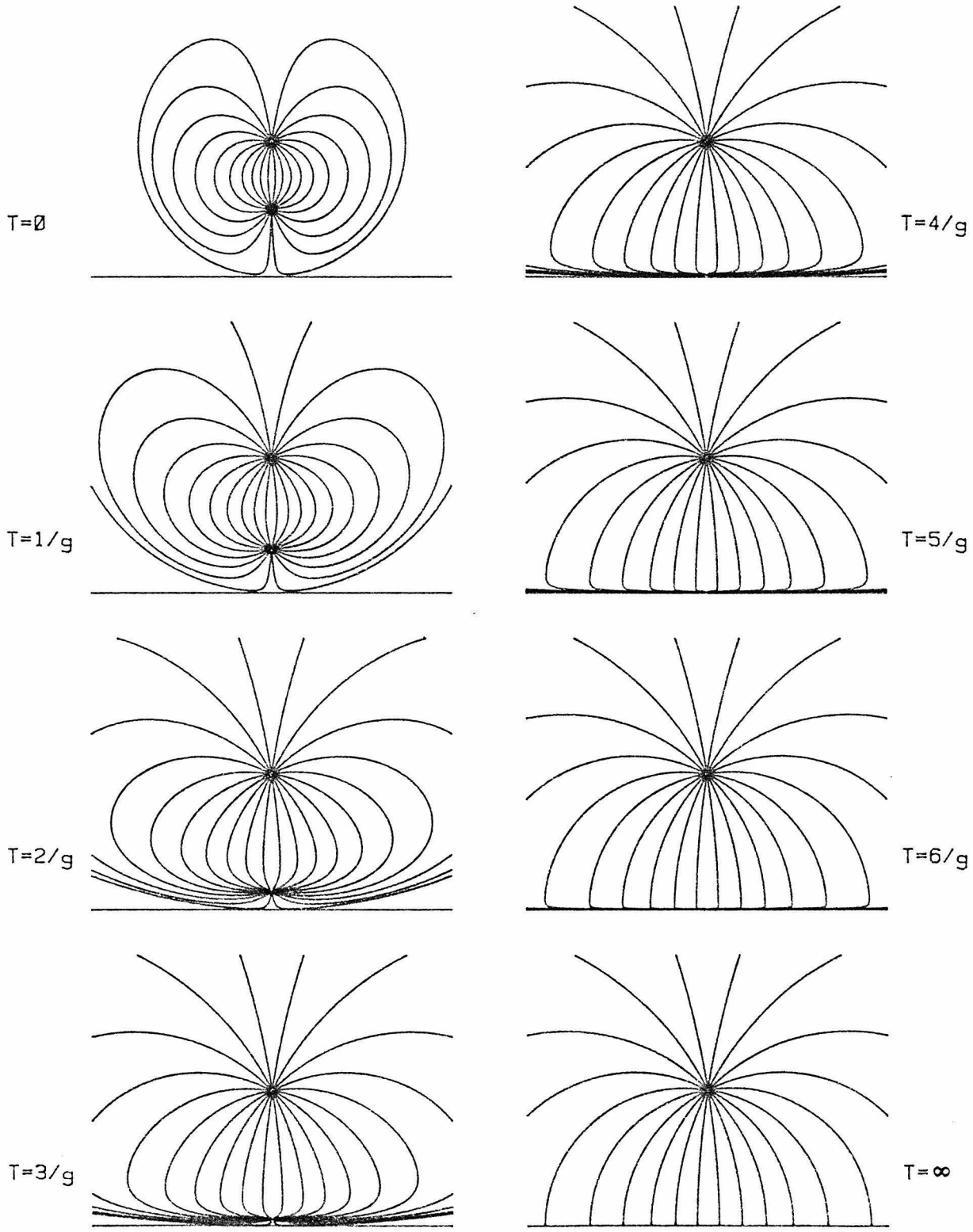

Fig. 4

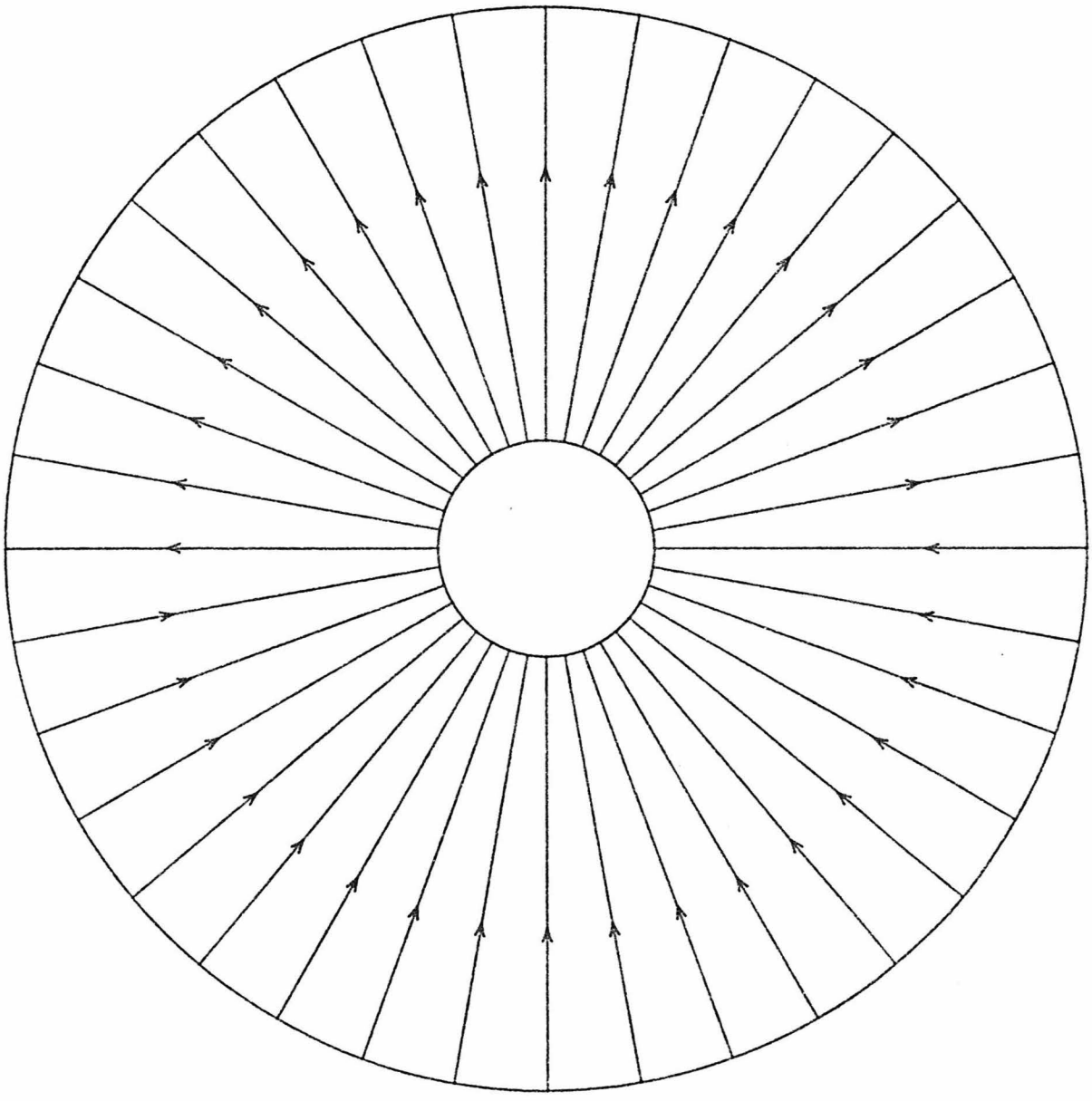

Fig. 5

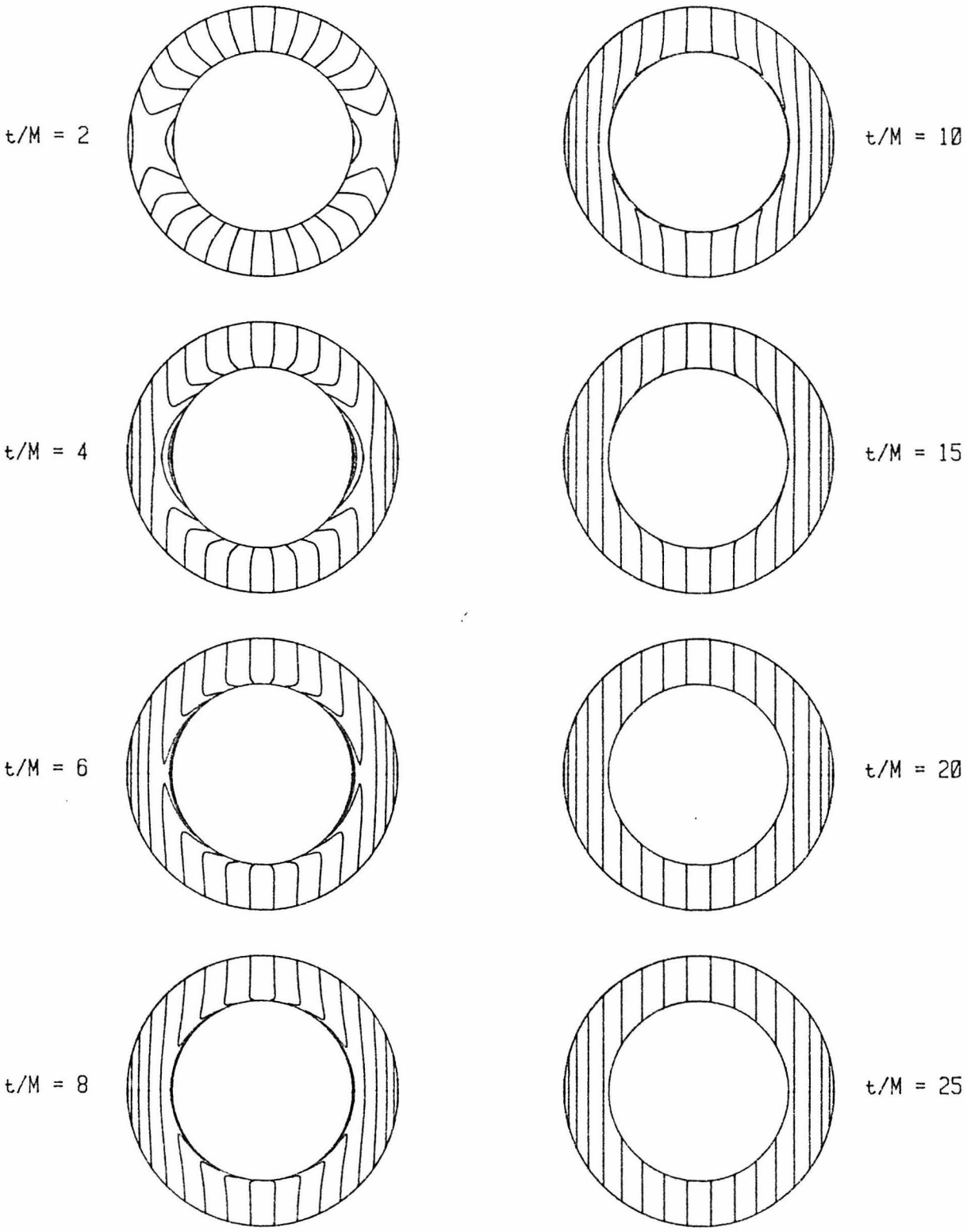

Fig. 6

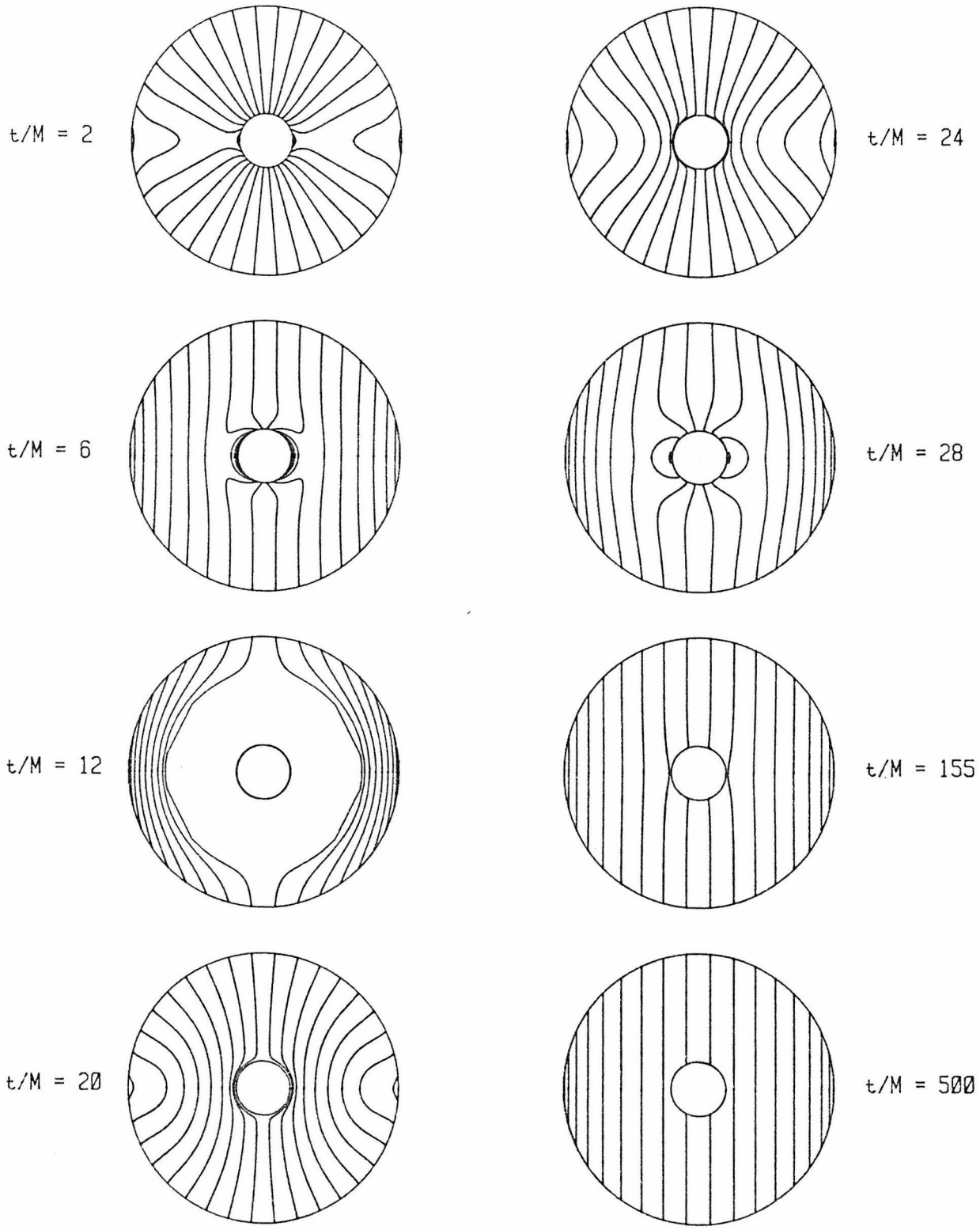

Fig. 7

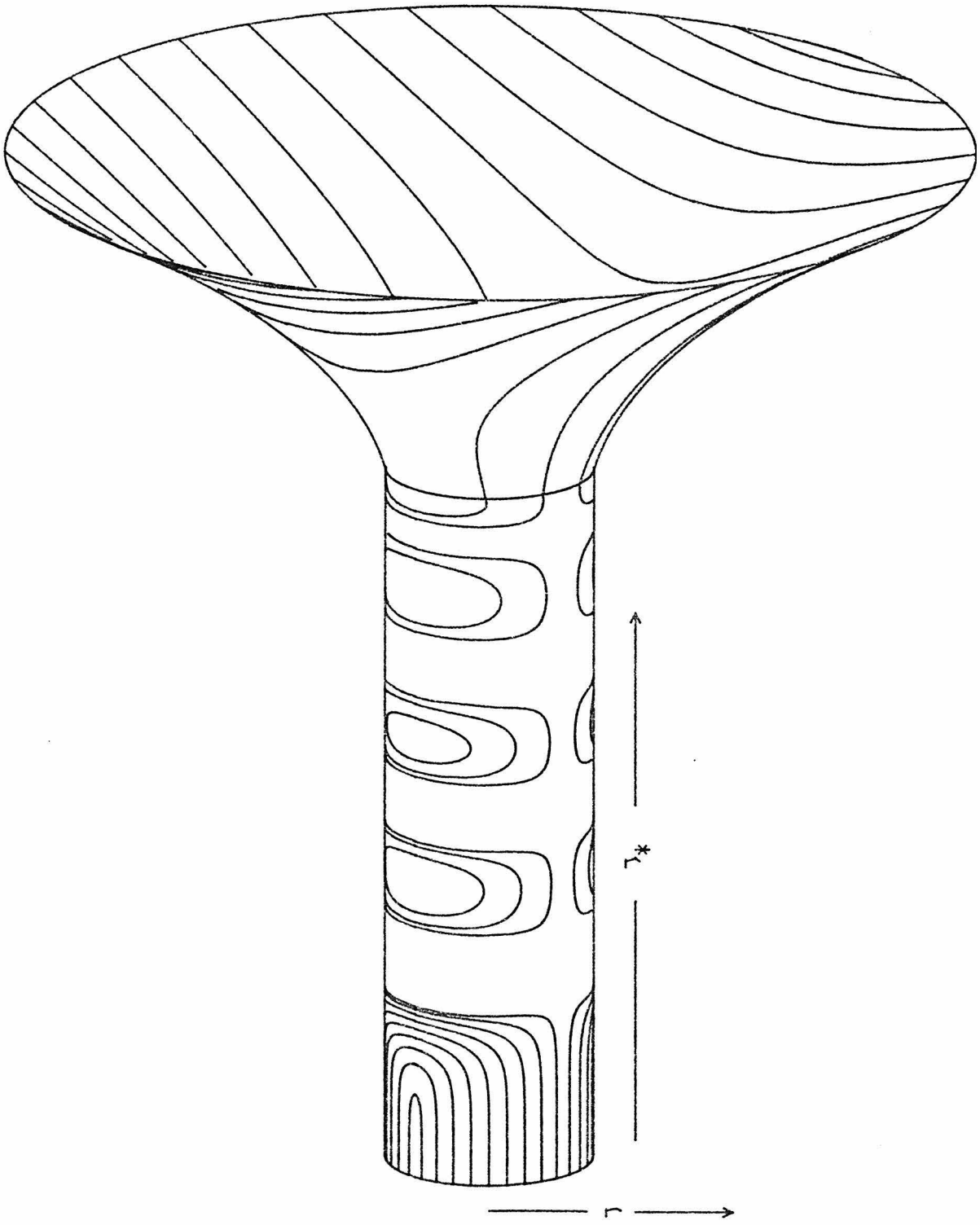

Fig. 8

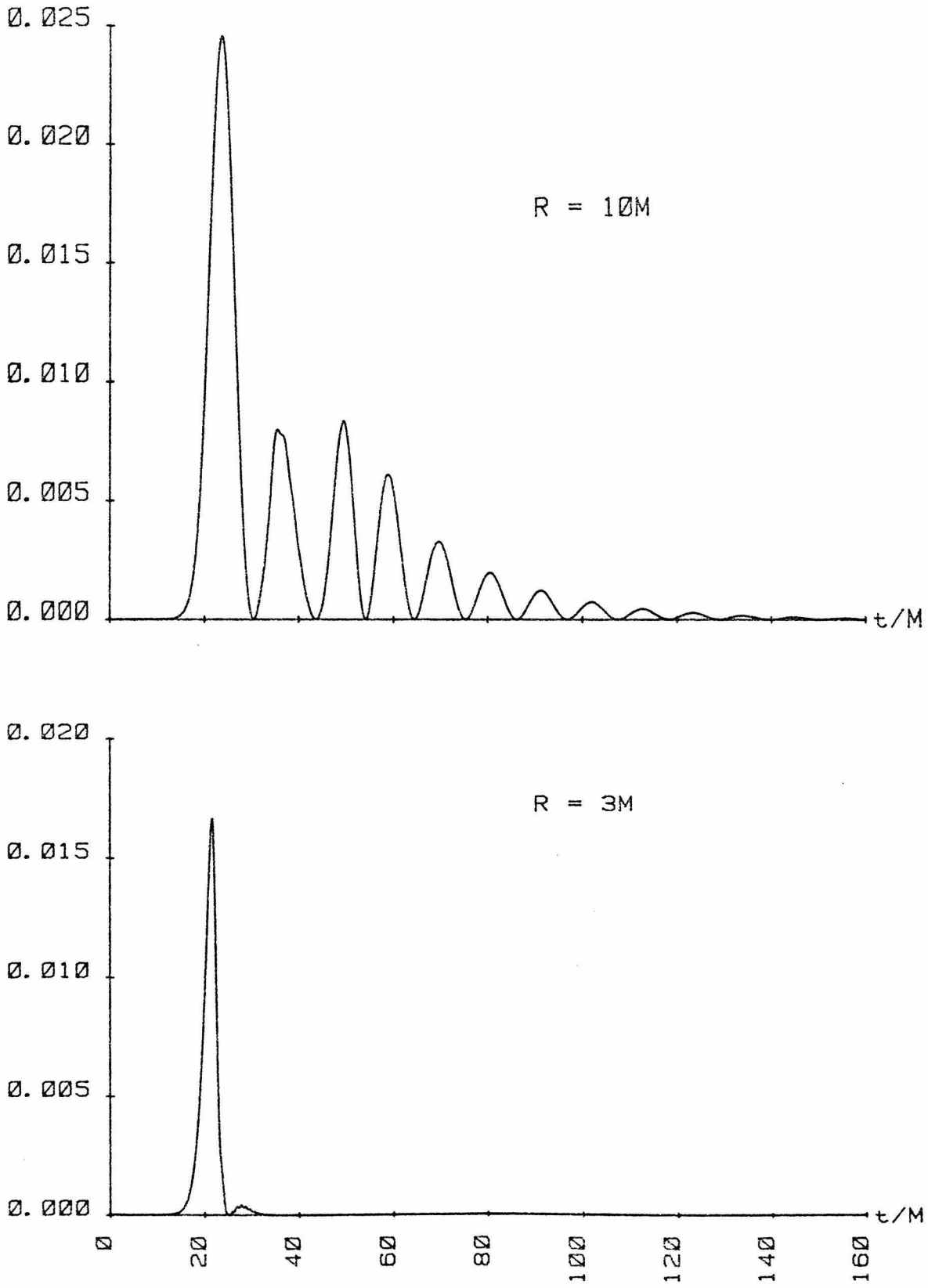
0.025
0.020
0.015
0.010
0.005
0.000
R = 10M
t/M
0.020
0.015
0.010
0.005
0.000
R = 3M
t/M
0
20
40
60
80
100
120
140
160

Fig. 9

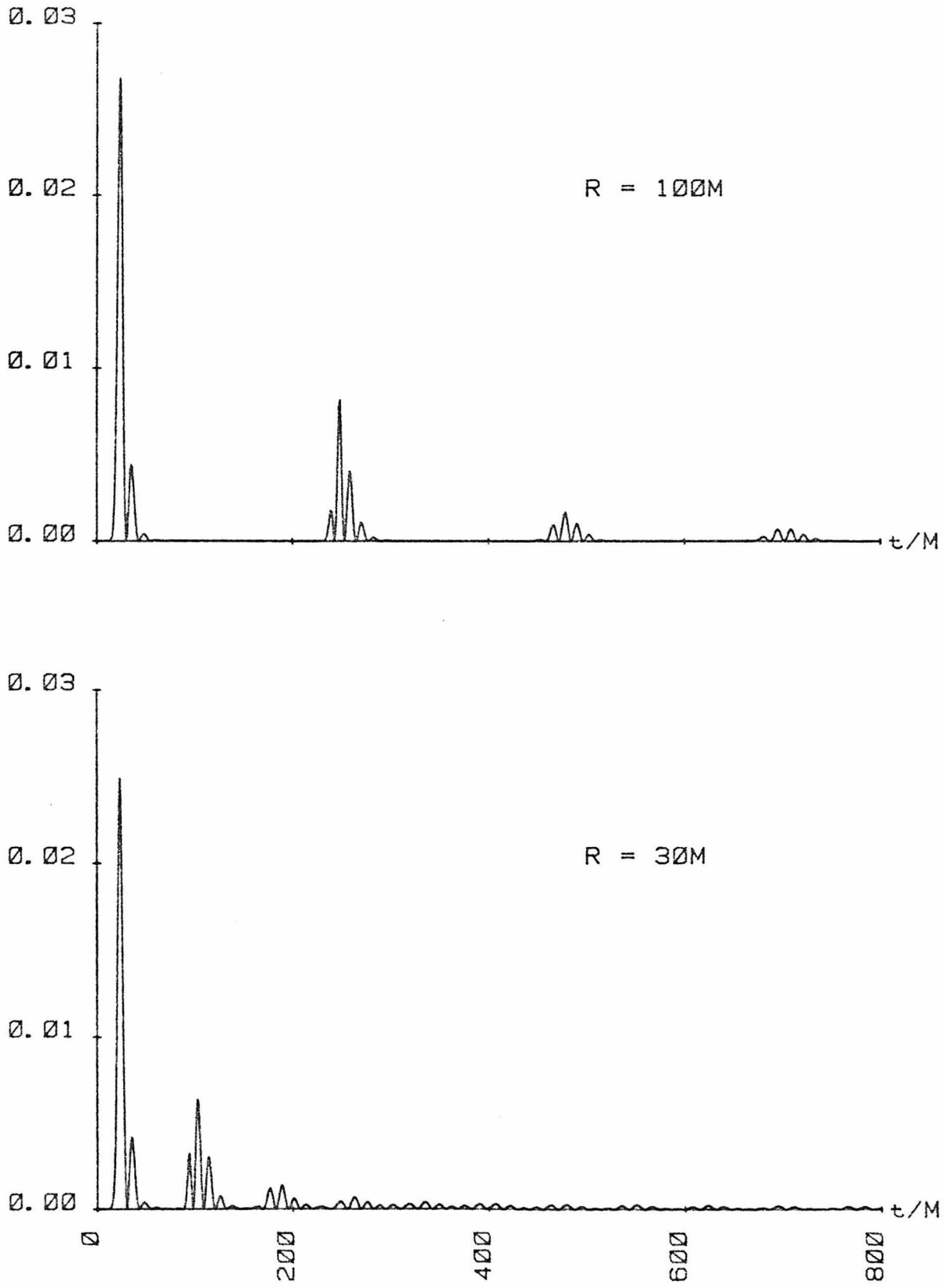
0.03
0.02
0.01
0.00
R = 100M
t/M
0.03
0.02
0.01
0.00
R = 30M
t/M
0
200
400
600
800

Fig. 10